Proteasome-Mediated Processing of Def1: a Critical Step in the Cellular Response to DNA Damage

Marcus D. Wilson

University College London

and

Cancer Research UK London Research Institute

PhD Supervisor: Dr Jesper Svejstrup

A thesis submitted for the degree of

Doctor of Philosophy

University College London

August 2013

Declaration

I Marcus D. Wilson confirm that the work presented in this thesis is my own. Where information has been derived from other sources, I confirm that this has been indicated in the thesis.

Abstract

DNA damage can pose an irreversible steric block to RNA polymerase II (RNAPII), preventing transcription. RNAPII becomes stalled at DNA lesions, blocking normal repair. As a 'last-resort' mechanism to clear the stalled polymerase - and repair the damage - the largest subunit of RNAPII is poly-ubiquitylated and degraded. In yeast, this process is dependent on the Def1 protein, through a previously unresolved mechanism. Using a combination of yeast genetic, biochemical and cell biological techniques this thesis reports the molecular mechanism of Def1 in this process.

Upon DNA damage induced RNAPII stall, Def1 becomes ubiquitylated and partially proteolytically processed by the 26S proteasome. This creates a biologically active, shorter form of Def1, termed pr-Def1. Removal of the C-terminus of Def1, which usually promotes nuclear export, results in nuclear accumulation of the N-terminal processed fragment. Nuclear pr-Def1 binds to stalled, mono-ubiquitylated RNAPII and recruits the Elongin-Cullin ubiquitin ligase complex, promoting RNAPII poly-ubiquitylation and degradation. Interestingly, Def1's ubiquitin-binding CUE domain and a novel ubiquitin homology domain in the Elongin complex mediate this interaction.

These results outline the multi-step mechanism of RNAPII poly-ubiquitylation, elucidate Def1 activation and function, and identify an atypical ubiquitin-like domain in the yeast Elongin complex.

Acknowledgement

First, and foremost, I would like to thank my PhD supervisor Jesper Svejstrup for giving me the opportunity to work in his lab and for his unceasing guidance over the last four years.

I would also like to thank all the members of the Svejstrup lab, past and present, for helpful discussions and providing a fantastic work environment. I would like to acknowledge my collaborators in the Svejstrup lab: Marco Saponaro, Mathias Leidl, Jane Walker, Michael Taschner, Jim Reid, Kotryna Temcinaite and Michelle Harreman. I would especially like to acknowledge Michelle Harreman, both for her teaching and close collaboration on the Def1 project. I would also like to thank my thesis committee - Helle Ulrich and John Diffley – for useful discussions and prompting me to ask the correct scientific questions.

The technical assistance provided by the LRI core services has proven invaluable, especially the mass spectrometry facility, cell services and fermentation services. I would also like to thank members of the public for their continued support of Cancer Research UK, and in particular the Rosetrees Trust for directly funding my PhD.

Last, but by no means least, I would like to thank my fiancée, parents and the rest of my family and friends for their support and encouragement.

Table of Contents

Table of figures

List of tables

Abbreviations

4-NQO	4-Nitroquinoline 1-oxide
5-FOA	5-Fluoroorotic Acid
6-AU	6-Azauracil
ATP	Adenosine triphosphate
BSA	Bovine serum albumin
ChIP	Chromatin Immunoprecipitation
CHX	Cycloheximide
CRL	Cullin-RING ligases
CS	Cockayne syndrome
CV	Column volume
DAPI	4',6-diamidino-2-phenylindole
DDR	DNA damage response
DHFR	Mouse Dihydrofolate reductase protein
DTT	Dithiothreitol
DUB	De-ubiquitylating enzyme
EDTA	Ethylenediaminetetraacetic acid
GAP	GTPase Activating Protein
GEF	Guanidine exchange factor
GFP	Green fluorescent protein
GG-NER	Global genome nucleotide excision repair
GRR	Glycine Rich Repeat motif
GST	Glutathione-S-Transferase
GTP	Guanidine triphosphate
HR	Homologous recombination
IP	Immunoprecipitation
IPTG	Isopropyl β-D-1-thiogalactopyranoside
LMB	Leptomycin B

MMS	Methylmethanosulphate
MTX	Methotrexate
NEB	New England Biolabs
NEM	N-ethylmaleimide
NES	Nuclear export sequence
NLS	Nuclear localisation sequence
NTS	Non-transcribed strand
PBS	Phosphate buffered saline
PCR	Polymerase chain reaction
PI	Protease Inhibitor mix
pr-Def1	Processed-Def1 protein
ROS	Reactive oxygen species
SD	Selective drop-out
SDS	Sodium dodecyl sulphate
TC-NER	Transcription coupled nucleotide excision repair
TEC	Transcription elongation complex
TS	Transcribed strand
TSS	Transcription start site
UBD	Ubiquitin Binding domain
UbH	Internal Ubiquitin Homology domain
Ubi	Ubiquitin
Ubl	Ubiquitin like protein
UV	Ultra-violet
WT	Wild-type (W303-1A *S. cerevisiae* strain)
XP	Xeroderma pigmentosa

Chapter 1. Introduction

1.1 Ubiquitin and Ubiquitylation

1.1.1 Ubiquitin as a post translational modification

Ubiquitin is an 8.5 kDa, 76-residue protein that commonly forms post-translational modifications on cellular proteins. As its name suggests, ubiquitin is universally expressed and highly conserved in eukaryotes (Figure 1.1, upper). Ubiquitylation creates an iso-peptide bond between the C-terminus of ubiquitin and the ε-amino lysine group of a target protein. Unlike other post-translational modifications, ubiquitin can be further modified itself; ubiquitin contains 7 lysine residues (Figure 1.1, lower) (Vijay-Kumar et al., 1987) and a solvent exposed N-terminus, all of which can be conjugated to another ubiquitin molecule, creating chains. Ubiquitin chains can pose an extremely complicated signal on a protein. Not only can multiple lysine residues on the same protein be mono-ubiquitylated, but also the ubiquitin itself can form chains of differing linkages, which targets a protein to different cellular fates. Chains are typically formed using the same target lysine, but mixed linkage chains have been reported (Peng et al., 2003, Kim et al., 2007). The flexibility of ubiquitin signalling helps to explain its importance in numerous cellular pathways.

Ubiquitin is added to a substrate protein at the end of an enzymatic activation cascade. Uba1 (the only E1 activating enzyme in *S. cerevisiae*) forms a high-energy thioester linkage with ubiquitin in an ATP-dependent process. Next, ubiquitin is transesterified onto a Ubc (E2 conjugating) enzyme (Olsen and Lima, 2013) and is finally transferred directly or indirectly to the substrate by an E3 ligase (Figure 1.2). The ubiquitin conjugation machinery determines ubiquitylation site usage and chain topology (Hofmann and Pickart, 1999, Petroski and Deshaies, 2005).

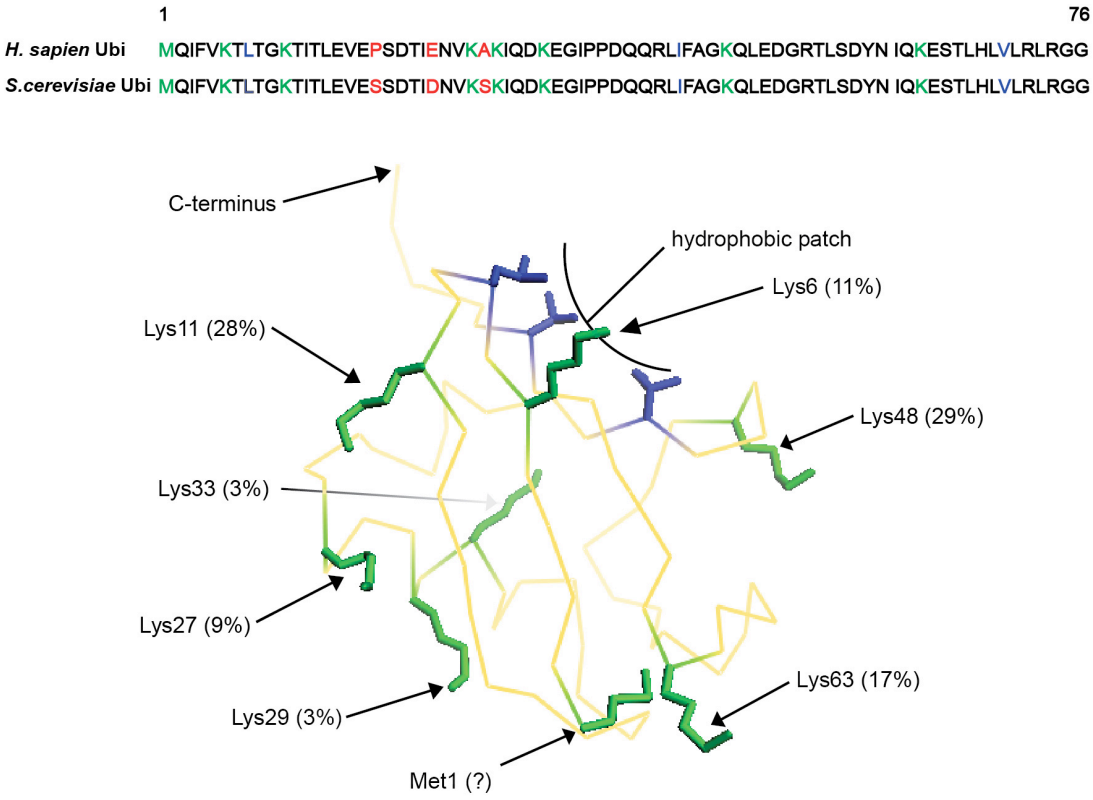

Figure 1.1: The structure of ubiquitin

(upper) Comparison of the primary sequence of ubiquitin from yeast and human, with non-conserved residues are highlighted in red. Sites of ubiquitin attachment are highlighted in green. The hydrophobic patch Leu-8, Ile-44 and Val-70 residues are highlighted in blue.
(lower) The structure of ubiquitin (pdb 1UBQ; (Vijay-Kumar et al., 1987), with residues highlighted as above. The ubiquitin ββαββαβ roll is a commonly found superfold (Kiel and Serrano, 2006), whereby the beta barrel (front) grasps the long α-helix (rear). The percentages refer to relative abundance of chain linkage in yeast (Xu et al., 2009a). Inspired by Komander 2009.

E2 conjugating enzymes do not play a benign role in the final ubiquitylation reaction. Instead, E2s help to determine the chain topology for E3s (Suryadinata et al., 2013, Eddins et al., 2006) and may even aid in substrate selection (Somesh et al., 2007, Bernier-Villamor et al., 2002). Different E2s preferentially pair with different E3s; for example, Cullin E3s bind to E2s with long C-terminal basic extensions (Pierce et al., 2009, Kleiger et al., 2009a).

There are between 60-100 E3 ubiquitin ligases in *S. cerevisiae* (Finley et al., 2012). E3s can be split into two catalytically separate families, RING domain and HECT domain-containing E3s. HECT E3s directly transfer ubiquitin to substrate, from an active site cysteine. The HECT domain comprises an N-terminal E2 binding lobe

and C-terminal catalytic lobe. Rsp5 is the only essential HECT E3 in yeast and has the most identified functions (Kaliszewski and Zoladek, 2008, Huibregtse et al., 1995).

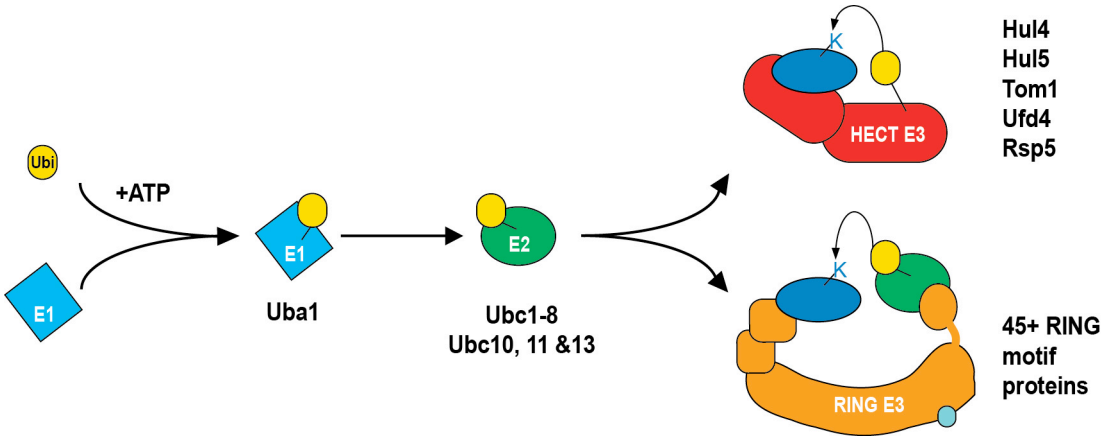

Figure 1.2: The ubiquitylation cascade

Ubiquitin is transferred from an E1 activating enzyme to an E2 conjugating enzyme and finally to substrate, directly (RING E3) or via an active HECT thioester (HECT E3). The directionality of the cascade is ensured through the use of a common binding interface (Eletr et al., 2005) and the relative affinities for Ubi-E2 and E2 (Pickart and Rose, 1985, Saha and Deshaies, 2008).

RING E3s bind to, and stimulate thioester transfer from a ubiquitin loaded E2, via altering the conformation of the E2 (Ozkan et al., 2005) and promoting the correct catalytic orientation (Duda et al., 2008). The largest sub-class of RING E3s is the modular Cullin-RING ligases (CRLs). CRLs are formed from one of three cullins in yeast (Cdc53, Rtt101 and Cul3), which fold as a ~110 Å elongated scaffold (Zheng et al., 2002). The C-terminal end of the cullin binds to the dynamic catalytic RING finger protein, Rbx1/Hrt1 (Duda et al., 2008). The N-terminal cullin repeats provide a platform to bind substrate adaptors (Figure 1.2), which allow a broad variety of targets to be ubiquitylated. The substrate adaptor component is typically a heterodimer comprised of a Skp1-like adaptor protein (either Skp1, Elc1 or Mms1) and one of a number of different substrate receptors: either an F-box protein, SOCS-box protein or DCAF-like protein. The 50-residue F-box motif is typically N-terminal in a protein and binds to Skp1 or Elc1, freeing the C-terminus for substrate interaction (Bai et al., 1996, Skowyra et al., 1997).

CRL activities are highly controlled. Rub1 (NEDD8 in humans), a ubiquitin-like modifier with 80% homology to ubiquitin, covalently links to, and activates CRLs (Duda et al., 2008). Lag2 (CAND1 in humans) binds and inactivates CRLs (Siergiejuk et al., 2009), in part through promoting the dissociation of substrate adaptor proteins (Pierce et al., 2013).

Chains are typically formed by the sequential addition of ubiquitins, requiring E2/HECT ubiquitin reloading (Kleiger et al., 2009b, Maspero et al., 2013). As a result, the poly-ubiquitylation and mono-ubiquitylation steps can often be separated; different E2 (Chen et al., 1993, Rodrigo-Brenni and Morgan, 2007) and E3 ligases (Hwang et al., 2010, Parker and Ulrich, 2009, Harreman et al., 2009) can be employed to perform poly-ubiquitin chain formation.

Thousands of proteins in yeast are ubiquitylated (Peng et al., 2003, Beltrao et al., 2012), each in a controlled manner through recognition of a degron signal. Substrate recruitment for the E3s can be mediated through the same polypeptide chain as the ligase domain. For example, Rsp5 contains three protein-interacting WW domains, which bind to proteins with PY-motifs (Sudol, 1996, Chang et al., 2000). This limits the possible list of substrates, so both HECT E3s and RING E3s utilise substrate adaptors to increase the number and specificity of potential ubiquitylation targets (Sullivan et al., 2007, Finley et al., 2012).

1.1.2 De-ubiquitylating enzymes (DUBs)

Poly-ubiquitylation is antagonised by de-ubiquitylating enzymes (DUBs). 20 DUBs have been found in yeast (Finley et al., 2012), which catalyse the hydrolysis of isopeptide bonds on substrate or in chains (reviewed by Komander et al., 2009). Unlike E3s, no singular DUB–activity is essential for viability in yeast and some DUBs have a broad range of enzymatic activity (Schaefer and Morgan, 2011). Indeed, upon cell lysis there is rapid reversal of all ubiquitylation, due to uncontrolled DUB action (Wilson et al., 2012, Finley et al., 2012). However, linkage

specificity has been reported for some DUBs (Edelmann et al., 2009, Mevissen et al., 2013, Ye et al., 2012, Chai et al., 2004).

DUBs have a critical role in providing free ubiquitin for ubiquitylation reactions, but also have key roles in antagonising ubiquitin signalling. DUBs can be controlled through interacting partners and post-translational modifications: for example, the DUB, Ubp3, is only active upon association with Bre5 (Cohen et al., 2003). Ubp3 is also further stimulated by phosphorylation upon osmotic stress (Sole et al., 2011). Another DUB, Ubp2, forms a complex with Rsp5 via Rup1, specifically antagonizing Rsp5 Lys-63 chain formation (Kee et al., 2005, Kim and Huibregtse, 2009, Kee et al., 2006).

1.1.3 Ubiquitin binding domains

Ubiquitin recognition poses a unique problem to cells: Ubiquitin itself is much larger than other post-translational modifications, making it impractical for a single domain to bind to both the ubiquitin and the ubiquitylated protein. In addition, the complexity of multiple chain topologies needs to be decoded. Different linkages lead to different cellular fates, requiring specific chain recognition. Ubiquitin recognition can be mediated through small, independently folding ubiquitin binding domains (UBDs) (Hofmann, 2009) or short ubiquitin-interacting peptide segments (Fradet-Turcotte et al., 2013).

UBDs have been divided into 20 or more distinct families depending upon sequence and fold (Husnjak and Dikic, 2012). *S. cerevisiae* contains 39 proteins with confirmed UBDs (some examples are listed in Table 1.1). Often these are involved in the ubiquitin conjugation reaction - by helping to orientate invading ubiquitin moieties during ligation (Polo et al., 2002, Shih et al., 2003, Hoeller et al., 2007) - or preventing the poly-ubiquitylation of a substrate (Herrador et al., 2013). Due to the broad function of ubiquitin in other cellular processes, UBDs are an integral part of signalling platforms (Hofmann, 2009, Acconcia et al., 2009).

Table 1.1: List of UBDs in *S. cerevisiae*

UBD	Binding mode	Ubiquitin motif	Example	Function	Reference
UIM	Single α helix	Hydrophobic patch	Rpn10	Proteasome subunit	(Elsasser et al., 2004)
UBA	Three helix bundle	Hydrophobic patch	Rad23 Dsk2	NER/ Proteasome shuttling factor	(Raasi et al., 2005)
UEV	Extended loop	Hydrophobic patch	Mms2	Lysine-63 conjugation	(Tsui et al., 2005)
PFU	Four β-strands and two α-helices	Hydrophobic patch	Doa1	Cdc48 adaptor	(Pashkova et al., 2010)
SH3v	Hydrophobic groove	Hydrophobic patch	Sla1	Actin cytoskeleton	(Stamenova et al., 2007)
UBZ	Inverted Single α helix	Hydrophobic patch/ C-terminus	Rad30	Translesion synthesis	(Bomar et al., 2007)
UBC	Catalytic core/β-sheet	C-terminus/ Hydrophobic patch	Ubc4	E2 enzymes	(Cook et al., 1993)
UBM	Helix turn helix	Hydrophobic patch	Rad2	NER	(Bomar et al., 2010)
CUE	Three helix bundle	Hydrophobic patch	Vps9 Def1	ER Ubiquitylation Rpb1 degradation	(Shih et al., 2003) (Ponting, 2002)
PRU	Three loops of PH domain	Hydrophobic patch	Rpn13	Proteasome subunit	(Husnjak et al., 2008)

Many structural studies have examined the interaction of ubiquitin and UBDs (Table 1.1). Ubiquitin recognition is mediated through a number of different folds, but tends to focus on the hydrophobic patch of ubiquitin (Winget and Mayor, 2010). The hydrophobic patch is formed by residues Val8-Ile44-Leu70 (Figure 1.1). Mutation of the isoleucine to alanine tends to ablate UBD interactions (the only reported exception has been presented in Bomar et al., 2010). Whist key residues in the hydrophobic patch mediate the majority of the interactions with UBDs, other, specific contacts are also important. For example, mutation of the β5 strand of ubiquitin ablates only the UIM-UBD interaction (Haririnia et al., 2008). Domains within the same family often display subtly different binding to ubiquitin. These subtle differences can lead to large functional consequences, in both the affinity to ubiquitin and recognition mode (Raasi et al., 2005, Komander et al., 2008).

As the UBD-Ubi interaction surface is small and principally hydrophobic, affinities tend to be low (Hurley et al., 2006). UBD interactions are often co-ordinated with other protein interaction motifs to help confer specificity and ensure robust protein interactions (Panier et al., 2012, Parker et al., 2007).

Whilst most UBDs have been identified through their binding to mono-ubiquitin *in vitro*, in their proper, cellular context they often display linkage specificity (Funakoshi et al., 2002, Raasi et al., 2005). The linkage specificity of UBDs is achieved through selection of the ubiquitin chain topology. Different chain conformations, whilst relatively dynamic (Ryabov and Fushman, 2006) have preferred states that can be fixed through the binding of UBDs (Husnjak and Dikic, 2012, Ye et al., 2012). Lys-6, -11, -27 and -48 ubiquitin chains preferentially form a closed conformation (Varadan et al., 2002), whilst Lys-29, -33, -63 and Met-1 linked chains form open, elongated structures (Varadan et al., 2004, Fushman and Walker, 2010).

Chain recognition can be achieved by individual UBDs: Rad23's second ubiquitin associated (UBA) domain preferentially binds to Lys-48 over Lys-63 chains (Raasi et al., 2005). This is achieved through the UBA sandwiching between two Lys-48 linked ubiquitins, using an additional ubiquitin-binding surface (Varadan et al., 2005). The NEMO UBD binds linear chains with 100x greater preference than other chain linkages, through direct binding to the glycine-methionine, C-N terminal linkage (Rahighi et al., 2009). Alternatively, using multiple UBDs both increases the relative avidity of ubiquitin interaction and can possibly lead to chain–linkage specificity (Sims and Cohen, 2009, Zhang et al., 2009). The length and flexibility of linker regions between repeated UBDs helps to determine specificity. For example, the two UIMs of RAP80 bind to Lys-63 linked chains (Sobhian et al., 2007), whereas Ataxin-3, which also has two UIMs, is a Lys-48 specific DUB (Chai et al., 2004). Swapping the linker region between the UIMs of RAP80 and Ataxin-3 reverses their inherent linkage specificity (Sims and Cohen, 2009).

The Dsk2 UBA domain was one of the first studied both biochemically and structurally (Hofmann and Bucher, 1996, Ohno et al., 2005), and displays one of

the highest UBD affinities reported (Raasi et al., 2005, Ohno et al., 2005). UBA domains wrap three helices around the ubiquitin hydrophobic patch (Dieckmann et al., 1998, Ohno et al., 2005). *In vivo* and *ex vivo* Dsk2 binds to Lys-48 linked chains (Funakoshi et al., 2002), fitting its function as a proteasome shuttle factor. However, the Dsk2 UBA domain does not exhibit any particular linkage preference on its own (Raasi et al., 2005), nor bind in a manner to exert such preference (Ohno et al., 2005). The Lys-48 selectivity of Dsk2 may be due to the interaction of more than one Dsk2 protein per ubiquitin chain (Lowe et al., 2006); the UBA domain of Dsk2 can dimerise (Sasaki et al., 2005).

The coupling of ubiquitin conjugation to ER degradation (CUE) UBD was identified from two studies of Vps9 binding to ubiquitin (Donaldson et al., 2003, Shih et al., 2003). CUE domains can bind to both to mono-ubiquitin and ubiquitin chains (Shih et al., 2003, Liu et al., 2012, Bagola et al., 2013). The CUE domain has a very similar fold to UBA domains (Prag et al., 2003, Kang et al., 2003), with a conserved mode of ubiquitin binding.

1.1.4 Ubiquitin-mediated proteolysis

Ubiquitylation is the main targeting signal for protein degradation. On a macroscopic scale, whole organelles and large protein complexes are targeted for autophagy through ubiquitylation (Nakatogawa et al., 2009).

Tagging with ubiquitin was originally identified to alter the half-life of a protein via ATP dependent proteasome degradation (Hershko et al., 1980). Further work elucidated that tagging by at least 4 ubiquitin moieties was required to target a protein for degradation (Thrower et al., 2000). All chain linkages except Lys-63 can lead to degradation (Xu et al., 2009a, Zhao and Ulrich, 2010). However, if the tagged polypeptide is shorter than 150 amino acids, even a single mono-ubiquitin is sufficient for proteasome-mediated proteolysis (Shabek et al., 2012). Furthermore, ubiquitin-independent proteasomal degradation has also been reported for a number of proteins (Jariel-Encontre et al., 2008, Ha et al., 2012).

The 26S proteasome is a 2.5 MDa complex comprised of 33 subunits (Finley, 2009, Beck et al., 2012); arranged into a 20S catalytic core particle capped with two 19S regulatory particles (Figure 1.3). The solvent accessible 20S barrel physically sequesters the proteolytic sites (Heinemeyer et al., 1997); the combination of three broad specificity proteases leads to the degradation of any entering polypeptide chain (Elsasser and Finley, 2005, Lee et al., 2001a).

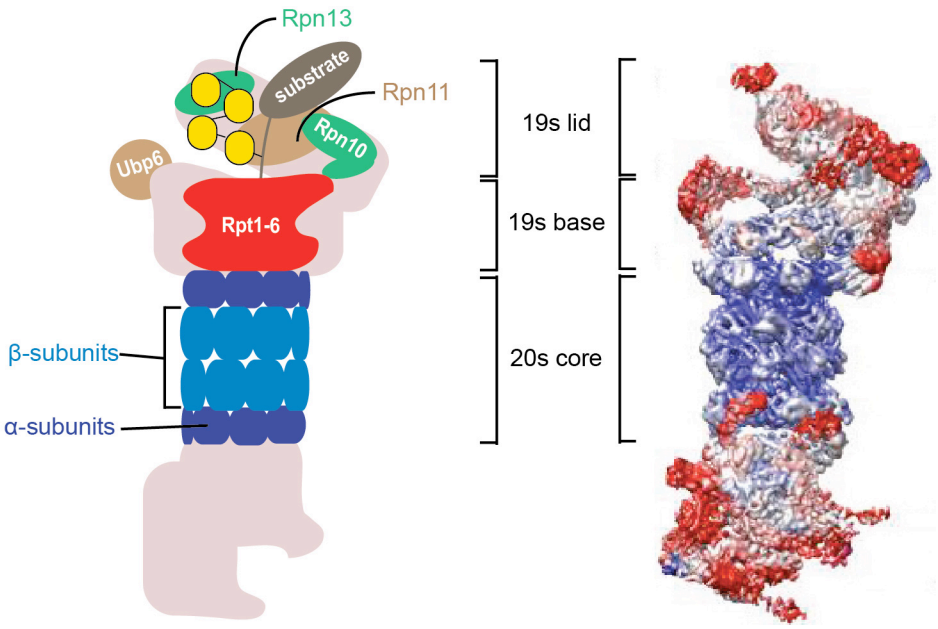

Figure 1.3: The 26S yeast proteasome

(Left) schematic representation of the 26S proteasome with labelled subunits. The ubiquitin interacting subunits Rpn10 and Rpn13 are coloured green, DUBs Ubp6 and Rpn11 are coloured brown and ATPase subunits Rpt1-6 are coloured red. In the core, the α -subunits Pre5-6, Pre8-10, Pup2 and Scl1 are coloured dark blue, whilst the β-subunits Pre1-4, Pre7, Pup1 and Pup3 are coloured light blue. Substrate (grey) is modelled as in Lander et al, 2012 (right) Cryo EM reconstruction of the yeast 26S core particle from (Beck et al., 2012)(pdb 4B4T) coloured according to resolution from blue (6.5 Å) to red (8.5 Å)

The 19S regulatory particle both recognises ubiquitylated substrates and unfolds globular proteins, allowing their passage into the 20S (Glickman et al., 1998, Navon and Goldberg, 2001). The base of the 19S forms a spiral hexameric ring (Lander et al., 2012), creating the dynamic helicase, which unwinds globular proteins in an ATP-dependent manner (Schrader et al., 2009, Matyskiela et al., 2013).

The 19S contains two associated DUBs; the zinc-metalloprotease Rpn11 cleaves the ubiquitin chain close to their base, whilst Ubp6 trims exterior ubiquitins (Verma et al., 2002, Guterman and Glickman, 2004). Ubiquitylated proteins are bound through the UIM domain of Rpn10 (Elsasser et al., 2004) and the PRU domain of Rpn13 (Husnjak et al., 2008); both subunits display a marked preference for poly-ubiquitin chains (Zhang et al., 2009). Interestingly, the ubiquitin receptors are not essential (Glickman et al., 1998). This may be due to redundancy with the proteasome shuttling factors: Rad23, Dsk2 and Ddi1 (Schauber et al., 1998, Funakoshi et al., 2002, Sirkis et al., 2006), which bind to and target ubiquitylated proteins to the proteasome (Elsasser et al., 2002, Rosenzweig et al., 2012).

The ubiquitin, chaperone-like, ATPase Cdc48 helps to deliver or aid unfolding of otherwise intractable ubiquitylated proteins to the proteasome (Dantuma and Hoppe, 2012). Accessory ubiquitin receptors help to target Cdc48 to multiple substrates and these can be subdivided into Ufd1-Npl4-Cdc48 complexes and Ubx-Cdc48 complexes. For example, the ER tethered transcription factor Spt23 is mono-ubiquitylated and partially processed by the proteasome (see 1.1.6; (Hoppe et al., 2000). However, the shorter, processed protein is still stably attached to an unprocessed protein at the ER membrane. This complex is dissociated by Cdc48-Ufd1-Npl4 complex, allowing nuclear accumulation of the transcription factor (Rape et al., 2001, Hitchcock et al., 2001).

1.1.5 Ubiquitin-like and ubiquitin homology domains

Genome-wide genetic analyses revealed a large number of ORFs that contained regions with homology to ubiquitin (Welchman et al., 2005). Ubiquitin-like proteins (Ubls) do not necessarily share high sequence homology to ubiquitin, but use the same β-grasp fold and conjugate to substrates via a C-terminal glycine. Six Ubls have been identified in yeast: Smt3 (yeast homologue of human SUMO1/2); Rub1 (NEDD8); Hub1 (Ubl5); Urm1 (URM1); Atg8 (GATE16) and Atg12 (ATG12). Each Ubl has its own conjugation machinery - which acts in a similar manner to the ubiquitylation cascade (Figure 1.2) - and targets proteins involved in numerous

cellular processes (Finley et al., 2012). Metazoans have evolved multiple Ubls with more diverse functions (van der Veen and Ploegh, 2012)

Horizontal gene transfer has also resulted in the formation of proteins containing internal ubiquitin homology domains (UbH domains). These domains do not act like the Ubls: they are not covalently conjugated to other proteins. Instead, integral UbH proteins utilise the ubiquitin fold and components of the ubiquitin machinery for their own ends. Whilst a large group of UbH proteins are implicated in ubiquitylation and proteasomal degradation, an increasing number have been found to be involved in other functions (May et al., 2004, Takai et al., 2001, Garrett et al., 1995).

Original classifications of UbH domains were based on sequence homology (Garrett et al., 1995); however, at a structural level the ubiquitin fold is extremely common (Kiel and Serrano, 2006). The broad *in silico* definitions have identified many possible internal UbH domains, most of which have not yet been validated structurally or biochemically. Where structural studies have been performed, the UbH domains invariably have a ubiquitin-like, β-grasp, superfold (Harper et al., 2011, Faesen et al., 2011). Integral UbH domains can also be referred to as ubiquitin fold domains (UFDs) (Faesen et al., 2012) or Ubls (Grabbe and Dikic, 2009), for clarity in this thesis the nomenclature UbH will be used.

The majority of work on integrated UbH proteins has focused on the UbH-UBA proteasome shuttle factors. Dsk2 and Rad23 simultaneously interact with the proteasome and ubiquitin chains, through their UbH and UBA domains respectively (Schauber et al., 1998, Wilkinson et al., 2001, Saeki et al., 2002). These proteins can protect ubiquitylated proteins from DUBs (Raasi and Pickart, 2003, Ng et al., 2003) and are essential for the degradation of a number of proteins (Verma et al., 2004). Rad23 is also involved in transcription-coupled nucleotide excision repair (TC-NER), independently of its UBA and UbH domains (see 1.4.2.2).

In metazoa, the majority of USP family DUBs contain UbH domains (Zhu et al., 2007). These domains do not share a common role (Faesen et al., 2012). In USP7/HAUSP two of the five UbH domains bind to the active site increasing the affinity for ubiquitin and the DUBs catalytic activity (Faesen et al., 2011), whereas

USP4 is catalytically inhibited by its UbH domain (Luna-Vargas et al., 2011). The N-terminal UbH in hUSP14 has no direct role on catalysis, but does help recruit the protein to the proteasome (Peth et al., 2009), whereas the equivalent yeast protein, Ubp6, is not recruited through its UbH domain (Rosenzweig et al., 2012).

UbH domains can bind to UBDs (Walters et al., 2003, Chartron et al., 2012). Apart from Rad23, these interactions are typically of much higher affinity than Ubi-UBD interactions; the normal Ubi-UBD hydrophobic contacts are aided by extra hydrogen bonding and electrostatic interactions (Chartron et al., 2012, Zhang et al., 2009).

Alternatively, UbH proteins interact via domains that do not usually bind Ubiquitin. These can bind to the normal hydrophobic patch on the UbH (Hanzelmann et al., 2010) or to an alternate position on the ubiquitin superfold (Pacold et al., 2000, Lowe et al., 2006). For example, the human UbH elongation factor Elongin B (see 1.3.1.2), binds to its interaction partner, Elongin C, via the β-sheet back face of the ubiquitin superfold (Brower et al., 1999, Babon et al., 2008). This interaction leaves the hydrophobic patch free and allows the formation of a stable heterodimeric complex (Kiel and Serrano, 2006).

1.1.6 Partial proteasomal processing

Proteasomes are extremely efficient at digesting substrate protein to short 5-20 residue peptides (Lee et al., 2001a). However, some studies have identified a small number of proteins that escape total degradation upon targeting to the proteasome, which are instead partially proteasomally processed.

Only 8 partially proteasomally processed proteins have been identified to date (Figure 1.4). In the early 1990s the p50 subunit of NF- κB1 was found to be formed, post translationally, from the full-length p105 precursor in an ATP and proteasome-dependent manner (Fan and Maniatis, 1991, Palombella et al., 1994) (Moorthy et al., 2006). The NF-κB2 subunit, p55, was also identified to be processed, from full-

length p100 protein (Xiao et al., 2001), as were the yeast homologs of NF-κB, Spt23 and Mga2 (Hoppe et al., 2000, Shcherbik et al., 2003). Fascinatingly, the NF-κB1 p105 protein can also be processed when expressed in yeast cells (Palombella et al., 1994, Kravtsova-Ivantsiv et al., 2009), a testament to the conserved nature of the processing reaction. Spt23 is processed from a p120 membrane-tethered fragment to a number of different protein fragments with a molecular weight of around 50 kDa (Hoppe et al., 2000). Transcription factors Curbitis interuptus (Ci; Aza-Blanc et al., 1997); its vertebrate homologs, Gli2 and Gli3 (Pan et al., 2006b, Wang et al., 2000); and mammalian specificity protein 1 (Sp1; Su et al., 1999) are also partially proteasomally processed.

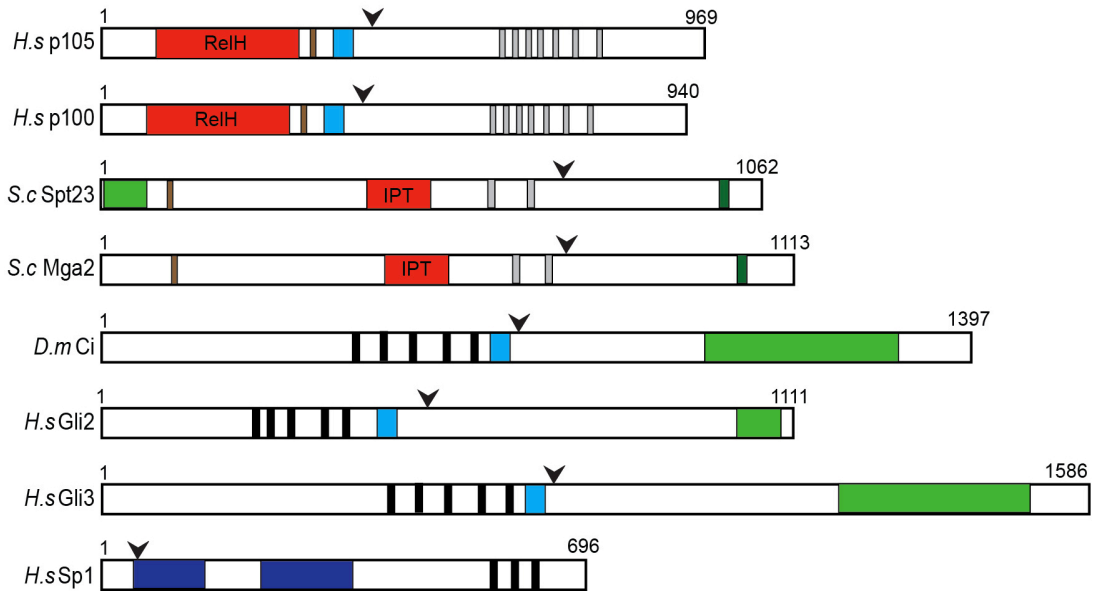

Figure 1.4: Schematic of the partially proteasomally processed proteins identified to date

Depicted proteins are to scale. An arrowhead identifies the approximate site of processing (note that this is highly dynamic). Domains are coloured as follows; red, rel homology/IPT domains; light blue glycine rich (GRR) or low complexity region; grey, ankyrin repeats; dark green, transmembrane regions; light green, transactivation domains; brown, NLS; dark blue, glutamine rich.

Whilst all the processed proteins identified to date have been transcription factors, the outcome of the processing reaction differs. NF-κB and its homologs, Spt23 and Mga2, are activated by the proteasomal degradation of their C-termini. The removal of the C-terminal ankyrin repeat regions of NF-κB exposes a nuclear localisation signal (NLS) (Orian et al., 1999). Spt23 and Mga2 are both ER-membrane bound

and processing liberates the proteins, allowing them to translocate into the nucleus (Hoppe et al., 2000, Rape et al., 2001, Hitchcock et al., 2001). Proteasomal processing, however, negatively regulates Ci and Sp1. Processing of Ci removes the transactivation domain, converting the DNA binding p75 fragment to a repressor (Aza-Blanc et al., 1997).

Twenty years of mechanistic studies of partial proteasomal processing has helped to elucidate the biochemistry of both partial and total protein degradation by the proteasome. The current model of partial proteolytic processing consists of two steps: proteasome-initiated cleavage and (bi-directional) degradation up to a blocking 'stop-transfer signal' (Lin and Ghosh, 1996, Piwko and Jentsch, 2006). The cleavage step requires proteasome recognition and an initiator site, which can be spatially removed from the final processed site (Schrader et al., 2009, Inobe et al., 2011). Initiator sites are thought to occur at unfolded regions of low complexity, close to the site of ubiquitylation (Prakash et al., 2004, Inobe et al., 2011), which may be inside the protein (Piwko and Jentsch, 2006, Liu et al., 2003). Internal initiation site usage appears to favour incomplete proteolysis (Kraut and Matouschek, 2011).

Proteasome recognition is principally mediated through ubiquitylation (Palombella et al., 1994, Inobe et al., 2011). Ubiquitin was directly shown to be required in extract-based *in vitro* reactions for p105 processing (Palombella et al., 1994, Orian et al., 1995, Sears et al., 1998) and lysines at the C-terminus of p105 are crucial for processing *in vivo* (Orian et al., 1999). Despite the frequent observation of poly-ubiquitin chains on processed proteins (Orian et al., 1999, Hoppe et al., 2000, Shcherbik et al., 2003), only mono-ubiquitylation is required for processing (Kravtsova-Ivantsiv et al., 2009, Rape et al., 2001). Ubiquitin remains attached to Spt23 and Mga2 after proteasomal processing, but it is not found on the partially processed proteins of higher eukaryotes, possibly due to the removal by proteasome associated DUBs during processing.

Partially processed proteins differ from normally degraded proteins in their ability to block the proteasome after the initiation of degradation. The cleaved C-terminal fragment has not been detected in any of the native processed proteins, suggesting

efficient complete proteasomal degradation of this section (Piwko and Jentsch, 2006). The N-terminal fragment is rescued by a stop-transfer signal that prevents the proteasome from completing degradation. In higher eukaryotes the stop-transfer signal is formed by the combination of a tightly folded domain followed by a simple low complexity region (Tian et al., 2005) (Figure 1.4). Low complexity regions have reduced coupling between nucleotide hydrolysis and substrate unfolding (Bachmair and Varshavsky, 1989, Daskalogianni et al., 2008). It is therefore conceivable that the combination of the 19S-resistant, stable domain allows the poorly bound low-complexity region to diffuse away from the proteasome mid degradation. Intriguingly, the transcription factor Sp1 lacks any recognisable components of this bi-partite stop signal (Figure 1.4). However, Sp1 does have glutamine rich regions (Roos et al., 1997), which significantly reduce the processivity of the proteasome (Kraut et al., 2012).

In *S. cerevisiae* the stop signal does not seem to require a region of low complexity. The IPT domain of Spt23 is required for processing and this domain forms very stable (resistant to up to 2.5M NaCl washing) homo-dimers (Rape et al., 2001). These dimerization domains are thought to block the proteasome, but do not have a simple coding sequence after them. In agreement with this observation, whilst normal p105 processing is observed upon expression in *S. cerevisiae*, this is not prevented by deletion of the GRR (Sears et al., 1998), which is absolutely required in mammalian cells (Lin and Ghosh, 1996). The observed discrepancy may be due to the inherent lower processivity of yeast proteasomes (Kraut et al., 2012).

Critically, the distance between the stop-transfer signal and newly formed C–terminus of the protein is not fixed, and can be altered by internal deletions around the proposed cleavage site (Sears et al., 1998, Lin and Ghosh, 1996, Piwko and Jentsch, 2006). However, the distance between the proteasome recognition signal and the initiator signal (Inobe et al., 2011) is crucial, as is the distance and orientation between the low complexity region and the tightly folded domain (Tian et al., 2005). The exact processing site for all processed proteins, bar Sp1, has not been identified (Su et al., 1999).

1.2 Nuclear Transport

The nucleus is the primary defining organelle of the eukaryotic cell, which spatially separates the coding DNA from protein translation and effector functions. As many nuclear processes require protein catalysts, import and export is required between the nucleus and cytoplasm.

The nucleus is encompassed by a phospholipid bilayer termed the nuclear membrane. The bilayer is punctuated by numerous aqueous channels, termed nuclear pore complexes (NPCs). Ions, small molecules and proteins <40kDa can freely diffuse through the NPC (Bonner, 1975), whereas RNA and larger proteins require the assistance of nuclear transport factors.

No ATP-driven subunits are part of the NPC. Nuclear transport is instead promoted by the relative affinities and concentrations of transport molecules on either side of the nuclear membrane (reviewed in Aitchison and Rout, 2012). The direction of transport is mediated through the interaction of karyopherins with Ran GTPase (Gsp1 in yeast). The GTP hydrolysis activity is spatially separated over the nuclear membrane. In the nucleus, Ran is maintained in a GTP-bound state, by the Ran guanidine exchange factor (GEF), Srm1 (Akhtar et al., 2001). In the cytoplasm, the Ran GTPase Activating Protein (GAP) Rna1 promotes the hydrolysis of GTP to GDP (Becker et al., 1995). As a result, transiting Gsp1 is interconverted on opposite sides of the nuclear membrane (Figure 1.5). Indeed, the direction of nuclear transport can be reversed by inverting the Ran gradient (Nachury and Weis, 1999).

1.2.1 Karyopherin family

All nuclear carrier proteins identified to date are part of the karyopherin family. Karyopherins are typically large with only around 20% sequence identity, but contain multiple, 50-residue HEAT repeats (Andrade et al., 2001). Most members resemble importin-β (Kap95), whereby each HEAT repeat forms two antiparallel

stacking α-helices, which assemble into a banana shaped structure (Xu et al., 2010).

14 karyopherins have been identified in yeast (Strom and Weis, 2001). The karyopherins principally involved in import are called importins. Conversely, export proteins are termed exportins and those implicated in two-way traffic are called transportins. The substrates and direction of travel for most karyopherins remain unclear. Karyopherins, except for Kap60, bind to their cargo directly, and this is the rate-limiting step in nuclear transport (Timney et al., 2006). Karyopherins are, by necessity, promiscuous and utilise multiple binding interfaces (Lee et al., 2003), sometimes used simultaneously (Hodges et al., 2005). There is redundancy between karyopherins: Kap123 mediates ribosome import but cells lacking this import factor utilise Kap121 (Rout et al., 1997). There are reports of proteins that can traverse the NPC without the aid of karyopherins and/or Gsp1 (Yen et al., 2001, Hanover et al., 2007), possibly via direct contact with NPC components.

1.2.2 Nuclear transport signals

Despite the large number of karyopherin proteins identified, only four nuclear targeting signals have been identified. The classical nuclear localisation signal (NLS) is the best-characterised nuclear targeting signal and comes in two flavours - mono-partite and bi-partite - both of which bind Kap60 (importin-α), and Kap123 (Kalderon et al., 1984, Hodel et al., 2001, Robbins et al., 1991). Only 57% of nuclear proteins in yeast contain an identifiable classical NLS (Lange et al., 2007).

The study of nuclear export has lagged behind nuclear import. The classical nuclear export signal (NES) was originally identified as a leucine rich motif in the human Protein Kinase A inhibitor (Wen et al., 1995). The NES is an extremely degenerate 15-residue peptide, with 4 hydrophobic residues regularly spaced. Over 200 proteins in yeast contain a variant of this motif, which binds directly to the exportin Xpo1/Crm1 (reviewed by Hutten and Kehlenbach, 2007, Figure 1.5). This hydrophobic-rich sequence only describes 40% of the known peptide signals that

can target nuclear export (Kosugi et al., 2008). Crm1 can also promote the nuclear export of non-NES containing proteins (Macedo-Ribeiro et al., 2009, Chan et al., 2011). Whilst the majority of nuclear export is mediated through Crm1, a number of proteins accumulate in the nucleus in strains defective for Crm1 (Maurer et al., 2001).

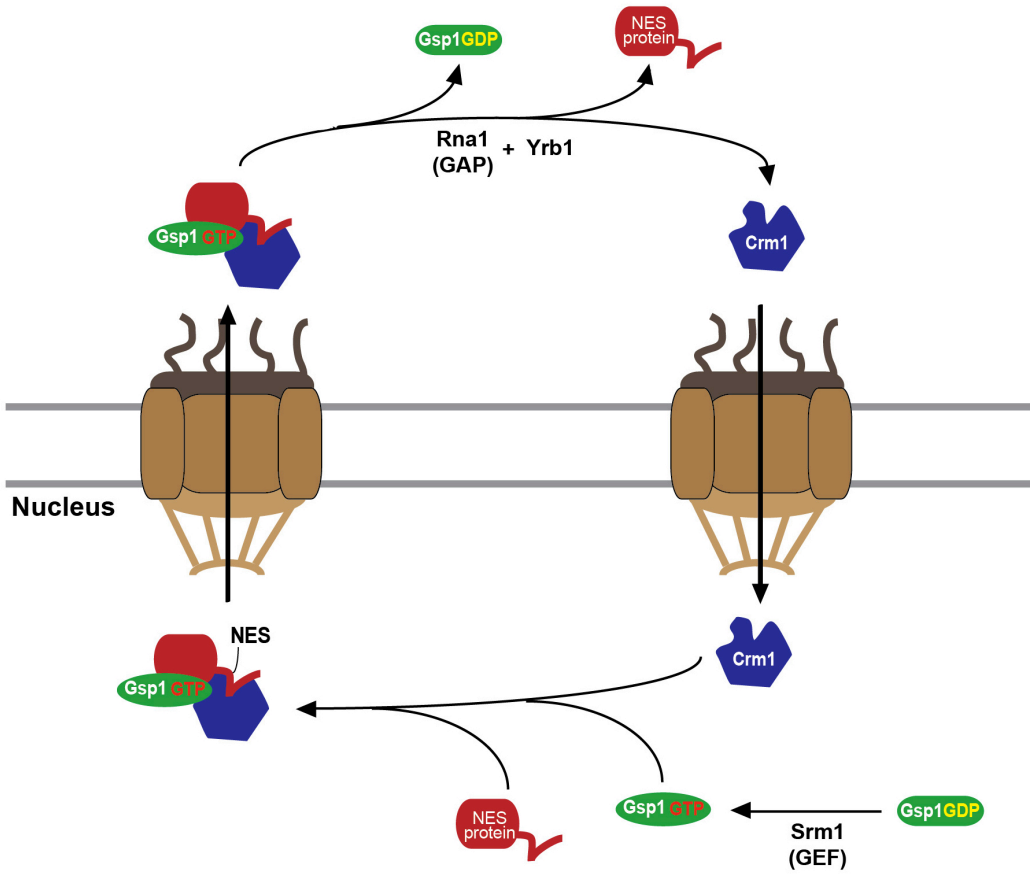

Figure 1.5: The classical nuclear export of proteins

The outside surface of Crm1 binds directly to the hydrophobic NES peptide, which induces the co-operative binding of Gsp1-GTP (Hutten and Kehlenbach, 2007, Dong et al., 2009). The complex transfers through the pore in a similar manner to other karyopherins, through interactions with NPC FG repeat proteins. Unlike import, GTP hydrolysis inefficiently promotes dissociation of the Crm1-Gsp1-cargo complex, which is aided by Yrb1 (Kunzler et al., 2001).

Despite early success with the well defined nuclear targeting signals outlined above, the other motifs have proved to be more degenerate: typically described instead by physiochemical rules, rather than an exact sequence pattern (Xu et al., 2010). Unlike other sub-cellular targeting signals found in the cell, nuclear targeting occurs

in the context of fully folded proteins. As a result, the dogma of short peptide signalling sequences is likely the exception rather than the rule. The karyopherins, Cse1 and Los1 specifically recognise the entire conformation of their targets - Kap60 and tRNA respectively (Matsuura and Stewart, 2004, Cook et al., 2009). In yeast up to 2000 proteins shuttle through the nuclear pore, yet the mechanism for this transport has been identified for only a handful of these proteins (Aitchison and Rout, 2012).

The shuttling protein need not necessarily have a transport signal, as mediator proteins could help specify subcellular localisation. This is often the case for the nuclear import of large complexes. Fully formed 12-subunit RNAPII is recognised by the NLS containing protein, Iwr1, which targets the complex for nuclear import (Czeko et al., 2011).

1.2.3 Control of nuclear localisation

Dynamic compartmentalisation, altering the subcellular localisation of a cargo protein, is an elegant method of regulation. This can be mediated through post-translational modification of transport signals, altering karyopherin binding (Harreman et al., 2004). For example, Kap121 imports the phosphate response transcription factor Pho4 into the nucleus when phosphate is limiting. When phosphate levels are restored, Pho4 is phosphorylated within its NLS, preventing Kap121 binding, and creating an Msn5 recognition site, promoting Pho4 export (Komeili and O'Shea, 1999, Kaffman et al., 1998).

Alternatively, proteins can be tethered to prevent their relocalisation (see discussion on Spt23 and Mga2 in 1.1.6; Hoppe et al., 2000). Nuclear pore components themselves can be phosphorylated, altering the permeability of the nucleus to numerous proteins (Makhnevych et al., 2003). Interestingly, a number of proteins accumulate in the nucleus upon transcription inhibition, as they are commonly exported with mRNA (O'Hagan and Ljungman, 2004, Lee et al., 1999b).

SUMOylated-PTEN and the small ribonucleotide reductase subunits, Rnr2 and Rnr4, relocalise to the cytoplasm after DNA damage (Bassi et al., 2013, Yao et al., 2003, Lee et al., 2008). A whole proteome study recently identified the translocation of around 100 proteins between the nucleus and cytoplasm as a response to DNA damage (Tkach et al., 2012). The induced transit mechanism for most of these proteins is unclear.

1.3 Transcription

In 1958 Francis Crick defined what is now known as the central dogma of biology: DNA is transcribed to RNA, which is then translated into an effector protein (Crick, 1958). A highly conserved, DNA-dependent, RNA polymerase catalyses the transcription stage in this process. In eukaryotes three RNA polymerases account for transcribing ribosomal RNA (rRNA), messenger RNA (mRNA) and transfer RNA (tRNA), respectively. RNAPII - responsible for transcribing mRNA - is arguably the most important and highly regulated of these.

RNAPII is a complex of 12 subunits; named Rpb1-Rpb12. Numerous structural studies of RNAPII have revealed the subunit architecture and catalytic mechanism of the transcription cycle (Gnatt et al., 2001, Cramer et al., 2001, Kettenberger et al., 2004, Cheung et al., 2011, Liu et al., 2013) (Figure 1.6 A). DNA is clamped between the upper jaw (comprised of Rpb1 and Rpb9) and lower jaw (chiefly Rpb5) (Gnatt et al., 2001). Roughly 18 bp of DNA is unwound at the upstream fork loop of Rpb2, and the non-transcribed strand (NTS) lies on the outside of the protein complex (Gnatt et al., 2001). The rudder and lid structures dissociate the 8-9 bp DNA-RNA hybrid, positioning RNA into a separate exit channel (Figure 1.6 B). The RNAPII active site is in the centre of the complex, formed between Rpb1 and Rpb2, and traversed by the bridge helix (Figure 1.6 B). RNAPII moves by a Brownian

ratchet mechanism, indirectly powered by the energy of RNA polymerisation (Bar-Nahum et al., 2005, Liu et al., 2013).

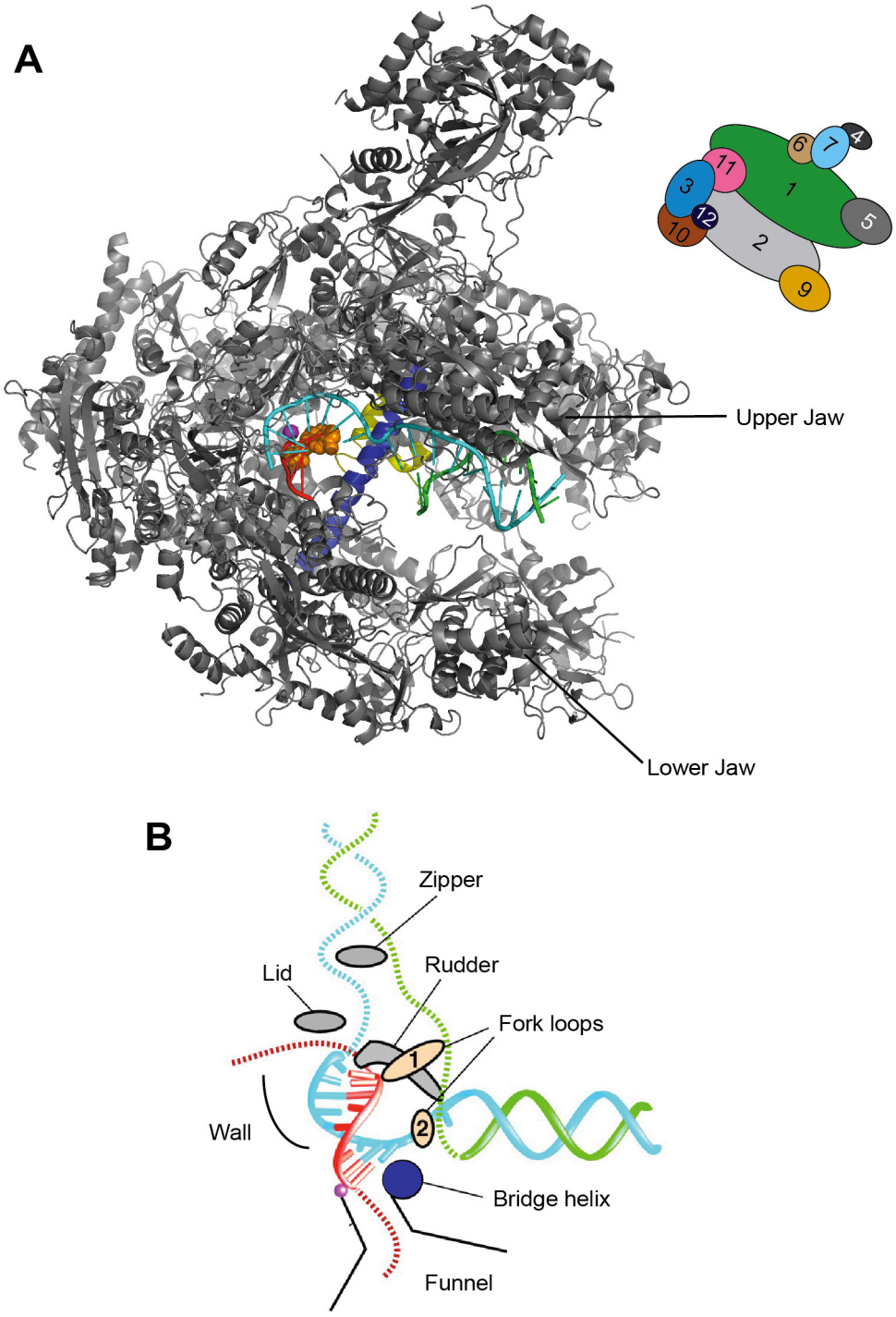

Figure 1.6: The RNAPII elongation complex

A. Overview of the RNAPII elongation complex (taken from Cheung et al., 2011; pdb 4A3F). Structure shows Transcribed strand (TS), cyan; Non-transcribed strand (NTS), green; 4 bp of RNA, red; Magnesium ion, purple; and bound NTP, orange. The key active site features of the trigger loop (navy blue) and bridge helix (yellow) are highlighted. Subunit position shown on the right, Rpb8 is behind the complex. Inspired by Kettenberger et al., 2004.
B. RNAPII catalytic center and transcription bubble. Features coloured as above. Modified from (Gnatt et al., 2001).

1.3.1 Transcription elongation

Many significant control steps take place during the production of mRNA concurrently with transcription elongation. The process of polymerisation is extremely processive. RNAPII transcription can continue for Mega bases: the human dystrophin gene is 2.3 Mbp long and takes around 16 hours to transcribe (Tennyson et al., 1995). Average transcription rates *in vivo* range from 1.5-4 kbp/min, dependent on species (Singh and Padgett, 2009), with reported speeds of up to 50 kbp/min (Maiuri et al., 2011). This discrepancy is not due to a change in the catalytic rate of RNA polymerisation but because RNAPII transcription is not a smooth continuous process, with many stochastic pauses and stalls.

1.3.1.1 Transcription pause and stall

Early footprinting and single-particle studies revealed frequent pausing and stalls of RNAPII during transcription (Krummel and Chamberlin, 1992, Zhou et al., 2013). RNAPII transcription elongation can be defined by periods of fast productive RNA polymerisation, interspersed with short pauses and arrests (Figure 1.7). One consequence of the rapid Brownian-ratchet motion of RNAPII transcription is the potential for reverse movement of the polymerase (termed backtracking)(Nudler, 2012). In an arrested, backtracked off-pathway state, the 3'hydroxyl-end of the RNA chain is displaced from the RNAPII active site, thus preventing forward catalysis. Whilst pauses do not always involve backtracking (Toulokhonov et al., 2007), a pause is converted into an arrest the longer a polymerase is in the non-productive state (Gu and Reines, 1995). Over 200,000 yeast genomic sites reproducibly lead to RNAPII pausing *in vivo*, of which 75% are backtracked (Churchman and Weissman, 2011).

The probability of pausing or stalling is partially dependent upon the transcribed sequence: A-T rich regions are hard to transcribe (Hawley et al., 1993, Tornaletti et al., 2008), leading to de-stabilisation of the RNA-DNA hybrid and reversal of the RNAPII (Nudler et al., 1997). RNAPII stall can also be due to the topology of the transcribed DNA (Garcia-Rubio and Aguilera, 2012). Backtracking is not just an off-pathway state; it is part of the RNAPII fidelity mechanism, which is promoted after mis-incorporation of a nucleotide (Nudler, 2012). Interestingly, the stronger a promoter is, i.e. the more RNAP is loaded onto a promoter, the faster the overall rate of transcription (Epshtein and Nudler, 2003). This can be partly explained through a de-chromatinisation of the template (Bintu et al., 2011), but also due to the co-operative effect of trailing polymerases pushing paused, leading RNAPII (Saeki and Svejstrup, 2009).

DNA must be compacted in order to fit into the nucleus. The most basic unit of chromatin compaction is the nucleosome, an octomer comprised of 2 copies each of Histone H3-H4 and H2A-H2B. Chromatin can pose a significant block to DNA processes, including transcription. However, the rate of transcription observed *in vivo* is similar to that reported *in vitro* on naked plasmid DNA (Singh and Padgett, 2009, Izban and Luse, 1992a). Moreover, transcription *in vitro* is severely inhibited by poly-nucleosomal DNA (Orphanides et al., 1998). *In vitro*, nucleosomes promote backtracking of RNAPII (Kireeva et al., 2005), which can be reversed by a trailing polymerase (Jin et al., 2010). Chromatin remodellers, histone chaperones, histone modifying proteins and transcript cleavage factor TFIIS (see below) can aid the inefficient transcription through nucleosomes *in vivo* (reviewed in Selth et al., 2010)
.

1.3.1.2 Basal Elongation factors

A whole host of protein factors assist in promoting efficient transcription elongation (Figure 1.7). Cells deleted for elongation factors are sensitive to RNAPII elongation inhibitors such as 6-azauracil (Hartzog et al., 1998). General elongation factors work in one of two ways, either by limiting the occurrence of RNAPII pauses or by

helping to rescue stalled RNAPII. A few relevant elongation factors are described below.

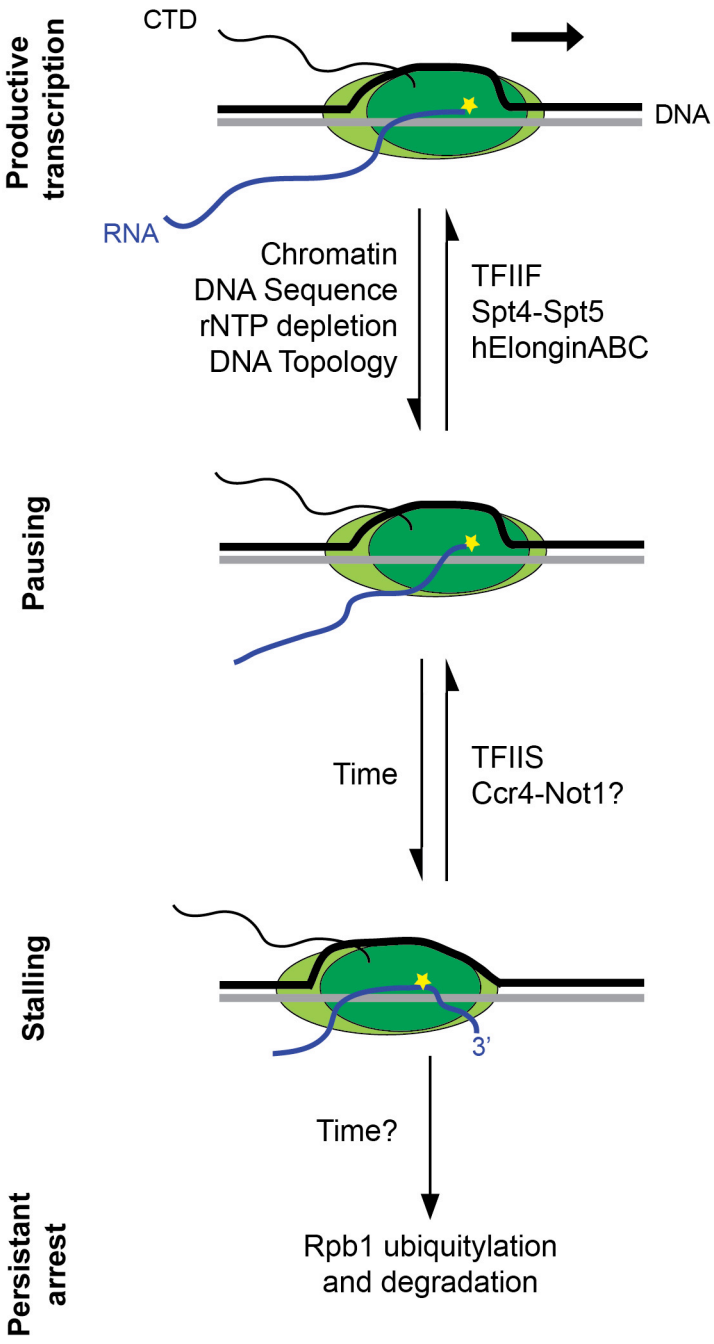

Figure 1.7: Schematic of RNAPII transcription elongation and backtracking

RNAPII shifts from productive transcription to off-pathway states. The factors that bias the equilibrium between states are named. RNAPII complex depicted in green, with the largest subunit Rpb1 depicted in dark green, active site depicted by a yellow star.

TFIIS shortens the length of stalls *in vivo* (Bengal et al., 1991), and can promote the read-through of difficult to transcribe sequences and DNA binding proteins blockages (Reines et al., 1992). The re-alignment of the 3' hydroxyl end of RNA, into the active site, is achieved through a weak intrinsic cleavage ability of RNAPII (Sigurdsson et al., 2010), which is drastically promoted by TFIIS (Izban and Luse, 1992b).

The mammalian Elongin ABC heterotrimer reduces the frequency of RNAPII pausing (Bradsher et al., 1993, Aso et al., 1995) through an unknown mechanism. Elongin A is the transcriptionally active subunit (Aso et al., 1996), which is partially redundant with the initiation and elongation factor TFIIF (Moreland et al., 1998). Elongin A is required for proper morphogenesis (Gerber et al., 2004, Yasukawa et al., 2012) and transcription in response to stress (Kawauchi et al., 2013). The Elongin C and Elongin B regulatory sub complex shares homology with Skp1 and ubiquitin respectively (Aso et al., 1995), and can form CRLs (Duan et al., 1995; see 1.5.3.2). The ubiquitin ligase and elongation features of the Elongin ABC complex can be separated (Yasukawa et al., 2012).

Clear Elongin A and Elongin C homologs have been identified in yeast, termed Ela1 and Elc1 (Aso and Conrad, 1997). However, no UbH domain-containing Elongin B homologue has been identified in *S. cerevisiae*. The Ela1-Elc1 dimer does not have any elongation stimulation activities (Koth et al., 2000), but can form an active ubiquitin ligase (Harreman et al., 2009).

1.3.1.3 Rpb1 CTD modifications

The largest subunit of RNAPII, Rpb1, contains a long C-terminal extension, thought to project away from the RNAPII complex (Meinhart and Cramer, 2004). The CTD consists of a heptapeptide sequence, Y-S-P-T-S-P-S, repeated 26 (yeast) or 52 (human) times (Liu et al., 2010). All 7 residues can be modified during transcription: the prolines are isomerised between *cis* and *trans* states and the hydroxyl groups

of serine, threonine and tyrosine are phosphorylated (reviewed recently by (Heidemann et al., 2013).

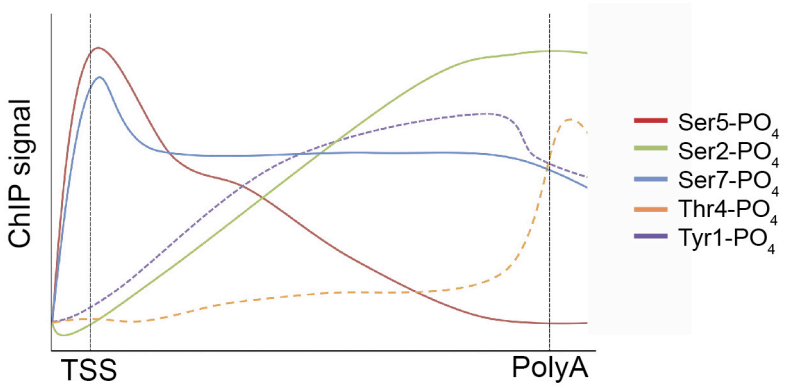

Figure 1.8: The CTD Phosphorylation cycle over a gene

Adapted from Heidemann et al., 2013, a representation of ChIP data from (Mayer et al., 2010) and (Mayer et al., 2012) and (Hintermair et al., 2012) Ser-5 and Ser-7 phosphorylation peak at the transcription start site (TSS). Phosphorylation of Ser-2 is the principle mark present during transcription elongation. Tyr-1 phosphorylation is concurrent with Ser-2 phosphorylation until the termination region, whilst Thr-4 phosphorylation peaks after the polyA signal.

The CTD is a regulatory platform, modulated by the CTD phosphorylation state (Figure 1.8). A wide variety of kinases, phosphatases and isomerases modify Rpb1's CTD during transcription, ensuring the correct recruitment of RNA processing factors, elongation factors and termination factors at their appropriate stages. There is significant cross-talk between the modifications, allowing bivalent marks to be recognised on adjacent repeats at specific transcription stages (Egloff et al., 2010, Ghosh et al., 2011).

1.3.2 Role of ubiquitin and the proteasome in transcription

In order to ensure a transient signal for transcription, many transcription factors are poly-ubiquitylated and short-lived (Meimoun et al., 2000, Salghetti et al., 2000). Mono-ubiquitylation is also important to activate a number of transcription factors *in situ* (Salghetti et al., 2001). Moreover, ubiquitylation can be required to activate a

transcription factor, upstream of transcription (Hoppe et al., 2000; see 1.1.6). Furthermore, ubiquitylation can directly affect RNAPII transcription: the Rpb1 and Rpb2 subunits are targeted by the E3 ligase Asr1, which leads to the ejection of Rpb4 and Rpb7 and RNAPII inactivation (Daulny et al., 2008).

Ubiquitylation of chromatin is essential for transcription elongation; H2B is mono-ubiquitylated at lysine 120 (Hwang et al., 2003) and this disrupts chromatin compaction (Fierz et al., 2011), as well as helping to recruit the numerous chromatin-modifying enzymes (Sun and Allis, 2002, Krogan et al., 2003). Efficient transcription requires the dynamic addition and removal of H2B ubiquitylation, by Rad6-Bre1 and Ubp8/Ubp10 respectively (Hwang et al., 2003, Wyce et al., 2007, Emre et al., 2005)

Proteolytic and non-proteolytic functions of the proteasome are used at active genes (reviewed by Geng et al., 2012). Genome-wide ChIP identified the genomic association of the proteasome with transcription (Auld et al., 2006). The proteasome co-immunoprecipitates with transcribing RNAPII and its proteolytic activity is important for the normal clearing of RNAPII from yeast termination regions (Gillette et al., 2004), but does not seem to be important *in situ* in other organisms (Scharf et al., 2011). The proteasome 19S particle has non-degradative roles in transcription initiation and elongation (Gonzalez et al., 2002, Ferdous et al., 2002). The 19S regulatory particle appears to be particularly important in transcription during stress conditions (Sulahian et al., 2006), possibly as the 19S alters chromatin by promoting histone acetylation (Lee et al., 2005).

1.4 DNA Damage and DNA Damage Repair Pathways

1.4.1 Types of DNA damage

DNA forms the basic inheritable genetic material of the cell. In an aqueous environment, the large, negative charged phosphate backbone prevents spontaneous hydrolytic cleavage, ensuring chemical stability. Nevertheless, endogenous damaging sources account for upwards of 10,000 chemical alterations on DNA each day, in a single mammalian cell (Lindahl and Wood, 1999, Ciccia and Elledge, 2010). This endogenous DNA damage can form as a by-product of normal cellular respiration, or base degradation and replication errors. On top of this background damage, exogenous sources of damage add to the damage load (Ciccia and Elledge, 2010).

The DNA double helix can be altered relatively harmlessly, from small chemical addition, up to the extremely toxic breakage of both strands, with a concomitant increase in risk of genetic loss. One potentially hazardous exogenous source of DNA damage is ultra-violet (UV) light. DNA absorbs UV-B light directly resulting in infrequent chemical cross-linking between adjacent thymines or cytosines, creating cyclopyrimidine dimers (CPDs), or less commonly, pyrimidine 6–4 pyrimidone photoproducts (6-4 photoproduct). CPDs and 6-4 photoproducts alter the normal conformation of DNA by 9^{o} and 44^{o} respectively (Kim et al., 1995, Lee et al., 1999a). Bulky aromatic chemical lesions can also perturb the structure of DNA (Kohda et al., 1991).

Mutation occurs when DNA damage remains unrepaired before DNA replication. The altered chemistry of the deoxyribose base often leads to the mis-incorporation of an incorrect base opposite the lesion. Alternatively, the repair pathways elicited are mutagenic themselves (Stallons and McGregor, 2010). One of the more immediate effects of DNA damage, often overlooked, is to sterically interfere with DNA-dependent processes, such as replication and transcription.

1.4.2 Repair of DNA damage

Multiple pathways with overlapping specificity restore damaged DNA to its correct state. As a testament to the essential nature of these pathways the presence, if not the directly conserved proteins, are present in all domains of life. Most pathways directly recognise the lesion and remove the damage through excision and gap filling. As it is particularly relevant to the work of this thesis, the basic repair pathways for bulky helix distorting lesions will be outlined in the next sections.

1.4.2.1 Direct repair of DNA damage

The direct reversal of DNA damage is both rapid and accurate (reviewed by Sancar, 2000). *S. cerevisiae* Phr1 binds to a CPD lesion by recognising the characteristic bend towards the major groove, but is only activated upon chromophore-associated absorption of light. A photo-excited electron is transferred to the CPD, splitting the unstable cross-linked bond, restoring the original pyrimidine ring and the bases to their monomeric forms. A similar enzyme is found in *E.coli* (Sancar and Rupert, 1978), as well as a 6-4 photoproduct reversing lyase (Todo et al., 1993). Mammals lack these direct reversal enzymes (Li et al., 1993).

1.4.2.2 Global genome nucleotide excision repair (GG-NER)

NER is the most versatile DNA repair pathway; NER factors recognise structural deformities in normal B-form helical DNA, rather than specific DNA lesions. NER consists of 4 distinct steps: damage recognition, DNA unwinding around the lesion, incision either side of the damage and resynthesis of the single-stranded gap. Two pathways for NER exist, global genome-NER (GG-NER; covered here), and Transcription coupled NER (TC-NER; discussed in 1.5.2) (Figure 1.9).

In vitro NER dual incision reactions require just six factors (Guzder et al., 1995), but over 30 proteins have been implicated *in vivo* (see Table 1.2). All these factors may exist as a single ‘repairosome’ (Svejstrup et al., 1995, Kong and Svejstrup, 2002), or associate in a stepwise manner (Prakash and Prakash, 2000).

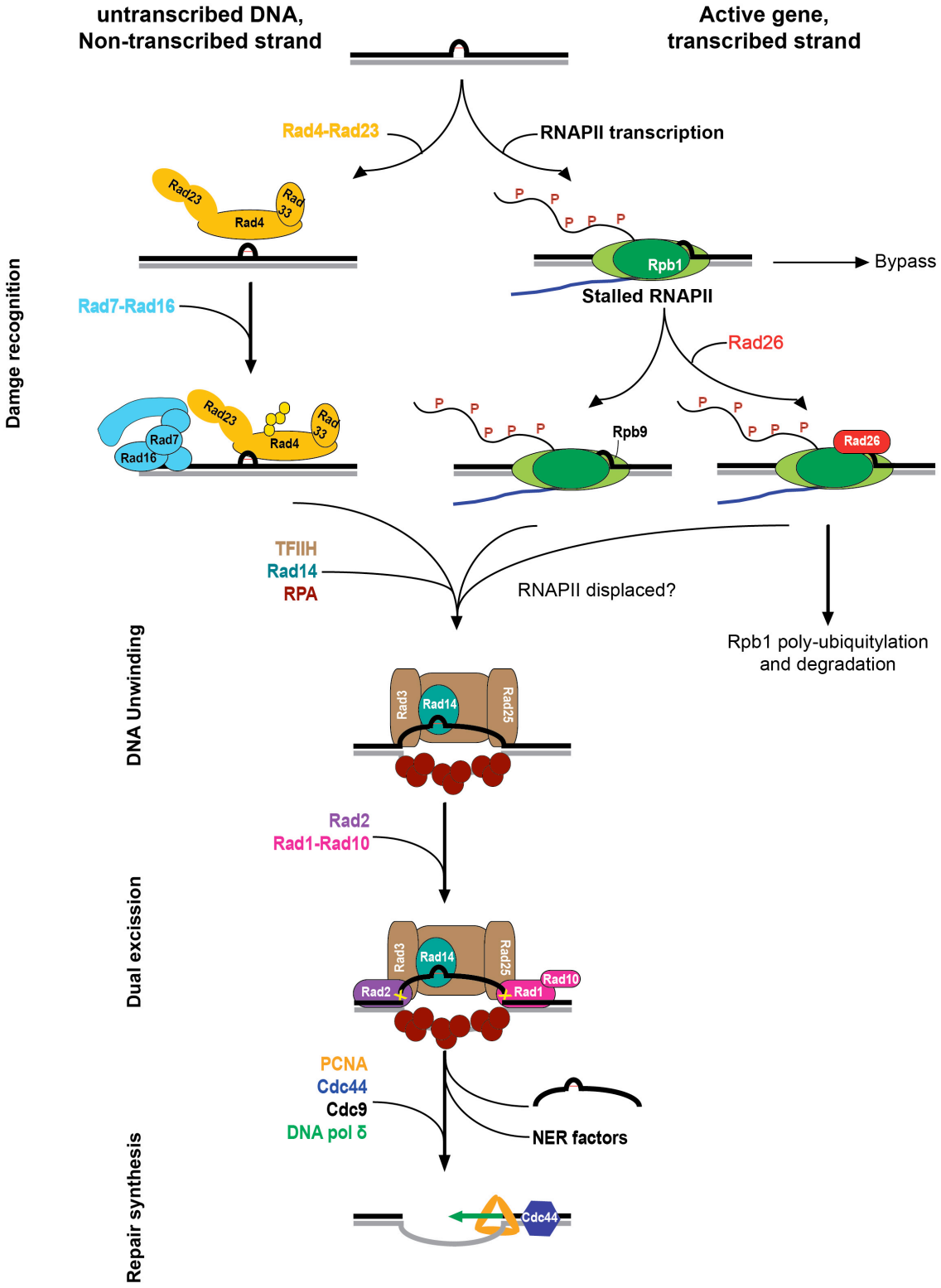

Figure 1.9: Schematic representation of Nucleotide excision repair pathways in yeast

Both GG-NER (left) and TC-NER (right) are represented. Key NER proteins are indicated. Not to scale. See text for detail.

Below, the molecular mechanism of NER is described, with emphasis on the yeast proteins. However, the mechanism and factors are conserved in all eukaryotes. The damage recognition components Rad7-16 and Rad4-23 bend DNA, facilitating binding of the Rad14 zinc finger protein to the lesion (Guzder et al., 1999, Min and Pavletich, 2007, Guzder et al., 2006). Rad4 helps to position TFIIH, signalling the commitment to excision (Sugasawa et al., 2001). The two helicases in TFIIH open up the DNA double helix, whilst the single-strand binding RPA heterotrimer coats the undamaged strand. Rad1-Rad10 and Rad2 are structure specific endonucleases, which are accurately positioned through their interaction with Rad14 (Guzder et al., 1996b) and TFIIH (Lafrance-Vanasse et al., 2012), respectively. The final gap-filling step has not been fully elucidated in yeast, but in human cells the clamp loader, PCNA, and DNA polymerase δ have been implicated, with final ligation catalysed by DNA ligase 1 (Mocquet et al., 2008).

Table 1.2: Yeast and human nucleotide excision repair proteins

Step	*S. cerevisiae*	*H. sapiens*	Function
Damage recognition	Rad7-Rad16	?	ATPase and ubiquitin ligase
	Abf1	?	DNA dependent ATPase with Rad7-16
	Elc1-Cul3	?	Ubiquitin ligase with Rad7-Rad16
	RNAPI	?	Stalls at site of damage?
	RNAPII	RNAPII	Stalls at site of damage
	Rad4-Rad23	XPC-HR23B	Binds damaged DNA
	Rad33/34	CEN2	Binds an protects Rad4-Rad23
	?	XPE-DDB2	Binds damaged DNA, ubiquitin ligase
DNA unwinding and recruitment	Rad14	XPA	DNA damage binding and verification
	Rfa1-3	RPA	ssDNA binding
	Rad3	XPD	5'-3' helicase (TFIIH subunit)
	Rad25	XPB	3'-5' helicase (TFIIH subunit)
	Rad26	CSB	DNA dependent ATPase (TC-NER)
	Rpb9	?	RNAPII subunit (TC-NER)
	Rad28?	CSA	Ubiquitin ligase (TC-NER)
Incision	Rad1-Rad10	XPF-ERCC1	5' endonuclease
	Rad2	XPG	3' endonuclease
Gap filling and ligation	Cdc44	RFC1	Clamp loader
	Dna Pol δ,ε	Dna Pol δ,ε	DNA replication
	Cdc9	DNA lig 1	DNA ligase
	PCNA	PCNA	Replication sliding clamp

Inactivating or attenuating mutations in components essential for the NER pathway in humans leads to the congenital autosomal recessive disorder Xeroderma pigmentosa (XP) (de Boer and Hoeijmakers, 2000). XP Patients are severely UV sensitive and have an increased risk of skin cancer. Mutations lie in 8 complementation groups, 7 of which are proteins of the NER pathway (XPA-XPG) (Table 1.2). Despite the high conservation between human and yeast NER, some important distinctions have been discovered (Boiteux and Jinks-Robertson, 2013). Whilst the majority of the identified NER homologs do appear to have homologous functions, there are no Rad7-Rad16 homologs in human cells. Similarly, the somewhat functionally related XPE-DDB2 factor does not appear to be present in yeast.

1.4.3 Signalling DNA damage/ The DNA damage checkpoint

Whilst repair of DNA is essential, uncontrolled enzymatic activity on DNA could be extremely harmful (Ciccia and Elledge, 2010). Multiple pathways exist to ensure correct spatial and temporal activation of repair enzymes.

Signalling is initiated from a broad range of sensing proteins that directly bind to DNA damage or repair intermediates. Often these are also part of the effector arm of the DNA damage response (DDR). In yeast the critical activator of the DDR is the PI3 kinase-related protein Mec1 (Pan et al., 2006a). Mec1 phosphorylates a large number of substrates (Albuquerque et al., 2008, Smolka et al., 2007), including downstream kinases Rad53 and Dun1 (Sweeney et al., 2005). Together these kinases promote damage specific transcription, block cell cycle progression, promote dNTP synthesis, and stabilise blocked replication forks (Segurado and Diffley, 2008, Zegerman and Diffley, 2010). Both GG-NER and TC-NER require Mec1 (Taschner et al., 2010).

1.4.3.1 Ubiquitin in DNA damage repair

Ubiquitin plays a key role in the repair of DNA damage, both as a signalling molecule and as a recruitment platform. Different ubiquitylation states of signalling molecules affect DNA repair pathway choice, through the recruitment of different effector proteins.

The trimeric sliding clamp protein, PCNA, binds to replicative DNA polymerases and aid their processivity; if the replication fork meets a blocking lesion then the fork stalls. Damage adjacent PCNA remains associated with DNA, and is marked by ubiquitylation at Lys 164 by Rad6 (E2) and Rad18 (E3) (Hoege et al., 2002, Daigaku et al., 2010). Mono-ubiquitylated PCNA is selectively recognised by components of trans-lesion polymerases (Bomar et al., 2007, Parker et al., 2007), which catalyse error-prone replication past DNA lesions as an alternative to DNA damage repair. PCNA poly-ubiquitylation is mediated by the Rad5 ubiquitin ligase, with the Lys-63 specific E2, Mms2-Ubc13 (Parker and Ulrich, 2009), leading to an error free, template switching, repair mechanism (Hoege et al., 2002).

Ubiquitylation plays a key role in NER. Elc1-Cul3-Rad7-Rad16 proteins form a complex that ubiquitylates Rad4 (Ramsey et al., 2004, Gillette et al., 2006), as well as other, unidentified, proteins. Whilst ubiquitylation eventually targets Rad4 for degradation, it is also important for its function. Rad23 may directly protect Rad4 from degradation (Ng et al., 2003), and is both an essential NER protein and a proteasome shuttling factor. Rad23 binds to Rad4 outside of both the UbH and UBD domains (Min and Pavletich, 2007) and the UBDs are dispensable for NER (Bertolaet et al., 2001). However, the UbH domain could help to recruit the 19S proteasome cap (Elsasser et al., 2002), which has a role in NER (Reed and Gillette, 2007). The NER and transcription complex TFIIH - via its Ssl1 subunit - can act as a ubiquitin ligase after DNA damage (Takagi et al., 2005b), although the target of this ligase is unclear.

The ubiquitin-mediated, inducible degradation of proteins is a critical step in the response to DNA damage. Degradation irreversibly shuts off dangerous damage repair pathways (Groisman et al., 2006). The key role of degradation of the largest

subunit of RNAPII, Rpb1, after stall at transcription lesion is the main subject of this thesis and covered in depth below (see section 1.5.3)

1.5 DNA Damage and Transcription

1.5.1 Transcription in the presence of DNA damage

The most immediate effect of DNA damage is not mutation, but creating a steric barrier to the normal reading of DNA. In the case of DNA replication a well-characterised Rad6-dependent pathway exists to bypass the lesion (see 1.4.3.1). The replication machinery is - by its very nature - dynamic and not stably associated with DNA, allowing polymerase exchange and DNA damage bypass. In contrast to replication, RNA polymerase cannot be dissociated from its template without loss of the transcript. RNA polymerases form very stable complexes on DNA (Kireeva et al., 2000, Dalal et al., 2006). This stability is both a blessing, ensuring high fidelity of long transcripts, but also a curse, as transcription can become blocked at DNA lesions (Svejstrup, 2007).

Upon UV irradiation transcription is rapidly halted in human cells (Mayne and Lehmann, 1982). UV-induced phosphorylation of free RNAPII prevents transcription initiation (Rockx et al., 2000, Heine et al., 2008). However, a specific transcription program is enacted in response to DNA damage. Microarray studies in *S. cerevisiae*, under a wide variety of cellular insults, found that around 20% of the transcriptome was altered, including many genes not implicated in DNA repair (Gasch et al., 2001). One branch of NER is reliant upon UV-induced new protein synthesis (Al-Moghrabi et al., 2003).

Small DNA lesions in the transcribed strand (TS) and most lesions in the NTS can be bypassed by RNA Polymerases (Zhou and Doetsch, 1993, Zhou et al., 1995).

Non-bulky, 8-oxoguanine and thymine glycol can inhibit or stall RNAPII transcription, but this can be overcome by general elongation factors (Charlet-Berguerand et al., 2006). Bulky, helix-distorting lesions force persistent RNAPII stall, either by steric hindrance or by directly inhibiting active site catalysis. UV induced CPDs, 6-4 photoproducts (Donahue et al., 1994), cisplatin adducts (Damsma et al., 2007), single strand gaps (Kathe et al., 2004), inter-strand cross-links (Jung and Lippard, 2006) and acetyl aminofluorine adducts (Donahue et al., 1996) all block RNAPII progression. In addition, smaller lesions may indirectly block RNAPII, through their high-affinity binding of DNA repair factors (Scicchitano, 2005).

Structural studies offer snapshots of RNAPII stalling at these lesions. A CPD causes stalling when it reaches the active site (Brueckner et al., 2007). Non-template adenine followed by a uridine can be fitted opposite the CPD, which remains permanently stuck. A recent study showed that a very slow and inefficient bypass of CPD lesions can occur *in vitro* and this may contribute to some resistance to UV irradiation *in vivo* (Walmacq et al., 2012).

Persistently stalled RNAPIIs act as direct sensors of damage. However, no surface conformational change is observed in crystal structures of RNAPII stalled at a lesion, arguing against this as a model for recruiting repair factors (Brueckner et al., 2007, Damsma et al., 2007). Direct RNAPII inhibition (Lee et al., 2002), rNTP depletion (Somesh et al., 2005) and endogenous transcription roadblocks (Hobson et al., 2012) can also induce persistent transcription stall, which may be indistinguishable from damage stalled RNAPII. In mammalian cells the DDR is activated upon transcription elongation inhibition, independent of DNA damage (Derheimer et al., 2007).

RNAPII stalled at a DNA lesion is extremely stable *in vitro* (t1/2~ 20 hours, Selby et al., 1997) and is now doubly dangerous: not only is transcription blocked at this gene, but the bulky RNAPII ternary complex also interferes with the normal DNA repair pathways. Mammalian RNAPII stalled at a CPD sterically blocks repair by a photolyase (Donahue et al., 1994). The cell has evolved two main mechanisms to cope with persistently stalled RNAPII: transcription coupled nucleotide excision

repair (TC-NER), and Rpb1 poly-ubiquitylation and degradation (Wilson et al., 2013).

1.5.2 Transcription Coupled-NER

TC-NER differs from GG-NER only in the recognition of the lesion; the basic lesion processing apparatus is the same (Figure 1.9). Unusually, the preferential repair of the transcribed strand was first observed in higher eukaryotes (Bohr et al., 1985), before *S. cerevisiae* (Terleth et al., 1989). RNAPII is the sensor of damage; repair is not only preferential for transcribed genes - which could be explained by increased chromatin accessibility - but also for the TS over the NTS (Sweder and Hanawalt, 1992). TC-NER is more rapid than GG-NER; lesions on the TS of a gene are repaired twice as fast as lesions on the NTS in yeast (Taschner et al., 2010). The principal UV photolesion, CPDs, are poorly recognised by GG-NER proteins (Sugasawa et al., 2001, Min and Pavletich, 2007). RNAPII engaged with DNA is a far better sensor of DNA damage than the Rad4 and Rad7-Rad16 complexes, which must first scan the entire genome slowly and peripherally (Lindsey-Boltz and Sancar, 2007).

TC-NER has two sub-pathways in yeast: one dependent upon Rad26 and the other on the non-essential RNAPII subunit, Rpb9. Rad26 was identified by sequence homology to the human TC-NER protein, Cockayne syndrome B protein (CSB) (van Gool et al., 1994) and is a DNA dependent ATPase (Guzder et al., 1996a). Both Rad26 and CSB contain a SNF2-like DNA helicase/translocase domain, but no observable helicase activity (Guzder et al., 1996a). Whilst cells lacking Rad26 are not sensitive to a number of DNA damaging agents (van Gool et al., 1994), *rad26Δ rad16Δ* cells are significantly more UV sensitive than *rad16Δ* single mutant cells (Verhage et al., 1996).

The exact role of Rad26 and CSB at damage-stalled RNAPII is still unclear. The *E. coli* homologue of Rad26, Mfd, directly displaces stalled RNAP away from DNA

(Selby and Sancar, 1993). In *S. cerevisiae*, Rad26 appears to be consistently associated with elongating RNAPII (Malik et al., 2010) and might even have some histone chaperone roles (Malik et al., 2012, Malik and Bhaumik, 2012). As a result, Rad26 could act as a general elongation factor and, in agreement with this hypothesis; Rad26 can promote elongation through 8-oxoguanine lesions (Lee et al., 2001b). In human cells CSB recruits NER factors and TFIIS in a stepwise manner (Fousteri et al., 2006), possibly through a chromatin modifying ability. Rad26 is dispensable for TC-NER near the promoter region of genes (Tijsterman et al., 1997) - where TFIIH is still resident after transcription initiation - possibly suggesting that Rad26's role is to recruit TFIIH to stalled RNAPII.

Intriguingly, overexpression of Rad26 can lead to increased repair of both TS and NTS strands (Bucheli and Sweder, 2004) and Rad26 has a role in the repair of repressed genes (Li et al., 2007). This effect may still be mediated through RNAPII, as antisense transcription is widespread throughout the genome (Xu et al., 2009b).

rad26Δ cells still have some residual TC-NER activity (Verhage et al., 1996), which can be attributed to a separate, Rpb9-dependent pathway (Li and Smerdon, 2002). The Rad26-independent pathway also involves the Rpb4 subunit, and is suppressed by the C-terminus of Spt5 and the Paf1 complex (Ding et al., 2010, Tatum et al., 2011). The contribution of each pathway is dependent upon the level of transcription and the position of the lesion within the gene (Li and Smerdon, 2002, Teng and Waters, 2000). The precise, molecular details of this pathway remain obscure.

In humans two autosomal-recessive diseases are directly linked to TC-NER, Cockayne syndrome (CS) and the milder UV sensitive syndrome ($UV^{S}S$). Most mutations leading to these syndromes map to Cockayne syndrome proteins CSA and CSB, and the recently discovered $UV^{S}SA$ protein (Hanawalt and Spivak, 2008, Nakazawa et al., 2012). The phenotype of patients is likely attributable to the roles of CSB and CSA in both repair and basal transcription (Gaillard and Aguilera, 2013). Multiple other accessory proteins have been implicated in the TC-NER pathway in mammals, including XAB2 (Kuraoka et al., 2008), HMGN1 (Birger et al., 2003), USP7 (Schwertman et al., 2012), and p300 (Datta et al., 2001).

Cockayne syndrome (CS) presents with severe developmental and neurodegenerative symptoms (Hanawalt and Spivak, 2008), but no cancer predisposition. Fibroblasts from CS patients cannot restart transcription after DNA damage and patients have mutations in CSA, CSB or TFIIH. The CSA protein forms a CRL complex with DDB2-CUL4a-RBX1 (Groisman et al., 2003, Fischer et al., 2011), which may ubiquitylate CSB at the end of TC-NER (Groisman et al., 2006). The direct sequence homologue of CSA in yeast is Rad28, which does not appear to play a role in TC-NER (Bhatia et al., 1996). $UV^{S}S$ is a less severe human syndrome, with patients displaying only mild UV sensitivity, but is similar to CS at the molecular level; mutations causing $UV^{S}S$ map to CSA, CSB and $UV^{S}SA$ (Spivak, 2005, Nakazawa et al., 2012)

It should be noted that genetic experiments performed in yeast on TC-NER are backed up by biochemical data, primarily using human proteins; however, a number of differences exist between the two systems (Boiteux and Jinks-Robertson, 2013). Even among the highly conserved proteins some obvious differences are clear. For example, yeast cells lacking Rad26 are not UV sensitive, but cells derived from CS patients cannot restart transcription after UV (Mayne and Lehmann, 1982) and are extremely sensitive to irradiation (van Hoffen et al., 1999). The damage sensing components of the GG-NER pathway are not required for TC-NER in humans, but in yeast, Rad4 is required for repair in the TS and TC-NER (den Dulk et al., 2006). A CSB/CSA-independent pathway has not been described in mammals to date.

1.5.3 Rpb1 poly-ubiquitylation and degradation

When the TC-NER pathway is either overloaded or unsuccessful, then an alternate and separate pathway is required to remove the stalled RNAPII and allow GG-NER repair factors access to the lesion. Treatment of mammalian cells with DNA damaging agents, such as cisplatin, results in the poly-ubiquitylation and

degradation of the largest subunit of RNAPII, Rpb1 (Bregman et al., 1996, Ratner et al., 1998, Mitsui and Sharp, 1999). At the time this was thought to be required for normal TC-NER, allowing Rpb1 to be removed from sites of damage, allowing access for TC-NER factors. Subsequent work in *S. cerevisiae* has shown that this degradation pathway is instead an entirely separate, more drastic 'last-resort' back-up pathway to failed transcription restart. Accordingly, TC-NER impairment leads to increased Rpb1 poly-ubiquitylation and degradation (Lommel et al., 2000, Woudstra et al., 2002, Chen et al., 2007).

Whilst originally identified as a response to DNA damaging agents that cause bulky lesions, Rpb1 poly-ubiquitylation and degradation occurs under all observed conditions of persistent RNAPII stall (Somesh et al., 2005, Anindya et al., 2007, Sigurdsson et al., 2010). Endogenous causes of stall, such as chromatin and *cis* transcribed sequence, do not lead to long arrests and are likely dealt with successfully by the help of elongation factors. However, if elongation factors are mutated, ineffective, or if RNAPII transcription elongation is otherwise inhibited, then RNAPII stalling persists. For example, treating human cells with the specific RNAPII elongation inhibitor α-amanitin leads to robust Rpb1 poly-ubiquitylation and degradation (Lee et al., 2002, Anindya et al., 2007). Similarly, depleting cellular rNTP pools with 6-azauracil (6-AU) promotes Rpb1 ubiquitylation in yeast (Somesh et al., 2005). Naturally occurring RNAPII pause sites are also associated with some degradation of Rpb1, such as those caused by clashes between transcription complexes during convergent transcription (Hobson et al., 2012). Blocking the transcript cleavage ability of RNAPII also induces Rpb1 poly-ubiquitylation (Sigurdsson et al., 2010). TC-NER cannot aid these blocked polymerases, as there is no damage to be removed and RNAPII remains associated with DNA. Rpb1 poly-ubiquitylation and degradation, however, strips the RNAPII complex from chromatin (Verma et al., 2011).

Rpb1 poly-ubiquitylation has been observed under a number of other conditions. This response seems to have been hijacked to prevent transcription by a number of viruses, for example (Akhrymuk et al., 2012). Two promising chemotherapeutic agents, triptolide and trabectedin, inhibit transcription elongation and induce wide-scale Rpb1 poly-ubiquitylation (Vispe et al., 2009, Manzo et al., 2012, Aune et al.,

2008). Rpb1 degradation has also been observed in conditions that have not been directly linked to transcription stalling. Treatment of mammalian cells with high levels of hydrogen peroxide induces Rpb1 degradation (Inukai et al., 2004), although this has been refuted (Mikhaylova et al., 2008). The specific transcription program induced upon rapamycin exposure promotes Rpb1 degradation (Jouvet et al., 2011).

Since the initial discovery of the 'last-resort' pathway it has proven to be more complex than originally envisioned. Even in *S. cerevisiae*, a host of factors are required to ensure processive poly-ubiquitylation of persistently stalled RNAPII and Rpb1 degradation (Figure 1.10). It is important to note that the poly-ubiquitylation can be separated into two catalytically separate steps, mono-ubiquitylation catalysed by the HECT E3 Rsp5, and poly-ubiquitylation, catalysed by the Elongin-Cullin complex (Harreman et al., 2009).

1.5.3.1 Rpb1 mono-ubiquitylation

The first ubiquitin ligase implicated in Rpb1 degradation was the *S. cerevisiae* Rsp5 protein (Huibregtse et al., 1997). Rsp5 is the only essential HECT ubiquitin ligase in yeast, with diverse roles, from intracellular trafficking to transcription factor activation (Kaliszewski and Zoladek, 2008). RNAPII was found to associate with the WW domains of Rsp5 via the CTD repeats of Rpb1 (Huibregtse et al., 1997, Chang et al., 2000, Somesh et al., 2005). As Rsp5 is an essential gene, most work has focused on the use of a temperature sensitive allele with a mutation of a single amino acid of the gene, shown to prevent its catalytic activity at the non-permissive temperature (Wang et al., 1999). Reduced levels of functional Rsp5 lead to increased steady state levels of Rpb1 and no detectable Rpb1-ubiquitylation in response to DNA damage (Beaudenon et al., 1999, Harreman et al., 2009).

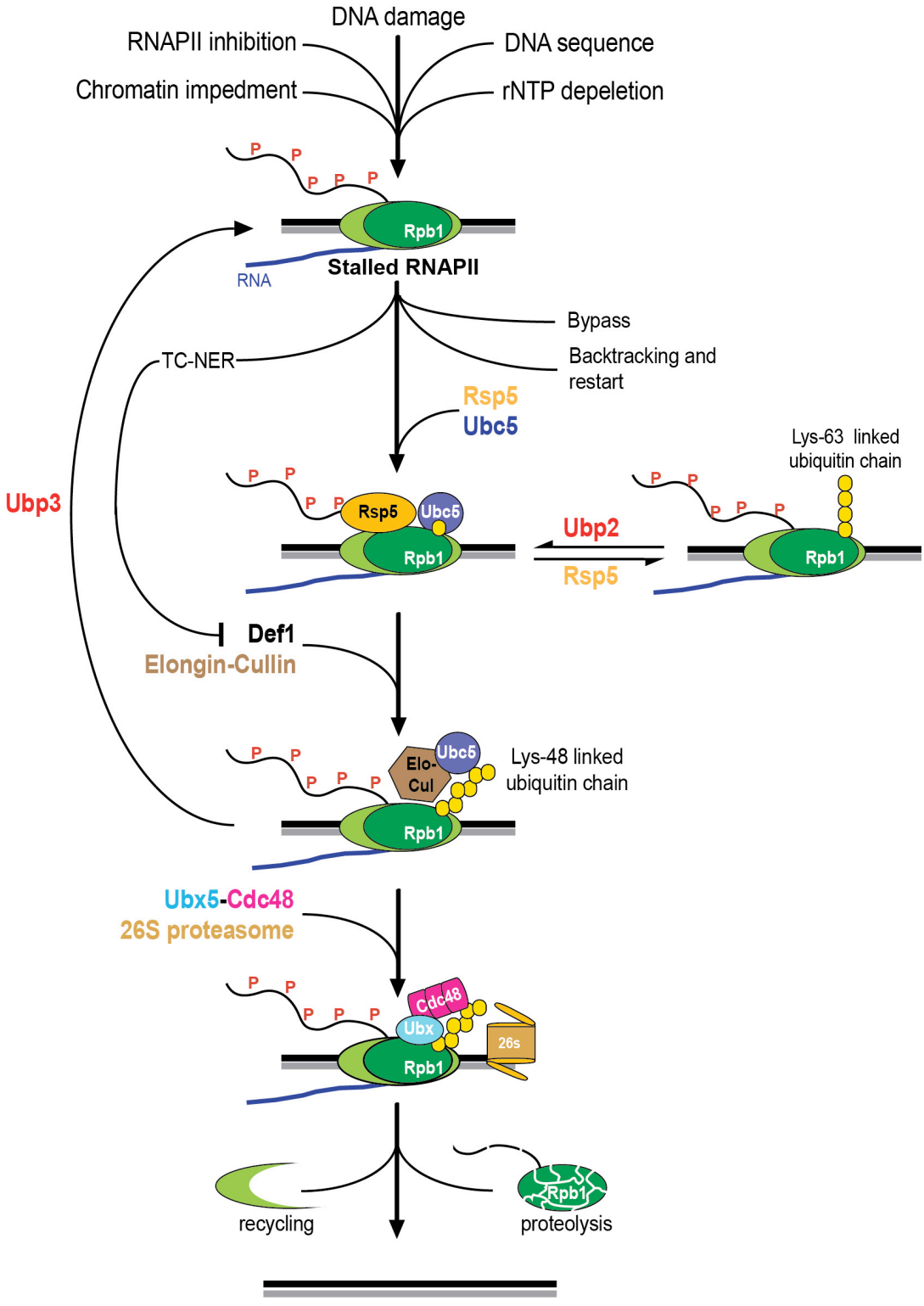

Figure 1.10: Model of Rpb1 poly-ubiquitylation and degradation in *S. cerevisiae*

Transcribing RNAPII becomes persistently arrested under a wide variety of conditions. As a last resort this can be dealt with by the sequential poly-ubiquitylation of Rpb1 and its degradation. See text for details. Modified from (Wilson et al., 2013)

As Rsp5 is involved in many cellular processes, it was critical to show a direct effect of the protein on Rpb1 poly-ubiquitylation. Indeed, Rsp5 inactivation directly leads to reduced levels of free ubiquitin in the cell (Krsmanovic and Kolling, 2004), which might potentially explain Rpb1 stabilisation. However, extract-based *in vitro* assays - where Rsp5 is inactivated - are unable to support Rpb1 ubiquitylation, in spite of the addition of excess ubiquitin in these assays (Reid and Svejstrup, 2006, Harreman et al., 2009). Adding pure Rsp5 back to this assay re-constitutes RNAPII poly-ubiquitylation (Harreman et al., 2009). Ubiquitylation of RNAPII can be reconstituted *in vitro* by using Uba1 (E1), Ubc5 (E2) and Rsp5, which together create poly-ubiquitin chains on Rpb1 only (Somesh et al., 2005), again suggesting a direct role for this enzyme. Rsp5 is known to assemble only single ubiquitin modifications or Lys-63 linked chains on substrates both *in vitro* and *in vivo* (Kee et al., 2005, Kim and Huibregtse, 2009, Kee et al., 2006), which are insufficient for proteasomal targeting (Zhao and Ulrich, 2010). Whilst this modified form may have a function in response to normal transcription stress (Katya Strasser, personal communication), it is not the principal ubiquitin chain found *in vivo* after DNA damage induced RNAPII stalling (Jung and Lippard, 2006). Instead, the Rsp5 associated DUB, Ubp2 (Kee et al., 2005, Kee et al., 2006), is thought to trim the Lys-63 chains back to a single mono-ubiquitin (Harreman et al., 2009)(Figure 1.10).

Many ubiquitin ligases have been implicated in the ubiquitylation of Rpb1 in mammalian cells, namely: CSA, BRCA1-BARD1, the VHL-Cullin complex and Nedd4. Furthermore, multiple different chain topologies have been reported on Rpb1 (Lee and Sharp, 2004, Jung and Lippard, 2006), with different observed ubiquitin banding patterns (Inukai et al., 2004). Cells deficient in CSA and CSB, or the CSB interacting protein UV^{S}SA, exhibit reduced levels of Rpb1 ubiquitylation after DNA damage (Bregman et al., 1996, Nakazawa et al., 2012). This, coupled with the observation that CSA can form a ubiquitin ligase (Groisman et al., 2003), led to the hypothesis that CSA directly ubiquitylates Rpb1 (Laine and Egly, 2006). CSA does interact with RNAPII after UV irradiation, but is selectively inhibited directly after DNA damage (Groisman et al., 2003). Furthermore, CS cells do not exhibit significant differences in the rate of degradation of Rpb1 after UV induced damage (Luo et al., 2001). The reduction in Rpb1 poly-ubiquitylation is now thought to be indirect; transcription is rapidly shut down after DNA damage in CS cells and

UV^{S}SA deficient cells (Mayne and Lehmann, 1982, Zhang et al., 2012), resulting in a reduction in the levels of RNAPII loaded onto chromatin, which reduces the amount of available substrate for ubiquitylation (Anindya et al., 2007).

The BRCA1-BARD1 complex has also been implicated in ubiquitylating RNAPII (Starita et al., 2005, Kleiman et al., 2005). In these studies a slower migrating band can be observed above the hyper-phosphorylated form of Rpb1. It is important to note that this cannot be simply interpreted as ubiquitylated Rpb1. A more reliable method, outlined in Anindya *et. al,* 2007, is to enrich for all ubiquitylated proteins from the cell, followed by Western blot and specific probing for Rpb1. Using the latter method Anindya and colleagues showed that only knock-down of Nedd4, one of the mammalian homologs of Rsp5, led to reduced levels of Rpb1-ubiquitylation and degradation. Nedd4 was also shown to bind to and ubiquitylate RNAPII *in vitro* and is now considered to have a homologous role to that of Rsp5 in Rpb1 mono-ubiquitylation (Anindya et al., 2007, Beaudenon et al., 1999).

Mono-ubiquitylated Rpb1 is thought to be constitutive at low levels in the unstressed cell (Woudstra et al., 2002, Sigurdsson et al., 2010, Wilson et al., 2012). This may be due to transitory stalled RNAPII complexes being recognised and mono-ubiquitylated, without being degraded. It is unclear whether this mono-ubiquitylation might have an additional functional role in RNAPII activity.

1.5.3.2 Rpb1 poly-ubiquitylation

After UV induced DNA damage, Rpb1 is poly-ubiquitylated with Lys-48 linked ubiquitin chains, removed from DNA and degraded by the proteasome (Ribar et al., 2006, Harreman et al., 2009, Verma et al., 2011). As Rsp5 only creates Lys-63 linked chains on substrates *in vivo* (Kee et al., 2006), another ubiquitin ligase is required to create a proteasome-targeting signal. Two papers revealed the role of an Elongin-Cullin CRL E3 complex, comprising Elc1 (Ribar et al., 2006), Ela1, Cul3 and Rbx1 (Ribar et al., 2007), in the poly-ubiquitylation and degradation of Rpb1 (Figure 1.11). In deletion strains that lacked these proteins, Rpb1 degradation did

not occur in response to a range of adduct-forming DNA damaging agents. Significantly, whilst there was no observed poly-ubiquitylation of Rpb1, mono-ubiquitylation was not compromised in these strains (Ribar et al., 2006, Ribar et al., 2007, Harreman et al., 2009). Elc1 and Cul3 have previously been reported to be part of another CRL, with Rad7-Rad16 (Ramsey et al., 2004, Gillette et al., 2006), which does not have a role in RNAPII poly-ubiquitylation or TC-NER (Ribar et al., 2006, Lejeune et al., 2009)

Confusion has surrounded the field over which ubiquitin ligase was the primary enzyme responsible for promoting the degradation of Rpb1, with compelling evidence for both Rsp5 and the Elongin-Cullin complex. However, work by Harreman and colleagues showed that RNAPII poly-ubiquitylation is a two-step process, involving both E3 ligases (Harreman et al., 2009). The authors reported that only pre-mono-ubiquitylated Rpb1, and not un-modified Rpb1, could be poly-ubiquitylated in an extract lacking functional Rsp5. They proposed that the Elongin-Cullin ubiquitin ligase complex, in the extract, acted in tandem with Rsp5 to produce a proteasomally competent Rpb1 for degradation. Furthermore, they found that a complex containing Elc1-Ela1-Cul3-Rbx1 co-purified and that it can only poly-ubiquitylate a pre-mono-ubiquitylated RNAPII *in vitro.* Whether this poly-ubiquitylation is an extension of the original mono-ubiquitylation or modification at another lysine on the surface of Rpb1 has yet to be determined. Rpb1 is ubiquitylated on multiple lysines (Somesh et al., 2007, Peng et al., 2003, Wagner et al., 2011, Kim et al., 2011); lysine choice may prove functionally important in dissecting the mechanism of action of the two distinct ubiquitin ligases.

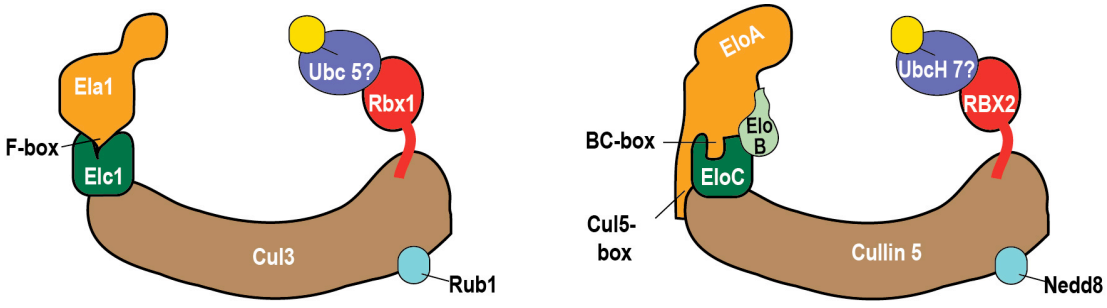

S. cerevisiae Elongin-Cullin

H. sapien Elongin-Cullin

Figure 1.11: The proposed Elongin-Cullin-E2 complexes in yeast and human cells

Components of the CRL like ligase and proposed E2 enzyme are coloured: red, the catalytic RING finger; brown, the structural scaffold cullin; green, the cullin adaptor protein Elc1 or Elongin BC; orange; the substrate adaptor protein Ela1 or Elongin A; light blue, Ubl activating protein Rub1 or Nedd8 and dark blue, the proposed E2 conjugating enzyme. Ubiquitin is coloured yellow. Key interaction motifs in the substrate adaptor proteins are highlighted.

The human homologue of Ela1-Elc1 is the Elongin ABC heterotrimer. Originally characterised as a positive regulator of transcript elongation (see 1.3.1.2), the Elongin ABC complex is also part of a CRL, with Cullin5 and Rbx2 (Yasukawa et al., 2008)(Figure 1.11). Elongin A interacts with the Elongin BC heterodimer via a BC-box motif: a degenerate 12-residue stretch upstream of the Elongin A transcriptional activity domain (Aso et al., 1996). Elongin B, which is absent from yeast, is a small protein with high homology to ubiquitin (Koth et al., 2000; see 1.1.5). Like in yeast, this mammalian complex can only efficiently poly-ubiquitylate Rpb1 when Nedd4 is present (Harreman et al., 2009), suggesting that there is an evolutional conservation of the two distinct, sequentially acting E3's in Rpb1 poly-ubiquitylation (Table 1.3). The mechanism of interaction between the substrate adaptor heterodimer differs across species (Figure 1.11). Ela1 contains an N-terminal F-box, which interacts with the Skp1-like Elc1 (Koth et al., 2000, Botuyan et al., 1999). Elongin A interacts with both Cullin-5 and Elongin C via its central SOCS-box (Mahrour et al., 2008, Yasukawa et al., 2012).

The Elongin BC heterodimer is known to associate with a wide variety of BC-box motif substrate adaptors to form functional CRLs (Duan et al., 1995, Kamura et al., 2001). Intriguingly, the pVHL-ElonginBC-CUL2-RBX1 complex (which lacks Elongin A) can bind to RNAPII after UV induced stress and has been shown to ubiquitylate the RNAPII subunits Rpb1-Rpb6. This requires the hyper-phosphorylation of the CTD of Rpb1 and hydroxylation of a proline in the linker region of Rpb1 (Kuznetsova et al., 2003, Mikhaylova et al., 2008). pVHL mediated ubiquitylation has been shown to be important in Rpb1 degradation in response to trabectedin (Aune et al., 2008) and pVHL catalysed poly-ubiquitylation of Rpb7 can prevent transcription (Na et al., 2003).

The Rpb9 subunit of RNAPII appears to play a role in Rpb1 ubiquitylation and degradation, as well as mediating the Rad26-independent TC-NER pathway (Chen

et al., 2007). Chen and colleagues demonstrated that cells lacking Rpb9 do not degrade Rpb1 in response to UV damage. Interestingly, one of the characterized sites of Rpb1 ubiquitylation, Lysine 695 (Somesh et al., 2007, Peng et al., 2003), is located close to the Rpb9-Rpb1 interaction surface. Rpb9 is required for efficient RNAPII elongation *in vivo* (Hemming et al., 2000); therefore, Rpb9 may help to sense the stalling state of the RNAPII complex and help recruit ubiquitylation factors.

1.5.3.3 Def1 protein

The *S. cerevisiae* protein Def1 (Degradation factor 1) also plays an important role in Rpb1 poly-ubiquitylation and degradation. Originally identified as an interacting binding partner of Rad26, Def1 is not involved in TC-NER (Woudstra et al., 2002). Instead, cells lacking Def1 are unable to degrade Rpb1 under a wide variety of transcription stalling conditions (Woudstra et al., 2002, Somesh et al., 2005). Consistent with a role in the poly-ubiquitylation of RNAPII, cells lacking Def1 display normal mono-ubiquitylation, but no poly-ubiquitylation after DNA damage. Furthermore, Def1 accelerates Rpb1 ubiquitylation *in vitro* and associates with Rpb1 after DNA damage (Somesh et al., 2005, Reid and Svejstrup, 2004). The mechanistic function of Def1 remains to be elucidated, but the protein is not absolutely required for catalysis *in vitro* (Harreman et al., 2009). Intriguingly, despite its role on chromatin, Def1 appears to localise primarily to the cytoplasm (Huh et al., 2003, Tkach et al., 2012).

Def1 has also been implicated in a number of other cellular processes. Def1 interacts with the telomere helicase Rrm3, and directly with telomeric DNA, leading to long DNA expansions at the end of chromosomes (Chen et al., 2005). Cells lacking Def1 are slow growing (Woudstra et al., 2002) and large (Jorgensen et al., 2002). Whole-genome, genetic studies have also suggested a role for Def1 in meiotic cross-over recombination (Jordan et al., 2007), peptide transporter subcellular localization (Cai et al., 2006), prion expression (Manogaran et al., 2011) and glutathione biosynthesis (Suzuki et al., 2011). Whole-genome tagging studies confirmed that Def1 is a fairly abundant protein, with an estimated 3380 copies

expressed per cell (Ghaemmaghami et al., 2003). A mammalian homologue of Def1 has yet to be identified; however, given the very high degree of conservation of the rest of the Rpb1 poly-ubiquitylation pathway (Table 1.3), it seems unlikely that this will turn out to be a yeast specific factor.

Table 1.3: Comparison of yeast and human proteins identified in the 'last-resort' pathway

	S. cerevisiae	Mammals
E1	Uba1	Uba1?
E2	Ubc4, Ubc5, ?	UbcH5c, UbcH7, ?
First E3	Rsp5	Nedd4
Second E3	Elc1-Ela1-Cul3-Rbx1	Elongin A-Elongin BC-CUL5-Rbx2 VHL-ElonginBC-CUL2-Rbx1
Accessory factors	Def1 Rpb9	? RPB9?
Rescue factors	Ubp2 Ubp3-Bre5	Usp2? USP10-G3BP?
Degradation factors	Cdc48-Ubx4/5 26S Proteasome	p97? 26S Proteasome

1.5.3.4 Rescue of poly-ubiquitylated Rpb1 by DUBs

Two DUBs have been implicated in the *S. cerevisiae* Rpb1 poly-ubiquitylation pathway. Ubp2 often acts in concert with Rsp5, in a complex to reverse Lys-63 poly-ubiquitin chains (see above). Ubp2 plays a mechanistic role with Rsp5, which ensures proper presentation of mono-ubiquitylated RNAPII (Harreman et al., 2009).

In contrast Ubp3 appears to completely remove Lys-48 linked ubiquitin chains, 'rescuing' Rpb1 from degradation (Harreman et al., 2009, Kvint et al., 2008). Ubp3 physically interacts with RNAPII and Def1, and cells that lack Ubp3 degrade Rpb1 at an accelerated rate (Kvint et al., 2008). Whilst this Rpb1 degradation is thought to be beneficial in the response to UV irradiation, Ubp3 promotes the stability of RNAPII on chromatin under other conditions of temporary transcription stalling. As a result, Ubp3 acts as a 'brake pedal' for ubiquitylation, allowing the large number of factors implicated with the restart of RNAPII to perform their function. Much like

many other pathways in the cell, ubiquitylation of Rpb1, if left unchecked, can prove more dangerous than simply lacking the pathway in the first place.

1.5.3.5 Rpb1 degradation/clearance

Poly-ubiquitylation leads to the rapid proteasomal degradation of Rpb1 (Luo et al., 2001, Ratner et al., 1998, Beaudenon et al., 1999). However, RNAPII is strongly and stably associated with chromatin (Kireeva et al., 2000). Elongation complexes containing ubiquitylated RNAPII *in vitro* appear just as stable, and its counterpart is present in a salt- and detergent-resistant chromatin cell fraction *in vivo* (Ratner et al., 1998, Lee et al., 2002). Furthermore, High avidity binding to DNA can prevent proteasome-mediated degradation (Coppotelli et al., 2011). This suggests that additional chromatin-associated machinery may be required to disassemble ubiquitylated RNAPII.

The ATPase Cdc48 is required for disassembling the RNAPII ternary complex from DNA and for feeding ubiquitylated Rpb1 to the 26S proteasome. Proteasomes from Cdc48 mutant cells are clogged with Rpb1 peptides, suggesting that Cdc48 is directly required to unwind Rpb1 for complete degradation by the proteasome (Verma et al., 2011). Cdc48 works with an adaptor protein, Ubx4 or Ubx5, to strip Rpb1 from the ternary complex. Interestingly, the Ufd1-Npl4 Cdc48 adaptor is also implicated genetically in the degradation of Rpb1, through an unknown mechanism.

The proteasome itself is recruited to chromatin to directly digest ubiquitylated Rpb1. The 26S proteasome is found to be genomically associated with highly active genes (Auld et al., 2006), and at sites of RNAPII accumulation (Gillette et al., 2004), suggesting that it is recruited to sites of transcription stall. In *C. elegans*, under conditions of transcription inhibition, RNAPII localises to discreet chromatin ‘degradation centres’ where it is degraded by the proteasome (Scharf et al., 2011).

Rpb1 is the only subunit of the RNAPII complex that is degraded in response to DNA damage (Malik et al., 2008, Chen et al., 2007). The other 11 subunits of RNAPII are thought to be recycled back into a new RNAPII complex. Other

subunits of RNAPII can be ubiquitylated basally and under different cellular stresses (Beltrao et al., 2012, Kleiman et al., 2005, Daulny et al., 2008, Na et al., 2003).

With Rpb1 degraded and the other subunits of RNAPII free to diffuse from chromatin, any lesions previously covered by the stalled RNAPII can now be repaired, presumably via normal GG-NER mechanisms.

1.5.3.6 Recognition of stalled RNAPII

It is critical that ubiquitylation and degradation of Rpb1 is confined to RNAPII that is persistently stalled, which must pose a different substrate to normally transcribing RNAPII or free RNAPII. CPD stalled RNAPII does not appear to undergo any major conformational change (Brueckner et al., 2007), which might be detected on the surface of the protein. Selection of substrate has been reported via two mechanisms.

The hyper-phosphorylated form of Rpb1 is the target for destruction (Mitsui and Sharp, 1999, Luo et al., 2001). The chromatin bound RNAPII CTD is cyclically phosphorylated during the transcription cycle (see 1.3.1.3). After termination all phosphorylation marks are removed, creating free, un-phosphorylated RNAPII competent for the next round of transcription (Heidemann et al., 2013).

Only serine-2 CTD phosphorylated RNAPII is ubiquitylated in yeast (Somesh et al., 2005). Serine-2 phosphorylation is indicative of RNAPII in the elongation phase of transcription (Yoh et al., 2007, Mayer et al., 2010). Rsp5 does not bind to the CTD when it is phosphorylated at serine-5 *in vitro* (Somesh et al., 2005). Furthermore, in cells lacking the CTD phosphatase Ssu72, which consequently display high serine-5 phosphorylation in the gene body, Rpb1 degradation was greatly reduced. Interestingly, the binding of Rsp5 to the RNAPII CTD can promote Serine-2 phosphorylation (Sogaard and Svejstrup, 2007).

RNAPII is hyper-phosphorylated after DNA damage (Rockx et al., 2000, Mitsui and Sharp, 1999, Heine et al., 2008). Whilst serine-2 is hyper-phosphorylated in yeast (Ostapenko and Solomon, 2003, Winsor et al., 2013), serine-5 is hyper-phosphorylated in mammalian cells, after stress (Lee et al., 2002, Zhou et al., 2000). The cognate E3 ligases in yeast and humans diverge in their specificity to phosphorylated Rpb1. Rsp5 recognises the serine-2 phosphorylated form of RNAPII, whilst the ElonginABC-CUL5 complex appears to bind specifically to the serine-5 phosphorylated form in humans (Yasukawa et al., 2008). This suggests that, although the exact details diverge, the mechanism of binding to phosphorylated RNAPII in response to stall is highly conserved.

The conformational state of the CTD may play a role in ubiquitin targeting. Rrd1, a CTD Proline isomerase, can release RNAPII from chromatin (Jouvet et al., 2010) and is required for efficient Rpb1 degradation (Jouvet et al., 2011). The prevalence of other CTD phosphorylation patterns, including tyrosine-1, threonine-4, and serine-7, are more widespread than previously anticipated. (Mayer et al., 2012, Akhtar et al., 2009, Hintermair et al., 2012). The role of these modifications, if any, in relation to the ubiquitylation of Rpb1 has not yet been resolved.

As the phosphorylation status of Rpb1's CTD is not specific to stalled RNAPII other recognition methods are required to ensure correct Rpb1 poly-ubiquitylation. Ubiquitylation *in vitro* is far more efficient for RNAPII that has been reconstituted into transcription elongation complexes (Somesh et al., 2005); RNAPII undergoes significant conformational changes upon incorporation into these RNAPII/RNA/DNA ternary complexes (Gnatt et al., 2001). Furthermore, transcribing up to a stall point in these elongation complexes - mimicking the *in vivo* situation – promotes the ubiquitylation of Rpb1 further (Somesh et al., 2005). A mechanism for this observation has been provided: unique among ubiquitin E2's so far described, Ubc5 plays an active role in the recognition of its substrate, stalled RNAPII. *ubc4Δubc5Δ* mutant cells cannot degrade Rpb1, and Ubc5 supports Rpb1 poly-ubiquitylation *in vitro* (Somesh et al., 2005). Ubc5 binds directly to the switch 2 domain of RNAPII (Somesh et al., 2007) and, critically, this domain is only well structured during elongation (Gnatt et al., 2001). By recognising a structural feature unique to the stalled-ternary complex, Ubc5 is confined to ubiquitylate off-pathway,

stalled RNAPII. In addition, one of the identified ubiquitylation sites in Rpb1, Lysine 330, is buried in this region. This is very close to the catalytic center of RNAPII, therefore, a large 8.5kDa post-translational modification in this region is likely to perturb RNAPII transcription activity.

As Rpb1 ubiquitylation is a two-step process, the poly-ubiquitylation apparatus must also be correctly targeted. In fact, Rsp5 mediated mono-ubiquitylation is constitutive in unstressed cells (Woudstra et al., 2002, Sigurdsson et al., 2010), suggesting that this may not be the key control step. Whilst it is not clear how the poly-ubiquitylation machinery is regulated in yeast, Def1 is recruited to RNAPII after UV damage (Reid and Svejstrup, 2004). In contrast, Elc1 co-immunoprecipitation with RNAPII - from crude yeast extracts - is not affected by UV irradiation (Harreman et al., 2009), although poly-ubiquitylation only occurs under these conditions. The mammalian Elongin ABC-CUL5 ligase co-localises to sites enriched with serine-5 phosphorylated RNAPII (Yasukawa et al., 2008). The Elongin ABC complex, unlike the yeast equivalents, is associated with RNAPII as elongation factors. It is conceivable that the second E3 is recruited to RNAPII in a stepwise manner; first, the substrate recognising Elongin ABC binds to RNAPII as an elongation factor, prior to recruitment of CUL5-RBX2 upon persistent transcription stall. Cdc48 also appears to associate constitutively with RNAPII, whilst the substrate adaptor protein Ubx5 (or Ubx4) associates only after DNA damage (Verma et al., 2011).

Rsp5 shuttles between the nucleus and cytosol (Cholbinski et al., 2011). When the NES of Rsp5 was mutated, leading to nuclear accumulation of Rsp5, degradation of Rpb1 was more extensive after UV irradiation, suggesting that the RNAPII degradation factors are, at least in part, regulated by their subcellular localisation. Dynamic compartmentalisation could offer an alternate way of confining RNAPII poly-ubiquitylation to after transcriptional stalling. A number of kinases are activated after DNA damage. Indeed, in human cells ATR and p53 are activated upon RNAPII stall, in the absence of any induced DNA damage (Derheimer et al., 2007) . Whilst Mec1 phosphorylation is required for TC-NER (Taschner et al., 2010), the role of the DDR in RNAPII poly-ubiquitylation is unclear. It is interesting to note that Rpb1 has been shown to be inducibly SUMOylated in response to

transcription stall (Chen et al., 2009), and this SUMOylation does not directly affect the rate of TC-NER or Rpb1 poly-ubiquitylation. SUMOylation does increase in TC-NER deficient strains and attenuates Rad53 activation.

1.5.3.7 Choice of degradation over TC-NER/restart

As a non-reversible, wasteful pathway it is imperative that degradation of Rpb1 is used as a last resort. The restart and TC-NER machinery must first act to sample the stalled RNAPII, with degradation the only option if these pathways fail.

There are different kinetics to transcription restart, TC-NER and degradation of Rpb1. Elongation factors that promote restart often travel with elongating polymerases (Aso et al., 1995, Otero et al., 1999), and as a result, they are localised to the site of stall without the need for 'time-wasting' recruitment. There are over 200,000 sites of paused RNAPII in the *S. cerevisiae* genome (Churchman and Weissman, 2011), which are most often rapidly reset by backtracking and restart. TC-NER is a fast process (Tijsterman et al., 1997, Svejstrup, 2002), with the majority of lesions being removed in under one hour in *S. cerevisiae* (Taschner et al., 2010). The degradation of Rpb1 under the same conditions occurs at a much slower rate. Degradation may be the least favoured pathway due to the slower kinetics of Rpb1 poly-ubiquitylation, suggesting a model whereby the time taken to form sufficient Lys-48 chains on Rpb1 for degradation allows TC-NER to progress (Daulny and Tansey, 2009). In this model both the slower kinetics of the two-step recruitment process, as well as the action of Ubp3 would allow sufficient time for DNA repair to be attempted first.

There is kinetic disparity between Rpb1 poly-ubiquitylation and Rpb1 degradation in human cells (Anindya et al., 2007). Ubiquitylation is very rapid and potentiated for three hours after UV irradiation, whereas levels of Rpb1 do not noticeably decrease until the three hour time point. This suggests that the disassembly of the ternary complex and proteasomal degradation of Rpb1 may be the rate-limiting step in the reaction. Whether this is also the case in yeast is unclear, due to the faster overall kinetics of Rpb1 ubiquitylation and degradation.

Whilst TC-NER and degradation can be viewed as two separate pathways, this does not mean that they are not interconnected. Cells that are unable to ubiquitylate and degrade Rpb1 still exhibit normal TC-NER, suggesting that TC-NER is by far the dominant pathway, and degradation and removal of RNAPII does not offer a quick solution to DNA repair. However, cells lacking both TC-NER and Rpb1 degradation components are highly UV sensitive. Interestingly, ubiquitylated RNAPII is enriched in immunoprecipitations of UV^{S}SA suggesting that the TC-NER and Rpb1-ubiquitylation pathways could be overlapping in humans (Nakazawa et al., 2012).

Def1 was first identified via its interaction with Rad26 in chromatin (Woudstra et al., 2002). Rad26 actively antagonises Def1 function, suggesting that degradation can only occur when the TC-NER machinery is not present at the stalled RNAPII (Woudstra et al., 2002); Rad26 could allow time for the TC-NER pathway to occur first. If TC-NER then fails, it is possible that Rad26 diffuses away from the lesion or its inhibitory activity is deactivated, allowing the equilibrium to shift promoting Rpb1 poly-ubiquitylation and degradation, mediated via Def1. The identity of the final signal for Rpb1 ubiquitylation over failed TC-NER is unclear. It would be expected that multiple signals, including the DDR converge on stalled RNAPII to determine which pathway is utilised.

1.6 Aims of this thesis

As outlined above, the ‘last-resort’ Rpb1 poly-ubiquitylation and degradation pathway has been well studied since its discovery, over twenty years ago. However, some key questions remain. Whilst the catalytic players have been identified in both yeast and human systems, how the signal for Rpb1 poly-ubiquitylation is activated and controlled is still unclear. The potential regulation through dynamic

compartmentalisation and post-translational modification is an intriguing possibility. In order to better understand how Rpb1 is degraded, better tools for studying protein ubiquitylation *ex vivo* were required. Chapter 3 outlines the development of a ubiquitin specific affinity resin, the MultiDsks. The MultiDsk protein allows the efficient protection and isolation of ubiquitylated proteins from extracts.

One essential player in the 'last-resort' pathway, Def1, was identified over 10 years ago, but its specific role in the Rpb1 poly-ubiquitylation pathway was unclear. Results, presented here in Chapters 5-7, have helped to elucidate the central place of this protein in the Rpb1 poly-ubiquitylation pathway. Def1 is processed after transcription stall, to a shorter, active fragment (Chapter 5). This fragment of Def1 is created by the proteasome after mono-ubiquitylation and accumulates in the nucleus (Chapter 6). Finally, in the nucleus Def1 acts as a bridging molecule between Elongin-Cullin ligase and stalled RNAPII substrate to promote efficient Rpb1 poly-ubiquitylation (Chapter 7).

Chapter 2. Materials & Methods

2.1 Buffers, Media and Solutions

Standard growth media was obtained from the media and cell services unit of the London Research Institute, Cancer Research UK. De-ionised water was used for all media. Solid media for plates was created by substituting water for agar, to a final concentration of 1.5% Agar. All media and solutions were shifted to the appropriate temperatures before use: bacteria media, 37^{o}C; yeast media, 30^{o}C; purification and assay buffers, 4^{o}C.

2.1.1 Bacteria Media

2.1.1.1 LB (rich medium)

1 % w/v bacto-tryptone (DIFCO)
0.5 % w/v yeast extract (DIFCO)
1 % w/v NaCl
pH adjusted to 7
+/- 100µg/ml Ampicillin (Melford Biosciences)
+/-35µg/ml Chloramphenicol (Sigma-Aldrich)

2.1.1.2 SOC medium (rich medium)

2 % w/v bacto-tryptone (DIFCO)
0.5 % w/v yeast extract (DIFCO)
10 mM NaCl
2.5 mM KCl
10 mM $MgCl_2$
10 mM $MgSO_4$
20 mM glucose
pH adjusted to 7

2.1.1.3 NZY medium

10 mg/ml yeast extract (DIFCO)
5 mg/ml NaCl
2 mg/ml Glucose
16 mg/ml NZ-Amine A (Sigma-Aldrich)
pH adjusted to 7

2.1.2 Yeast media

2.1.2.1 YPD

1 % w/v yeast extract (DIFCO)
1 % w/v peptone (DIFCO)
2 % w/v glucose
For fluorescence studies supplemented with 24 µg/ml adenine and 10mM Tris pH 8.

2.1.2.2 Selective drop-out media (SD media)

2 % sugar (glucose, raffinose or galactose)
6.7 mg/ml Yeast nitrogen base without amino acids (DIFCO)
1.4 mg/ml Yeast Synthetic Drop-Out Medium Supplement (Sigma-Aldrich)
12 µg/ml adenine
+/- 80 µg/ml leucine
+/- 40 µg/ml histidine
+/- 40 µg/ml uracil
+/- 40 µg/ml tryptophan
+/- 1 µg/ml 5-Fluoroorotic acid (5-FOA) (Sigma-Aldrich)

2.1.2.3 Sporulation media

50mM Potassium acetate pH 7.0

6 µg/ml adenine
20 µg/ml uracil
40 µg/ml leucine
20 µg/ml tryptophan
20 µg/ml histidine

2.1.2.4 TE/LiOAc

Tris-EDTA pH 7.5
100 mM lithium acetate

2.1.2.5 PEG/TE/LiOAc

Tris-EDTA pH 7.5
100 mM lithium acetate
40% Polyethylene glycol (PEG) 3350

2.1.3 General solutions

2.1.3.1 Phosphate Buffered Saline (PBS)

137 mM NaCl
2.7mM KCl
10 mM Na_2HPO_4
2 mM NaH_2PO_4
pH adjusted to 7.5

2.1.3.2 Phosphate buffer

700mM Na_2HPO_4
300 mM NaH_2PO_4

pH adjusted to 7.4 or 8.1 as required

2.1.3.3 PBS TWEEN

137 mM NaCl
2.7mM KCl
10 mM Na_2HPO_4
2 mM NaH_2PO_4
0.025% TWEEN 20

2.1.3.4 Saline

137 mM NaCl
2.7mM KCl

2.1.3.5 Tris-EDTA (TE)

10 mM Tris-Cl pH 7.5 or pH 8.0
1 mM EDTA pH 8.0

2.1.3.6 Borate buffer

40mM Sodium Borate
70mM Boric Acid
pH ~9

2.1.3.7 Tris-Borate-EDTA (TBE)

89 mM Tris-Cl
89 mM Boric Acid
2 mM EDTA
A 10 x stock buffer was routinely used to prepare 1 x TBE.

2.1.3.8 5 x DNA loading buffer for agarose electrophoresis

20 mM EDTA pH 8.0
30 % glycerol
0.05 % bromophenol blue

2.1.3.91.5 x SDS-PAGE loading buffer

98 mM Tris-Cl pH 6.8
15 % glycerol
3 % SDS
0.015 % bromophenol blue
150 mM β-Mercaptoethanol

2.1.3.10 5 x SDS-PAGE loading buffer

325mM Tris-Cl pH 6.8
50 % glycerol
10 % SDS
0.05 % bromophenol blue
500 mM β-Mercaptoethanol

2.1.3.11 SDS-PAGE running buffer

A 20x stock solution of MES, MOPS or Tris-Acetate (BioRad or Invitrogen) buffer was diluted with dH_20.

2.1.3.12 Western transfer buffer

25mM Tris-base
192mM Glycine
20% Methanol

0.02% SDS

2.1.3.13 100x Protease Inhibitor (PI) mix

28.4 µg/ml leupeptin
137 µg/ml pepstatin A
17 mg/ml phenylmethylsulfonyl fluoride
33 mg/ml benzamindine
Dissolved in ethanol

2.1.4 Bacteria Purification Buffers

2.1.4.1 STE

10mM Tris pH 8
1mM EDTA
100mM NaCl
1xPI

2.1.4.2 MultiDsk wash buffer 1

1xPBS
450mM NaCl
10% glycerol
0.1mM EDTA
0.1% Triton X-100
1X PI
2mM Dithiothreitol (DTT)

2.1.4.3 MultiDsk wash buffer 2

50mM Phosphate buffer pH 7.4

50mM NaCl
10% glycerol
1mM β-Mercaptoethanol
1xPI
0.2% Triton X-100

2.1.4.4 GST lysis buffer

1xPBS
15mM Phosphate buffer pH 7.4
10% glycerol
0.2% Triton X-100
1X PI
2mM β-Mercaptoethanol

2.1.4.5 GST Wash buffer 1

1xPBS
250mM NaCl
10% glycerol
0.1% Triton X-100
1X PI
2mM β-Mercaptoethanol

2.1.4.6 GST wash buffer 2

50mM Phosphate buffer pH 7.5
50mM NaCl
10% glycerol
0.3% Triton X-100
1X PI
1mM β-Mercaptoethanol

2.1.4.7 GST Elution buffer

50mM Phosphate buffer pH 8.1
300mM KCl
10% glycerol
1xPIs
0.05% Triton X-100
15mM Glutathione
pH adjusted to >8.1

2.1.4.8 GST HRV 3C buffer

50mM Tris pH 7.5
150mM NaCl
1mM EDTA
1mM DTT
0.01% Triton X-100

2.1.4.9 Nickel lysis buffer

1xPBS
15mM Phosphate buffer pH 7.5
150mM NaCl
10% glycerol
0.2% Triton X-100
1X PI
2mM β-Mercaptoethanol
15mM Imidazole

2.1.4.10 Nickel wash buffer

1xPBS

450mM NaCl
10% glycerol
0.1% Triton X-100
1X PI
2mM β-Mercaptoethanol
20mM Imidazole

2.1.4.11 Nickel elution buffer

1xPBS
15mM Phosphate buffer pH 7.5
150mM NaCl
10% glycerol
0.2% Triton X-100
1X PI
2mM β-Mercaptoethanol
300mM Imidazole
pH adjusted to ~7.5

2.1.4.12 Mono S buffer A

1xPBS
15mM Phosphate buffer pH 7.4
10% glycerol
1X PI
2mM β-Mercaptoethanol

2.1.4.13 Mono S buffer B

1xPBS
900 mM NaCl
15mM Phosphate buffer pH 7.4

10% glycerol
1X PI
2mM β-Mercaptoethanol

2.1.4.14 Dialysis buffer 1

100mM HEPES pH 7.5
5% glycerol
2mM DTT

2.1.4.15 Dialysis buffer 2

50 mM HEPES pH 7.5
150 mM NaCl
10% glycerol

2.1.5 Yeast purification buffers

2.1.5.1 Cell lysis buffer

150 mM Tris-Acetate pH 7.8
50 mM potassium acetate
1 mM EDTA
5 mM DTT
20 % Glycerol
0.01 % NP40
1 x PI

2.1.5.2 Myc wash buffer 1

150 mM Tris-Acetate pH 7.8
500 mM potassium acetate

1 mM EDTA
5 mM DTT
10 % Glycerol
0.01 % NP-40
1 x PI

2.1.5.3 Myc wash buffer 2

50 mM Phosphate buffer pH 7.5
50 mM NaCl
1 mM β-Mercaptoethanol
10% glycerol
0.01% NP-40

2.1.5.4 TEV cleavage buffer

50 mM Phosphate buffer pH 7.5
150 mM NaCl
1 mM β-Mercaptoethanol
10% glycerol
0.01% NP40

2.1.6 Assay buffers

2.1.6.1 Degradation buffer (D-buffer)

150 mM Tris-Acetate pH7.4
100 mM potassium acetate
1 mM EDTA
0.1% Triton X-100
10% glycerol
2mM N-ethylmaleimide (NEM)
10 μM MG132

1x PI

2.1.6.2 Degradation buffer (D250-buffer)

150 mM Tris-Acetate pH7.4
250 mM potassium acetate
1 mM EDTA
0.1% Triton X-100
10% glycerol
2mM N-ethylmaleimide (NEM)
10 µM MG132
1x PI

2.1.6.3 High salt degradation buffer (D500-buffer)

150 mM Tris-Acetate pH7.4
500 mM potassium acetate
1 mM EDTA
0.1% Triton X-100
10% glycerol
2mM N-ethylmaleimide (NEM)
10 µM MG132
1x PI

2.1.6.4 Low salt degradation buffer (D50-buffer)

150 mM Tris-Acetate pH7.4
50 mM potassium acetate
1 mM EDTA
0.2% Triton X-100
10% glycerol

2mM N-ethylmaleimide (NEM)
10 μM MG132
1x Protease Inhibitor mix

2.1.6.5 Proteasome buffer (P-buffer)

25mM Tris pH 7.5
100mM NaCl
10% glycerol
2mM ATP
5mM MgCl2
1mM DTT
0.25mg/ml [4.5 μM] BSA

2.1.6.6 Binding buffer (B-buffer)

20mM Tris pH 7.5
200mM NaCl
0.05% Triton X-100
1x Protease Inhibitors
1 mM β-Mercaptoethanol
15% glycerol
75ug/ml BSA

2.1.6.7 Binding Phosphate buffer (BP-buffer)

1xPBS
50mM NaCl
0.05% Triton X-100
1x Protease Inhibitors
1 mM β-Mercaptoethanol
15% glycerol
75ug/ml BSA

2.1.6.8 Ubiquitylation buffer (U-buffer)

25mM Tris pH 7.5

125mM NaCl

2mM $MgCl_2$

1mM DTT

3.75mM ATP

2.1.7 RNA extraction buffers

2.1.7.1 Buffer Y1

1M Sorbitol

100mM EDTA pH 7.4

0.1% β-Mercaptoethanol

2.2 DNA Techniques

2.2.1 Plasmids

Table 2.1: Plasmids used in this study

Name	Description	Source
pRS423	AmpR, 2μ, URA3	(Sikorski and Hieter, 1989)
pRS414-DEF1	AmpR, CEN, TRP; DEF1 expressed from own promoter and terminator	JW
pRS414-MTH-DEF1	AmpR, CEN, TRP; as above, but 9xMyc-2xTEV-6xHis-DEF1	MDW
pRS414-MTH-DEF1-TEV	AmpR, CEN, TRP; as above, but TEV site inserted at DEF1 amino acids 522-523 (note: N-terminal TEV sites were removed during JSY1191 strain construction)	JW
pRS414-def1$_{CUEm}$	AmpR, CEN, TRP; as pRS414-DEF1, but CUE domain mutated (I54A, I55A, F33A, P34A)	MDW
pRS414-def1$_{Ubm}$	AmpR, CEN, TRP; as pRS414-DEF1, but Def1 mutated at K281R, K288R, K328R, K329R	MH
YIPlac204-TEV118	AmpR, TRP; pGAL10, NLS-9xMyc-TEV-2xNLS	(Uhlmann et al., 2000)
pRS425-Myc-TEV	AmpR, 2μ, LEU; pGAL10, NLS-9xMyc-TEV-2xNLS	MDW

pGEX-6p1	AmpR, GST	GE healthcare
pGEX-Def1$_{1-500}$	AmpR, GST-Def1-1-500-6xHIS. Codon optimised by Genscript	MDW
pGEX-Def1$_{1-500CUEm}$	AmpR, GST- Def1-1-500-6xHIS. CUE mutated at I54A, I55A, F33A, P34A	MDW
pGEX-Dsk2	AmpR, GST-Dsk2	(Anindya et al., 2010)
pGST-MD	AmpR, GST-6xHis-MultiDsk	(Wilson et al., 2012)
pGEX-Rsp5	AmpR, GST-Rsp5	(Somesh et al., 2005)
pET21-Ubc5	AmpR, 6xHis-Ubc5	(Parker and Ulrich, 2009)
pST44	AmpR polycistronic low copy number vector	(Tan, 2001)
pST44-Elc1-Ela1	AmpR, His-Elc1, Ela1. Polycistonic, codon optimised by Genscript	MDW
pST44-Elc1-Ela1$_{1-250}$	AmpR, His-Elc1, Ela1 residues 1-250	MDW
pST44-Elc1-Ela1$_{1-300}$	AmpR, His-Elc1, Ela1 residues 1-300	MDW
pST44-Elc1-Ela1$_{1-350s}$	AmpR, His-Elc1, Ela1 residues 1-350	MDW
pGEX-Ubi	AmpR, GST-Ubiquitin	(Anindya et al., 2010)
pGEX-Ubi$_{I44A}$	AmpR, GST-Ubiquitin (I44A mutated)	(Anindya et al., 2010)
pGEX-Ela1$_{250-379}$	AmpR, GST-Ela1 C-terminus residues 250-379	MDW
pPS815	AmpR, 2µ, URA, pADH1, SV40 NLS-GFP-LacZ	(Lee et al., 1996)
pPS1372	AmpR, 2µ, URA, pADH1, SV40 NLS-NES-GFP2	(Taura et al., 1998)
pBOW3 NLS-GFP-def1$_{500-738}$	AmpR, 2µ, HIS, pADH1, SV40 NLS-GFP-DEF1500-738	MDW
pBOW3 NLS-GFP$_2$-def1$_{500-540}$	AmpR, 2µ, HIS, pADH1, SV40 NLS-GFP2-def1500-540	MDW
pYC2/NT	AmpR, CEN, URA, pGAL1	Invitrogen
pYC2-DEF1	AmpR, CEN, URA, pGAL1, DEF1,	MH
pYC2-def1$_{1-500}$	AmpR, CEN, URA, pGAL1, DEF11-500	MH
pYC2-def1$_{CUEm}$	AmpR, CEN, URA, pGAL1, DEF1 CUE mutated (I54A, I55A, F33A, P34A)	MDW
pYC2-def1$_{1-500/CUEm}$	AmpR, CEN, URA, pGAL1, DEF11-500 CUE mutated (I54A, I55A, F33A, P34A)	MH
pYC2-NES-DEF1	AmpR, CEN, URA, pGAL1, Consensus NES, DEF1	MDW
pYC2-NES-def1$_{1-500}$	AmpR, CEN, URA, pGAL1, Consensus NES, DEF11-500	MDW
pYM28	AmpR, CEN, HIS, eGFP	(Janke et al., 2004)

Plasmids were created for this study by: MDW = Marcus Wilson; JW = Jane Walker; MH = Michelle Harreman

Def1 mutations and N-terminal tags were introduced into a yeast *DEF1*-expression plasmid (pRS414-DEF1) containing the endogenous *DEF1* promoter, ORF, and terminator regions, using standard PCR methods. For galactose-inducible overexpression of *DEF1*, the appropriate DNA sequence was amplified by PCR from these plasmids and cloned into the pYC2 vector (Invitrogen).

The MultiDsk construct was created from the coding sequence for the yeast Dsk2 ubiquitin binding domain (residues 327-373). This was repeated in tandem 5 times, incorporating a low complexity 8-amino acid spacer between repeats (Figure 1A). The sequence was codon optimised and synthesised (GenScript USA, Inc.), and cloned into GST fusion expression vector pGs-21a, producing pGST-MD.

The sequence coding for Def1 amino acids 1-500 with a C-terminal 6xHis tag was codon-optimised and synthesised by GenScript USA Inc. The coding region was sub-cloned into pGEX-6P1 (GE healthcare). Mutation in the CUE domain was performed by PCR using mutant primers. Sequences can be provided upon request.

The coding regions of Elc1 and Ela1, complete with polycistronic spacer sections as described by Tan et al (Tan, 2001), were codon-optimised and synthesized by Genscript USA Inc. A 6xHis tag was included at the N-terminus of Elc1 and cloned into pST44 polycistronic vector. C-terminal Ela1 deletions were created by amplifying the corresponding regions from codon-optimised Elc1-Ela1 and subcloning into vector pST44.

Sequences expressing the TEV protease were sub-cloned from construct 118 in Uhlmann *et al* (2000) into pRS425. The TEV recognition site was incorporated between amino acid residues 522 and 523 of Def1, inserting the sequence Glu-Asn-Leu-Tyr-Phe-Gln (using the native Gly-523 residue of Def1 as the final part of the TEV recognition consensus site), by site directed mutagenesis.

To create the NLS-GFP-DEF1$_{500\text{-}738}$ plasmid, the *DEF1* region coding for amino acids 500-738 was first cloned into a pRS423-based plasmid (pBOW3), containing the *ADH1* promoter and terminator separated by multiple cloning sites. Sequences encoding NLS-GFP were amplified from pYM28 (eGFP; EUROSCARF) with the SV40 nuclear localization signal (NLS) encoded in the primers, and then cloned in frame with DEF1$_{500\text{-}738}$. The construct has 4 amino acid spacers between each feature. All final constructs were confirmed by DNA sequencing.

2.2.2 Polymerase chain reaction (PCR)

PCR for cloning and strain creation were performed with the high fidelity KOD Hot start DNA polymerase kit (Novagen), as per manufacturer's instructions. Analytical PCR was performed using GoTaq DNA polymerase (Promega), as per manufacturer's instructions. Primers were synthesised upon request by Sigma-Aldrich or DNA Technologies. Thermal cycling conditions were optimised for each PCR.

2.2.3 DNA purification

DNA was purified from restriction digests, agarose gels or PCR using the QIAquick PCR/gel purification kit (Qiagen), following manufacturer's instructions.

2.2.4 Cloning

Appropriate Restriction enzymes (New England Biolabs [NEB]) were incubated with purified DNA and NEB buffer, at 37^{o}C for 2-4 hours. Cut plasmids were dephosphorylated using Calf intestinal phosphatase (NEB). Digested DNA was purified using the QIAquick gel purification kit (Qiagen). DNA quantification was performed using a Nanodrop spectrophotometer (Thermo Scientific). DNA ligations were set up with a 3:1 molar ratio of insert: vector, using Roche T4 DNA ligase and reaction buffer. The reaction was allowed to proceed for 3 hours at 25 °C prior to bacterial transformation. See Table 2.1 for a description of the plasmids created and used in this study.

2.2.5 Mutagenesis

Point or deletion mutations were created by using the QuikChange II XL kit, or mutated primers and 2-step overlap PCR. Site-directed mutagenesis was carried out using the QuikChange II XL kit (Stratagene), according to the manufacturer's instructions. The presence of point mutations/deletions was confirmed by sequencing.

2.2.6 Sequencing

Standard Sanger sequencing reactions were set up using the BigDye sequencing kit (Applied Biosystems) using standard conditions. Sequencing was performed at the London Research Institute sequencing facility.

2.2.7 Agarose gel electrophoresis

Horizontal gel electrophoresis was performed to separate DNA, using 0.8-2% agarose gels, stained with 0.5µg/ml ethidium bromide (Sigma-Aldrich). Gels were run in TBE (see 2.1.3.7) and samples loaded in DNA loading buffer (see 2.1.3.8).

2.2.8 Quantitative PCR

qPCR reactions were carried out using iQ Custom SYBR Green SuperMix (BioRad), with primers used at a final concentration of 0.2µM, and a total final volume of 20 µl. Standard thermal cycling and melt curve conditions were used in a CFX-96 Real-Time System (BioRad). Quantification of Ct values was performed in Excel (Microsoft).

2.3 RNA Techniques

2.3.1 Extraction of total RNA from cells

Total cellular RNA was isolated after zymolase (100units) treatment of $1x10^7$ cells in buffer Y1 (see 2.1.7.1) for 15 minutes at 30^oC, with gentle agitation. Cells were lysed and RNA extracted using the RNAeasy mini kit (Qiagen), following manufacturer's specifications. Genomic DNA contaminant was removed by on column DNase digestion (Qiagen).

2.3.2 Reverse transcription

Reverse transcription was performed using the Applied Biosystems Taqman RT kit. 1.5µg of RNA was used per reaction using oligo dT primers.

2.4 Bacterial Techniques

2.4.1 Transformation of bacterial competent cells

Top10 (Invitrogen) or XL-10 Gold (Stratagene) competent cells were used for transformations of newly ligated plasmids, as per manufacturer's specifications. BL-21 DE3 (RIL) (Invitrogen) cells were transformed with plasmid for recombinant protein expression, and selected using ampicillin and chloramphenicol containing LB-media.

2.4.2 Extraction of plasmid DNA

Plasmid DNA was extracted from 2ml or 100ml of overnight bacteria cultures using the QIAprep miniprep or midiprep kits (Qiagen) respectively, following manufacturer's specifications.

2.4.3 Overexpression of recombinant proteins.

Transformed BL-21 DE3 (RIL) cells were grown overnight in starter culture in LB-100µg/ml ampicillin-35 µg/ml chloramphenicol, at 37˚C. Typically 600-800 ml of LB-Ampicillin/chloramphenicol was inoculated with 15ml of overnight starter culture and allowed to reach an optical density (OD_{600}) of 0.6. IPTG was added to a final concentration of 0.5 or 1 mM, and the culture was shifted to 25˚C or 30˚C for 4 hours. Cells were harvested by centrifugation at 6000g for 20 minutes, washed once in PBS, and frozen in liquid nitrogen

2.5 Yeast Techniques

2.5.1 Yeast strains

All *Saccharomyces cerevisiae* strains used in this study were grown and manipulated using standard techniques (Sherman, 1991) and congenic with W303-1A unless stated.

Table 2.2: Yeast strains used in this study.

Strain number	Strain name	Genotype	Source
	W303-1a	*MATa ura3 leu2-3, 112 his3-11,15 trp1-1 ade2-1 can1-100*	R. Rothstein
	W303 diploid	*MATa/MATalpha ura3 leu2-3, 112 his3-11,15 trp1-1 ade2-1 can1-100*	R. Rothstein
	Sub592	*MAT* a *lys2–810 leu2–3,-112 ura3–52 his3-Δ200 trp1–1[am] ubi1-Δ1::TRP1 ubi2-Δ2::ura3 ubi3-Δub-2 ubi4-Δ2::LEU2* [pUB39] [pUB221-hismyc-ubi]	(Spence et al., 2000)
RJD1144	*Pre1-flaghis*	*MAT***a** *his3Δ200 leu2-3,112 lys2-801 trp1Δ63 ura3-52 PRE1^{FH}::Ylplac211 (URA3)*	(Verma et al., 2000)
JSY1175	*Ubp2-his-tev-myc*	*MATa ura3 leu2-3, 112 his3-11,15 trp1-1 ade2-1 can1-100, Ubp2-6xhis-2xtev-9xmyc::TRP, FLAG-Rsp5 ::URA*	MDW
JSY568	*Δdef1 ::URA3*	*W303 MATa leu2-3,112 his3-11,15 trp1-1 ade2-1 can1-100 ∆def1::URA3*	(Woudstra et al., 2002)
JSY645	*Δdef1::TRP1*	W303 MATa ura3 leu2-3,112 his3-11,15 ade2-1 can1-100 ∆def1::TRP1	(Woudstra et al., 2002)
JSY1176	*def1 1-100 HA*	W303 MATa ura3 leu2-3,112 his3-11,15 ade2-1 can1-100, def1$_{1-100}$-3HA::HIS3	MH
JSY1177	*def1 1-200 HA*	W303 MATa ura3 leu2-3,112 his3-11,15 ade2-1 can1-100, def1$_{1-200}$-3HA::HIS3	MH
JSY1178	*def1 1-300 HA*	W303 MATa ura3 leu2-3,112 his3-11,15 ade2-1 can1-100, def1$_{1-300}$-3HA::HIS3	MH
JSY1179	*def1 1-600 HA*	W303 MATa ura3 leu2-3,112 his3-11,15 ade2-1 can1-100, def1$_{1-600}$-3HA::HIS3	MH
JSY1180	*def1 1-700 HA*	W303 MATa ura3 leu2-3,112 his3-11,15 ade2-1 can1-100, def1$_{1-700}$-3HA::HIS3	MH
JSY1181	*def1 1-738 HA*	W303 MATa ura3 leu2-3,112 his3-11,15 ade2-1 can1-100, DEF1-3HA::HIS	MH
JSY1182	*DEF1/def1$_{1-500}$-HA*	MATa/MATalpha ura3 leu2-3, 112 his3-11,15 trp1-1 ade2-1 can1-100, DEF1/def1$_{1}$-500-3HA::HIS3	MH
JSY1183	*def1 1-530 HA*	W303 MATa ura3 leu2-3,112 his3-11,15 ade2-1 can1-100, def1$_{1-530}$-3HA::HIS3	MH
JSY1190	*Def1 WT*	As JSY 568, but with DEF1 knock-in (KI) at genomic DEF1 locus	MDW
JSY1191	*Def1-TEV*	As JSY568, but with def1-TEV522 KI at genomic DEF1 locus	MDW
JSY1192	*rsp5-1*	W303 MATa ura3 leu2-3,112 his3-11,15 ade2-1 can1-100 rsp5 I733S::pRS303	(Harreman et al., 2009)
GAC202	*GAC202*	Matα *his3-11 leu2-3,112 ura3-52 lys2-801 trp1-1 pdr5Δ::KanMX6 pre3-Δ2::HIS3 pup1Δ::leu2-HIS3* [pRS317-pup1-T30A] [YCplac22-pre3-T20A] gal^{-}	(Collins et al., 2010)

GAC201	*GAC201*	Matα *his3-11 leu2-3,112 ura3-52 lys2-801 trp1-1 pdr5Δ::KanMX6 pre3-Δ2::HIS3 pup1Δ::leu2-HIS3* [pRS317-PUP1] [YCplac22-PRE3] gal$^-$	(Collins et al., 2010)
JSY1193	*4xUbm*	As JSY568, but with def1 K281R, K288R, K328R, K329R at genomic DEF1 locus	MDW
JSY1218	*Def1-DHFR*	*MATa ura3 leu2-3, 112 his3-11,15 trp1-1 ade2-1 can1-100.* Def1-DHFR-HA::URA	MDW
JSY1194	*eGFP-DEF1*	As JSY568, but with eGFP-DEF1 at genomic DEF1 locus	MDW
JSY1195	*eGFP-DEF1 GAC202*	Matα *his3-11 leu2-3,112 ura3-52 lys2-801 trp1-1,* but with eGFP-DEF1 at genomic DEF1 locus	MDW
	DEF1-GFP	MATa his3Δ1 leu2Δ0 met15Δ0 ura3Δ0, DEF1-GFP::HIS3	(Huh et al., 2003)
JSY1196	*def1$_{CUEm}$*	As JSY568, but with def1 I54A, I55A, F33A, P34A at genomic DEF1 locus	MDW
JSY1197	*eGFP-def1$_{CUEm}$*	As JSY568, but with eGFP-def1 I54A, I55A, F33A, P34A at genomic DEF1 locus	MDW
JSY1198	*9xMyc-TEV-his-DEF1*	As JSY568, but with 9xMyc-2xTEV-6xHis-DEF1 at genomic DEF1 locus	MDW
JSY1199	*9xMyc-TEV-his-def1$_{CUEm}$*	As JSY568, but with 9xMyc-2xTEV-6xHis -def1 I54A, I55A, F33A, P34A at genomic DEF1 locus	MDW
JSY642	*DEF1-6xHA*	W303 MATa ura3 leu2-3,112 his3-11,15 ade2-1 can1-100 def1::pHAHIS304	(Reid and Svejstrup, 2004)
JSY919	*RPB1-3xHA*	MATa ura3-52, trp1-1, prb1-1122, prc1-407, pep4-3, leu2-3, 112 nuc1::LEU2 RPB1-3HA::URA	(Reid and Svejstrup, 2004)
JSY 951	*Rpb3-FLAG*	W303, MATa ura3-1 leu2-3,112 his3-11,15 trp1-1 ade2-101 lys2Δ can1-100, RPB3-FLAG::TRP1	(Sigurdsson et al., 2010)
RAT7-1	*Rat7-1*	matα ura3-52, leu2∆1, his∆200, rat7-1.	(Gorsch et al., 1995)
MNY8	*Mny8*	Mata leu2, his3, trp1, ura3.pDC-CRM1T539C::LEU2	(Neville and Rosbash, 1999)
JSY1201	*Mny8, GFP-Def1*	Mata leu2, his3, trp1, ura3.pDC-CRM1T539C::LEU2. GFP-Def1::URA	MH
JSY1202	*Def1 CUEm, 9xMyc-TEV-his -Elc1*	As JSY1196 with 9xmyc-2xTEV-6xHis at N-terminus of Elc1::URA (see JSY 1116)	MDW
JSY 1116	*9xMyc-TEV-his -Elc1*	MATa ura3 leu2-3, 112 his3-11,15 trp1-1 ade2-1 can1-100. 9xmyc-2xTEV-6xHis at N-terminus of Elc1::URA	(Harreman et al., 2009)
JSY 1205	*Δela1*	MATa ura3 leu2-3, 112 his3-11,15 trp1-1 ade2-1 can1-100. Δela1::URA3	MDW
JSY 1203	*Ela1$_{1-250}$*	MATa ura3 leu2-3, 112 his3-11,15 trp1-1 ade2-1 can1-100, Ela1 1-250::HIS	MDW
JSY 1204	*Ela1 WT*	MATa ura3 leu2-3, 112 his3-11,15 trp1-1 ade2-1 can1-100, Ela1::HIS	MDW
JSY 1206	*Def1-his-TEV-9xMyc*	MATa his3Δ1 leu2Δ0 met15Δ0 ura3Δ0, Def1-his-TEV-9xMyc::HIS	MT
JSY1207	*Ela1$_{1-250-ub}$*	MATa ura3 leu2-3, 112 his3-11,15 trp1-1 ade2-1 can1-100, Ela1 1-250-4xgly-UbiquitinG76V::HIS	MDW
JSY 1208	*Def1 del 400-445*	As JSY568, but with def1 lacking residues 400-445	MDW
JSY 1209	*Def1 del 430-490*	As JSY568, but with def1 lacking residues 430-490	MDW
JSY 1210	*Def1 del 480-520*	As JSY568, but with def1 lacking residues 480-520	MDW
JSY 1211	*Def1 del 506-575*	As JSY568, but with def1 lacking residues 506-575	MDW
JSY1212	*Def1 del 400-500*	As JSY568, but with def1 lacking residues 400-500	MDW
JSY 1213	*Def1 del 400-600*	As JSY568, but with def1 lacking residues 400-600	MDW

JSY1214	*Def1 del 500-600*	As JSY568, but with def1 lacking residues 500-600	MDW
JSY1215	*9xMyc-TEV-his -Elc1, Ela1 WT*	MATa ura3 leu2-3, 112 his3-11,15 trp1-1 ade2-1 can1-100, 9xmyc-2xTEV-6xHis at N-terminus of Elc1::URA, Ela1::HIS	MDW
JSY1216	*9xMyc-TEV-his -Elc1, Ela1$_{1-250}$*	MATa ura3 leu2-3, 112 his3-11,15 trp1-1 ade2-1 can1-100, 9xmyc-2xTEV-6xHis at N-terminus of Elc1::URA, Ela1 1-250::HIS	MDW

Strains were created for this study by: MDW = Marcus Wilson; MH = Michelle Harreman; Michael Taschner = MT.

2.5.2 Generation of Yeast strains

Yeast Deletions or C-terminal tags were created using a PCR technique. An auxotrophic marker gene was amplified, with homology to the start and end (gene knockout), or the end of the coding region of interest (Schneider et al., 1995). 1-3µg of PCR product was transformed into yeast cells and transformants were selected on SD media plates (amino acid coded for by the auxotrophic marker). Correct integration was checked by PCR analysis and Western blotting.

Def1 genomic truncations were created by homologous recombination of PCR products (5'- truncation sequence - HA tag - STOP codon – *HIS3* selection marker - 3' truncation sequence) into haploid or diploid yeast, and selection on SD plates lacking Histidine. The truncations were confirmed by genomic PCR and Western blot analysis. Heterozygous diploids were sporulated on sporulation media for 7 days. Tetrads were partially digested with zymolase and dissected on a Singer msm micromanipulator.

Inserting GFP at the N-terminus of Def1 via recombination, without altering the DEF1 promoter, created strain JSY1201. The PCR product (5'- homology to upstream *DEF1* promoter – *URA3* selection marker – *DEF1* promoter – GFP in frame with the beginning of the Def1 coding sequence), created by two-step PCR, contained a *URA3* resistance cassette 1 kb upstream of the GFP tag.

Strains (JSY1191, 1193-1199 and 1208-1214) were created by inserting, via recombination, different versions of *DEF1* into the genomic locus in the *Δdef1::URA* strain (JSY568). Strains in which the *URA3* marker had been replaced by the

relevant version of *DEF1* were selected on 5-Fluoroorotic acid. PCR analysis and Western blotting we used to check for correct integration. Growth of the strains was checked by dilution series growth assays. JSY1190 served as a control for experiments with these strains. As described above, the wild-type *DEF1* gene was integrated into *Δdef1::URA* (recreating a wild-type *DEF1* locus), creating *Def1 WT*.

Strains JSY1203 1204, 1215 and 1216 were created by homologous recombination of PCR products (5'- truncation sequence - STOP codon – *HIS3* selection marker - 3' truncation sequence) into haploid yeast. The JSY 1207 PCR product was created by two-step PCR (5'- truncation sequence -4xglycine-ubiquitin (G76V) - STOP codon – *HIS3* selection marker - 3' truncation sequence) and transformed as above. Correct integration was confirmed by PCR analysis, and expression by quantitative PCR of Ela1 transcript levels and Elc1 co-immunoprecipitation.

2.5.3 Yeast Growth conditions

Logarithmically growing yeast cells – $0.5x10^7$-$3x10^7$ cells/ml - were used for all analyses. Typically cells were grown at 30^oC, unless otherwise indicated, in YPD medium (2.1.2.1) or SD medium (2.1.2.2). Yeast cell density was assessed using a Z2 Coulter Particle Count and Size Analyzer (Beckman-Coulter), with particle gating from 2.5-7.5 µm.

Table 2.3: Drugs used in Yeast liquid media in this study

Drug	Source	Solvent used	Final concentration
4-Nitroquinoline 1-oxide (4-NQO)	Sigma	Acetone	8µg/ml or 10µg/ml (where indicated)
Nocodazole	Sigma	DMSO	15µg/ml
Leptomycin B	Calbiochem	Ethanol	100ng/ml
MG132	Calbiochem	DMSO	50µM
Cycloheximide (CHX)	Sigma	DMSO	35µg/ml
Rapamycin	Calbiochem	DMSO	200ng/ml

6-Azauracil (6-AU)	SIgma	Water	250µg/ml
Methotrexate (MTX)	Sigma	100mM Tris pH9	10 µM

Drugs used in this study are listed in Table 2.3, Drugs were added to cells in liquid media, with the equivalent volume of solvent added as a minus treatment control.

In the case of proteasome inhibitor MG132 and nuclear export inhibitor Leptomycin B, the drugs were added prior to the start of the experiment. MG132 was added 1 hour prior to the start of the experiment; accumulation of poly-ubiquitylated proteins was used as a measure of activity (Figure 6.3 A). Leptomycin B was added 30 minutes prior to the experiment, and assayed using the control construct NLS-NES-GFP_2 (pPS1372).

2.5.4 UV treatment of cells

Logarithmically growing yeast cells were harvested at 800g, washed once in saline solution (2.1.3.4), and resuspended in 1% of the initial volume (around 10^9cells/ml). The cell suspension was placed in large Pyrex dishes and distributed evenly. Cells were exposed to 300J/m^2 of 254nm UV light, using a calibrated UV box. The Pyrex dishes were washed with saline to gather all yeast, spun down and resuspended in the original media. Timepoints were taken where indicated.

2.5.5 Yeast cell transformations

Yeast cells were grown overnight in the appropriate medium and diluted to early logarithmic phase (typically 2-5x10^6 cells/ml). Cells were allowed to grow until they reached a density between 1-2.5x10^7 cells/ml, harvested by centrifugation and washed once in sterile water, followed by a second wash in TE/LiOAc (see 2.1.2.4). Cells were resuspended at 10^9 cells/ml in TE/LiOAc. 50µl of this cell suspension was added to PCR product (1-3µg) or plasmid (100ng), 70µg of boiled salmon sperm carrier DNA, 35µl of DMSO and 300µl of PEG/TE/LiOAc (2.1.2.5) and

incubated for 30 minutes at 30^{o}C. A negative control without PCR DNA was always performed. The cell mixture was heat shocked at 42^{o}C for 15 minutes, washed once in water and plated. For auxotrophic selection SD plates lacking histidine, leucine, tryptophan and/or uracil were used and cells were plated directly. For 5-FOA selection, cells were plated on YPD agar for 14 hours before replica plating onto SD 5-FOA plates. Plates were incubated at 25^{o}C or 30^{o}C until distinct colonies could be selected: typically 2-3 days.

2.5.6 Yeast Dilution series growth assays

Overnight yeast cultures were diluted to early logarithmic phase and allowed to grow. Equal numbers of cells were harvested and resuspended in an equal volume of sterile water. Ten fold serial dilutions were created, and dilution series from 10^{6} to 10^{0} cells were spotted linearly on YPD agar or SD agar plates. Multiple plates were spotted concurrently with different sugar sources (glucose or galactose) or incubated at different temperatures. After growth, the plates were photographed using a GelDoc XR (BioRad).

2.5.7 Galactose-induced overexpression in yeast cells.

Typically the gene of interest was cloned into a vector containing the GAL1 promoter and CYC1 terminator region (see Table 2.1), to promote galactose inducible expression. Cells were grown overnight in SD glucose media lacking the selecting amino acid. Cells were harvested and washed twice in sterile water before resuspension in SD raffinose media and incubated at 30^{o}C for three hours. Galactose was added directly to a final concentration of 2% and the indicated time points were taken.

2.5.8 Isolation of genomic DNA

The MasterPure Yeast DNA purification kit was used to isolate total DNA from 10^{8} cells, following the manufacturers instructions, typically 0.5µL of resuspended DNA was used in subsequent PCR reactions. For quick genomic DNA extraction 10^{7}

cells were harvested and resuspended in 0.2% SDS and boiled for 10 minutes. 1 µl of the supernatant was used in PCR reactions.

2.5.9 Whole cell extracts at sub-zero temperatures and chromatin enrichment

Yeast cells were harvested at 800g and washed once in PBS. Cells were resuspended directly in 2 volumes of cold D-buffer (2.1.6.1) or cell lysis buffer (2.1.5.1) and drops were added to liquid nitrogen, to create yeast 'popcorn'. The popcorn was either ground by hand using a liquid nitrogen cooled pestle and mortar, or disrupted using a freezer mill (Spex CertiPrep). Extent of cell disruption was assessed using optical microscopic measurements and grinding stopped when 90% of cells were disrupted.

Lysis via mechanical disruption at liquid nitrogen temperatures does not significantly solubilise chromatin (Kong and Svejstrup, 2002, Takagi et al., 2005a). As a result the above extract was spun at high speed (3900g for 10 minutes) and the pellet resuspended in D-buffer containing 4mM $MgCl_2$. The extract was sonicated (output 30%, 3 cycles 10s), followed by the addition of 2 units of Benzonase (Novagen) per ml of extract and incubated at 25^{o}C for 20 minutes. The extract was then spun at 3900g for 10 minutes, and the soluble fraction was taken. This fraction was now highly enriched for histone proteins.

2.5.10 Alkaline quick whole cell extract preparation

Whole cell extracts were created essentially as described (Kushnirov, 2000). Briefly, 1-2x10^{7} cells were pelleted and resuspended in 100mM Sodium Hydroxide for 5 minutes at room temperature. Cells were pelleted and the supernatant discarded. The pellet was resuspended directly in 1.5x SDS loading buffer (2.1.3.9) and heated to 99^{o}C for 5 minutes, before placing on ice. Samples were re-heated and spun at 14 000g for 1 minute before loading on SDS-PAGE gels.

2.5.11 Whole cell extract via glass bead beating

$3x10^8$ Yeast cells were harvested by centrifugation and washed once in PBS before flash freezing in liquid nitrogen. Thawed pellets were resuspended in 700µl D-buffer (2.1.6.1) and roughly 500µl 0.5mm diameter Glass beads (BioSpec Products) were added. The cells were disrupted using a FastPrep-24 cell homogenizer (MP Biosystems), using 6 rounds of beating at an intensity of 5.5, for 30 seconds each. Samples were incubated on ice between disruptions, to reduce heating of the sample. The extracts were clarified twice at 20,000g for 10 minutes. Protein concentrations for extracts were estimated using the Bio-Rad protein assay or Nanodrop, using an extinction coefficient of 50.

2.5.12 S-35 labelling of proteins

Cells were grown to early logarithmic phase, and transferred to –methionine SD media for 30 minutes. Cycloheximide (25 µg/ml) was added at the indicated time points, before an S-35 chase was performed. 100nCi of S-35 labelled methionine (Perkin-Elmer) was added to the media for 10 minutes, to radioactively label any synthesised protein in this time period. $1x10^7$ cells were harvested and washed extensively in media containing cycloheximide to remove unincorporated methionine and cell extracts created by alkaline quick whole cell extraction (Kushnirov, 2000).

2.6 Protein Techniques

2.6.1 SDS-PAGE

Precast 4-12% Bis-Tris gradient polyacrylamide Criterion gels or 3-8% Tris-Acetate gradient Criterion gels (BioRad) were commonly used for protein separation. Gels were run in Criterion MES, MOPS or Tris-acetate buffer (BioRad) depending on protein size and separation required. Electrophoresis was carried out in Criterion gel tanks, typically at 180V.

Proteins were directly detected by staining the gel with InstantBlue (Expedion) or the SilverQuest silver staining kit (Invitrogen) following the manufacturers directions. Alternatively, proteins were transferred and subjected to Western blot (see below).

2.6.2 Western blotting

After electrophoresis, SDS polyacrylamide gels were incubated in transfer buffer (2.1.3.12). H-bond C-extra Nitrocellulose membrane (Amersham) was placed on top of the gel and sandwiched between Whatman 3MM paper in a Criterion Blotter (BioRad) filled with transfer buffer. Transfer was typically performed for 90 minutes at 500mA. After the transfer the membrane was washed briefly in water and then stained using Ponceau S solution (Sigma-Aldrich) and the image scanned, to confirm transfer and loading. The membrane was then washed in PBS and blocked in PBS TWEEN (2.1.3.3) containing 5% milk powder (Marvel) for 1-16 hours.

Blotted proteins were detected using primary antibodies listed below (Table 2.4) at the stated dilutions in either 5% or 1% milk powder or 3% BSA, typically overnight at 4^{o}C. After the initial incubation the membrane was washed three times, for 10 minutes each, in PBS TWEEN. Membranes were incubated with the appropriate secondary antibody: anti-rabbit HRP (GE Healthcare), 1:10,000; anti-mouse HRP (GE Healthcare), 1:10,000; anti-mouse TrueBlot HRP (eBioscience), 1:1000; anti-rabbit TrueBlot HRP (eBioscience), 1:1000. The secondary antibody was incubated for 1 hour at room temperature, followed by three 10-minute washes in PBS TWEEN. The membranes were then incubated with SuperSignal Pico or Dura ECL reagents (Thermo Scientific) for 5 minutes and exposed to Amersham Hyperfilm ECL.

Figures were created using linear exposures - scanned using an Epson perfection V700 PHOTO scanner set at 720dpi at 24-bit colour. To quantify gel bands ImageJ v1.44 (W. Rasband, NIH) was used as per program specifications.

Table 2.2: Western blot antibodies used in this study

Antibody	Epitope	Source	Supplier	Dilution
4H8	Rpb1 CTD	Mouse, m	In house	1: 10,000
8WG16	Rpb1 CTD	Mouse, m	In house	1: 1,000
9E10	Myc tag	Mouse, m	In house	1: 5,000
9E11	Myc tag	Mouse, m	In house	1: 5,000
α-Pgk1	Pgk1	Mouse, m	Invitrogen	1: 10,000
α-His	6xHis	Mouse, m	Clonetech	1: 1,000
12CA5	HA tag	Mouse, m	Abcam	1:1,000
α-Ela1	$Ela1_{115-214}$	Mouse, p	Abcam	1:1,000
P4D1	ubiquitin	Mouse, m	Millipore	1:1,000
1Y26	Rpb3	Mouse, m	Abcam	1:1,000
α-Def1	$Def1_{388-738}$	Rabbit, p	This study	1:1,000

m=monoclonal
p=polyclonal

2.6.3 Analysis of pr-Def1

pr-Def1 was visualised via Western blot using an anti-Def1 antibody or tag specific antibody, where indicated. The antibody exhibits increased specificity for this lower processed band. Def1 was always visualised immediately after the experiment, and using the quick whole cell extract method (2.5.10).

2.6.4 Analysis of ubiquitylated proteins ex vivo

Poly-ubiquitylated substrate enrichment assays were performed using multiDsk conjugated to GST beads (GE healthcare)(2.7.2). Typically, 2 mg of yeast protein extract in 750 µl was incubated with 15 µl of this resin (60µg protein) for 2 hours at 4˚C before beads were extensively washed with D500-buffer (2.1.6.3), and with D50-buffer (2.1.6.4). Beads were resuspended in 1.5x SDS loading buffer and subjected to SDS-PAGE. In order to ascertain ubiquitin depletion, ubiquitin specific

antibodies were used (Table 2.4). In order to visualise individual ubiquitylated proteins, specific antibodies were used.

For the protection assay, yeast extract was incubated with MultiDsk at 30˚C for the indicated times, and then resuspended directly in SDS loading buffer prior to SDS-PAGE and Western blotting as above.

2.6.5 Immunoprecipitations (IPs)

Extract was prepared using either glass bead beating (2.5.11), or mechanical grinding at liquid nitrogen temperatures (2.5.9). Extracts were derived from strains JSY1199, 1198, 1116, 1202, 1206, 1215 and 1216, and UV-irradiated 1 hour prior to harvesting. Typically immunoprecipitations were performed with 15µl Protein A/G antibody cross-linked agarose beads (2.7.1). Typically 3.5mg of extract was used, in a total volume of 750µl (JSY1199, 1198 and 1206), and 20mg was used in a total volume of 13ml (JSY 1116, 1202, 1215 and 1216). IPs were incubated at 4^{o}C for two hours and washed 3 times in D250-buffer (2.1.6.2) and once in D50-buffer (2.1.6.4.), before directly resuspending in 1.5x SDS loading buffer (2.1.3.9) and separated by SDS-PAGE. In order to remove the background signal from Antibody heavy and light chain upon Western blotting, TrueBlot secondary antibodies were used.

2.7 Protein Purification

2.7.1 Antibody cross linking to beads

Cross-linking was performed as described (Harlow and Lane, 1999). Briefly, an equal mix of Protein A and Protein G Agarose beads (Pierce) were incubated with 3-5mg of antibody/ml of resin overnight at 4^{o}C. Beads were washed extensively with PBS and Borate buffer before coupling at room temperature for one hour using dimethylpimelidate. Incubating the beads with 1M Tris pH9 stopped the reaction, and beads were washed with PBS. The beads were stored as a 4x slurry in PBS

with 0.01% Sodium azide, at 4°C. Cross-linking was checked via detection of only the light antibody chain in SDS-PAGE.

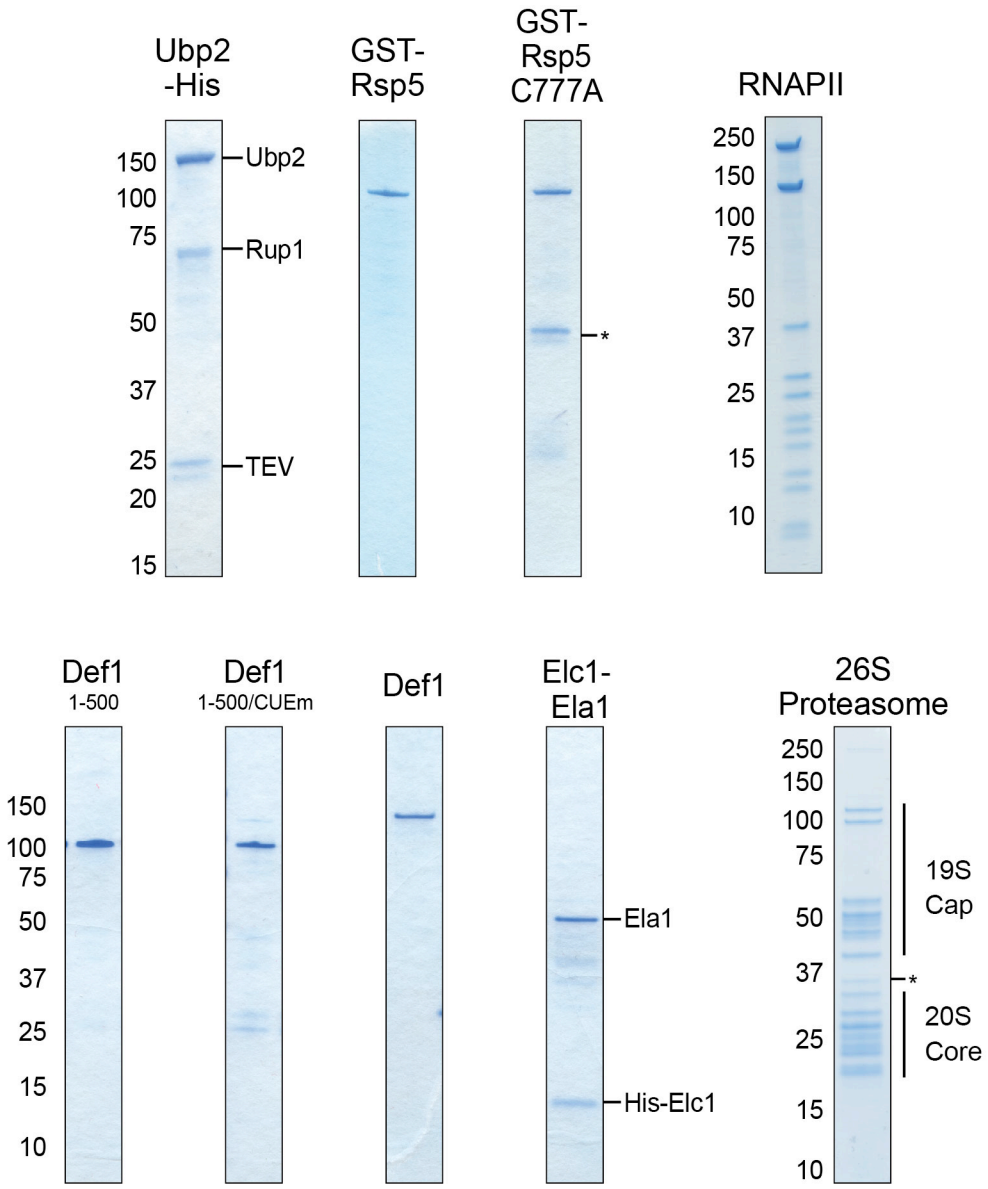

Figure 2.1: InstantBlue stained gel slices of Proteins purified in this study

Asterisks indicate minor unidentified contaminants. Proteins in a complex are labelled. MultiDsk and Ela1 C-terminal deletions are included elsewhere (Figure 3.1 & Figure 7.5)

2.7.2 MultiDsk purification

MultiDsk expression plasmid pGST-MD was propagated in BL-21 (DE3) cells, selected via ampicillin and expressed as above (2.4.3). Cells were lysed and protein solubilised essentially as described (Frangioni and Neel, 1993). Briefly, thawed pellets were resuspended in STE buffer with lysozyme (100µg/ml). After 15 minutes on ice *N*-lauryl sarcosine was added to a final concentration of 1.5%, to denature all proteins. After brief sonication (20% output 4 cycles15s on) and centrifugation at 10 000g 5 minutes, Triton X-100 was added to the supernatant to a final concentration of 3%. The Triton (added at a w:w ratio of 1:8) masks the sarcosine by forming mixed micelles (Dekker et al., 2002). Pre-equilibrated glutathione agarose beads (GE healthcare) were added and the slurry incubated for 2-4 hours at 4˚C. The beads were washed thoroughly in MultiDsk wash buffer 1 (2.1.4.2), followed by a low salt wash (2.1.4.3). For most purposes the protein was left bound to beads, stored as a 4x slurry in PBS +0.01% Sodium azide, at 4^{o}C. The protein was eluted by incubating the resin overnight in GST elution buffer (2.1.4.7) (4 ml elution buffer per ml resin). The purified protein was then dialysed in Dialysis buffer 2 (2.1.4.15).

2.7.3 Standard GST-Glutathione purifications

Glutathione-S-Transferase (GST), GST-Ubiquitin, GST-Ubiquitin I44A, GST-Ela1$_{250\text{-}379}$ and GST-Dsk2 were all purified using the same protocol, after recombinant overexpression (2.4.3). Cells were lysed via sonication (30% output 6 cycles 15s on) in GST lysis buffer (2.1.4.4) containing lysozyme (100µg/ml). The extract was clarified at high speed and pre-equilibrated glutathione agarose beads (GE healthcare) were added and incubated for 4 hours at 4˚C. The slurry was washed first in batch, and then on column with 100CV of GST wash buffer 1(2.1.4.5) followed by 50CV of GST wash buffer 2 (2.1.4.6). SDS-PAGE gels stained with InstantBlue, using BSA as a standard, estimated purity and protein concentration. GST-Dsk2 protein was cleaved and eluted using overnight FactorXa cleavage (GE healthcare), and dialysed in Dialysis buffer 1 (2.1.4.14)

2.7.4 Rsp5 purifications

GST-Rsp5 and GST-Rsp5 C777A were purified after recombinant overexpression (2.4.3). Cells were lysed in GST lysis buffer (2.1.4.4) containing lysozyme (100µg/ml), via sonication (30% output 6 cycles 15s on). The extract was clarified at high speed and pre-equilibrated glutathione agarose beads (GE healthcare) were added and incubated for 2-4 hours at 4˚C. The slurry was washed first in batch, then on column with 100CV of GST wash buffer 1(2.1.4.5) and then 50CV of GST wash buffer 2 (2.1.4.6) before elution overnight in GST elution buffer (2.1.4.7).

2.7.5 RNAPII purification

Rpb1-3xHA or Rpb3-FLAG RNAPII was purified essentially as described (Cramer et al., 2001). Briefly 100l of yeast cells (JSY919 or 951) were lysed via ball milling and clarified. Extract was passed over a heparin column, eluted with high salt and salted out using ammonium sulphate. The pellet was resuspended and bound to an Rpb1 CTD specific, 8WG16 column (2.7.1) for 4 hours at 4^{o}C. RNAPII was eluted using high glycerol and the protein containing fractions were loaded onto an anion exchange, Mono Q (GE healthcare) column.

2.7.6 Full-length Def1 purification

Pure, full length Def1 was purified as a side fraction from the final Mono Q stage of RNAPII purification (2.7.5)

2.7.7 Def1 1-500 purifications

Def1 1-500 and 1-500/CUEm were purified after recombinant overexpression (2.4.3). Cells were lysed in Nickel lysis buffer (2.1.4.4) containing lysozyme (100µg/ml), via sonication (30% output 6 cycles 15s on). The extract was clarified at high speed and pre-equilibrated Nickel-NTA beads (Qiagen) were added and incubated for 4 hours at 4˚C. The slurry was washed first in batch, then on column with 150CV of Nickel wash buffer (2.1.4.10) before elution using imidazole, in Nickel elution buffer (2.1.4.11). Eluate was diluted by two to reduce salt and

imidazole levels and bound to pre-equilibrated glutathione agarose beads (GE healthcare) for 2-4 hours at 4˚C. The slurry was washed with 75CV of GST wash buffer 1(2.1.4.5) and then 10CV of GST wash buffer 2 (2.1.4.6) before proteolytic elution overnight using Turbo 3C protease (AG Scientific Inc.) (50ng/ml of resin) in HRV 3C buffer (2.1.4.8). Eluted protein was finally concentrated by Nickel affinity chromatography, as above. The resulting proteins were dialysed in Dialysis buffer 1 (2.1.4.14).

2.7.8 Ubc5 purification

Yeast Ubc5 was purified after recombinant overexpression (2.4.3). Cells were lysed in Nickel lysis buffer (2.1.4.4) containing lysozyme (100µg/ml), via sonication (30% output 6 cycles 15s on). The extract was clarified at high speed and pre-equilibrated Nickel-NTA beads (Qiagen) were added and incubated for 4 hours at 4˚C. The slurry was washed first in batch, then on column with 150CV of Nickel wash buffer (2.1.4.10) before elution using Imidazole in Nickel elution buffer (2.1.4.11)

2.7.9 Elc1-Ela1 purifications

His-Elc1-Ela1 complex was induced in BL-21 DE3 *E.coli* cells, using 0.5mM IPTG at 25^{o}C for 4 hours. Cells were lysed in Nickel lysis buffer (2.1.4.4) containing lysozyme (100µg/ml), via sonication (30% output 6 cycles 15s on). The extract was clarified at high speed and pre-equilibrated Nickel-NTA beads (Qiagen) were added and incubated for 4 hours at 4˚C. The slurry was washed first in batch, then on column with 150CV of Nickel wash buffer (2.1.4.10) before elution using Imidazole in Nickel elution buffer (2.1.4.11). The eluate was diluted by two – in order to reduce the Imidazole and salt concentration. The proteins were then cleaned through a Mono Q (GE healthcare) column; Elc1-Ela1 complex does not bind to Mono Q resin. The flow through was loaded onto a cation exchange Mono S column, washed with 5CV of Mono S buffer A (2.1.4.12) and eluted using a salt gradient with Mono-S buffer B (2.1.4.13). Heterodimer containing fractions were dialysed in Dialysis buffer 1 (2.1.4.14).

Ela1 C-terminal deletions ($Ela1_{1-150}$, $Ela1_{1-250}$, $Ela1_{1-300}$, $Ela1_{1-350}$) were purified similarly to the full-length protein in a heterodimer with Elc1. The complexes eluted at a lower salt concentration on the Mono-S column to the full-length protein, but otherwise expressed and behaved identically.

2.7.10 Ubp2 purification

Ubp2 was purified from strain JSY1125, where Ubp2 and Rsp5 are tagged at their genomic locus. Cells were broken open in cell lysis buffer (2.1.5.1) by ball milling, followed by a clarification centrifugation. The supernatant was loaded onto 9E10/9E11 conjugated antibody column (2.7.1), at a rate of 0.2ml/min. The column was washed thoroughly in 50CV of myc wash buffer (2.1.5.2) and 20CV of myc wash buffer 2 (2.1.5.3). Bound proteins were eluted by overnight TEV protease cleavage (produced by the Protein Production facility, London Research Institute) in TEV cleavage buffer (2.1.5.4) (50ng of TEV protease/ml of beads). Eluted Ubp2 still contained a C-terminal 6xHis tag. Contaminating Rsp5 was removed by incubation of the cleaved supernatant with M2 agarose FLAG-beads (Sigma). Rup1 bridging factor co-purified with Ubp2 at stoichiometric levels, as has been observed previously (Kee et al., 2005).

2.7.11 Proteasome purifications

26S and 20S proteasomes were purified essential as described (Verma et al., 2000), using a FLAG-HIS tagged Pre1 strain (RJD1144). Briefly, 20l of yeast cells were grown and lysed in the freezer mill. Clarified supernatant was mixed with anti-Flag M2 agarose (Sigma) for 4 hours at 4^{o}C. Beads were washed extensively in physiological salt and 5mM $MgCl_2$ containing buffer, and eluted in 4CV of the same buffer with 200µg/ml 3xFLAG peptide. Critically to ensure intact 26S proteasome 5mM ATP was used in all buffers, in the 20S purification this was omitted. Proteasome activity was checked via an immunogenic peptide assay.

2.7.12 Protein concentrations

Protein concentration estimations were performed using a Bradford assay (Bio-Rad protein assay), whereby 20µl of protein added to 1ml of diluted Bradford reagent and incubated for 5 minutes. The reaction was visualised on an ultraspec 110 pro spectrophotometer at A_{595}, if the reading was in the linear range (0.1-0.7), this was taken as the approximate concentration of protein in mg/ml. More accurate estimates were then performed by running the pure protein on SDS-PAGE and InstantBlue staining; the stained protein band was compared with known BSA standard.

For proteins with unusual Bradford reactions and InstantBlue stain (i.e Def1), concentration measurements were further performed with NanoDrop measurements using a calculated extinction coefficient (Protparam http://web.expasy.org/protparam/).

2.7.13 Dialysis

Purified proteins were dialysed in Slide-a-lyzer Dialysis cassettes (Pierce) with a molecular cut off of 10,000 Da, into either Dialysis buffer 1(2.1.4.14) or 2 (2.1.4.15). Cassettes were resuspended in a volume equal to 300 times the cassette volume. The buffer was replaced three times and dialysed for 2 hours each.

2.8 *In vitro* Biochemistry

2.8.1 Ubiquitylation assays

Def1 and RNAPII Ubiquitylation assays were performed essentially as described for RNAPII ubiquitylation (Somesh et al., 2005) using purified components. Briefly, all components (below) were added to U-buffer at a final volume of 40µl (2.1.6.8) and incubated at 30^{o}C for 90 minutes. The reaction was stopped upon addition of

5x SDS-PAGE running buffer (2.1.3.10) to the reaction, and proteins resolved via SDS-PAGE and detected by Western blotting.

E1	rUba1	0.3 pmol	Boston Biochem
E2	yUbc5	2 pmol	2.7.8
E3	GST-Rsp5	50 nmol	2.7.4
Ubi	yUbiquitin	250 pmol	Boston Biochem
	hUbiquitin No lysines	250pmol	
DUB	Ubp2	5 pmol	2.7.10
Substrate	Def1	20 pmol	2.7.6
	RNAPII	20 pmol	2.7.5

Mono-ubiquitylated RNAPII was purified away from the ubiquitylation components by first depleting GST-Rsp5 using glutathione beads. This was followed by separation from non-ubiquitylated RNAPII using anion exchange mini Q column chromatography (GE Healthcare)

2.8.2 Proteasome processing assays

In vitro proteasome assays were performed in P-buffer (2.1.6.5) at 30^{o}C or 4^{o}C, where stated. Purified yeast 26S and 20S proteasome (10nM) were added to reactions with Def1 or ubiquitylated Def1 (2.8.1) (1.5 μM). MG132 was used to inhibit the proteasome at concentrations of 10 μM or 100 μM and lactacystin at 50 μM, where indicated. Pure RNAPII (2.7.5) or mono-ubiquitylated RNAPII (2.8.1) was added at ten-fold molar excess to Def1 (150 μM). The reaction was initiated upon the addition of Def1 and stopped by addition of 5xSDS page loading buffer (2.1.3.10) at the indicated times. Proteins were then resolved via SDS-PAGE and detected by Western blotting. The proportion of Def1 converted to processed bands was assessed as the amount of upper band remaining, quantified by ImageJ (see 2.6.2).

2.8.3 Ubiquitin chain binding assay

The poly-ubiquitin chain-binding assay was performed essentially as described in (Anindya et al., 2010). 20µl of GST, GST-Dsk2 or GST-multiDsk (200µg total each) were washed in Binding buffer (2.1.6.6). 400µl of B-buffer with 50µg/ml of either Lys-48 or Lys-63 linked ubiquitin chains (Enzo) were incubated with the beads for 2 hours at 4^{o}C. The beads were washed three times in B-buffer and resuspended directly in 1.5x SDS-PAGE loading buffer (2.1.3.9)

2.8.4 Ubiquitin binding assay

15µl of GST, GST-Ubiquitin, GST-ubiquitin I44A or GST-Ela1$_{250\text{-}379}$ (2.7.3)(100µg total each) were washed in B-buffer (2.1.6.6). 700µl of B-buffer with 55µg/ml of either recombinant Def1 1-500 or recombinant Def1 1-500/CUEm (2.7.7) were incubated with the beads for 2 hours at 4^{o}C. The beads were washed three times in B-buffer and resuspended directly in 1.5x SDS-PAGE loading buffer (2.1.3.9).

2.8.5 Elc1-Ela1 binding assays

Def1 1-500, Def1 1-500/CUEm (2.7.7) and Dsk2 (2.7.3) were immobilised on Affigel-15 as per the manufacturers instructions, at a concentration of 2 µg/µl. The UBDs of RAP80 and Ataxin-3 (Boston Biochem) were similarly cross-linked to Agarose beads, and diluted using empty quenched Affigel-15 beads to 2µg/µl. Empty Affigel-15 beads - with cross-linker blocked by ethyl-ethanolamine - were used as empty bead controls.

Pure recombinant His-Elc1-Ela1 proteins (2.7.9) were incubated with 15µl of pre-blocked Affigel-protein beads, in 700µl of BP-buffer (2.1.6.7) with 55µg/ml of recombinant heterodimer complexes. After a two-hour incubation, beads were washed three times in BP-buffer and directly resuspended in 1.5x SDS-PAGE loading buffer (2.1.3.9).

For the *ex vivo* ubiquitin binding assay (Figure 7.4 B) extracts were prepared from chromatin (2.5.9) from strain JSY1116, one hour after UV damage. 8mg of extract

was incubated in 700µl of D-buffer (2.1.6.1), at 4°C for two hours and washed 3 times in D250-buffer (2.1.6.2) and once in D50-buffer (2.1.6.4.), before directly resuspending in 1.5x SDS loading buffer (2.1.3.9) and separated by SDS-PAGE.

2.8.6 RNAPII binding assays

Mono-ubiquitylated RNAPII-3HA was created as described (2.8.1). Control RNAPII-3HA was not ubiquitylated, by omitting ubiquitin in the reaction. 20 pmol of RNAPII in U-buffer (2.1.6.8) was bound to 15µl of anti-HA affinity matrix (Roche) for 1 hour at 4°C, before washing once in U-buffer and twice in BP-buffer (2.1.6.7). Pure recombinant His-Elc1-Ela1 (30µg/ml) (2.7.9), Def1 1-500 and Def1 1-500/CUEm (35µg/ml) (2.7.7) were added to a total volume of 700µl in BP-buffer. Proteins were incubated with the beads at a 20 molar excess to RNAPII, for 2 hours at 4°C. Bound complexes were washed three times in BP-buffer, before directly resuspending in 1.5x SDS loading buffer (2.1.3.9).

2.9 Fluorescence microscopy

Cells were grown to logarithmic phase and, where appropriate, treated with drugs (2.5.3) or UV irradiated (2.5.4) as described previously. Where indicated (Figure 6.8 & Figure 6.7) cells were fixed for 30 minutes at their reaction temperature, using 3.75% Formaldehyde. 10mM Tris pH 8 was added to media 1 hour prior to visualisation, to enhance GFP fluorescence.

Typically $5x10^6$ cells were harvested at no greater than 800g, and washed once in sterile water. Cell pellets were incubated with 20µl of Vectashield containing 4',6-diamidino-2-phenylindole (DAPI) (Vector laboratories) for five minutes before 1µl was added to 1% Agar on microscope slides (for technique see yeast resource centre http://depts.washington.edu/yeastrc/pages/plasmids_protocols.html). Coverslips were immediately applied and sealed using Nail varnish (Revlon).

Cells were visualized on a DeltaVision workstation (Image Solutions), using an X100 UplanSApo 1.40 NA oil objective lens on an Olympus inverted microscope (IX71). Images were acquired and deconvolved using SoftwoRX software (Applied Precision), using 5 iterations with low noise reduction.

Assessment of Def1 nuclear localisation was scored by eye, when there was convincing overlap between green GFP signal and Blue nuclear DAPI stain. Only cells with positive nuclear DAPI stain were counted. Quantification was performed in Excel (Microsoft) and Prism (GraphPad Software).

Chapter 3. Results I

MultiDsks: A Ubiquitin Specific Affinity Resin

3.1 Aims

Post-translational modification by ubiquitin has emerged as an extremely common event resulting in multiple cellular fates (see Introduction 1.1). Studying protein ubiquitylation *ex vivo* has been hampered by two key technical limitations: the difficulty in achieving high affinity enrichment of native ubiquitylated proteins and the transient nature of the modification in extracts.

Ubiquitylated proteins are subject to rapid proteasomal degradation and aberrant de-conjugation of ubiquitin by intracellular de-ubiquitylating enzymes (DUBs), exposed upon cell lysis (Finley et al., 2012). To counteract this problem, chemical inhibitors of ubiquitin proteases have commonly been used in cell lysis buffers, to reduce unwanted, non-targeted, loss of ubiquitin from target proteins. These inhibitors are non-specific, short-lived in aqueous solutions, only partially inhibit ubiquitin proteases, and can cause aberrant covalent modifications. One inhibitor, Iodoacetamide, has been reported to create covalent modifications on protein substrates that could be confused with ubiquitin remnants on digested peptides (Nielsen et al., 2008). Whilst the majority of DUBs are cysteine proteases, the Rpn11 subunit of the proteasome is a Zinc-metalloprotease (Verma et al., 2002), not inactivated by the majority of inhibitors used. Alternatively, lysates can be prepared under denaturing conditions, thereby inactivating any protease activity. However, this renders these proteins unusable for further extracellular assays.

Enrichment of ubiquitylated proteins from cells has been performed using a number of different methods, each with problematic technical caveats. N-terminal tagging of ubiquitin and using a tag-specific affinity resin allows efficient depletion of tagged ubiquitin and any conjugated proteins. However, this requires the tricky replacement of all ubiquitin in the cell with the tagged version (for example, yeast have several genes encoding ubiquitin precursors), or risk competition from the

abundant endogenous form of the protein (Ziv et al., 2011). It is also conceivable - considering the small size and many possible modifications of ubiquitin - that the addition of any tag may perturb the function of the molecule *in vivo*. Nevertheless multiple proteomic and targeted studies have utilised N-terminally His-tagged ubiquitin (Peng et al., 2003, Kirkpatrick et al., 2005, Jeon et al., 2007), a small tag with the benefit of allowing the experiments to be carried out under denaturing conditions. High background and concerns over artefactual effects of ubiquitin overexpression has resulted in an increased use of strategies that utilise endogenous ubiquitin.

As an alternative to ubiquitin-tagging, ubiquitin specific antibodies may be used to deplete ubiquitin from extracts. However, such antibodies have proven to be of low affinity and show specificity for certain chain subtypes (Newton et al., 2008). Recent studies have made use of GG-peptide antibodies (Wagner et al., 2011, Kim et al., 2011), which have proven useful to identify ubiquitylated proteins after trypsin digestion.

Isolation of native, un-modified ubiquitylated proteins has relied upon using ubiquitin-binding domain (UBD) containing proteins, typically fused to GST (Layfield et al., 2001). Using a complete UBD protein can bias the recruitment to mono- or linkage-specific ubiquitylated proteins (Raasi et al., 2005, Funakoshi et al., 2002) and has been shown to exhibit high background – due to interaction with non-ubiquitylated proteins (Kang et al., 2007). Moreover, the affinity of ubiquitylated substrates for UBDs is low ($K_d \approx$ 15-500μM) (Hurley et al., 2006). Furthermore, immobilised GST-Dsk2 protein, for example, is unstable, degrading entirely - even in its purified form - within two weeks at 4^{o}C.

In a recent paper (Hjerpe et al., 2009), the authors produced a recombinant protein comprised of 4 ubiquitin binding domains in tandem (termed TUBEs). Not only did the TUBE-1 protein bind ubiquitin with high avidity, but it could also be used to protect ubiquitylated proteins from ubiquitin-specific proteases in cell extracts. Unfortunately, TUBEs are only available commercially, limiting their usefulness.

Inspired by the TUBEs paper we decided to create a higher affinity, freely available tool to help study protein ubiquitylation, namely a high-avidity, ubiquitin-specific affinity resin, hereafter called MultiDsk.

3.2 Results

3.2.1 Creation and purification of the MultiDsk resin

The artificial MultiDsk protein relies on the ubiquitin affinity of multiple UBDs. The UBA domain, from the C-terminus of the ubiquitin-binding protein Dsk2, was chosen. Dsk2 helps to target poly-ubiquitylated proteins to the proteasome for degradation (Saeki et al., 2002); through binding ubiquitylated substrates via its UBA domain, and to the proteasome via an N-terminal ubiquitin homology domain (Elsasser et al., 2002). The UBA UBD of Dsk2 has been well characterised (Raasi et al., 2005, Ohno et al., 2005), and exhibits relatively high affinity, of approximately 15μM to mono-ubiquitin (Ohno et al., 2005). Our laboratory has previously used the GST tagged full-length Dsk2 protein to enrich ubiquitylated proteins from extracts (Anindya et al., 2007, Harreman et al., 2009). The engineered MultiDsk protein instead consists of five Dsk2 UBA domains in tandem, each separated by a 7-amino acid flexible linker. An N-terminal GST tag and a C-terminal 6xHis tag were included to ease purification and allow the protein to be immobilised (Figure 3.1A). By obtaining a codon-optimised version of the sequence (GenScript USA, Inc.), we hoped to achieve higher levels of bacterial expression, aiding purification.

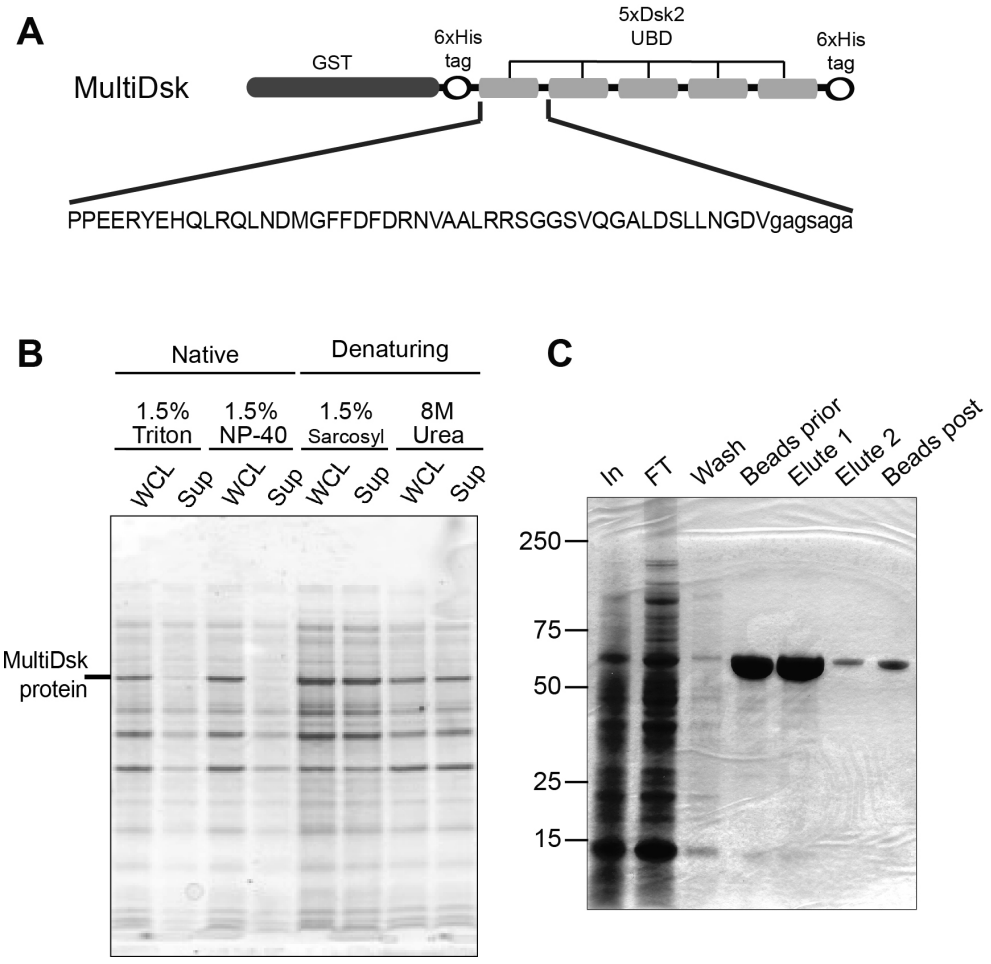

Figure 3.1: Schematic and purification of MultiDsk

A. Schematic representation of the MultiDsk protein, including primary sequence of one Ubiquitin binding repeat, including the 7-amino acid spacer section (lower case).
B. MultiDsk protein is insoluble under native cell lysis conditions**.** *E.coli* post-induction cell pellets were resuspended in STE buffer supplemented with the indicated chemicals. A sample was taken before and after the cells were lysed using extensive sonication and lysozyme treatment. Gel was stained with InstantBlue. WCL- whole cell lysate; Sup- supernatant after cell lysis.
C. MultiDsks were purified as described in Materials and Methods (2.7.2). Gel was stained with InstantBlue. Molecular weight marker positions on the left are in kDa. In-Input; FT- flow-through.

MultiDsk expression studies were performed to maximise protein yields (data not shown). Under a wide range of temperatures, induction times, and IPTG concentration, the protein was expressed extremely well. However, the expressed protein was consistently found to be insoluble under native cell lysis conditions (Figure 3.1 B). We therefore used mild denaturing conditions to solubilise the protein, found almost exclusively in inclusion bodies. Instead of harsh, urea-based denaturation - which cannot be rapidly reversed - the bacterial cells were first

solubilised with sarcosyl. Sarcosyl coats the hydrophobic core of proteins in a similar manner to SDS (Frangioni and Neel, 1993, Dekker et al., 2002). The extract - including MultiDsk protein - was then refolded by removing the denaturant, by forming mixed triton-sarcosyl micelles (Frangioni and Neel, 1993). Using this approach, both the Dsk2 binding domains (as tested by the ability to bind ubiquitylated proteins) and the N-terminal GST protein (as judged by its ability to bind to glutathione resin) refolded properly. Despite denaturation-renaturation process leading to a 50% loss of starting MultiDsk protein (Figure 3.1 C, Flow-through), yields of around ~15 mg of active, pure protein per litre of bacteria culture were routinely obtained (Figure 3.1 C). Where appropriate, MultiDsk protein was eluted using reduced glutathione from the resin and dialysed before use. However, MultiDsk protein, immobilised on glutathione beads, was highly pure and stable, retaining activity for at least 6 months upon storage at 4^{o}C.

3.2.2 MultiDsks can deplete all ubiquitylated proteins from extract

We next tested the ability of pure immobilised MultiDsk protein to enrich ubiquitylated proteins from yeast extracts. In order to ease visualisation, and to prevent any chain linkage specificity imparted from a ubiquitin antibody, we commonly utilised a yeast strain where the only copy of ubiquitin is His-Myc tagged (SUB592, from Spence et al., 2000). To ensure that the tag was not affecting ubiquitylation or MultiDsk association wild-type extracts were also used, where indicated.

Upon GST pull-down, a strong signal was observed for poly-ubiquitylated - low to high molecular weight - ubiquitin conjugates when MultiDsk was coupled to beads, but not when using GST alone (Figure 3.2 A, compare lane 2 to lanes 4,6,8,10,12). The amounts of total immobilised protein and bead volume were kept constant throughout this experiment, by supplementing GST protein for MultiDsk protein, to yield the final MultiDsk concentration stated. Depletion of ubiquitylated proteins by MultiDsk exhibited a clear concentration dependence; only relatively modest

amounts of MultiDsk protein was required to remove ubiquitylated proteins from the extract. At a concentration of 1.6-3.2 μM, virtually all ubiquitylated proteins were depleted from the extract (Figure 3.2 A compare input, lane 1, with the flow throughs in lane 3, lane 11, and lane 13). The MultiDsk resin binds efficiently to ubiquitylated proteins in extracts from a number of different organisms (Wilson et al., 2012 and Marco Saponaro and Gabriele Piergiovanni, personal communication): a testament to the high conservation of ubiquitin between species. Fascinatingly, the resin exhibits high avidity, specifically towards ubiquitin. Immunoblots using antibodies raised against NEDD8 and SUMO, which are Ubiquitin-like proteins, did not show any appreciable enrichment from extracts (data not shown). These experiments were performed using yeast extracts; it remains to be seen whether this would also be case in more complex organisms with a greater number of ubiquitin-like proteins.

Each ubiquitin in a chain can be modified on 7 internal lysine residues and its N-terminal methionine, creating a vast array of different possible chain linkages. Different ubiquitin-binding proteins can bind different ubiquitin chain conformations (see introduction, 1.1.3). This specificity permits the different fates of different ubiquitylated proteins to be read through a 'ubiquitin code' (Komander and Rape, 2012). Importantly, MultiDsk resin can deplete all ubiquitylated proteins from extracts (Figure 3.2 A lane 13 Flow through), regardless of chain linkage. It was imperative to investigate whether MultiDsk was capable of enriching all ubiquitylated species more or less equally, to ensure that specific linkages were not over-represented in the final pull-down. Full-length Dsk2 protein has previously been shown to have some specificity for Lys-48 linked poly-ubiquitin chains (Funakoshi et al., 2002). In contrast, MultiDsk does not appear to discriminate between chain topologies, at least for pure Lys-48 and Lys-63 poly-ubiquitin chains (Figure 3.2 B). Compared to the inputs, the enrichment of the isolated chains appears to be equal. The apparent discrepancy of levels between Lys-48 and Lys-63 chains observed is due to the ubiquitin-blotting antibody used displaying a far higher affinity for Lys-63 linked chains than for Lys-48 chains. This is clear from the difference between the Ponceau-S detected protein loading and the Western blot inputs shown and has already been documented by the manufacturers (Enzo).

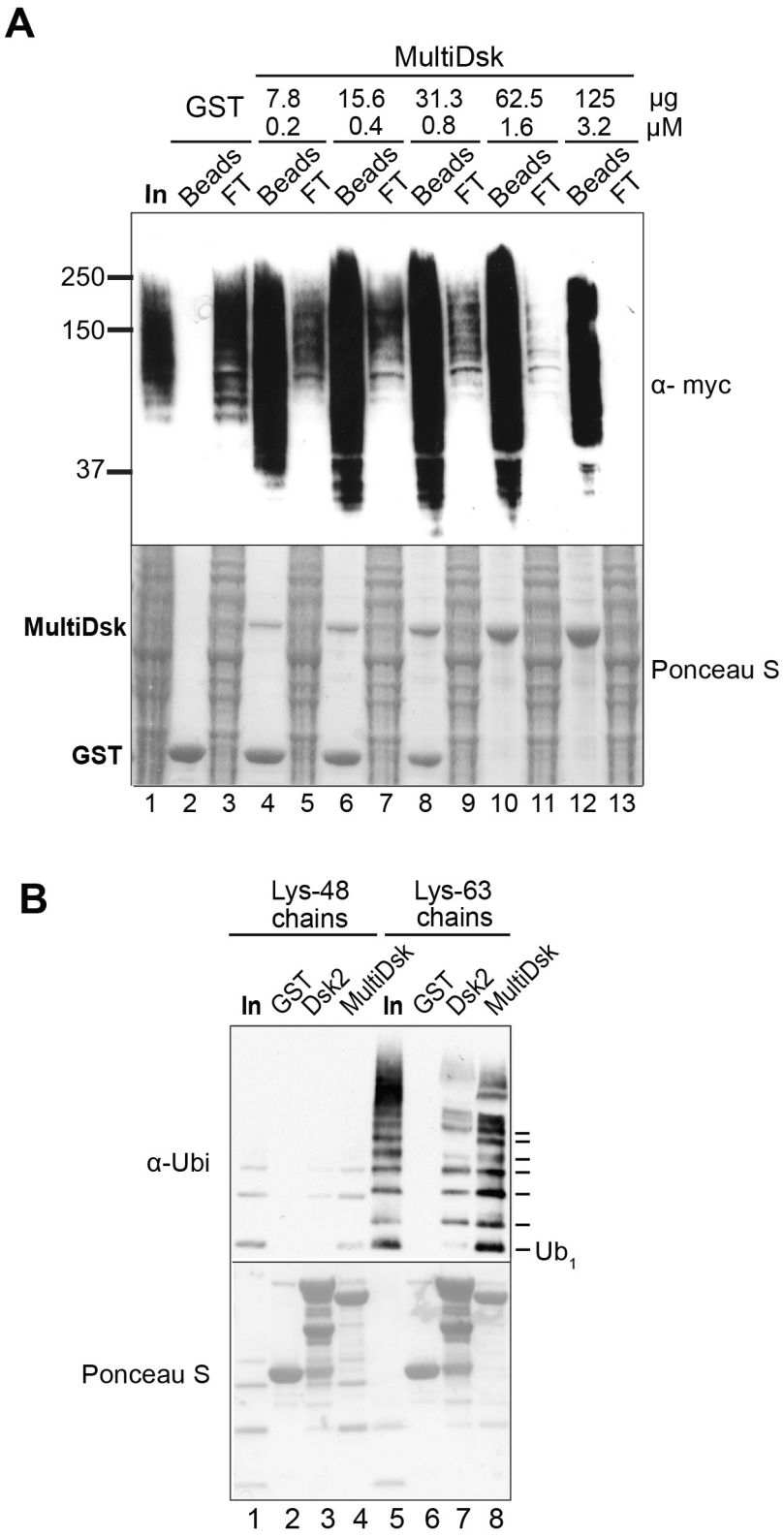

Figure 3.2: MultiDsk binds efficiently to ubiquitylated proteins

A. 2 mg of yeast whole cell lysate from strain SUB592 expressing Myc-His-tagged ubiquitin was incubated with glutathione affinity beads. Differing amounts of GST protein, alone or as a

mixture with GST-MultiDsk protein were mixed with agarose beads so that equal amounts of total protein and bead bed volumes were used in each experiment. The flow-through not bound to the beads was retained and loaded at equivalent levels to the Input (Lane 1). After electrotransfer, the membrane was stained with Ponceau S to reveal total protein in samples (lower panel), and Western blot was performed using anti-Myc antibodies to detect ubiquitylated species (upper panel).
B. GST alone, full length GST-Dsk2 protein, or MultiDsk, bound to beads, were incubated with 20 µg of synthetic Lys-48 or Lys-63 linked ubiquitin chains for 2 hours. After Western transfer, the membrane was stained with Ponceau S to reveal total protein in samples (lower panel), and Western blot was performed using anti-ubiquitin antibody (P4D1) to detect ubiquitylated species (upper panel).

Similarly, MultiDsk does not show obvious preference for mono-ubiquitin over short poly-ubiquitin chains. The ubiquitin chains purchased are of variable length, due to the inefficiency of coupling. Roughly equal levels of free single ubiquitin are enriched *in vitro* compared to chains of 5-6 ubiquitin moieties (Figure 3.2 B compare lanes 1 and 4, 5 and 8). This is in stark contrast to the immobilised full-length Dsk2 protein, which does not interact very well with free unconjugated ubiquitin (Figure 3.2 B compare lanes 5 and 7), and has previously been shown to underestimate mono-ubiquitylated protein levels in extracts (Zhang et al., 2009).

3.2.3 MultiDsks can protect ubiquitin chains

The MultiDsk resin is able to isolate virtually all ubiquitylated proteins from a cell extract. Relatively little protein was required, suggesting MultiDsk displays a high avidity for ubiquitin chains. The binding of ubiquitylated protein by MultiDsk is stable in both high salt and detergent (Figure 3.3 C), and is almost as stable as the GST-glutathione interaction. As a principally hydrophobic binding (Ohno et al., 2005, Lowe et al., 2006), the binding surface of Dsk2 UBA domain and ubiquitin is large. This, coupled with the high affinity of interaction between MultiDsk and ubiquitin, led us to postulate that the resin might help to sterically block, and prevent the action of, yeast DUBs in the extract. To assess the ability of MultiDsk to protect poly-ubiquitin chains from de-ubiquitylation and degradation we incubated protein in crude extracts at physiological 30^{o}C temperature (Figure 3.3 A).

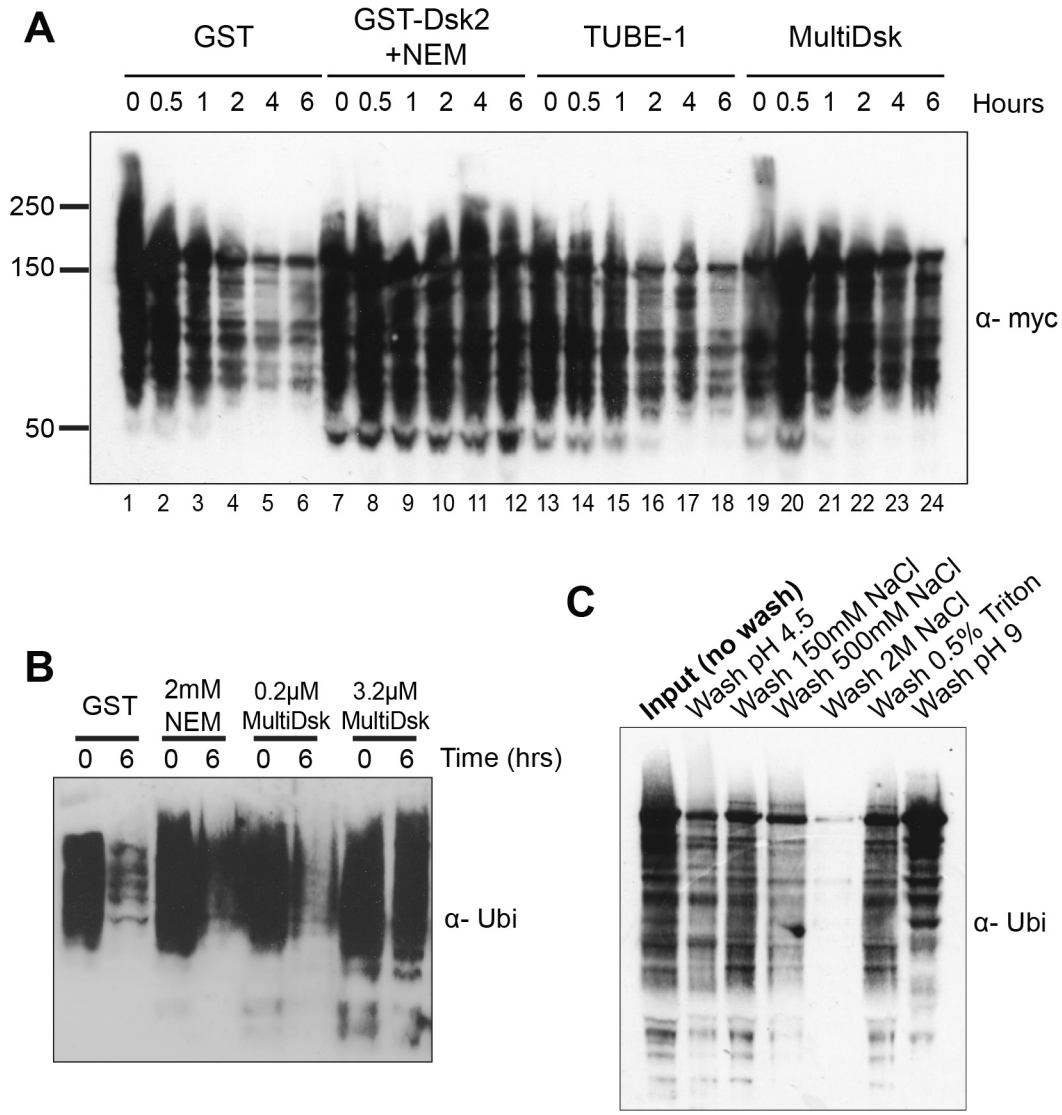

Figure 3.3: Protection of poly-ubiquitin chains in extract

A. Extract from strain SUB592 was incubated with equivalent amounts of GST, GST-Dsk2, commercially available TUBE-1, and MultiDsk (1.6 μM) and incubated at 30˚C for the indicated time. Total protein extracts were subject to Western blot and probed using anti-myc antibody.
B. As (A), except using wild-type cells and probing using a ubiquitin antibody. Different concentrations of MultiDsk proteins were used in the extract.
C. MultiDsk beads were incubated for 2 hours with 2mg of yeast extract and spun down. They were then washed three times under the stated conditions, before elution in sample loading buffer. Western blot was performed using anti-ubiquitin antibody (P4D1) to detect ubiquitylated species.

Over a 6-hour time-course, there is a loss of high molecular weight ubiquitin conjugates when yeast extract is incubated with GST control protein only (Figure 3.3, lanes1-6). In contrast, MultiDsk protein offered significant protection, despite use at a relatively low concentration (1.6 μM, or 0.4 μg MultiDsk per mg crude

yeast extract [lanes 19-24]), with a large retention of ubiquitylated species in solution. Whilst MultiDsk was not as effective as using a combination of GST-Dsk2 and a high concentration of chemical inhibitor (5 mM NEM [lanes 7-12]), it was significantly more potent than the commercially available alternative TUBE-1 (LifeSensors [lanes 13-18]). The chemical inhibitor, NEM, was the principal protecting agent in the GST-Dsk2–NEM mixture, as NEM on its own was sufficient to protect ubiquitylated proteins (Figure 3.3 B), whereas Dsk2 in isolation was not. Varying the concentration of MultiDsk protein used in extract affected the extent of protection, suggesting a direct stoichiometric affect of binding. Near complete ubiquitin-protein protection was observed by using a concentration of 3.2 µM or 0.8 µg MultiDsk per mg of crude yeast extract, over the 6-hour time course (Figure 3.3 B). In support of the direct stoichiometry hypothesis, this was also the estimated concentration required to completely deplete ubiquitylated proteins from the extract. When ubiquitylated proteins from extracts were pre-bound to the MultiDsk resin they were also protected from a broad range of purified DUBs (purchased from Boston Biochem), added *in vitro* (data not shown). These data show that the MultiDsk protein can be used not only as an affinity resin, but also as a protecting agent after cell lysis.

3.2.4 MultiDsks can be used to assess the changing ubiquitylation state of a protein

By using a resin that specifically enriches all ubiquitylated proteins we can assess how protein ubiquitylation changes under different conditions. When only a very small sub-fraction of the total cellular pool of a particular protein is ubiquitylated this cannot normally be visualised, as the signal from the unmodified version of the protein is typically much stronger and obstructs the signal from the modified form. It is also worth noting that all molecular weight shifts of 5-10 kDa should not be automatically assigned to ubiquitin, as many other post translational modifications can similarly alter electrophoretic mobility. Furthermore, for large proteins it is often impossible to observe the shift in molecular weight brought about by addition of the relatively small ubiquitin protein.

By using the MultiDsk resin to pull-out all ubiquitylated proteins - and wash away non-ubiquitylated contaminants - it is then possible to probe via Western blotting for the protein(s) of interest. To ensure that this is not due to contamination of non-ubiquitylated protein, an electrophoretic mobility shift - due to the addition of the extra molecular weight of ubiquitin or poly-ubiquitin - can often be observed by comparing to the migration of the input protein in the crude extract.

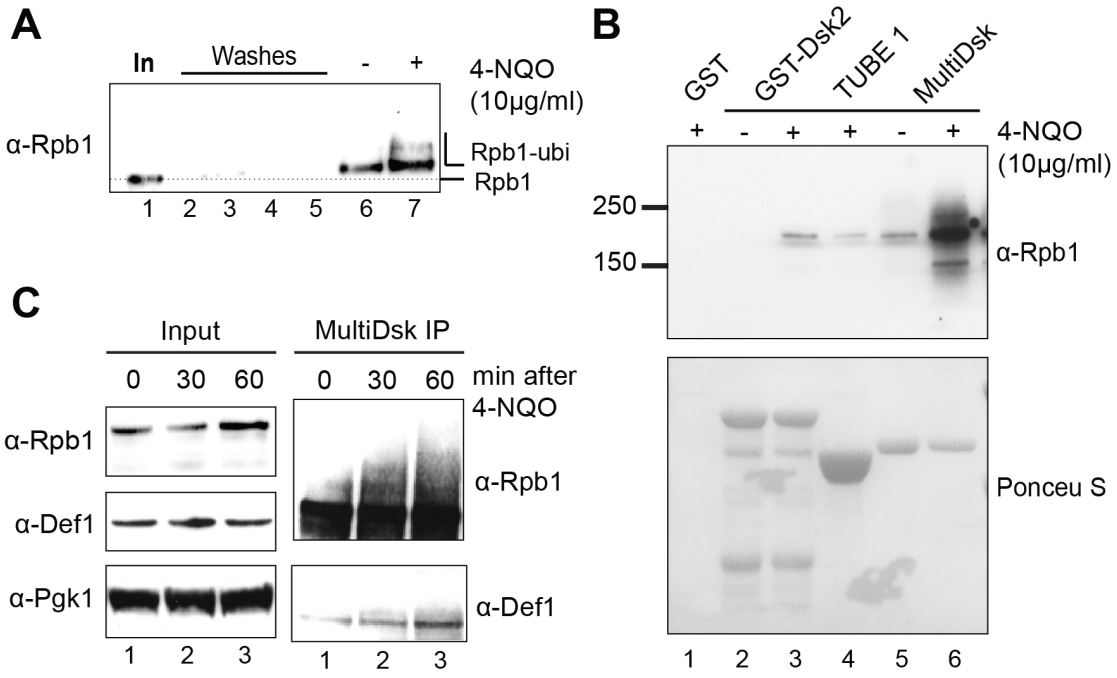

Figure 3.4: MultiDsks can be used to characterise the kinetics of ubiquitylation of a specific protein species

A. Cells were either treated with 4-NQO for one hour, or left untreated, as indicated. Equal amounts of extracts were incubated with MultiDsk resin. Dilute input extract (1%) and washes from the beads were also loaded. Proteins were analysed by Western blotting using anti-Rpb1 antibody, 4H8.
B. Exponentially growing yeast cells were either treated with 4-NQO for one hour, or left untreated, as indicated. Equal amounts of the extracts were incubated with agarose beads loaded with GST alone, GST-Dsk2 protein, commercial TUBE1, or MultiDsk. Proteins were eluted via boiling in sample buffer and subjected to Western blot analysis using the anti-Rpb1 antibody, 4H8 (upper panel). Ponceau S staining (lower panel) shows relative amounts of affinity proteins used.
C. Yeast cells were harvested at the indicated time after treatment with 4-NQO, incubated with MultiDsk resin, and isolated proteins were analysed by Western blotting using either 4H8, or an anti-Def1 antibody, as indicated.

This method was used for the 215kDa largest subunit of RNAPII, Rpb1, which becomes poly-ubiquitylated in response to DNA damage (Svejstrup, 2007 and see Introduction section 1.5.3). This is hypothesised to occur as RNAPII becomes persistently stalled at DNA lesions and needs to be removed. Importantly, this protein is also subject to numerous other post-translational modifications that have sometimes previously been misinterpreted as ubiquitylation events (Starita et al., 2005). To inflict consistent and reproducible DNA damage, 4-nitroquinoline 1-oxdide (4-NQO) was used. 4-NQO is commonly called a UV mimetic drug, which upon metabolism readily forms bulky DNA adducts on purines in DNA (Tanooka and Tada, 1975). These lesions are repaired by the nucleotide excision repair pathway, and promote the degradation of Rpb1 (Beaudenon et al., 1999). Using an Rpb1 CTD specific antibody, a signal in the MultiDsk pull-downs was observed, with a notable electrophoretic mobility shift compared to the Input (Figure 3.4A, compare lane 1 with lane 6 and 7 [stippled line]), corresponding to specific enrichment of ubiquitylated forms of Rpb1. Mono-ubiquitylation of Rpb1 appears to be relatively constitutive, as has been reported previously (Woudstra et al., 2002, Sigurdsson et al., 2010). The slower migrating, poly-ubiquitylated forms of Rpb1 resulting from DNA damage can also be detected (Figure 3.4 A, compare lanes 6 and 7).

Previously, GST-Dsk2 protein has been used to follow the ubiquitylation status of Rpb1 (Anindya et al., 2007, Harreman et al., 2009, Verma et al., 2011). To compare the MultiDsk to GST-Dsk2 and the commercially available TUBE-1 protein, roughly equal amounts of these proteins were immobilised on glutathione beads (Figure 3.4B, lower panel) and incubated with equal amounts of yeast extract. A weak ubiquitylated signal for Rpb1 was observed after DNA damage, when using the GST-Dsk2 protein (Figure 3.4B lanes 2 and 3). This correlated with overall reduced enrichment of ubiquitin conjugated proteins. A similarly weak Rpb1 signal was obtained when using the commercially available ‘TUBE- 1’ protein for ubiquitin enrichment (Figure 3.4B, lane 4). Only extract treated with 4-NQO was used in this case, and the TUBE-1 was more efficient than the single UBD GST-Dsk2 resin, though more TUBE-1 was also used (compare lanes 3 and 4). In both cases, a single band, corresponding to mono-ubiquitylated Rpb1, was observed with little or no higher molecular weight poly-ubiquitylation signal observed at the exposure

shown. In contrast, MultiDsk is much more efficient at enriching ubiquitylated Rpb1, so that both the constitutive, mono-ubiquitylated form (Figure 3.4B, lane 5), and the increased signal from induced Rpb1 mono-ubiquitylation and poly-ubiquitylation - stimulated by DNA damage - can be more readily observed (lane 6).

One of the benefits of using a resin that enriches only ubiquitylated proteins is that novel ubiquitylation targets can be identified. Any protein bound to the MultiDsk resin should be ubiquitylated; therefore using an antibody to the protein of interest will reveal if, and to what extent, it is ubiquitylated. Poly-ubiquitylation of Rpb1 has been shown to be reliant on Def1 (Woudstra et al., 2002), though little mechanistic detail, or information on how it is activated, has been reported (see subsequent Results chapters). By using a Def1-specific antibody we could use the MultiDsk ubiquitin pull-downs to assess if Def1 was modified. The Def1 antibody used throughout this thesis is a polyclonal rabbit antibody, raised against the C-terminal 350 amino acids of Def1. Unexpectedly, we observed the appearance of a band that cross-reacted with the Def1 antibody in MultiDsk extract pull-downs (Figure 3.4C), which increased with time upon exposure to 4-NQO. This band migrates at a slightly higher position than would be expected for unmodified Def1, suggesting that this is a new, DNA damage-inducible, mono-ubiquitylated form. This was Def1 specific band, no such band was observed upon enrichment of ubiquitylated proteins from *Δdef1* cells. There is a low basal level of Def1 mono-ubiquitylation, and possible higher molecular weight Def1 ubiquitin conjugates observable using this technique. Whether this is related to RNAPII ubiquitylation or part of the normal cellular degradation of Def1 is unclear. Indeed, previously ubiquitylation has been misinterpreted as having important functional consequences, when instead its role was in normal cellular recycling (Davies et al., 2010). However, the formation of mono-ubiquitylated Def1 has similar kinetics to that of the poly-ubiquitylation of Rpb1 and these events are indeed inherently interlinked. Furthermore, the mono-ubiquitylation of Def1 appears to be crucial for its function (see results presented in section 6.2.1). The MultiDsk resin can be used on any protein of interest under a wide variety of conditions, to identify dynamic changes in their ubiquitin post-translational modification state.

3.2.5 MultiDsks can be used to help purify ubiquitylated proteins to homogeneity

The MultiDsk resin allows the specific isolation of ubiquitylated proteins from cell extracts. As the MultiDsk protein can be eluted from glutathione beads by adding reduced glutathione, a second purification step can be introduced to specifically isolate the ubiquitylated form of a chosen protein.

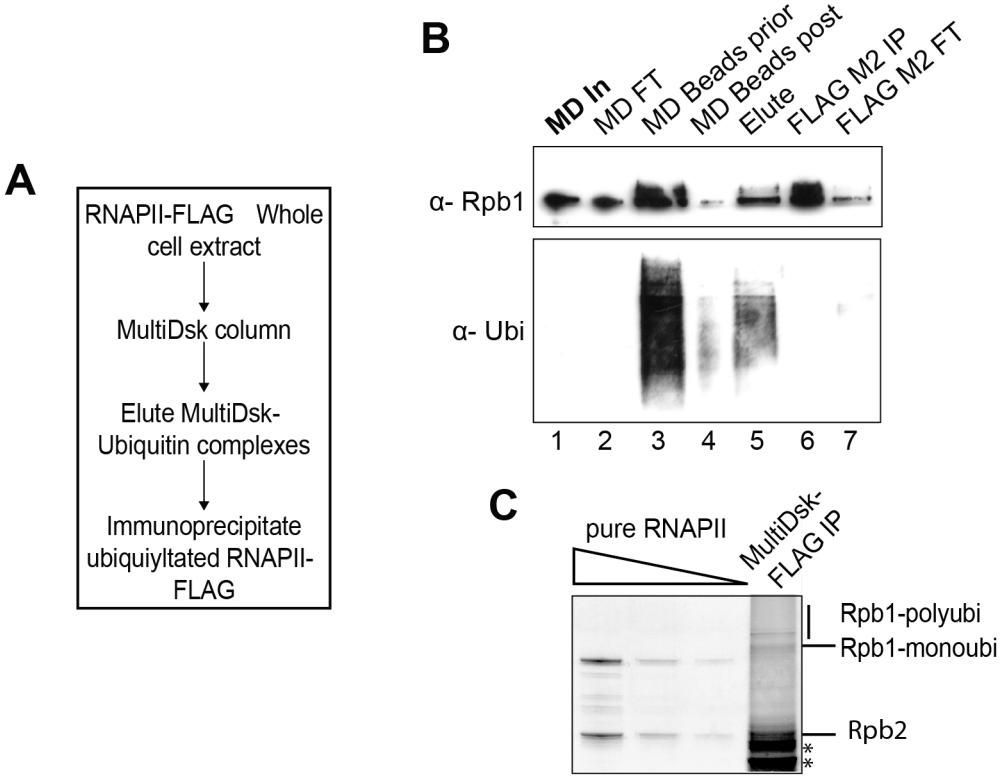

Figure 3.5: MultiDsks can be used to purify a specific ubiquitylated protein

A. A schematic of purification of ubiquitylated RNAPII from 4-NQO treated Rpb3-FLAG tagged cells. Cells were treated with 10µg/ml 4-NQO for one hour before extract was created.
B. Western blot of two-step purification, probed with anti-Rpb1 antibody (4H8) and anti-ubiquitin antibody (P4D1). MD-MultiDsk; In-input; FT-flow-through; IP-Immunoprecipitation.
C. Silver stain comparing FLAG immunoprecipitate post-MultiDsk enrichment (lane 6 from B) to pure Rpb3-FLAG tagged RNAPII. Different concentrations of pure RNAPII are loaded for comparison. Bands at corresponding heights are labelled, non-specific background bands from residual MultiDsk proteins are indicated by asterisks.

The validity of this approach was illustrated by the specific purification of ubiquitylated RNAPII from extracts prepared from an Rpb3-FLAG strain (Figure 3.5 A). Cells were treated with 4-NQO 1 hour prior to harvesting and cell lysis. Stringent washing allows the removal of non-modified forms of RNAPII from the MultiDsk beads (Figure 3.5 B lane 3). After glutathione elution, the ubiquitylated, FLAG-tagged, RNAPII can be purified using an anti-FLAG M2 affinity resin (Figure 3.5 B, lane 6). The high affinity antibody-epitope interaction allowed stringent (1M NaCl) washing that removes not only all the other ubiquitylated proteins, but also the majority of the MultiDsk protein that initially bound ubiquitylated-RNAPII. In a silver stain of the FLAG Immunoprecipitate, bands corresponding to Rpb2 and a shifted Rpb1 band can be observed (Figure 3.5 C), compared to RNAPII purified by conventional means (Cramer et al., 2001).

3.3 Conclusions

The MultiDsk protein is a novel protein tool useful for depletion and protection of ubiquitylated proteins *ex vivo*. MultiDsk binds strongly and specifically to ubiquitylated protein species and allows the unbiased enrichment of a small, often unstable pool of proteins. The resin provides a useful tool for the analysis of protein ubiquitylation and will be used extensively elsewhere in this thesis.

Chapter 4. Discussion I

MultiDsks: A Ubiquitin Specific Affinity Resin

The data presented here indicate that the MultiDsk protein offers an excellent alternative to the previously used methods for studying protein ubiquitylation. The MultiDsk can be used to obtain pure, native, non-tagged ubiquitylated proteins from cell extracts, as well as to ensure the maintenance of the their ubiquitylation state, via a strong protective function, which blocks cellular de-ubiquitylating enzymes (DUBs).

4.1 The High Avidity Interaction of MultiDsk

By combining multiple ubiquitin binding domains (UBDs) from the yeast Dsk2 protein, a dramatic synergistic increase of affinity for ubiquitylated proteins was achieved. The amount of ubiquitylated protein isolated with MultiDsk was far greater than that obtained with the single UBD containing GST-Dsk2 and significantly greater than the commercially available TUBE-1 protein.

In all likelihood, the interaction of the MultiDsk is imparted through the synergistic action of the multiple UBDs engaging with the same ubiquitin chain. Whilst only 4 ubiquitin moieties are sufficient to target proteins to the proteasome (Thrower et al., 2000), *in vivo* chains of all topologies often extend much further Kim and Huibregtse, 2009. The TUBE-1 protein displays approximately 1,000 times greater avidity to poly-ubiquitin chains compared to a single UBD (Hjerpe et al., 2009). Whilst the affinity for each UBD to ubiquitin is thought to remain constant, the co-operative action of multiple binding surfaces, engaging simultaneously, increases the overall avidity. Indeed, the relationship is probably non-linear for the interaction of subsequent UBDs, due to the reduced entropic penalty after the initial UBD binding.

The increased avidity of the MultiDsk protein over the TUBE-1 protein is likely due to the increased individual affinity of each UBD and the presence of a fifth, additional UBD. The UBA domain from HR23A, which is used in the TUBE-1 protein, has a K_d of 40-60μM (Hjerpe et al., 2009, Withers-Ward et al., 2000), whilst the Dsk2 UBA domain has a much higher individual affinity, with a K_d of around 15μM (Ohno et al., 2005). Whilst the MultiDsk resin appears to be more efficient at enriching ubiquitylated proteins than all other alternatives, the exact biophysical data to substantiate this case is lacking. Further work to provide quantitative values of affinity - using a technique such as surface plasmon resonance - is required to confirm the observed comparative, qualitative high avidity.

4.2 Specificity of MultiDsk

Importantly, the MultiDsk resin does not appear to discriminate between different kinds of ubiquitin chains. This is at least the case for the two most prevalent ubiquitin chains present in the cell, Lys-48 and Lys-63. Similarly, the binding to single free ubiquitin and mono-ubiquitylated proteins is better for MultiDsk than the single UBD protein, GST-Dsk2. The full-length Dsk2 protein is known to interact specifically with Lys-48 chains (Funakoshi et al., 2002), whilst the isolated UBA domain alone does not show such preference (Raasi et al., 2005, Ohno et al., 2005). Some isolated UBA domains do exhibit Lys-48 specificity (Varadan et al., 2005, Trempe et al., 2005), through dual ubiquitin interaction surfaces, the second of which contains a conserved phenylalanine residue. This is not present in Dsk2's UBA (Ohno et al., 2005, Zhang et al., 2008). Therefore, the chain topology preference of the Dsk2 protein may be due to the exact spatial orientation of its UBA domain within the full-length protein, or its oligomerisation state (Lowe et al., 2006, Sasaki et al., 2005).

The MultiDsk construct was deliberately designed with a flexible linker between UBA domains, possibly allowing the free rotation of these domains to accommodate multiple chain topologies. Lys-48 and Lys-63 chain linkages only

account for roughly half of all chain linkages in yeast cells (Xu et al., 2009a). Unfortunately, synthetic poly-ubiquitin chains of the untested linkages are not currently available, preventing *in vitro* interaction studies with MultiDsk. However, all ubiquitylated proteins were depleted from cell extracts, suggesting that MultiDsk can also interact with the other, minor chain linkages. Future biochemical experiments are required to assess whether MultiDsk exhibits any chain preference.

The ubiquitin field is increasingly recognising the importance of Ubiquitin-like (Ubl) proteins, which can also covalently mark proteins post-translationally (van der Veen and Ploegh, 2012). The exact prevalence of these modifications is unclear, but for Smt3 (yeast SUMO) targeting appears to be restricted (Hannich et al., 2005). These Ubl modifications tend to utilise their own conjugation apparatus (Johnson and Gupta, 2001), recognition apparatus (Pfander et al., 2005) and deconjugation enzymes (Cope et al., 2002). However, recent work has suggested that the highly ubiquitin-homologous Rub1 - or human Nedd8 - can be utilised by ubiquitin ligases, integrated into ubiquitin chains and recognised by UBDs (Hjerpe et al., 2012, Leidecker et al., 2012, Singh et al., 2012). Critically, Rub1 interacts, with a similar affinity as Ubiquitin, with the UBA domain from the human homologue of Dsk2 (Singh et al., 2012). In our experiments, MultiDsk pull-downs did not appear to appreciably enrich Rub1 or Smt3 conjugates. However, these proteins were identified using human isoform specific antibodies with poor Ubl detection in crude extracts. Direct *in vitro* evidence and better - yeast specific - antibodies are required to further substantiate these conclusions.

4.3 Using MultiDsk as a Protein Reagent

The MultiDsk protein also acts to preserve poly-ubiquitylated proteins in extracts, avoiding the need for hazardous chemical DUB inhibition. The MultiDsk protein provides a significant protective role at concentrations as low as 0.2 μM (Figure 3.3 B), making it suitable for use in even large-scale extract-based experiments. It is interesting to note that the protective role of both the MultiDsks and commercial

TUBE- 1 was not complete at the concentrations used in this study. A previous report (Hjerpe et al., 2009) suggested that a TUBE- 1 concentration of 1.6 μM was sufficient for complete protection from cellular DUBs. However, these protection assays were performed using human extracts, rather than *S. cerevisiae* extracts, suggesting that the problem posed by non-specific DUBs is greater in yeast. It is likely that the MultiDsk protein protects poly-ubiquitin chains through direct steric occlusion of DUB enzymes from their substrates.

One of the expected problems of working with proteins as reagents is their inherent low stability (Taverna and Goldstein, 2002). Proteins unfold and degrade under non-physiological temperatures, pHs and salt concentrations. However, the MultiDsk protein can withstand complete unfolding and refolding (Figure 3.1 C). Furthermore, the interaction of MultiDsk with ubiquitylated proteins is stable under a range of pHs and <1M sodium chloride (Figure 3.3 C). In the Svejstrup lab, GST-Dsk2 was previously used to enrich ubiquitylated proteins. This protein is unstable in its purified state (see Figure 3.4 B, lower panel lanes 2 and 3), and unusable within 2 weeks after storage at 4^{o}C. The MultiDsk protein appears to be far more stable; MultiDsk resin retains activity for upwards of 6 months and can be stored pure at -20^{o}C for up to a year.

Unfortunately, as a tool for assessing the whole ubiquitome, the large amount of MultiDsk protein required, coupled with the inability to easily release bound ubiquitylated proteins, somewhat limits MultiDsk use in mass spectrometry. However, as a tool for assessing the ubiquitylation state of an individual protein, MultiDsk is a uniquely specialised reagent. The resin was used to follow the ubiquitylation status of two proteins, Rpb1 and Def1, after treatment with DNA damage. It is important to note that by pulling out the ubiquitylated protein in its native state, the molecular weight shifts could be due to numerous post-translational modifications, one of which is probably ubiquitylation. Some post-translational modifications occur concurrently; Rpb1 SUMOylation and ubiquitylation occurs under the same transcription stall conditions (Chen et al., 2009) and SUMO directed ubiquitin E3 ligases have been identified (Uzunova et al., 2007). Care must be taken not to over-interpret MultiDsk pull-down data.

We have shown that it is possible to purify *in vivo* ubiquitylated proteins using the MultiDsk resin coupled to traditional protein purification techniques. As the majority of the MultiDsk protein can be removed using high salt washes, a native ubiquitylated form of a protein can be isolated and used for further biochemistry, eliminating the need for *in vitro* ubiquitylation reactions. However, as only a sub-fraction of cellular proteins tend to be ubiquitylated; a larger amount of extract starting material is required to enrich proteins to the same extent.

Since publication (Wilson et al., 2012), the plasmid expressing the MultiDsk protein has been requested by multiple laboratories worldwide and is proving to be a valuable research tool for the isolation of ubiquitylated proteins in a number of different systems.

4.4 Implications for the Rpb1 Poly-ubiquitylation Pathway

The MultiDsk resin was used to assess the ubiquitylation status of two proteins involved in the 'last-resort' Rpb1 poly-ubiquitylation pathway (see 1.5.3). The high avidity of MultiDsk enabled the total depletion of the ubiquitylated forms of the proteins from extracts and allowed the ubiquitin status of Rpb1 and Def1 to be evaluated, after treatment with DNA damaging agents. RNAPII mono- and poly-ubiquitylation are separate steps that are catalysed by different E3 ligases. Whilst initial mono-ubiquitylation is required for the subsequent poly-ubiquitylation of Rpb1 (Harreman et al., 2009), there is a basal level of mono-ubiquitylation under normal, unstressed, conditions. The extent of this mono-ubiquitylation has been unclear, partially due to the preference of the GST-Dsk2 resin, which was used previously, for poly-ubiquitin chains (Funakoshi et al., 2002, Zhang et al., 2009). MultiDsk does not seem to display such a preference (Figure 3.2 B). Illuminatingly, the levels of Rpb1 between the input (loaded with 1% of protein used in the assay) and pull-downs were roughly equivalent; suggesting that at least 1% of all total RNAPII is modified by mono-ubiquitin, in the absence of induced transcription stress (Figure

3.4 A). Whether this mono-ubiquitylation has a functional relevance, outside of its role as an intermediate in degradation, is currently unclear.

Def1 has not been previously shown to be ubiquitylated from whole genome approaches, or from more tailored, directed investigations (Peng et al., 2003) attesting to the high sensitivity of the MultiDsk. resin. However, since this project was initiated, a number of studies have identified three separate ubiquitylated Def1 peptides (Starita et al., 2012, Beltrao et al., 2012). Further work in this thesis has identified four additional lysine residues of Def1 that are ubiquitylated in response to DNA damage (see section 6.2.1). Interestingly, it appears that Def1 is inducibly mono-ubiquitylated with a similar kinetic to that of Rpb1 poly-ubiquitylation. Since we know that Def1 is required for this Rpb1 poly-ubiquitylation, it is tempting to speculate that Def1 mono-ubiquitylation plays a role in the activation of this protein. Evidence for a role for Def1 ubiquitylation is covered later (see section 6.2.1).

In order to explain the substantial Rpb1 degradation that is observed after DNA damage, the minor fraction of poly-ubiquitylated Rpb1 must be very short lived, and under constant turnover. However, it is interesting to note that RNAPII poly-ubiquitylation can be separated from degradation (Verma et al., 2011). We have tended to interpret the two events as inherently linked, due to the rapid proteasomal degradation of poly-ubiquitylated Rpb1 (Luo et al., 2001, Beaudenon et al., 1999). For all the experiments shown in this thesis both Rpb1 ubiquitylation and degradation were observed under the same conditions, even if not shown. RNAPII can also be modified with non-degradable, Lys-63 chains (Harreman et al., 2009). In future studies it would be critical to ascertain the nature of the ubiquitylation status of Rpb1 and whether this leads to proteasomal degradation.

Notably, Rpb1 levels do not appear to reduce in the inputs of Figure 3.4 C, despite robust poly-ubiquitylation. This may be due to the Rpb1 antibody used, which is specific towards hyper-phosphorylated Rpb1, known to be induced upon DNA damage (Rockx et al., 2000, Mitsui and Sharp, 1999). The phosphorylation state of Rpb1 helps to distinguish it for poly-ubiquitylation (see introduction, 1.5.3.5). As a result, whilst the overall levels of Rpb1 may be decreasing, the phosphorylated levels detected with this antibody may be higher, leading to the apparent lack of

Rpb1 degradation. This phospho-specific antibody was not used to measure Rpb1 degradation elsewhere in the rest of this thesis.

Chapter 5. Results II
Def1 Partial Proteolytic Processing

5.1 Aims

Def1 protein - from the yeast *Saccharomyces cerevisiae* - was originally identified by the Svejstrup lab as an interacting partner of Rad26p in chromatin (Woudstra et al., 2002). Whilst Rad26 is the key yeast protein mediating transcription coupled-nucleotide excision repair (TC-NER), Def1 does not appear to function directly in this pathway. Instead, Def1 is a critical player in the alternate, back-up pathway to TC-NER, namely the poly-ubiquitylation and degradation of Rpb1. Cells that lack Def1 exhibit normal TC-NER and are not UV sensitive, but do not poly-ubiquitylate and degrade Rpb1 after DNA damage. This effect is direct: poly-ubiquitylation of RNAPII can be reconstituted in an extract based *in vitro* assay and is entirely reliant upon Def1 (Reid and Svejstrup, 2004).

Def1 has also been implicated directly in telomere maintenance and mitochondrial retention (Chen et al., 2005). Genetic studies have revealed a number of cellular deficiencies in *def1Δ* cells (Jordan et al., 2007, Manogaran et al., 2011, Cai et al., 2006, Suzuki et al., 2011). Despite a clear role in ubiquitylation of chromatin-associated RNAPII, localization studies assigned Def1 to the cytoplasm (Huh et al., 2003, Tkach et al., 2012).

In spite of years of extensive research on Def1 the molecular role of the protein in the mechanism of Rpb1 poly-ubiquitylation was still unknown. Intriguingly, prior to work presented here, Western blots of extracts from DNA damaged cells - with antibodies raised against Def1 - showed a faster migrating, cross-reacting, band that was not present in the untreated controls. This band was also reproducibly observed under other conditions of transcription stress. The aim of my project was to further investigate the nature of this inducible, smaller form of Def1. Some of this work overlapped with the efforts of Michelle Harreman, a postdoctoral fellow in the

Svejstrup lab. Therefore, some of the figures presented below were the product of Michelle Harreman's experiments. These are clearly labelled as such.

5.2 Results

5.2.1 The faster migrating band corresponds to a N-terminal fragment of Def1

Def1p is a 738 amino acid protein with a predicted molecular weight of 86 kDa. The protein contains only one identified functional domain; a CUE domain identified *in silico* (Ponting, 2002; Figure 5.1 A). Strikingly, greater than 40% of the C-terminal half of the protein sequence is composed of glutamines, possibly explaining the unusual mobility of Def1 on SDS-PAGE: Def1 runs at around 120 kDa (Figure 5.1 B). As observed previously (see above), a collection of similar, faster-migrating, protein bands, cross-reacting with the Def1 antibody, appear after 4-NQO treatment (Figure 5.1 B), or after exposure of cells to 254 nm UV-B light (Figure 5.1 C). These conditions are known to cause bulky, helix-perturbing DNA damage (Kim et al., 1995, Tanooka and Tada, 1975) and block the path of RNAPII along a transcribed gene (Svejstrup, 2007). Long RNAPII pauses are signals for DNA repair, or eventually RNAPII poly-ubiquitylation. Intriguingly, the faster-migrating Def1 bands appear at a similar kinetic to that of Rpb1 poly-ubiquitylation (Figure 5.1 C) and subsequent degradation (Figure 5.1 B). The faster-migrating Def1 bands runs at a molecular weight of around 90kDa, commonly as a doublet. These bands are only observed if the processed samples are run immediately after cell lysis. The bands are not stable in extracts even in the presence of SDS-PAGE loading buffer, possibly due to the action of uninhibited vacuolar proteases. It should be noted that the Def1 antibody shows some preference for the lower form of Def1 over the full-length protein. As a result, the lower, p90, bands are often clearly seen in Western blots, with no appreciable reduction in the full-length p120 Def1 signal.

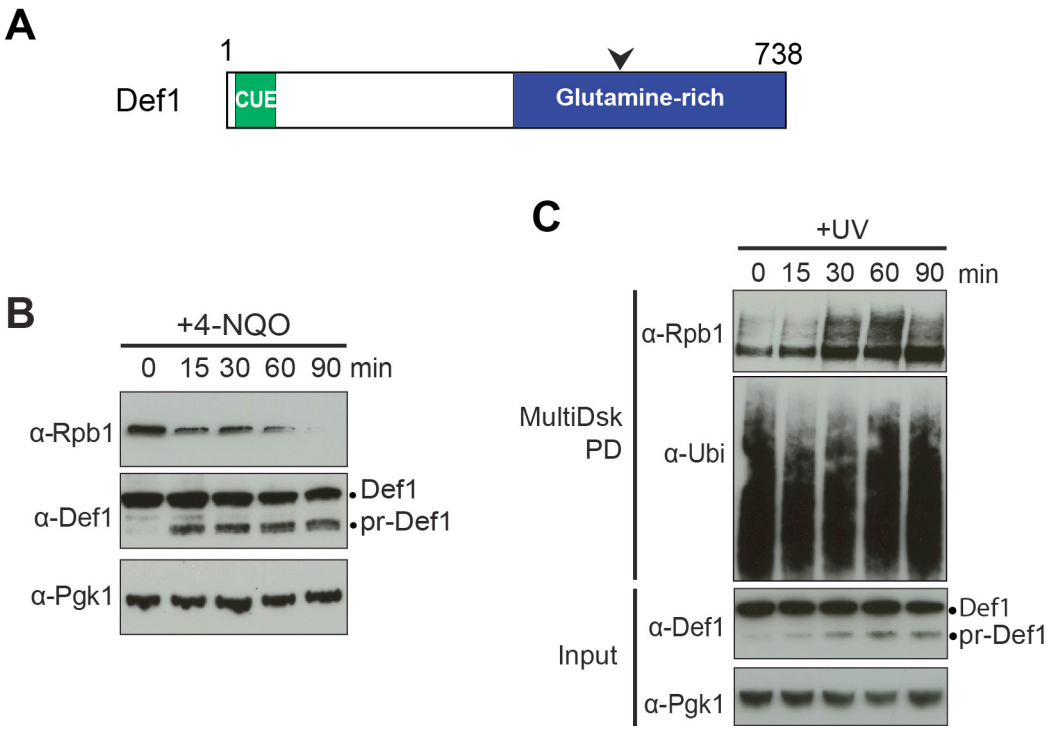

Figure 5.1: A faster migrating Def1 band appears after transcription stress

A. Schematic representation of Def1 indicating the CUE domain, approximate area of processing site (arrow), and glutamine rich region.
B. Quick extracts (2.5.10) from 4-NQO exposed cells, Immunoblotted using antibodies against Rpb1 (8WG16), Def1, and Pgk1 (loading control).
C. Extracts from UV-irradiated cells analysed by Western blotting at the indicated times as in (B). Ubiquitylated Rpb1 isolated from the extract using MultiDsk pull-down (PD) and probing for Rpb1 (4H8) (as Figure 3.4). Ubiquitin pull-down loading confirmed by probing for ubiquitin (P4D1).

In order to assess the conditions under which the faster migrating band was observed, cells were subjected to a number of cellular stresses (Figure 5.2). The lower band (hereafter referred to as processed-Def1 or pr-Def1) might be formed as a general response to DNA damage in a separable, independent pathway to Rpb1 degradation. Alternatively, these processes may be inherently interlinked. Rpb1 degradation occurs as a consequence of persistent transcription stall. This is commonly induced using DNA damaging agents, which chemically alters the read DNA so it can no longer be transcribed. RNA synthesis can also be blocked by the depletion of rNTP pools, leading to RNAPII stalling in the absence of DNA damage (Archambault et al., 1992). 6-azauracil (6-AU) inhibits IMP dehydrogenase, the rate-limiting enzyme in biosynthesis of GTP. 6-AU treatment rapidly leads to the depletion of cellular GTP pools (Exinger and Lacroute, 1992) and the stalling of

RNAPII. After inducing stalling by treatment with 6-AU, the processed form of Def1 also appears (Figure 5.2 A). The appearance of pr-Def1 after 6-AU treatment is slow, compared to treatment with DNA damaging agents. Similarly treating cells with 6-AU leads to slower RNAPII poly-ubiquitylation, compared to treatments that cause DNA damage (Somesh et al., 2005).

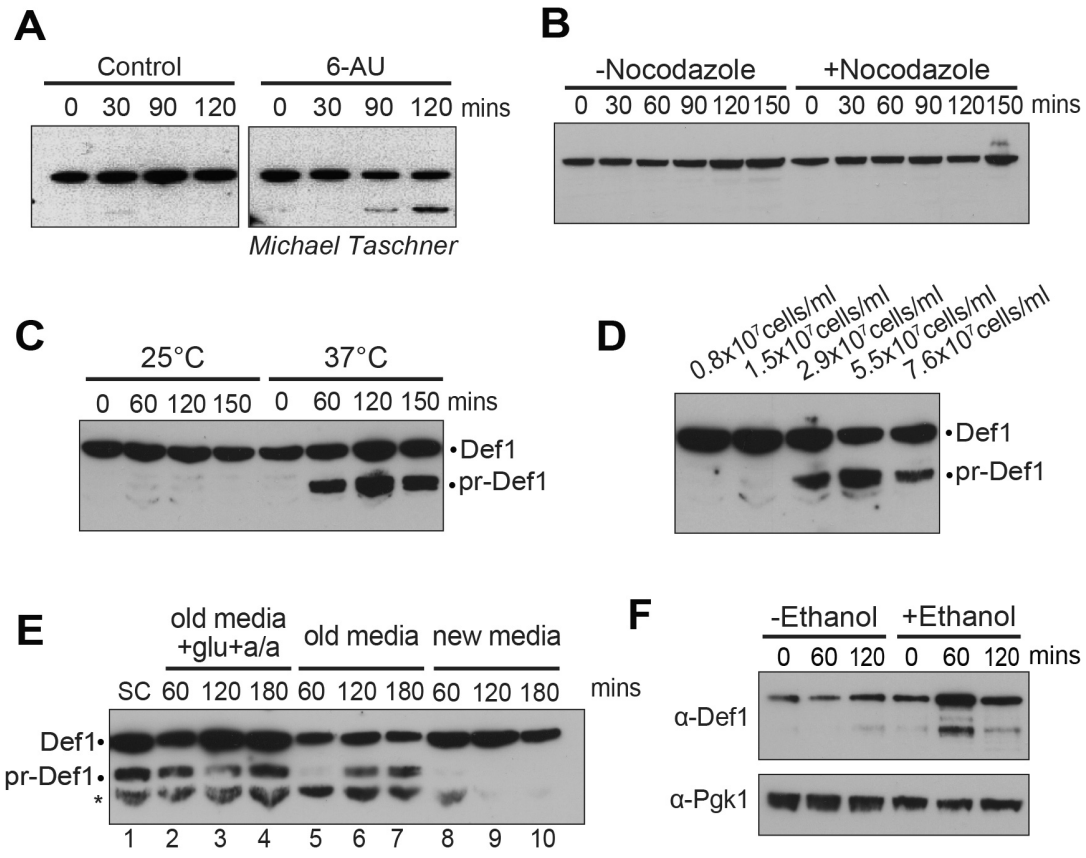

Figure 5.2: pr-Def1 occurs after cellular stress

A. Cells were incubated in the absence (control) or presence of 6-azauracil (6-AU), and extracts analysed by Western blot using the Def1 antibody. Michael Taschner performed this experiment.
B. Cells were G2 arrested using nocodazole; by the final time point all cells in nocodazole treated sample were double-budded, whilst the control cells showed a normal asynchronous budding pattern. Quick extracts were run on SDS-PAGE and Western blotted using the anti-Def1 antibody.
C. Extracts from cells grown at below (25^{o}C) and above (37^{o}C) optimal growth conditions. Cells were shifted from 30^{o}C and samples taken at the indicated timepoints. Western blotting was performed with the anti-Def1 antibody.
D. Quick extracts from equal cell numbers were created from the same culture as it proceeded through logarithmic growth. Cells were counted every 90 minutes and 1.5x10^{7} cells extracted. Western blot using anti-Def1 antibody.

E. Stable logarithmic-phase growing cells were harvested and resuspended in pre-warmed YPD (2.1.2.1). Either fresh YPD (lanes 8-10), YPD supernatant taken from stationary phase cells (lanes 5-7) or YPD taken from stationary phase culture supplemented with 2% glucose and 40 µg/ml amino acids was used. Lane 1 corresponds to equivalent cell numbers from the stationary phase culture (SC). Quick extracts were analysed by Western blot using the Def1 antibody. Asterisk corresponds to non-specific band occasionally observed with the Def1 antibody.
F. Cells were incubated with YPD supplemented with or without 3% ethanol, for the indicated time periods. Quick extracts were analysed by Western blot using anti-Pgk1 and anti-Def1 antibodies.

The treatment of cells with DNA damaging agents or transcription inhibitors not only blocks RNAPII, but also perturbs normal yeast cell cycle progression. To discount the possibility that the faster migrating pr-Def1 band is formed in a cell cycle-specific manner, cells were treated with a microtubule depolymerisation agent, nocodazole, blocking cells in G2 phase (Figure 5.2 B). No processed band was formed as the cells became synchronised, confirmed by the observation of cells in a dual-budded state. Treatment of *MATa* cells with α-factor arrests them in the G1 phase of the cell cycle (Bucking-Throm et al., 1973). Similarly to nocodazole treatment, α-factor treatment did not result in the processing of Def1 (data not shown). This data suggests that pr-Def1 forms as the direct result of transcription stress, rather than due to any off-target or downstream signalling effects of the agents used.

Interestingly, Def1 also becomes processed under a wide variety of other cellular stresses. Cells shifted to a permissive, but higher than optimal, growth temperature also produce pr-Def1 (Figure 5.2 C). As cells entered late logarithmic growth phases, and cell density increased, Def1 was also processed (Figure 5.2 D). Puzzlingly, this occurred at middle-to-late log growth phase, when growth conditions are not limiting. This was not due to direct overcrowding; cells at a low cell density incubated with old media - taken from cells at high cell density - also exhibited Def1 processing (Figure 5.2 E lanes 5-8). Supplementing the old, pre-used media with essential amino acids and glucose did not prevent the formation of pr-Def1 (Figure 5.2 E, lanes 2-4), suggesting that the processing stimulus in this case is an accumulating waste product, rather than a declining nutrient source. Despite growth in aerobic conditions, *S. cerevisiae* commonly respires anaerobically in the presence of excess glucose (Crabtree, 1928). This produces

ethanol as a by-product, which becomes toxic at high concentrations. Addition of 3% ethanol - a concentration that the strain used in this study could tolerate (Dinh et al., 2008) - was sufficient to induce some Def1 processing (Figure 5.2 F). This suggests the Def1 processing seen at high cell density may, at least in part, be due to the accumulation of toxic metabolic by-products.

In conclusion, pr-Def1 formation occurs not only in response to transcription stress, but also more widely as a response to a variety of cellular stresses. Whether these stress conditions trigger Def1 processing by affecting transcript elongation through RNAPII is presently unclear and requires further study. The remainder of the current work will focus completely on the robust induction of pr-Def1 observed upon DNA damage, and on its effect on Rpb1 ubiquitylation and degradation.

5.2.2 The N-terminal fragment is not a new protein product of Def1

To investigate the identity of the faster-migrating pr-Def1 band, the genomic version of Def1 was tagged at either the N- or C-terminus (JSY 1198 and 642, respectively). After treating the tagged strains with agents that cause DNA damage, extracts were subjected to Western blotting to detect the proteins, using polyclonal antibodies raised against Def1. When tagging the protein at its N-terminus, the migration of both the full-length Def1 protein and pr-Def1 was shifted upwards in the gel, compared to the wild-type protein (Figure 5.3 A, left). This suggests both forms of Def1 contain the N-terminal tag and consequently both are of higher molecular weight than their wild-type equivalents. In contrast, whilst the full-length protein - tagged at the C-terminus - was shifted upwards in the gel, the pr-Def1 band was not (Figure 5.3 A, right), strongly indicating that pr-Def1 does not contain the C-terminal tag. Indeed, pr-Def1 could not be detected when using an antibody against the C-terminal tag (data obtained by Michelle Harreman, not shown). These results suggest that pr-Def1 corresponds to an N-terminal product of Def1.

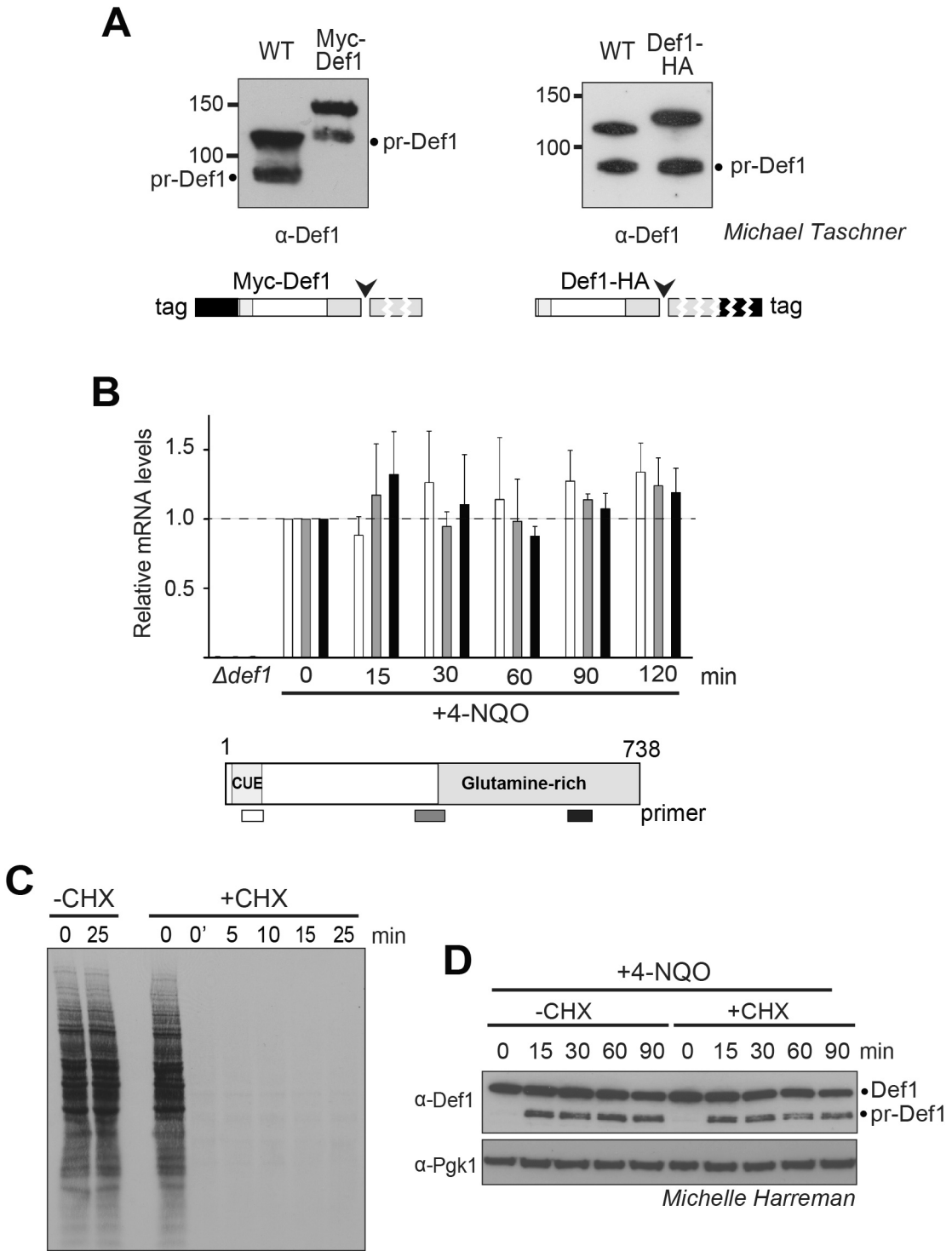

Figure 5.3: Full length Def1 protein is processed to an N-terminal fragment

A. Western blot showing WT or tagged Def1, after incubation of cells with 4-NQO for 1 hour. (Left panel) The WT strain was compared to a N-terminally Myc tagged strain (JSY1198). (Right panel) as above, but with cells expressing C-terminally 6xHA-tagged Def1 (JSY642), performed by Michael Taschner.
B. Quantification of relative mRNA levels of Def1 after 4-NQO treatment. Quantification normalised to β-actin levels in each sample, then against untreated conditions (time$_0$). Primers

were used from the start (white), middle (grey) and end (black) of the Def1 gene. Error bars correspond to the standard deviation across three biological replicates.
C. Def1 processing occurs post-translationally. (Left) Autoradiogram of SDS-PAGE gel, showing cellular proteins, radioactively labelled *in vivo*. Protein synthesis was inhibited by the addition of 25 µg/ml cycloheximide to mid-log cells at time 0, and new protein synthesis measured by incorporation of radioactive label in proteins (S35-methionine pulse initiated at the times indicated after cycloheximide inhibition). Time point 0' was transferred to grow in radioactive methionine immediately after addition of cycloheximide.
D. Cells were pre-treated with cycloheximide (CHX) – to block protein translation – 5 minutes prior to the addition of 4-NQO. Quick extracts were collected for analysis by Western blot using anti-Def1 antibody.

The N-terminal pr-Def1 fragment could arise through three possible mechanisms. Firstly, upon cellular stress and transcription stall, a different mRNA product might be transcribed from the *DEF1* gene that encodes only the N-terminal section of Def1. This could occur through alternate stop-site usage or splicing removing the 3' end of the gene. To assess these possibilities, the level of Def1 mRNA was measured under pr-Def1-inducing conditions by treating cells with 4-NQO (Figure 5.3 B). Three separate primer sets were used that amplified the start, middle, or end of the coding region, respectively (Figure 5.3 B lower). Def1 mRNA levels did not change significantly across the body of the gene, including the 3' coding end of the gene (Figure 5.3 B, black bars), suggesting that the mRNA product was not altered by DNA damage. It is worth noting that overall *DEF1* mRNA levels did decrease after damage induction; however, this was not significantly reduced when compared with total mRNA (the data presented here has been normalised to the mRNA from the housekeeping gene β-actin). The half-life of *DEF1* mRNA produced from the *GAL* promoter is around 5 minutes (data not shown). Assuming that this is also true for *DEF1* mRNA produced from its own promoter, the mRNA detected at the time-points used here should be predominantly synthesised after DNA damage.

A second possible explanation for the formation of the shorter pr-Def1 band is that Def1 is being alternately translated after DNA damage, or co-translationally cleaved, forming the N-terminal, pr-Def1 fragment. A direct, metabolic labelling, pulse-chase approach to detect the formation of pr-Def1 from full-length Def1 was not successful. The pr-Def1 band formed is a minor proportion of the total cellular Def1 and was below the detection limit of the experiment performed.

Instead, the relationship between pr-Def1 formation and translation was assayed by blocking protein synthesis. In these experiments, cells were first pre-incubated with cycloheximide, an inhibitor of the translocation step of translation, before DNA damage was induced. In order to assay the effectiveness of cycloheximide, cells were treated with a pulse of S-35-Methionine before or after the addition of cycloheximide (Figure 5.3 C). Addition of cycloheximide almost immediately shut-off protein synthesis. Indeed, even the earliest time point (0', corresponding to the time taken between addition of cycloheximide and the addition of S-35-Methionine) showed little to no radioactive methionine incorporation. As a result cells were pre-treated with cycloheximide for only 5 minutes, to shut-off all protein production, prior to the addition of damage inducing 4-NQO. As can be seen in Figure 5.3 D, even in the absence of new protein synthesis, pr-Def1 still forms after transcription stress, suggesting that pr-Def1 formation is not dependent on active translation.

The pr-Def1 band was not formed as a result of altered transcription or translation. Therefore, only one option remains: pr-Def1 protein must be formed from the full-length protein post-translationally, in all likelihood as the result of a proteolytic cleavage event. All subsequent experiments presented in this thesis are consistent with this hypothesis; pr-Def1 appears to be the proteolytically cleaved product formed from full-length Def1. We have not been able to detect the C-terminal fragment of the protein, despite using multiple different detection methods (data not shown). We, therefore, assume that the C-terminus is degraded during the proteolytic cleavage or immediately thereafter.

5.2.3 Mapping the site of processing: activity of truncation mutants

The data above suggest, but do not prove, that the pr-Def1 (p90) fragment is created post-translationally, by proteolysis, from full-length Def1 (p120). This suggests there is a direct site of proteolytic cleavage, which consistently produces two similar molecular weight N-terminal fragments. Unfortunately, due to the unusual electrophoretic mobility of Def1, the molecular weight of the supposed p90

pr-Def1 fragment was unclear. In order to map the processing site of Def1, a library of C-terminal genomic truncations of the *DEF1* gene were created (JSY 1176-1181), for comparison to the processed band on Western blot.

When the endogenous *DEF1* gene is truncated by recombination, small C-terminal deletions had little or no effect on the growth of cells, whilst large C-terminal truncations resulted in a similar slow-growth phenotype as the null strain (Figure 5.4 A). Interestingly, a former Svejstrup lab postdoc, Jim Reid, had previously obtained preliminary evidence that $Def1_{1-400}$ and $Def1_{1-500}$ could not be generated using this method, a result confirmed by Michelle Harreman. This was not an artefact of the method used: a diploid strain expressing both $Def1_{1-500}$ and a wild-type copy of Def1 could be created (JSY 1182). This strain grew normally and could be sporulated and tetrad dissected into haploid spores. However, only two of the four spores were ever viable and these contained the wild-type, full-length version of Def1 (Figure 5.4 B), as confirmed by PCR. We therefore surmised that expressing the shorter Def_{1-400} or $Def1_{1-500}$ was extremely detrimental to the cell. As pr-Def1 is also an N-terminal product, we hypothesised that genomically deleting the C-terminus artificially mimicked constitutive processing of Def1.

When GAL-regulated Def1 was expressed on plates containing galactose, this rescued the slow growth phenotype of *Δdef1* cells. In contrast, and in support of the above hypothesis, galactose driven expression of $Def1_{1-500}$, prevented the growth of *Δdef1* cells (Figure 5.4 C), exacerbating the slow growth phenotype. As the over-expression of $Def1_{1-500}$ is toxic to the cell, it seems reasonable to hypothesise that the formation of pr-Def1 - induced by DNA damage and transcription stress – is harmful if not tightly controlled. Over-expression of the Def1 C-terminal fragment ($Def1_{500-738}$) concomitantly with $Def1_{1-500}$ did not overcome the toxicity of the N-terminal fragment (data not shown).

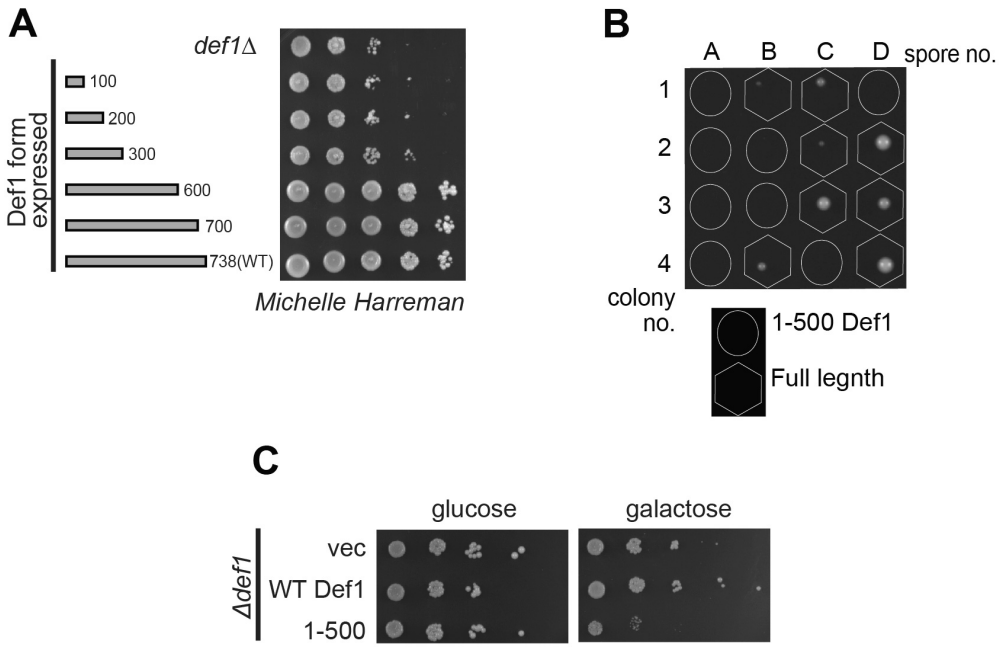

Figure 5.4: Def1 C-terminal deletions can be toxic to the cells

A. Dilution growth series (2.5.6) of cells expressing Def1 N-terminal fragments, grown on YPD-agar. No viable clones could be acquired for *def1*$_{1\text{-}400}$ or *def1*$_{1\text{-}500}$. Michelle Harreman performed this experiment.
B. Spores (A-D) from 4 different tetrads (1 through 4) from a heterozygous *DEF1/def1*$_{1\text{-}500}$ diploid, with haploid spore genotype indicated.
C. Dilution series of *Δdef1* yeast cells (carrying the *GAL*-driven plasmid indicated on the left), grown on SD -Uracil Agar glucose or galactose as indicated.

The data above suggest that the toxic Def$_{1\text{-}400}$ or Def1$_{1\text{-}500}$ polypeptides may artificially mimic the processed form of Def1 observed after DNA damage. In order to test this hypothesis, it was necessary to fine map the exact site. Smaller C-terminal genomic truncations were created, with the aim of comparing these against the processed band on Western blot. As the deletion of the last 138 amino acids of Def1 (Def1$_{1\text{-}600}$) was viable whilst Def1$_{1\text{-}500}$ was lethal we surmised that genomic truncations in the region of 500-600 would be very informative. No transformants were obtained for Def1 truncations between 1-500 and 1-520, suggesting expression of these proteins was also toxic to cells. Truncations over 540 amino acids in length were viable with no obvious phenotype. A strain with the N-terminal 530 amino acids of Def1 expressed was viable but found to be temperature sensitive (Figure 5.5 A, JSY 1183). The Def1$_{1\text{-}530}$ protein migrated at a marginally higher position in gel than the endogenously induced pr-Def1 band (Figure 5.52 B). Assuming that pr-Def1 is not post-translationally modified in a

different manner to Def1$_{1-530}$, this suggests that the exact site of processing lies somewhere in the region encompassed by residues 520-530.

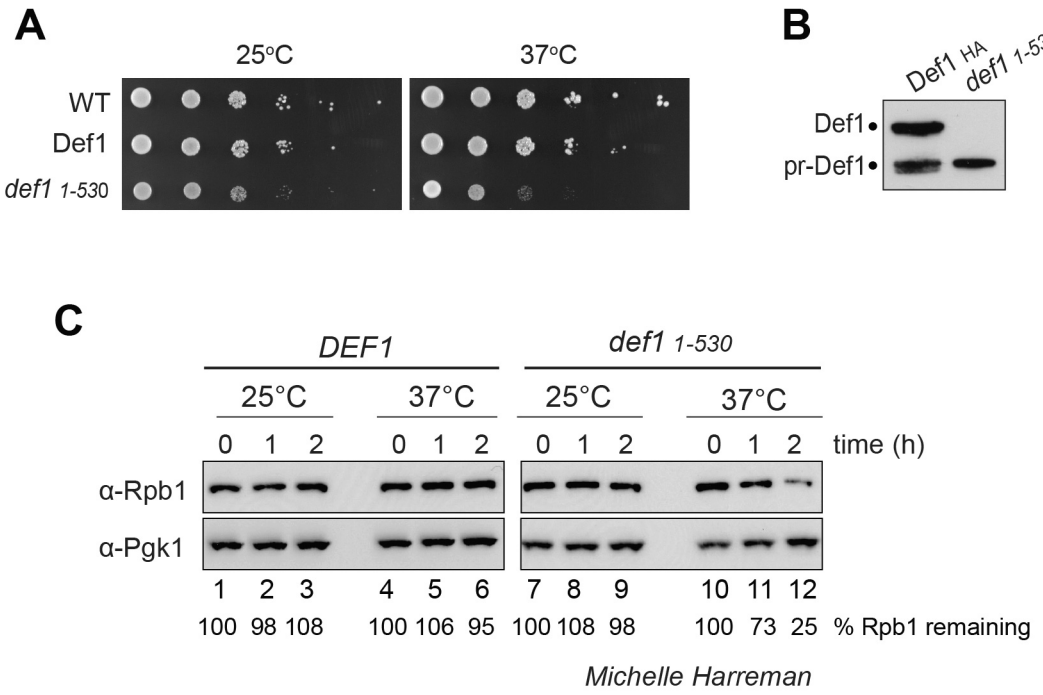

Figure 5.5: Expression of Def1$_{1-530}$ is tolerated in cells

A. Dilution growth series of Wild-type cells compared to cells with a C-terminal HA tag (JSY 1181), and cells lacking the last 208 amino acids of Def1 with a C-terminal HA tag (JSY1183). Cells were plated on YPD-agar and grown at the indicated temperatures. Michelle Harreman created these strains.
B. Western blot showing Def1 from *def1$_{1-530-HA}$* and 4-NQO treated Def1-HA cells, respectively.
C. Western blots of extracts from Def1-HA and *def1$_{1-530-HA}$* cells grown at permissive (25°C) or restrictive temperature (37°C) for the indicated times. Anti-Rpb1 (8WG16) and anti-Pgk1 antibodies were used for the Western blot. Michelle Harreman performed this experiment.

In order to assess what was causing the slower growth of the *def1$_{1-530}$* strain, various cellular proteins were examined after shifting to the non-permissive temperature, 37°C. The total protein content of the samples was not altered, as measured by Ponceau-S stain and the Pgk1 loading control (Figure 5.52 C lower panel). The protein levels of Def1$_{1-530}$ were also not detectably altered. Growth was retarded at higher temperatures for the Def1$_{1-530}$ strain, but protein concentration was normalised by loading equal amounts of whole cell extract. Def1 has a critical role in the degradation of Rpb1 (Woudstra et al., 2002). The slow growth of the

$Def1_{1-530}$ strain may be, at least partly, due to the reduction in the levels of the essential Rpb1 protein. In fact, Rpb1 levels decreased steadily, the longer the $Def1_{1-530}$ strain was incubated at 37°C, to just 25% of the original starting levels after 2 hours (Figure 5.52 C, upper panel). The cognate wild-type strain did not exhibit a reduction in Rpb1 levels at 37°C under the same conditions, despite some pr-Def1 formation (Figure 5.2C). This suggests that elevated temperature activates the $Def1_{1-530}$ protein to promote the aberrant degradation of Rpb1, even in the absence of damage-induced transcription stalling.

5.2.4 Mapping the site of processing: inactivation of proteolytic cleavage

In a further attempt to map the site of processing, and attempt to disrupt it, we decided to create a form of Def1 that was insensitive to damage-induced proteolysis. Strains with small internal deletions in Def1 were made, with the aim of removing the protease cleavage and/or recognition site. As proposed earlier, the pr-Def1 processing site probably lies in the region near residues 520-530. We first created mutations in this region, which did not affect the processing of Def1 appreciably (data not shown). Therefore, larger internal deletions of 40-70 amino acids between residues 400 and 575 were created (JSY1208-1211). These internal deletions changed the electrophoretic mobility of the full-length protein, but not in proportion to the size of the deletion (Figure 5.6 A). The amino acid composition radically alters Def1 electrophoretic mobility, and unsurprisingly this is also the case for these small internal deletions. Importantly, none of the deletions - even those spanning the proposed processing site – blocked the processing of Def1 after DNA damage (Figure 5.6 A) or at high cell density (data not shown). The deletions did, however, shift the site of processing; the faster migrating, processed band also changed electrophoretic mobility compared to the wild-type protein. This suggests that the processing site is not a fixed short amino acid sequence. Rpb1 degradation was not altered in any of the internal deletion strains (Figure 5.6 A, upper panel). As Def1 has an unusual electrophoretic mobility, the distance between processed and full-length bands cannot be directly inferred. One

possibility is that the proteolytic cleavage of Def1 occurs at a fixed length from the C-terminus of Def1. However, tagging Def1 at the C-terminus did not affect the site of processing (Figure 5.3 A), suggesting that if there is some kind of 'molecular ruler' marking the site of cleavage, it must be reliant on Def1's primary sequence rather than other domains added to the protein.

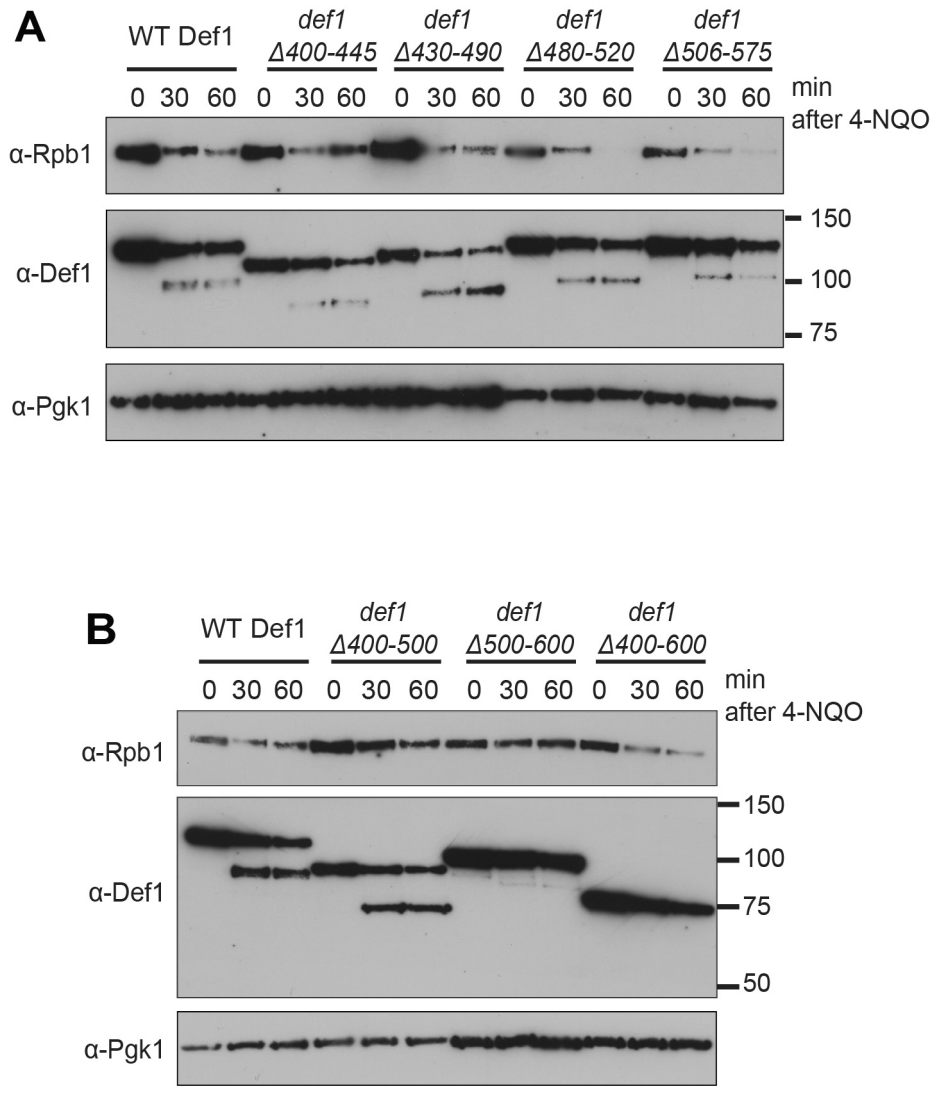

Figure 5.6: Def internal deletions shift the site of processing

A.Quick alkaline extracts from WT Def1 (JSY1190) and Def1 small (40-70 residue) internal deletion strains indicated, before and after treatment with 4-NQO for 30 and 60 minutes. Western blot using anti-Rpb1 (8WG16), anti-Def1, and anti-Pgk1 antibodies.
B. As (A) with larger (100-200 residue) internal deletions of Def1.

Larger internal deletions removing hundreds of amino acids were created around the proposed processing site of Def1, and the strains expressing these were found to be viable (JSY1212-1214). 4-NQO treatment of cells with Def1 residues 400-500 deleted resulted in the shifted mobility of both full-length and processed band, suggesting alternate processing site usage (Figure 5.6 B), as above. However, Def1 proteins with internal deletions from 400-600 and 500-600 no longer appeared to be processed after DNA damage. Interestingly, whilst the 506-575 deleted strain did exhibit Def1 processing, albeit at a different position, the 500-600 deletion did not. Surprisingly, the $Def1_{\Delta\ 400\text{-}600}$ and $Def1_{\Delta\ 500\text{-}600}$ strains exhibited normal Rpb1 degradation after DNA damage, suggesting that Def1 was still functional in these cells, without any detectable proteolytic processing. Both these strains exhibit a slight growth defect at 30°C. Similar to the Def1 protein expressed by the $def1_{1\text{-}530}$ strain, $Def1_{\Delta\ 400\text{-}600}$ and $Def1_{\Delta\ 500\text{-}600}$ might, under certain conditions, behave like the processed band without the need for proteolytic processing. Additional experiments are required to investigate these intriguing strains further.

5.2.5 The N-terminal processed product of Def1 is the biologically active fragment

pr-Def1 is an N-terminal proteolytic fragment formed in response to transcription stress. pr-Def1 appears to be the active form of the protein: the pr-Def1-like, *def11-530* can degrade Rpb1 spontaneously upon heat stress (Figure 5.5 C). However, a more direct link between the formation of the shorter activated version of Def1 and Rpb1 poly-ubiquitylation was still lacking.

In order to help answer this question, a TEV cleavable form of Def1 was created (JSY 1191). TEV protease is the catalytic domain from the highly specific N1a protease from Tobacco Etch Virus (Dougherty et al., 1989, Parks et al., 1995). The N1a protease fragment helps to cleave the Tobacco etch virus polyprotein, at the consensus ExxYxQG peptide motif. TEV protease's high specificity has been

utilised previously to create the specific, induced, cleavage of a modified cohesion subunit, outside of its normal cellular context (Uhlmann et al., 2000).

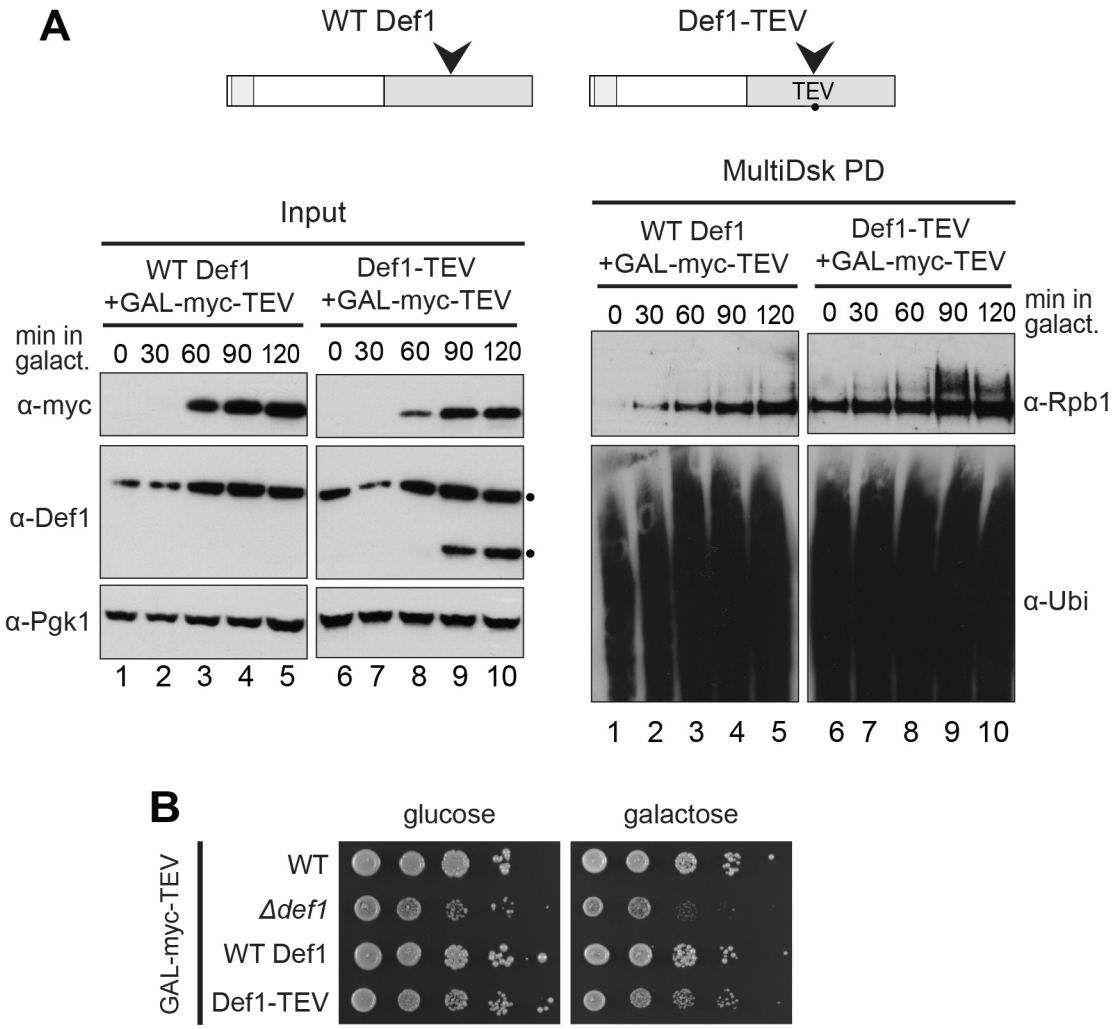

Figure 5.7: Def1-TEV poly-ubiquitylates Rpb1 in the absence of damage

A. Western blot of extracts from cells expressing WT Def1, or Def1 containing a TEV protease cleavage site. Both cell types contained galactose inducible Myc-tagged TEV protease. Western immunoblot of cell extracts of Def1 and TEV protease induction (anti-myc), and Pgk1 are shown (left panel). MultiDsk ubiquitin enrichment was performed on the extracts and immunoblotted for Rpb1 (4H8) and ubiquitin (P4D1) (right panel).
B. Yeast dilution growth assay of the indicated strains transformed with galactose inducible Myc-tagged TEV protease plasmid. Cells grown on SD –Leucine Agar containing glucose and galactose as indicated.

To mimic the generation of pr-Def1, without induced transcription stress, we placed a consensus TEV protease cleavage site into the approximate region that is normally subject to proteolytic cleavage (between residue 522 and 523 of Def1;

Figure 5.7 A, upper panel). Inserting the TEV cleavage site does not measurably affect the normal function of the Def1-TEV protein: the TEV site does not affect normal proteolytic processing or Rpb1 degradation (data not shown), or normal growth (Figure 5.7 B, glucose). *GAL*-regulated TEV protease - containing a Myc tag and nuclear localisation signalling (NLS) - was expressed from a transformed plasmid in these strains. Upon galactose induction of TEV protease Def1-TEV was proteolytically cleaved (Figure 5.7 A, left panel). This induced cleavage is at a similar position to that observed in the wild-type Def1 protein upon transcription stress, as estimated by comparing the electrophoretic mobility of the two bands. As expected, Def1 lacking a TEV cleavage site was not cleaved in the presence of TEV protease (Figure 5.7 A, left panel lanes 1-5). Importantly, concurrent with the emergence of the TEV-cut Def1 form, Rpb1 became poly-ubiquitylated, independently of induced transcription stalling (Figure 5.7 A right panel). No poly-ubiquitylation of Rpb1 was observed when the TEV protease is expressed with a non-cleavable wild-type version of Def1. This suggests that the proteolytic nicking of Def1 is sufficient to induce the aberrant poly-ubiquitylation of Rpb1, and partially reconstitute the proteolytic processing, even in the absence of damage-induced transcription stalling.

It is important to note that the extent of Rpb1 poly-ubiquitylation is lower compared to irradiation of cells with UV (Figure 5.1 C), despite roughly equal levels of cleaved Def1. Indeed, a noticeable reduction in the total cellular levels of Rpb1 could not be detected after expression of TEV protease in the Def1-TEV strain. Furthermore, there was only a slight growth defect of the Def1-TEV strain, compared to the wild-type Def1 strain, on galactose plates (Figure 5.7 B), suggesting that constant Def1-TEV cleavage was not overly detrimental to cell growth. Whether this was because the TEV-cleaved form of Def1 does not truly mimic pr-Def1, or if Rpb1 degradation requires other signalling events, is presently unclear. There is no induced transcription stall in this experiment. As Def1 is thought to promote the poly-ubiquitylation of stalled mono-ubiquitylated RNAPII, this is likely the limiting factor in these conditions. The ubiquitylation observed is possibly the aberrant poly-ubiquitylation of RNAPII that is temporarily paused or arrested, a natural consequence of all on-going transcription (Sigurdsson et al., 2010).

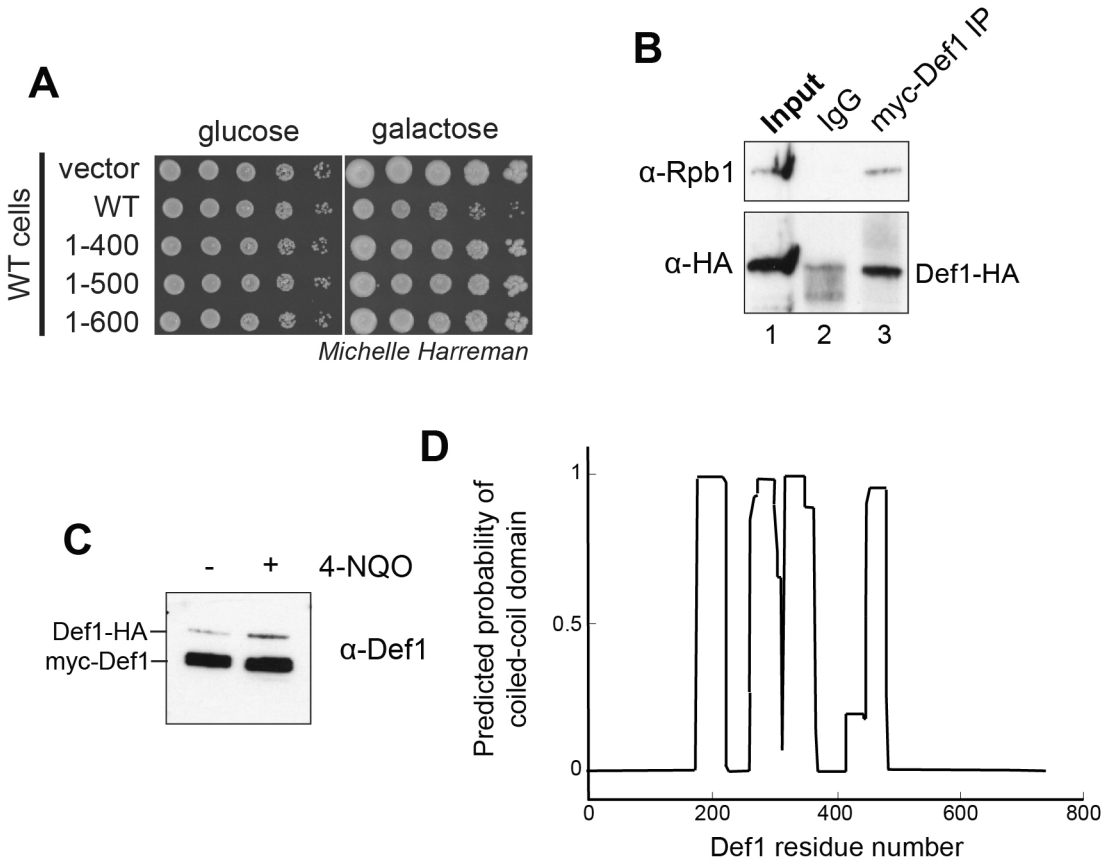

Figure 5.8: Def1 acts as an oligomer

A. Dilution series of Wild-type yeast cells (carrying the *GAL*-driven plasmid indicated on the left), grown on SD -Uracil Agar glucose or galactose as indicated.
B. Western blot showing Def1-HA and Rpb1 retained on immobilized Myc-Def1 beads after anti-myc immunoprecipitation (IP, see 2.6.5). IP from cells expressing both Myc-Def1 and Def1-HA (JSY642 with pRS414-MTH-DEF1)
C. Western blot of extracts from the above strain, immunoprecipitated for Myc epitopes and probed using anti-Def1 antibody.
D. Coiled-coil domain prediction plot of Def1 created using COILs server (http://embnet.vital-it.ch/software/COILS_form.html).

It was surprising that $Def1_{1-400}$ or $Def1_{1-500}$ was extremely toxic to haploid cells, but not to diploid cells expressing a normal wild-type copy of *DEF1* (Figure 5.4 B). The absence of a dominant negative effect of Def1 truncations was also observed when overexpressing $Def1_{1-400}$ and $Def1_{1-500}$ in wild-type cells, where a normal version of Def1 was expressed (Figure 5.8 A). This suggests that the wild-type version of Def1 is helping to sequester the toxic fragment, possibly via direct interaction. To ascertain if Def1 oligomerises, cells expressing a C-terminally HA-tagged form of Def1 (JSY 642) were transformed with a plasmid expressing an N-terminal Myc

tagged form of *DEF1,* from its own promoter. In these cells both forms of Def1 protein were expressed roughly equally. Immunoprecipitation of the Myc-tagged form of Def1 co-precipitated the other Def1-HA form (Figure 5.8 B), suggesting that the protein exists as a multimer *in vivo*. Myc-tagged Def1 could still interact with Rpb1, but whether this was at the same time as interacting with another copy of Def1 requires further investigation. The association of Def1 with a partner appears to be somewhat inducible by DNA damage (Figure 5.8 C); increased levels of higher molecular weight Def1-HA appeared to associate with Myc-Def1 after 4-NQO treatment for one hour.

Whilst the exact stoichiometry of the Def1 self-interaction is unclear, it seems probable that Def1 forms as multimers rather than just as a dimer. Presumably, under constant galactose induction of $Def1_{1-400}$ or $Def1_{1-500}$, the amount of these proteins would exceed that of the endogenous wild-type Def1. However, despite the higher protein level, such expression is not toxic in wild-type strains, suggesting that the full-length protein can sequester multiple copies of the toxic $Def1_{1-500}$ or $Def1_{1-400}$. Def1 is predicted, with high probability, to have multiple coiled-coil regions (Woudstra et al., 2002, Figure 5.8 D). Coiled-coil domains typically consist of multiple α-helical-like secondary structures wound around each other in a rope-like manner (Yu, 2002). Coiled-coils are a common structural motif associated with oligomerisation of proteins, either as dimers (such as leucine zippers), trimers (in keratin) or pentamers (Malashkevich et al., 1996). Whether the identified coiled-coil domains in Def1 associate inter- or intra-molecularly is unclear. It is interesting to note that the most C-terminal predicted coiled-coil domain ends at around residue 481, before the proposed proteolytic processing site. Def1 also contains a CUE domain at its N-terminus. Whilst principally described as a ubiquitin binding domain (UBD), CUE domains in solution can dimerise (Kang et al., 2003). The oligomeric state of Def1 is clearly important for its function and deserves further study.

5.3 Conclusions

The faster migrating protein doublet that cross-reacts with a Def1 antibody on Western blots is a product of the Def1 protein. Full-length Def1 is post-translationally processed, by proteolytic processing, creating an N-terminal fragment, termed pr-Def1. The exact site of proteolytic processing is unknown, but appears to be in the range of 520-530 amino acids from the N-terminus of Def1.

Def1 is processed in response to RNAPII stalling and this processed protein - if expressed at high enough levels - is dangerous to the cell. The results presented here suggest pr-Def1 is the active form of Def1 and that it is toxic if aberrantly expressed and/or expressed at too high abundance. This toxicity is mediated, at least in part, through the degradation of Rpb1. Interestingly, we have found that the pr-Def1 protein is extremely short lived in protein extracts, and *in vivo*, suggesting that it is rapidly removed, as would be expected for such a toxic protein.

Chapter 6. Results III
Def1 Protein Control

6.1 Aims

The data presented in the previous results chapter indicate that Def1 is proteolytically processed to an active fragment. However, the identity and control of the protease responsible for this cleavage was unknown. When Def1 processing was artificially mimicked - creating active fragments of Def1 – it promoted the aberrant poly-ubiquitylated of Rpb1. Confining the removal of the C-terminus, to occur only after transcription stress, appears to be crucial in order to prevent the inappropriate degradation of Rpb1.

Furthermore, the mechanism by which removal of Def1's C-terminus activates the protein was still unclear. Expression of a C-terminus fragment of Def1 did not prevent the toxicity of over-expressing $Def1_{1-500}$. Previous experiments have shown that full-length Def1 protein can interact with RNAPII and Rad26 (Reid and Svejstrup, 2004, Woudstra et al., 2002). Furthermore, pure Def1 can promote the formation of - albeit non-physiological - Rsp5-catalysed Lys-63 linked ubiquitin chains on RNAPII *in vitro* (Somesh et al., 2005). This would suggest that full-length Def1 is still biochemically functional. If this is the case, why is it necessary to proteolytically activate Def1 and why is this fragment toxic?

One intriguing possibility is that the C-terminus might control Def1 through altering its sub-cellular localisation. Despite Def1's primary role in chromatin, previous studies have shown that the protein primarily localises to the cytoplasm (Huh et al., 2003, Tkach et al., 2012). The second of these studies observed no change in the steady state localisation of Def1 after the induction DNA damage. Importantly, in both studies, the authors used a C-terminal GFP tagged form of Def1. They, therefore, did not visualise the active N-terminal fragment of interest under investigation here. The molecular mechanism of Def1 proteolytic processing, its

control and effect on sub-cellular localisation were investigated and the results are presented in this chapter.

6.2 Results

6.2.1 Def1 processing is ubiquitin-dependent and requires Rsp5

One of the benefits of working in *S. cerevisiae* is the large number of strains with gene disruptions available. Assaying the formation of pr-Def1 in many different genetic backgrounds was therefore possible, using the Def1 antibody. We undertook a candidate approach to assess Def1 processing in strains that had already been implicated in Def1 interaction, or involved in the Rpb1 degradation pathway. In most cases processing was not affected, however, this was not the case when the ubiquitin ligase Rsp5 was inactivated (Figure 6.1 A).

Rsp5 is a HECT domain Ubiquitin ligase responsible for many processes *in vivo*, including the mono-ubiquitylation of Rpb1 (Kaliszewski and Zoladek, 2008). As Rsp5 is an essential protein in yeast (Wang et al., 1999), a temperature sensitive allele, termed *rsp5-1*, was used. At the permissive temperature, 25^{o}C, Rsp5 function is not impaired: Def1 processing and Rpb1 degradation occurs as normal (Figure 6.1 B). Shifting cells to the non-permissive temperature, 37^{o}C, for 90 minutes inactivates the protein (Harreman et al., 2009, Beaudenon et al., 1999). Rsp5-inactivated cells, treated with 4-NQO, exhibit greatly reduced pr-Def1 formation, and no Rpb1 degradation (Figure 6.1 A). Whilst total Def1 levels appear to be reduced in the *rsp5-1* strain, this is a loading artefact (Figure 6.1 A, compare Pgk1 loading to Def1 blots). Def1 is not processed, and therefore stabilised when Rsp5 is inactivated. Def1 processing, and subsequent Rpb1 degradation, can be observed in the wild-type control (Figure 6.1 B, left panel). Some Def1 processing is even observed without 4-NQO treatment; possibly due to the increased temperature, used during the assay, causing some transcription stress (see Figure 5.2 C).

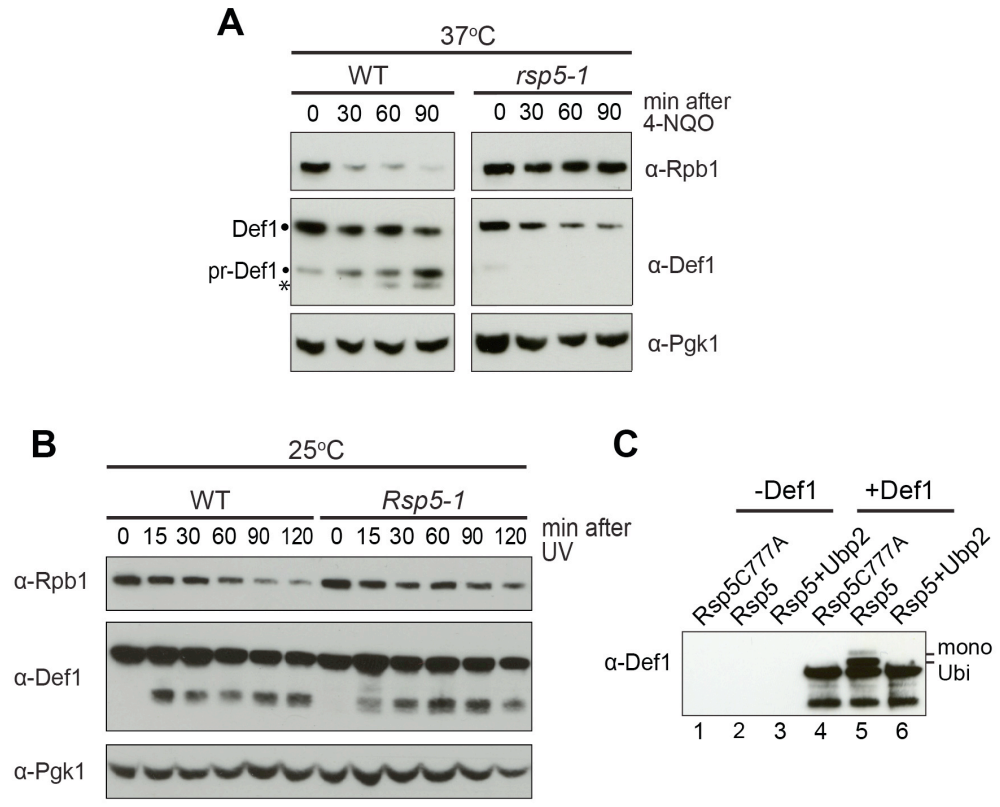

Figure 6.1: Def1 processing requires ubiquitylation by Rsp5

A. Western blot of extract from WT and *rsp5-1* cells, grown at 37°C (non-permissive temperature) for 2 hours before addition of 4-NQO for the indicated times. Asterisk denotes an unrelated or non-specific band, occasionally observed with the anti-Def1 antibody.
B. Quick extracts from WT and Rsp5-1 strains treated with 4-NQO at the permissive temperature, 25°C. Western blot probed using anti-Rpb1 (8WG16), anti-Def1 and anti-Pgk1 antibodies.
C. Western blots of Def1 ubiquitylation, reconstituted *in vitro* using highly purified proteins (Def1, ubiquitin, Uba1, Ubc5, Rsp5 and Ubp2; see 2.8.1). An Rsp5 catalytic site mutant (C777A) and the de-ubiquitylating enzyme Ubp2 were used as specificity controls. Western immunoblot using anti-Def1 antibody.

It was important to show a direct role for Rsp5 in the processing of Def1. Rsp5 is a promiscuous enzyme *in vivo* and also mono-ubiquitylates Rpb1, which might conceivably act as the signal for Def1 processing. As we have previously shown that Def1 becomes mono-ubiquitylated upon DNA damage (Figure 3.4 C), we therefore hypothesised that Rsp5 might be the ligase catalysing this ubiquitylation. Def1 ubiquitylation was reconstituted *in vitro*, using highly purified Uba1 (E1), Ubc5 (E2), Rsp5 and ubiquitin. Two bands of reduced electrophoretic mobility were observed, corresponding to the oligo mono-ubiquitylated forms of Def1. These

were only present upon addition of pure active Rsp5 (Figure 6.1 lane 5); when an active site mutant form of Rsp5 was used (Rsp5 C777A, lane 4) ubiquitylation was absent. This mono-ubiquitylation can be trimmed back by Ubp2 (lane 6), a ubiquitin protease commonly associated with Rsp5 (Kee et al., 2005). Furthermore, pure recombinant Def1$_{1\text{-}500}$, mimicking pr-Def1, can associate with immobilised pure recombinant Rsp5 (data not shown). Def1 contains two degenerate PY motifs, possibly the recognition sites for the WW-domains of Rsp5 (Sudol, 1996, Chang et al., 2000). However, the binding to Rsp5 requires further investigation.

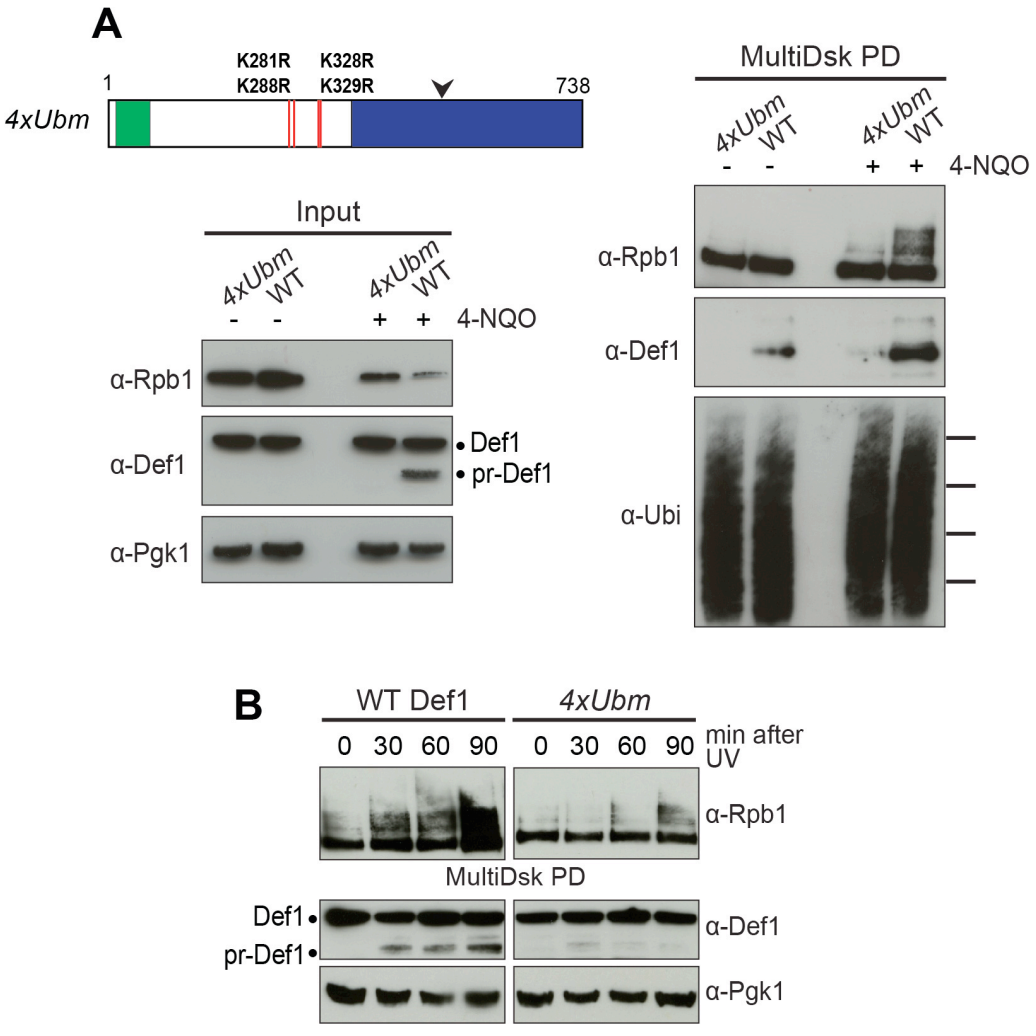

Figure 6.2: Mutation of Def1 ubiquitylation sites reduces processing and Rpb1 degradation

A. Comparison of extracts from Def1 KI (WT) and a strain with 4 identified ubiquitin sites mutated from lysine to arginine (*4xUbm*, JSY1193), before and after treatment with 4-NQO for

30 minutes. Schematic with the position of mutated lysine residues indicated (top left). Cells were treated with and without 4-NQO for 1 hour. Western blot of extracts probed using anti-Rpb1 (8WG16), anti-Def1 and anti-Pgk1 antibodies (left panel). MultiDsk pull-down from extracts, immunoblotted for Rpb1 (4H8), Def1 and ubiquitin (P4D1) (right panel).
B. Western blot showing time course of cells from the above strains after UV irradiation. Western blot of extracts probed using anti-Def1 and anti-Pgk1 antibodies and MultiDsk pull-down probed with anti-Rpb1 (4H8).

From the *in vitro* ubiquitylation reaction described above, two ubiquitylated Def1 peptides were identified by mass spectrometry. Both these peptides contained two lysines; it was not possible to identify which of these was ubiquitylated. A strain was created where these four lysines (K281, K288, K328 and K329) were all mutated to the closely related - but non-ubiquitylatable – arginines (*4xUbm*, JSY1193; Figure 6.2 A schematic). Mutation of these sites greatly reduced DNA damage-inducible mono-ubiquitylation of Def1 (Figure 6.2 A, right panel). The under-ubiquitylated Def1 was processed far less efficiently after transcription stress (Figure 6.2 A, left panel & B). Damage induced poly-ubiquitylation (Figure 6.2 A and B) and degradation of Rpb1 (Figure 6.2 A, left panel) was also markedly reduced in the *4xUbm* strain. This suggests that ubiquitylation of Def1 is important for efficient pr-Def1 formation and again suggests a link between the processing of Def1 and Rpb1 degradation.

Def1 is probably only ubiquitylated at just one or two sites on each molecule, as is implied from both the *in vivo* and *in vitro* molecular weight shifts. Interestingly, despite mutating four ubiquitylated lysines, Def1 mono-ubiquitylation and processing was not fully abrogated, suggesting that ubiquitylation can occur at alternative sites, with reduced efficiency. Ubiquitylation is often a promiscuous reaction that can target lysines in a local, conformational area (Danielsen et al., 2011). Def1 is lysine-rich between residues 200-335 (14% of all residues in this area are lysines): these residues may lie close to each other in both primary and tertiary structure. Other ubiquitylation sites on Def1 have been reported using whole ubiquitome profiling (Starita et al., 2012, Beltrao et al., 2012). Therefore, additional lysines might also need to be mutated in order to totally ablate Def1 ubiquitylation and processing. Another possibility (discussed below) is that ubiquitylation is not absolutely required for processing, but significantly enhances its efficiency.

6.2.2 Def1 processing requires the proteasome

Whilst Def1 ubiquitylation greatly enhances its processing, the identity of the protease responsible for the proteolytic cleavage was still unclear. Surprising results, presented here, point to a role of the proteasome in this process.

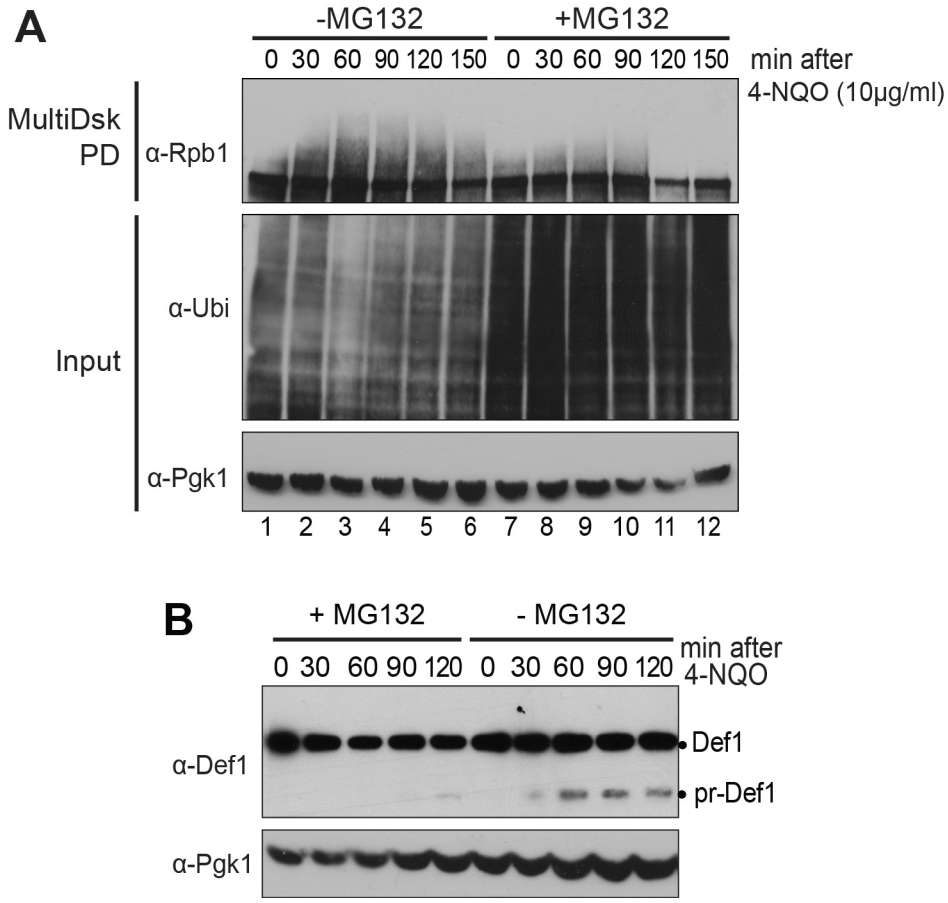

Figure 6.3: Rpb1 poly-ubiquitylation and def1 processing is reduced when the proteasome is inhibited

A. Time-course of treatment of the proteasome inhibitor sensitive strain (GAC202) after addition of 4-NQO (10 µg/ml). Cells were pre-treated for an hour with or without the proteasome inhibitor MG132. Western blot of total cellular ubiquitylated proteins (P4D1) and anti-Pgk1 (lower) and MultiDsk pull-down probed for Rpb1 (4H8).
B. Western blot of extracts from GAC202 cells treated (or not) with the proteasome inhibitor MG132, prior to incubation with 4-NQO for the indicated times.

MG132 is a potent, specific inhibitor of the chymotryptic activity of the proteasome (Lee and Goldberg, 1998b). MG132's use in yeast has been limited due to its low efficiency inhibition of the yeast proteasome and its effective export by the multi-drug resistance pump, Pdr5 (Lee and Goldberg, 1998a). A strain, deleted for the gene encoding this pump, and with active site mutations in trypsin and caspase-like subunits of the proteasome core particle, is highly sensitive to MG132 (Collins et al., 2010, GAC202). When treating GAC202 cells with MG132, high molecular weight ubiquitin conjugates accumulate (Figure 6.3 A, middle panel), signifying the inhibition of proteasome-mediated protein degradation. As shown previously, DNA damage induces the poly-ubiquitylation of Rpb1 (Figure 3.3 C and 5.1 C), which under normal conditions is cleared by proteasomal degradation (Beaudenon et al., 1999, Verma et al., 2011). Combining pre-treatment of MG132 and DNA damage would, thus, be expected to result in increased levels of Rpb1 poly-ubiquitylation: as Rpb1 is both becoming ubiquitylated and prevented from being degraded. Unexpectedly, however, the opposite was observed under these conditions: there was a reduction in the poly-ubiquitylated form of Rpb1 in response to both 4-NQO and MG132 compared to 4-NQO treatment alone (Figure 6.3 compare lanes 1-6 and 7-12). Whilst it has been observed that poly-ubiquitin conjugation is somewhat limited during proteasome inhibition – as free ubiquitin concentration becomes limiting (Hjerpe et al., 2012) - the result is still striking. This suggests that the proteasome has a role upstream of its function in degrading Rpb1, possibly in promoting the poly-ubiquitylation of Rpb1.

The mono-ubiquitylated form of Rpb1 was not affected by proteasome inhibition. Cells lacking Def1 also exhibit normal Rpb1 mono-ubiquitylation, but no poly-ubiquitylation, after DNA damage (Woudstra et al., 2002). As pr-Def1 is believed to be the active form of Def1, it is conceivable that the proteasome plays a role in the proteolytic processing step of Def1. The formation of pr-Def1 was therefore assessed under the same conditions as Rpb1 poly-ubiquitylation. Pre-inhibiting the proteasome before 4-NQO treatment greatly reduced the formation of pr-Def1 (Figure 6.3 B). Def1 processing was normal without MG132 treatment and in the congenic wild-type strain to GAC202, even when treated with MG132 (data not shown).

There are multiple possible explanations for the role of the proteasome in Def1 processing. Processing may be mediated directly, via the proteolytic action of the proteasome. Alternatively, the proteasome might act indirectly, by degrading an inhibitor of pr-Def1 formation, after transcription stress. Finally, despite the high specificity of MG132, this compound could also be inhibiting other cellular proteases, which process Def1. MG132 is not widely used in yeast cells so possible off-target effects have not been investigated fully.

In order to ascertain whether the proteasome can directly proteolytically process Def1, the reaction was reconstituted *in vitro*. Adding highly purified yeast proteasome to purified Def1 protein led to the rapid appearance of a faster migrating band, reminiscent of pr-Def1 (Figure 6.4 A). Indeed, the lower, proteasome-generated, Def1 band is of equivalent size to the pr-Def1 band observed *in vivo* after DNA damage (Figure 6.4 B, compare lanes 2 and 3). No further Def1 degradation products were observed, suggesting that only partial proteasomal processing - rather than total Def1 degradation - is occurring in this reaction. The conversion of the full-length protein to the smaller processed version occurs in a time-dependent manner. These data suggest that Def1 is partially proteolytically processed directly by the proteasome.

As expected, inhibiting the pure 26S proteasome protein with MG132 drastically reduces the formation of the processed product *in vitro* (Figure 6.4 A left panel). In order to ascertain whether processing can occur independently of the purified proteasome, or if MG132 is not completely inhibiting the proteasome, the experiment was performed in the presence of excess MG132 and another proteasome inhibitor, lactacystin, which inhibits all protease activity of the proteasome (Fenteany et al., 1995) (Figure 6.4 C).

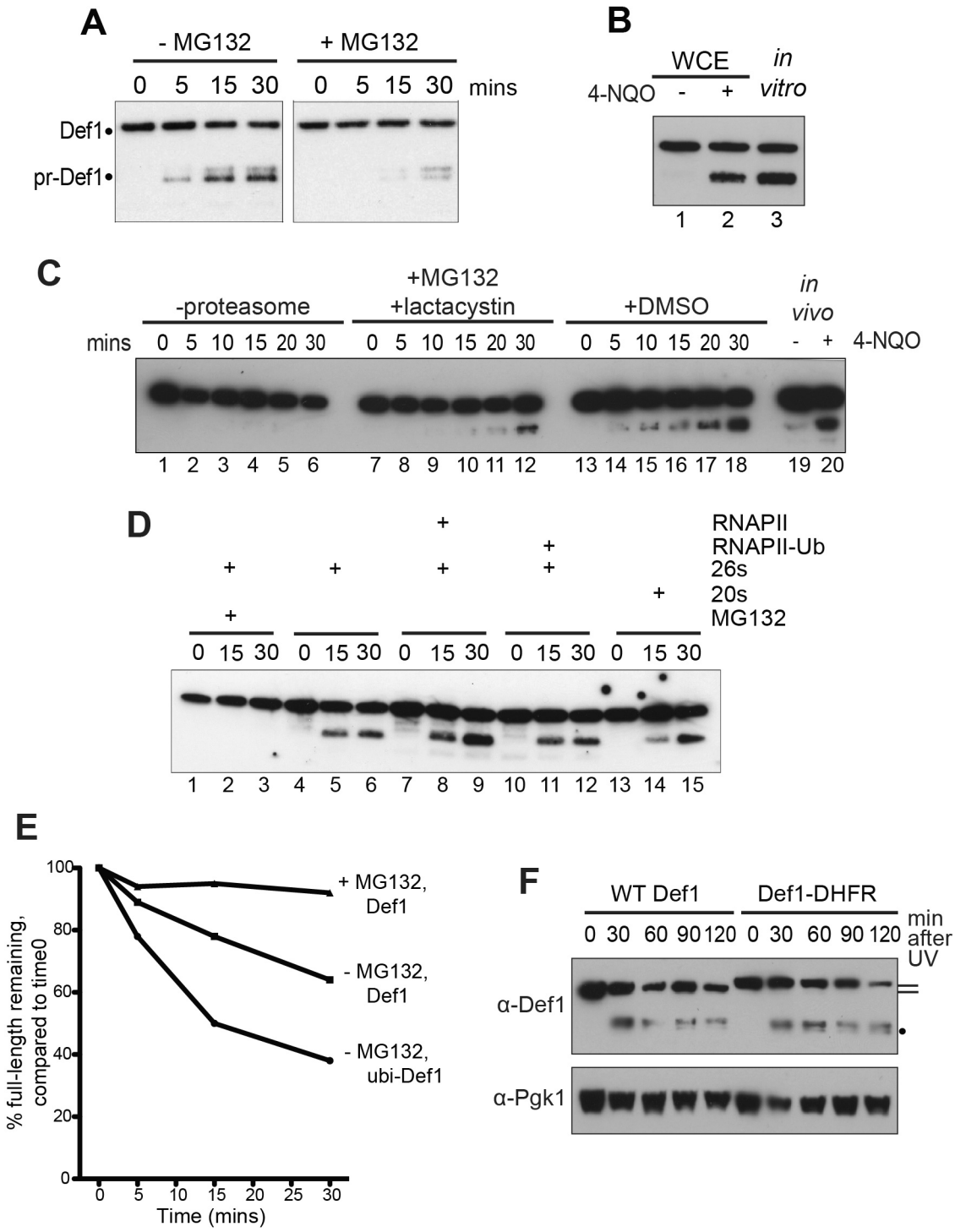

Figure 6.4: Def1 is directly processed by the proteasome

A. Reconstitution of Def1 processing with purified Def1 and 26S proteasome at 30°C (2.8.2), in the absence or presence of MG132. An immunoblot using anti-Def1 antibody showed no other bands than presented here.
B. Comparison of quick extracts from cells treated with or without 4-NQO for 30 minutes, with *in vitro* processed Def1 (lane 3).

C. *In vitro* proteasome proteolytic reaction performed at 30°C: without Drug control (+DMSO, lanes 13-18); large excess of MG132 (100μM) and lactacystin (50μM) (lanes 7-12); and without the addition of proteasome (lanes 1-6). Quick extracts with and without 4-NQO treatment are loaded as a control for the processed band(s) (lane 19 & 20).
D. *In vitro* proteasome assay performed at 4°C, with MG132 inhibitor (lanes 1-3), or with 26S proteasome (lanes 4-6), or 20S proteasome (lanes 13-15). The assay was also performed with 26S proteasome and pure RNAPII (lanes 7-9) and 26S proteasome and pure, mono-ubiquitylated RNAPII (lanes 13-15).
E. Proteolysis of full-length, ubiquitylated Def1 (ubi-Def1), or un-modified Def1 (Def1) over time in response to incubation with proteasome in the absence (-) or presence (+) of MG132. Def1 was ubiquitylated *in vitro* prior to the assay (see Figure 6.1 C). Western blot quantifications (ImageJ) of the disappearance of full-length or ubiquitylated Def1 were normalised to 100% at starting time point 0.
F. Western blot of quick extracts of wild-type and Def1 with mouse Dihydrofolate reductase (DHFR) attached to the C-terminus. Cells were grown for 3 hours in media containing methotrexate (Piwko and Jentsch, 2006) before treatment with 4-NQO.

Intriguingly, even with the very high amounts of inhibitor used, some residual *in vitro* processing of Def1 still occurred (lanes 7-12). Whilst processing is far slower than without inhibitor (lanes 13-18), no observable pr-Def1 formation occurs - over the time course of the experiment - when proteasome is not added (lanes1-6). This observation is not unprecedented: reconstituted NF-κB p105 processing in extracts shows a reduction of only around 50% of processing in the presence of great excess of MG132 (Kravtsova-Ivantsiv et al., 2009). Further study of this effect has been hampered due to the inherent instability of the Def1 protein, which appears to spontaneously 'self-cleave' during longer incubations at 30°C (see lower band in ubiquitylation reaction in Figure 6.1 C). Intriguingly, this spontaneous cleavage appears to occur at the same site as normal *in vivo* processing. Further work is required to investigate this finding. A fascinating possibility is that the proteasome is inhibited in the *in vitro* reaction presented in Figure 6.4 C, but that it is the binding of Def1 to the proteasome that then induces breakage at an inherently unstable site in Def1.

Performing the proteasome-processing assay at 4°C still permits production of the active processed fragment, albeit at a slower rate (Figure 6.4 D). Partial processing has been re-constituted previously for the p105 subunit of NF-κB1, using pure components with 20S proteasome (Moorthy et al., 2006). We could also observe partial processing by the 20S proteasome particle (Figure 6.4 D, lanes 13-15) that lacked the 19S caps, normally critical for the unwinding and feeding of substrates into the proteasome (Lee et al., 2001a). However, the efficiency of processing was

reduced compared to the reaction with complete 26S proteasome (compare lanes 4-6 and 13-15).

Both the *in vivo* and the *in vitro* data points to a direct role for the proteasome in the partial proteolytic processing of Def1, which cleaves and degrades Def1's C-terminus, allowing the active N-terminal pr-Def1 fragment to escape. Proteolytic cleavage is commonly used to produce active proteins from their inactive precursors (Hengartner, 2000, Berg et al., 2002). Partial proteolytic processing has been reported previously in a number of different studies (see introduction, 1.1.6). Not all proteasome-mediated protein degradation requires ubiquitylation of the target protein (Jariel-Encontre et al., 2008). However, previous cases of partial proteolytic processing have required ubiquitylation of the processed protein, at least *in vivo*, in order to target the protein to the proteasome (Palombella et al., 1994, Hoppe et al., 2000).

However, in the *in vitro* system outlined above, ubiquitylation is not absolutely required for proteasomal processing. This appears to be at odds with the previous observations of Def1 DNA damage-inducible ubiquitylation, and subsequent processing (section 6.2.1). In order to investigate the role of ubiquitylation in pr-Def1 formation *in vitro*, ubiquitylated Def1 was created as described previously (Figure 6.1 C). Ubiquitylated Def1 is more rapidly proteasomally processed *in vitro* than its non-ubiquitylated counterpart; quantification of the upper, full-length bands show more rapid loss in overall signal of the ubiquitylated Def1 band, compared to the non-ubiquitylated Def1 band (Figure 6.4 E). These observations, whilst not in strict agreement with the requirement for Rsp5 and its identified ubiquitylation sites observed *in vivo*, are not unprecedented. In other reconstituted systems ubiquitylation seems to play an accessory - but stimulatory - role in processing, however, the same proteins *in vivo* require ubiquitylation (Moorthy et al., 2006, Kravtsova-Ivantsiv et al., 2009, Kraut and Matouschek, 2011). It is interesting to note that the ubiquitylation sites identified are in the N-terminal section of Def1; however, the pr-Def1 bands do not appear to be ubiquitylated.

Further study into the ubiquitin-dependent processing of Def1 has been hampered due to the inherent instability of the Def1 protein, which spontaneously cleaves

during the lengthy ubiquitylation-reaction incubation *in vitro* (Figure 6.1 C). One potential possibility is that direct Def1 ubiquitylation is not required for processing *in vivo*: instead it is the association with mono-ubiquitylated RNAPII that triggers Def1 proteasomal cleavage. According to this model, the requirement of Rsp5 for Def1 processing would be indirect. Rsp5 would be necessary for RNAPII mono-ubiquitylation, instead of Def1 ubiquitylation, by the same enzyme. If this were the case, one would expect to see an increase in the formation of pr-Def1 when excess, purified, mono-ubiquitylated RNAPII is added to the *in vitro* processing reaction, but this was not observed (Figure 6.4 D, lanes 10-12).

The exact mechanism of proteasomal degradation is still unclear. In the case of partial proteasomal processing, the proteasome might act as an exo-peptidase; chewing up the substrate from the C-terminus, until it is blocked or reaches a stop signal in the processed protein (Orian et al., 1999). Alternatively, the proteasome may act at an internal initiation site and process the fragment bi-directionally (Piwko and Jentsch, 2006). In order to test these two possibilities, we created a strain expressing Def1 protein with mouse Dihydrofolate reductase (DHFR) and a HA tag at its C-terminus (JSY1218). Previous studies have used DHFR to block the proteasome (Piwko and Jentsch, 2006, Prakash et al., 2004, Kraut and Matouschek, 2011). DHFR, when bound to methotrexate, is refractive to 19S unwinding and is extremely stable *in vivo* (Johnston et al., 1995). When cells expressing the Def1-DHFR fusion protein were pre-incubated with methotrexate, and then treated with 4-NQO, Def1 was still processed. This suggests that the DHFR tag did not block the processing reaction, and argues against the processing reaction occurring from the C-terminus. Instead, processing by the proteasome may be initiating from an internal Def1 site. This preliminary experiment requires further optimisation to assert this conclusion. Unfortunately, the ‘stable’ Def1-DHFR C-terminus could not be visualised using either a mouse DHFR antibody or HA antibody, suggesting it may still have been degraded by the proteasome as an exo-peptidase. This may be because Def1 can be processed independently of the 19S subunit (Figure 6.4 D), possibly bypassing the inhibitory role otherwise observed for mouse DHFR.

6.2.3 Def1 changes steady state subcellular localisation after UV irradiation

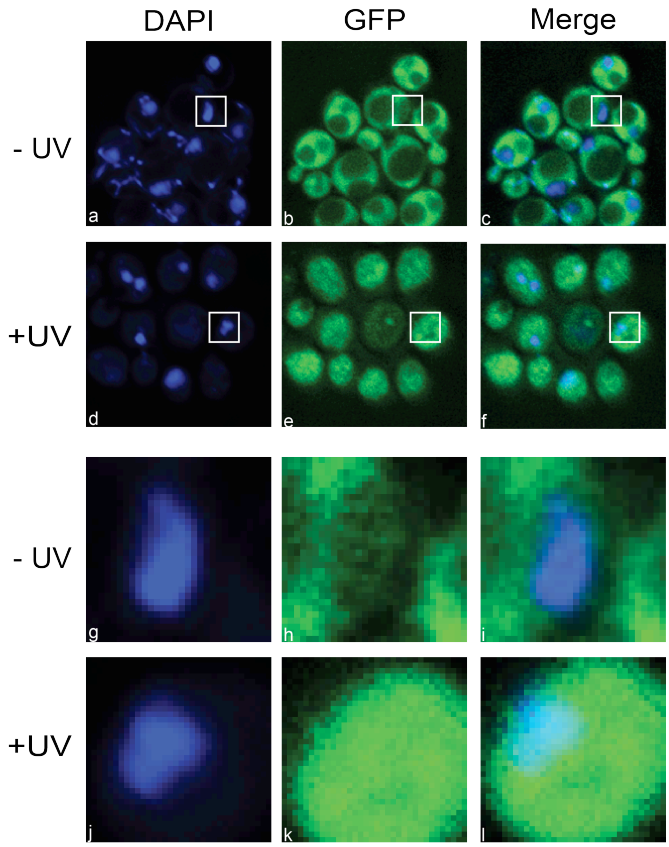

Figure 6.5: GFP-Def1 changes subcellular localisation after DNA damage

Localisation of N-terminally GFP-tagged Def1 in untreated and UV-irradiated cells. Live cells were visualised 1 hour after irradiation, the nucleus is marked by DAPI staining. (Upper panels) A typical field of cells. (Lower panels) Enlargement of the yeast cell, indicated by white box, in the top panels. Please note that although the number and size of vacuoles differed from experiment to experiment, it had no influence on the nuclear accumulation observed.

Previous studies have shown that Def1 is localised to the cytoplasm (Huh et al., 2003, Tkach et al., 2012), despite its involvement in RNAPII poly-ubiquitylation on chromatin. These studies relied on a C-terminally GFP-tagged Def1, allowing visualisation of the full-length protein, but not pr-Def1. By engineering DNA encoding an N-terminal enhanced green fluorescent protein (eGFP) tag into the *DEF1* genomic locus (JSY1194), the localisation of both full-length and processed forms of Def1 could be ascertained. As eGFP fluoresces in live cells, intact non-fixed cells could be visualised. Without UV treatment, Def1 localises predominantly

to the cytosol. Def1 is largely absent from two patches in the cell, one of which is attributable to the nucleus, identified by the blue nuclear DAPI staining (Figure 6.5, panel c and zoom in on one cell panel i). The other, typically larger, GFP signal exclusion zone is the yeast vacuole. The vacuole changes in size during cell cycle progression and due to different nutrient conditions. As a result, the size of the vacuole varies between different experiments, which did not alter the results obtained. Cells were also imaged 1 hour after UV irradiation and under these conditions the eGFP signal was distributed across the whole cell. Notably, there is considerable overlap between the blue, DAPI-stained genetic material and the green, GFP Def1 signal (Figure 6.5, panel f and l). This indicates that, after UV treatment, Def1 can change its subcellular localisation, and partially redistribute to the nucleus.

6.2.4 pr-Def1 changes subcellular localisation after UV irradiation

It was important to ascertain whether it is specifically pr-Def1 that is capable of changing its subcellular localisation, rather than the whole cellular pool of Def1. Moreover, it was unclear whether the apparent change in sub-cellular distribution of Def1 was just an artefact of exposing cells to UV radiation. This remained a possibility as the GFP signal became visible across the whole cell, including the vacuole, after UV irradiation. Hence, UV treatment might theoretically destroy these intracellular compartments, allowing free diffusion of GFP-Def1.

Cells expressing a C-terminally GFP-tagged form of Def1 exhibited normal cellular morphology after UV treatment. Furthermore, these cells did not show appreciable relocalisation of GFP signal after treatment with UV, suggesting that the cellular compartments remained intact (Figure 6.6 A, panel e). Moreover, the lack of Def1-GFP in the nucleus suggests that it is only the N-terminal fragment that changes sub-cellular distribution after UV treatment (compare Figure 6.6 A, panel f with Figure 6.5 panel f). Upon quantification, only the N-terminally, GFP-tagged Def1 strain exhibited significant overlap of nuclear DAPI stain with GFP signal after

irradiation (Figure 6.6 A, right). Around 20% of cells in both strains exhibited some overlap of DAPI with GFP signal, in the absence of DNA damage, which may reflect the lower sensitivity threshold of the experimental system.

Def1 was also N-terminally eGFP-tagged in the MG132 sensitive yeast strain (eGFP-Def1 GAC202, JSY1195) and pre-treated with MG132 prior to irradiation. This allowed the role of the proteasome - and thus the processing of Def1- in the sub-cellular re-distribution of Def1 to be investigated. As shown above, inhibition of proteasomal activity ablates the DNA damage-dependent processing of Def1 (Figure 6.3 B). Without inhibition of the proteasome, the GFP-Def1 signal was observed across the whole cell after UV treatment (Figure 6.6 B, panel f), as seen previously. When the proteasome was inhibited, however, the cellular localisation of Def1 was not appreciably altered by DNA damage. After UV irradiation the majority of cells still displayed predominantly cytosolic localisation of Def1 (Figure 6.6 B, compare panel f with l; see also quantification on the right), suggesting that proteasome-dependent generation of pr-Def1 is required for Def1 accumulation in the nucleus.

Proteasome inhibition does not completely block GFP-Def1 spreading in all the cells. From the quantification of two biological replicates, approximately 40% of cells exhibit overlap of the nuclear and Def1 signal after DNA damage and MG132 treatment, compared to approximately 80% of cells after only DNA damage (Figure 6.6 B, right). This partial effect may be due to incomplete inhibition of the proteasome, which allows some residual Def1 processing (see Figure 6.3 B, +MG132). It should be noted that MG132 treatment of cells affected their morphology: there was a decrease in the number of budded cells, consistent with a reduction in cell growth. MG132 treatment also resulted in the emergence of cytosolic Def1 foci, which were more pronounced after DNA damage (Figure 6.6 B, panels h and k). Human cells exhibit cytosolic foci of unfolded ubiquitylated proteins, termed aggresomes, upon proteasome inhibition (Johnston et al., 1998). Whether the yeast foci observed upon proteasome inhibition are aggresomes, containing Def1, is unclear and requires further study.

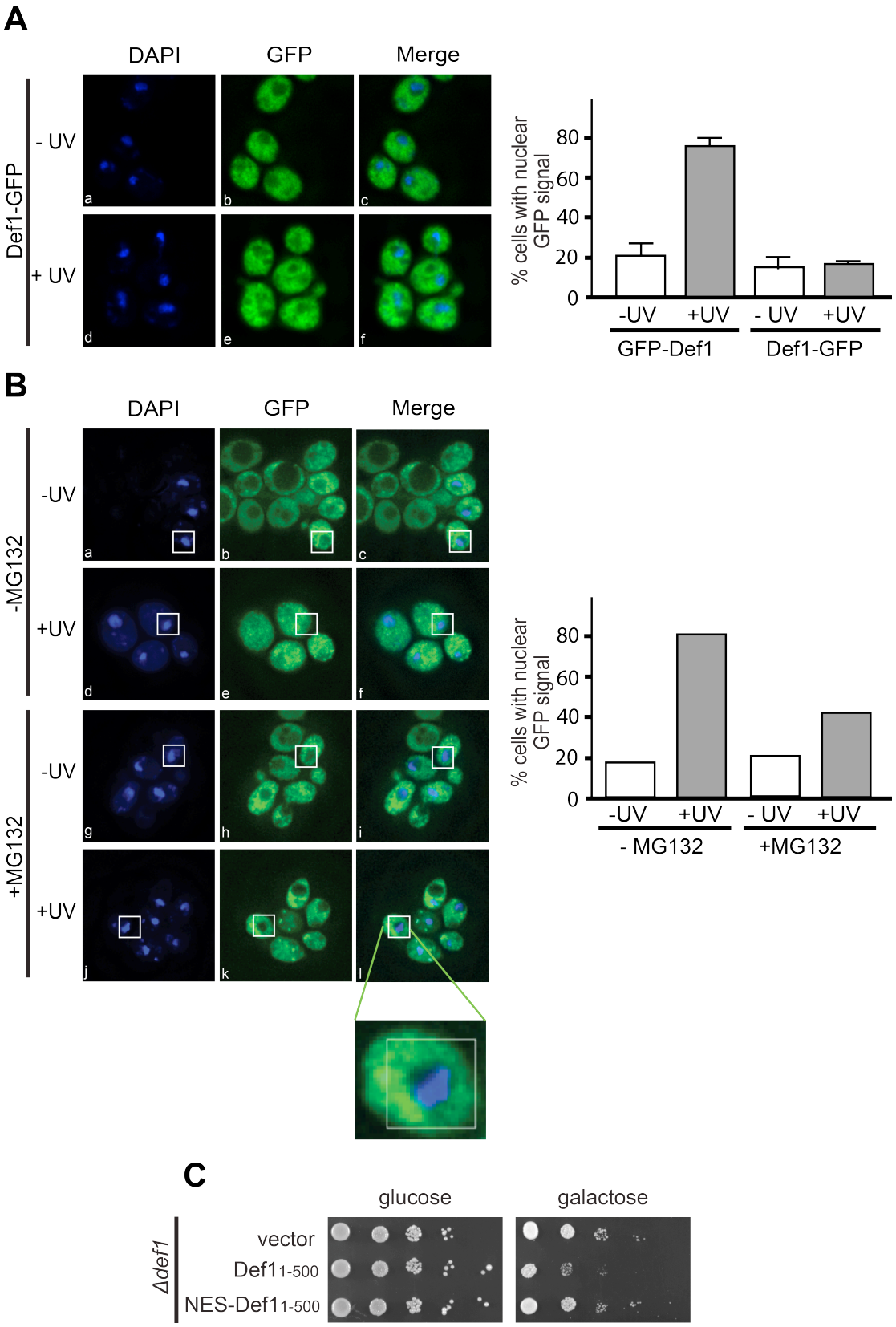

Figure 6.6: accumulation of pr-Def1 in the nucleus after DNA damage mediates its toxicity

A. A typical field of cells showing localisation of C-terminally GFP-tagged Def1 in untreated and UV-irradiated cells as Figure 6.5 (left panel). Quantification of Def1 nuclear accumulation in cells expressing N-terminally tagged GFP-Def1 or C-terminally tagged Def1-GFP, respectively, with or without UV-irradiation as indicated (right panel). Error bars indicate standard deviation of three biological replicates, counting a total of 200-300 cells for each condition.
B. Localisation of GFP-Def1 in proteasome-sensitive GAC202 cells incubated in the absence or presence of MG132 for 1 hour prior to UV irradiation and visualised one hour hence. (Left panel) A typical field of cells. (Right panel) Quantification of Def1 nuclear accumulation in proteasome active and inhibited cells, with and without UV treatment. Data obtained from around 200 cells from two biological replicates.
C. Yeast growth analysis of Δdef1 cells with (right panel) or without (left panel) galactose induction of 1-500 Def1 or 1-500 Def1 with a consensus Nuclear Export Signal (NES) at the N-terminus.

Over-expression of the first 500 amino acids of Def1 is toxic to cells (Figure 5.4 C). As the active pr-Def1 form is localised to the nucleus, we considered the possibility that the forced export of $Def1_{1-500}$ from the nucleus might suppress its toxicity. Indeed, appending a nuclear export signal (NES; Wen et al., 1995) to the N-terminus of $Def1_{1-500}$ partially rescues the toxic phenotype (Figure 6.6 C, compare vector to NES-$Def1_{1-500}$). This suggests that the toxicity mediated by the $Def1_{1-500}$ is at least partially dependent upon its nuclear localisation. This is not a complete rescue; possibly because $Def1_{1-500}$ is still imported to the nucleus before it is shuttled out again, and thus allowed access to RNAPII. $Def1_{1-500}$ is also under constant galactose expression, resulting in very high levels of expression; this might overload the NES-dependent export pathway, resulting in some growth retardation.

6.2.5 The C-terminus of Def1 promotes its steady state cytoplasmic localisation

The data above indicate that Def1 can accumulate in the nucleus upon partial proteasomal processing. Under normal, non-stressed, steady state conditions the protein appears to be largely cytoplasmic, spatially excluded from its substrate in the nucleus. As a result, Def1 processing and dynamic compartmentalisation may help to control Def1 function, by restricting access to stalled RNAPII on chromatin. Def1 may be actively excluded from the nucleus by its C-terminus, whereby the

removal of this section – after transcription stress - allows active import into the nucleus.

There are several shortcomings of this hypothesis. First, this model does not explain how the signal of persistently stalled RNAPII is transduced to the cytosol, leading to the processing of Def1. Second, previous data indicated that full-length Def1 can be extracted from chromatin (Woudstra et al., 2002) and can associate with nuclear RNAPII (Reid and Svejstrup, 2004). Finally, the Svejstrup lab has shown that some poly-ubiquitylation and degradation of Rpb1 is required to deal with 'everyday' transcription stalling (Sigurdsson et al., 2010, Hobson et al., 2012). As a result, some Def1 might be required, even in the absence of DNA damage, due to some basal transcription-stress.

An alternative possibility is that full-length Def1 can be present both in the nucleus and cytoplasm, but appears to be mainly steady state cytosolic because it is actively pumped out of the nuclear compartment. In this model, Def1 constantly samples the nucleus for RNAPII stalling, and may become proteolytically processed, on chromatin *in situ,* when stalling occurs, allowing its nuclear retention. The two models - nuclear exclusion versus nuclear export - differ in their prediction for the function of the C-terminus of Def1: in the former it inhibits nuclear import, and in the latter it directs nuclear export.

In order to distinguish between these models, the relative distribution of control proteins in the strains used in this study was first required. A protein with both a nuclear localisation signal (NLS) and a NES was distributed around the whole cell, indicating a dynamic balance between the NLS targeting the protein to the nucleus and the NES directing it to the cytoplasm (Figure 6.7, panels a-c), as has been observed previously by others (Taura et al., 1998). A construct with a NLS, GFP protein and β-galactosidase (β-gal) was used as a positive control for nuclear localisation (Figure 6.7, panels d-f). The β-galactosidase acts as a control protein-tag that does not affect the localisation of the hybrid protein, which is directed to the nucleus by the N-terminal NLS (Lee et al., 1996).

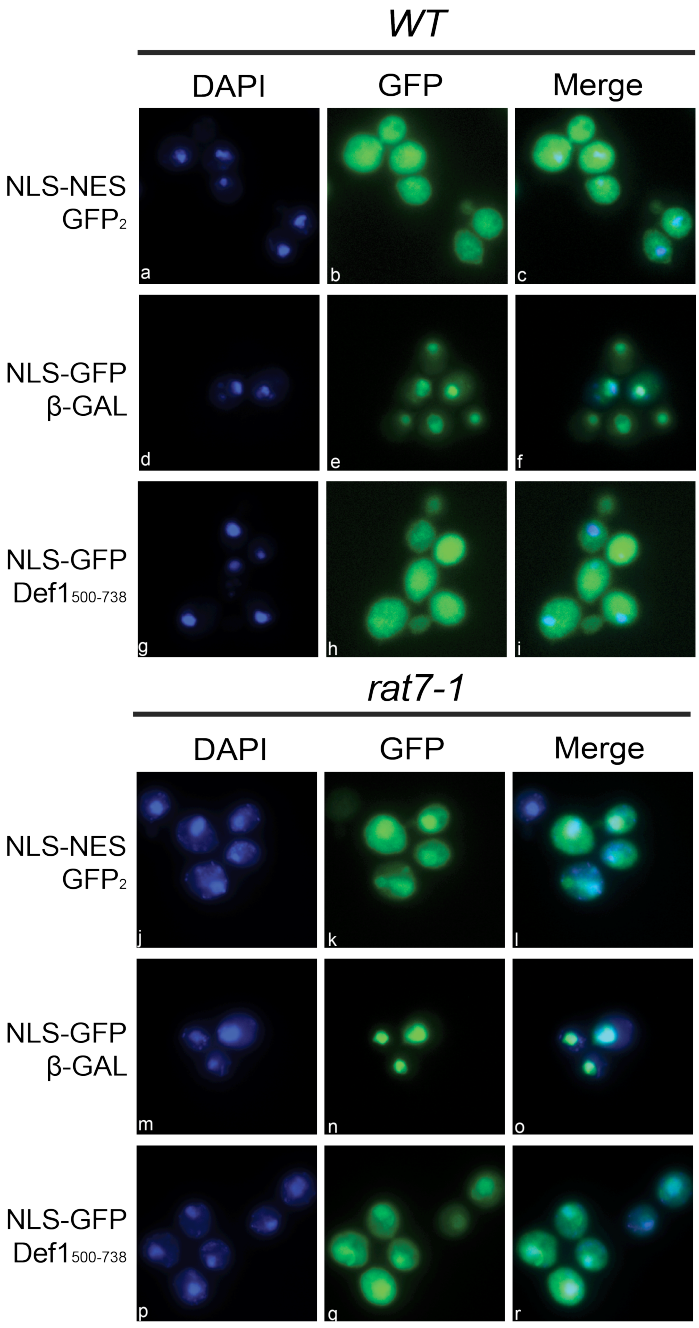

Figure 6.7: The C-terminus of Def1 promotes the nuclear export of Def1

Localisation of NLS-GFP proteins in fixed cells. Wild-type (upper panel) or *rat7-1* (lower panel) cells expressing NLS-NES-GFP_2 (pPS1372), NLS-GFP-β-galactosidase (pPS815), or NLS-GFP-$Def1_{500-738}$ were grown at 23°C and shifted to 30°C for 2 hours before fixing in formaldehyde.

To test the role of the C-terminus of Def1, the β-gal control tag was substituted with the last 238 amino acids of Def1 (NLS-GFP-$Def1_{500-738}$). If the C-terminal polypeptide of Def1 - removed by proteolysis in processing - normally prevents

entry to the nucleus, then the NLS-GFP-Def1$_{500-738}$ construct would only appear in the cytosol. In contrast, if this domain promoted nuclear export, then the fusion protein would be able to move into the nucleus, before being pumped out. Interestingly, the C-terminus of Def1 radically altered the localisation of NLS-GFP, mirroring the pattern observed for the NLS-GFP$_2$-NES (Figure 6.7, panels g-i): the GFP signal was distributed equally over the entire cell. This suggests that the C-terminus of Def1 does not interfere with nuclear import and may actively promote nuclear export.

To further test this hypothesis, a temperature-sensitive *rat7-1* strain was used. Rat7/Nup159 is a core component of the nuclear pore complex. In the *rat7-1* strain most nuclear export is inhibited at the non-permissive temperature (Gorsch et al., 1995). Analysing the same constructs described above in the *rat7-1* strain showed marked nuclear accumulation of both the NLS-GFP$_2$-NES and NLS-GFP-Def1$_{500-738}$ proteins (Figure 6.7, panels j-l, p-r), indicating these were captured in the nucleus, unable to be re-exported after NLS-directed import. Interestingly, this marked effect was observed even at the semi-permissive temperature of 30^{o}C. These observations suggest that the C-terminus of Def1 is acting like a NES, to promote the export of Def1 from the nucleus, rather than preventing its entry. Whilst the artificial test proteins used here are distributed throughout the whole cell, this is not the case for the full-length Def1 protein. This is possibly due to the relative strength of any NLS found within Def1 compared to the SV40 NLS sequence used in the constructs tested here. The SV40 NLS is near to the ideal consensus sequence recognised by Kap60 (importin-α) (Lange et al., 2007). Def1 contains a predicted, but weak, lysine-rich NLS encompassed by the CUE domain (residues 74-80). A high level of NLS sequence conservation promotes improved nuclear import (Hodel et al., 2006). Furthermore, the positioning of the NLS in Def1 might alter its ability to bind Kap60. Thus, the import activity of this NLS may normally be overwhelmed by the activity of the - so far poorly defined – Def1 C-terminal nuclear export signal.

The C-terminus of Def1 is sufficient to promote nuclear export of another protein. The majority of proteins actively exported from the nucleus contain a short leucine rich NES, which is bound directly by the Crm1/Xpo1 exportin (Hutten and Kehlenbach, 2007). No clear leucine rich region could be identified in Def1, either

manually or by using NES prediction tools (http://www.cbs.dtu.dk/services/NetNES/). In agreement with the lack of a NES-like sequence, the export of Def1 does not seem to rely on Crm1. This was visualised using a strain carrying a *CRM1* mutation, sensitising the protein to Leptomycin B (LMB) inhibition (MNY8; Neville and Rosbash, 1999). LMB inhibits Crm1 in *Schizosaccharomyces pombe* and its homologue in mammalian cells, Exportin-1, by covalently binding to a conserved cysteine residue in the proteins' NES-binding domain. The *S. cerevisiae* MNY8 strain has this sensitising cysteine mutation, making it possible to rapidly block NES-directed export by addition of LMB to the media (Neville and Rosbash, 1999).

Addition of LMB to MNY8 cells transformed with the NLS-GFP_2-NES protein rapidly led to the accumulation of the protein in the nucleus, as nuclear export for this NES-containing protein was blocked (Figure 6.8 A, panels j-l). Movement of Def1 in the same strain background was observed by N-terminally eGFP tagging Def1 genomically (JSY1201). This strain did not accumulate eGFP-Def1 in the nucleus after extensive LMB treatment (Figure 6.8 A, panels d-f), suggesting the dynamic shuttling of Def1 was not appreciably affected. Therefore, Def1 nuclear export is probably not mediated via the classical Crm1/NES pathway. Instead, export may be mediated through one of the other, poorly characterised, nuclear export pathways identified in yeast (Strom and Weis, 2001).

Remembering the striking range of phenotypes observed by making Def1 C-terminal genomic deletions ($Def1_{1-500}$, was lethal, $Def1_{1-530}$ was viable but temperature sensitive and $Def1_{1-540}$ had no discernable phenotype) (Figure 5.5), we hypothesised that the region encompassing amino acids 500-540 might contain a sequence required for nuclear export. However, appending Def1 residues 500-540 to a protein with an N-terminal NLS-and two GFPs was not sufficient to alter its subcellular localisation, suggesting that this region is not sufficient, by itself, to promote nuclear export (Figure 6.8 B, compare panels c and f). The export signal may be a large conformational element, which cannot be described by short, simple tracts of primary sequence. No export sequences have been identified for the other, non-Crm1 dependent, export pathways found in yeast. It is more likely that recognition is mediated through tertiary structure (Xu et al., 2010) and therefore the entire C-terminus of Def1 may be required for export. In connection, it

is interesting to note that the C-terminal region of Def1 is glutamine rich, and poly-glutamine expansions have been shown to promote nuclear export (Chan et al., 2011). In this paper, a large poly-glutamine section was sufficient to ensure nuclear export. However, this was mediated via the Exportin-1-NES pathway. In contrast, if the glutamine rich region of Def1 helps to promote nuclear export in yeast, it is probably not dependent upon the Crm1-NES pathway.

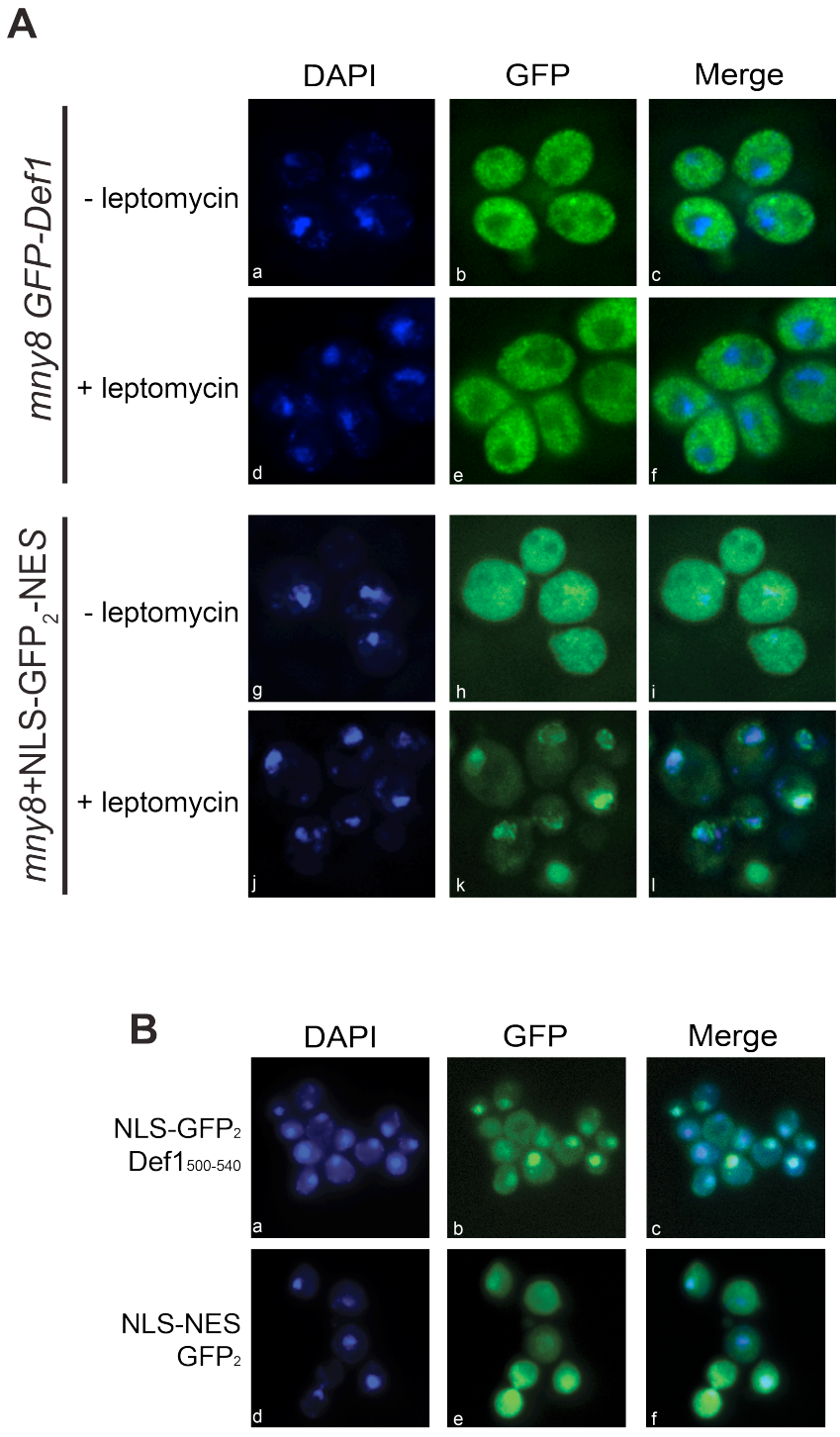

Figure 6.8: Def1 is exported in a Xpo1 independent manner

A. Localisation of GFP proteins in fixed Leptomycin B (LMB) sensitive MNY8 cells. MNY8 cells with the T539C LMB sensitising mutation in Crm1 were incubated with or without LMB for 30 minutes before fixing in formaldehyde and visualising. MNY8 cells, with eGFP-Def1, were generated by Michelle Harreman.
B. A typical field of cells showing the localisation of NLS-GFP proteins under steady state conditions. Cells were transformed with vectors promoting the expression of NLS-GFP_2-$Def1_{500-540}$ and NLS-NES-GFP_2.

6.2.6 Conclusions

In this chapter, evidence has been provided for the manner in which Def1 is processed to an active N-terminal fragment, how this is controlled, and why it is necessary to control the protein. Def1 is ubiquitylated by the HECT E3 ligase Rsp5 and blocking this ubiquitylation ablates partial proteolytic processing. Ubiquitylation may target Def1 to the proteasome, where instead of being totally degraded it is partially processed, releasing an active N-terminal fragment. This active, pr-Def1 fragment appears to be no more active biochemically than the full-length protein. Instead, Def1 is controlled at a cellular level, through dynamic compartmentalisation. The pr-Def1 fragment accumulates in the nucleus, as the C-terminus normally promotes the nuclear export of full-length Def1. The partial proteasomal processing of Def1 creates an elegant, irreversible control step, in order to mediate Def1 access to its substrate. Exactly how the C-terminus of Def1 facilitates nuclear export remains unclear, but it is not mediated through the canonical NES-Crm1 pathway

Chapter 7. Results IV
The Role of Def1 in the Nucleus

7.1 Aims

The previous results chapter outlined that pr-Def1 accumulates in the nucleus after its C-terminus has been proteolytically removed. Up to this point the protein has been termed as 'active' and 'toxic', but what mediates this toxicity is not known. Aberrant expression of pr-Def1-like molecules leads to the poly-ubiquitylation and degradation of Rpb1. The manner in which nuclear pr-Def1 mediates this process was investigated and the results are presented in this chapter.

Def1 lacks any clear enzymatic activity domains, so instead, may act as a scaffold for binding components of the RNAPII poly-ubiquitylation pathway. We set out to find what pr-Def1 was binding to in the nucleus and how this leads to the degradation of Rpb1. Previous studies have found that full-length Def1 can interact with Rad26 (Woudstra et al., 2002) and RNAPII (Reid and Svejstrup, 2004). RNAPII poly-ubiquitylation is a multi-step process involving many protein factors (see 1.5.3), all of which could be potential pr-Def1 interactors. We also wanted to investigate which part of Def1 was responsible for any binding and whether this was also responsible for mediating RNAPII poly-ubiquitylation.

7.2 Results

7.2.1 Def1 requires its N-terminal CUE domain for activity

Def1 has a putative N-terminal CUE (coupling of ubiquitin conjugation to endoplasmic reticulum degradation) ubiquitin-binding domain (UBD), identified via loose sequence homology (Ponting, 2002). CUE domains have been reported to

bind ubiquitin; structural and mutational data has revealed that this interaction is mediated via hydrophobic interactions (Shih et al., 2003, Kang et al., 2003). A hydrophobic pocket within the CUE domain fold accommodates the Leu8-Ile44-Val70 patch of ubiquitin. The mutation of four key residues in the CUE domain pocket ablates ubiquitin-binding activity (Shih et al., 2003). In Def1 these residues were predicted to correspond to Phe32-Pro33 and Ile54-Ile55. We mutated these residues to alanine, hereafter termed CUE mutant (CUEm Figure 7.1 A, left). Over-expression of wild-type Def1 in *Δdef1* cells, leads to a rescue of the slow growth phenotype of these cells. Such rescue was also observed for over-expression of the mutant protein (Figure 7.1 A, right), suggesting that the full-length CUEm protein can be both expressed and is not detrimental to growth. However, over-expression of the CUE mutated 1-500 Def1 ($Def1_{1\text{-}500/CUEm}$) was not toxic, unlike the expression of the cognate non-mutant $Def1_{1\text{-}500}$ (Figure 7.1 A, right). This dramatic rescue suggests that the CUE domain is critical to the function of pr-Def1.

Mutating the CUE domain at the genomic locus of Def1 (*def1*$_{CUEm}$, JSY 1196) does not affect the formation of pr-Def1, in response to UV irradiation (Figure 7.1 B). Furthermore, the mutations do not prevent the induced accumulation of pr-Def1 in the nucleus after UV damage (Figure 7.1 C, compare panels f to l), suggesting that the function of the CUE domain lies downstream of Def1 activation. Indeed, *def1*$_{CUEm}$ displays reduced poly-ubiquitylation of Rpb1 after UV irradiation (Figure 7.1 B, upper). Despite the correct processing of Def1 and relocalisation to the nucleus, a functional CUE domain is thus required to induce poly-ubiquitylation of Rpb1.

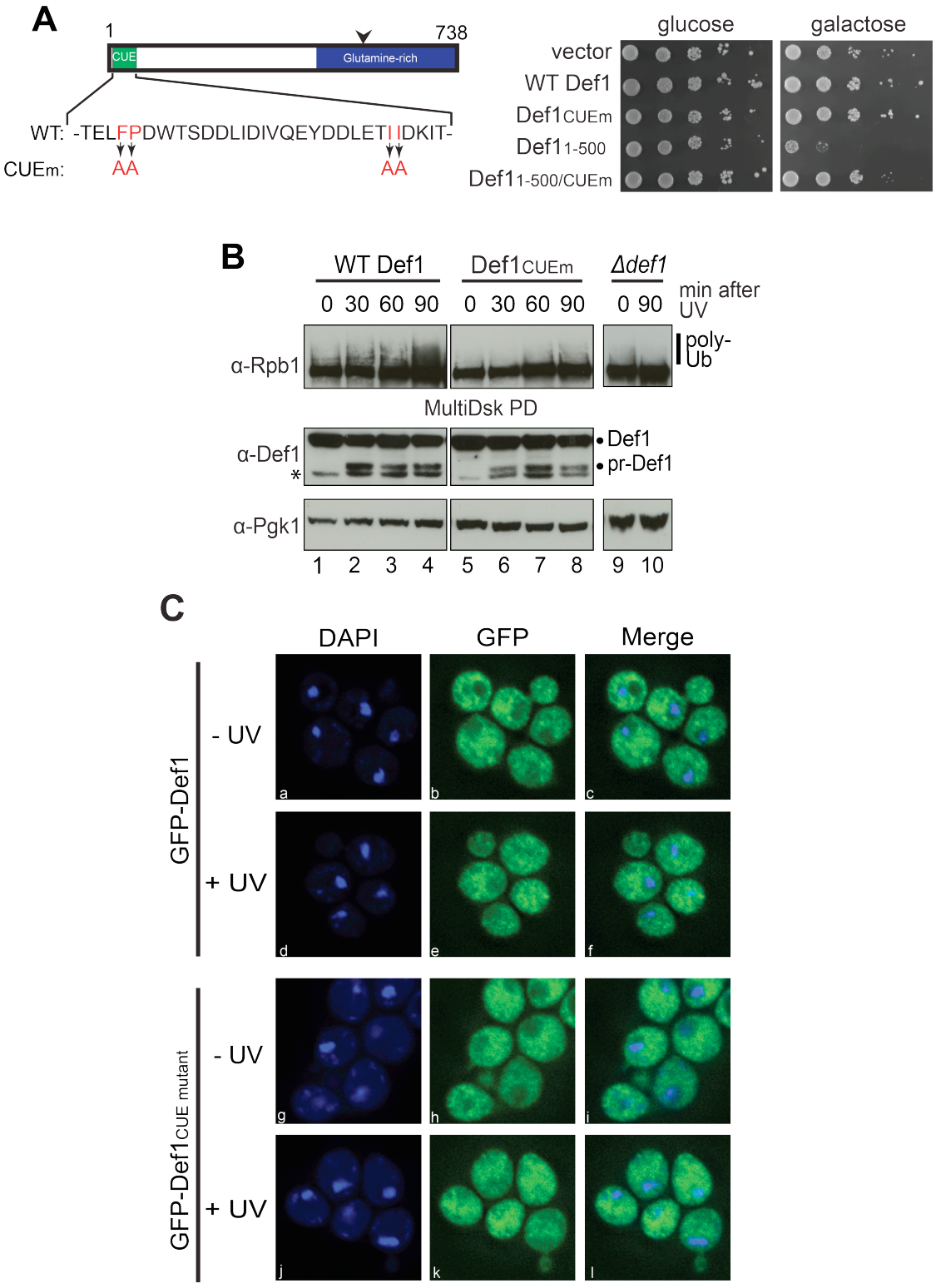

Figure 7.1: The CUE domain of Def1 is essential for Def1-dependent poly-ubiquitylation of Rpb1

A. (Left) Schematic of Def1 showing the 4 key residues of the CUE domain, which were mutated (F33A, P34A. I54A, I55A). (Right) Yeast growth assay of *Δdef1* cells (carrying the *GAL*-driven plasmid indicated on the left) on glucose or galactose, as indicated.
B. Western blot of extracts from KI def1 (WT), *def1$_{CUEm}$* (JSY1196) or *Δdef1* strains. Cells were UV-irradiated and extracts taken at the indicated time-points taken. Western immunoblot for Def1 and Pgk1 in cell extracts is shown. MultiDsk ubiquitin enrichment was performed on the extracts and immunoblotted for Rpb1 (4H8). Asterisk indicates a non-specific antibody band.
C. A typical field of live cells showing localisation of Def1 in GFP-Def1 wild-type and GFP-Def1$_{CUEm}$ cells, in untreated and UV-irradiated conditions. DNA was stained by DAPI.

The primary hypothesis investigated was that nuclear CUEm pr-Def1 was deficient in a binding event, required for Rpb1 poly-ubiquitylation. The CUE domain of Def1 was predicted to bind mono-ubiquitin (Shih et al., 2003). To assess this *in vitro* we purified the first 500 amino acids of Def1, with a C-terminal His tag (Def1$_{1\text{-}500\text{-}His}$), from *E.coli*. It was assumed that this protein would mimic the functions of pr-Def1. The CUE domain mutations were also incorporated in this protein, creating Def1$_{1\text{-}500/CUEm\text{-}His}$. Def1$_{1\text{-}500\text{-}His}$ binds to immobilised GST-ubiquitin, but not to GST alone, or to GST-ubiquitin with a mutation in the hydrophobic patch (GST-Ubi I44A) (Figure 7.2 A, left). In contrast, Def1$_{1\text{-}500/CUEm\text{-}His}$ interacts very poorly with GST-Ubiquitin, despite roughly equal protein amounts added to the assay (Figure 7.2 A, right). The bound Def1 runs at a lower position to the Input due to a loss of the C-terminal 6xHis tag during the experiment. Intriguingly, Def1$_{1\text{-}500}$ appears to bind preferentially without the C-terminal tag, suggesting that either this form is enriched from the Def1$_{1\text{-}500}$ population, or binding to ubiquitin induces the loss of the 6xHis tag. These results confirm that Def1 does contain a UBD and that this is the N-terminal CUE domain identified bioinformatically.

The *def1$_{CUEm}$* strain cannot promote efficient poly-ubiquitylation of Rpb1. Moreover, the CUE domain of Def1 can bind to immobilised ubiquitin. As RNAPII requires mono-ubiquitylation before a subsequent poly-ubiquitylation step (Harreman et al., 2009) - which involves Def1 (Woudstra et al., 2002) – the most obvious target of Def1's CUE domain would be mono-ubiquitylated RNAPII. In order to test this hypothesis directly, mono-ubiquitylated RNAPII-HA was created using pure E1, E2 (Ubc5), E3 (Rsp5) and NoK ubiquitin - where all internal lysine residues are mutated, to prevent the formation of poly-ubiquitin chains. The reaction is robust and results in a molecular weight shift and slight smear of multiple mono-ubiquitins added to Rpb1 (Figure 7.2 B, compare lanes 3&4). As a control, RNAPII-HA was

left un-ubiquitylated by omitting ubiquitin in the reaction. The ubiquitylation reactions were then incubated with a HA-affinity resin and washed extensively before incubation with recombinant Def1$_{1\text{-}500\text{-}His}$ proteins. Surprisingly, Def1$_{1\text{-}500\text{-}His}$ bound well to immobilised RNAPII, but not to mono-ubiquitylated RNAPII (Figure 7.2 B, lanes 3 & 4). Furthermore, when the CUE domain of Def1 was mutated this did not affect the observed binding pattern (Figure 7.2 B, lanes 6 & 7). Def1$_{1\text{-}500/CUEm\text{-}His}$ bound poorly to mono-ubiquitylated RNAPII, but equally as well to unmodified RNAPII as Def1$_{1\text{-}500\text{-}His}$. These results suggest that, unexpectedly, Def1 interaction with RNAPII is neither dependent on its CUE domain, nor is it stimulated by the ubiquitylation of RNAPII. It is, of course, impossible to rule out that the *in vitro* ubiquitylated RNAPII is not the proper substrate for Def1s CUE domain, or recombinant Def1 is not competent for RNAPII-Ubi binding. While the above experiment was performed using artificial reaction conditions and substrates, multiple other attempts to test the CUE domain dependence of Def1 binding to mono-ubiquitylated RNAPII were also unsuccessful (data not shown).

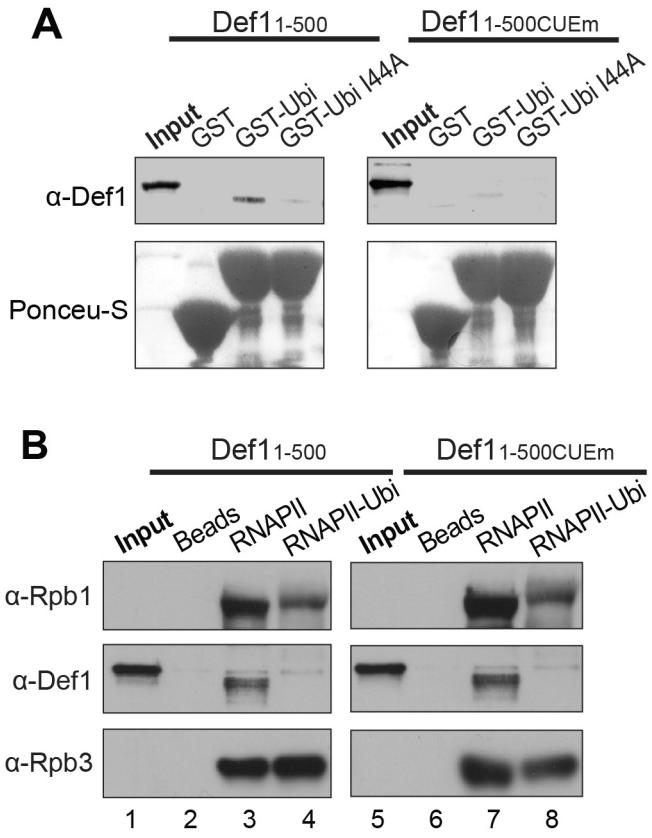

Figure 7.2: The CUE domain of Def1 binds ubiquitin but not RNAPII.

A. Binding of purified, recombinant $Def1_{1\text{-}500\text{-}His}$, or $Def1_{1\text{-}500/CUEm\text{-}His}$ to immobilized GST, GST-ubiquitin or GST-ubiquitin with a hydrophobic patch mutation I44A. 5% of input and bound proteins were loaded onto an SDS-PAGE gel, followed by anti-Def1 immunoblotting. Ponceau S is shown as a loading control for the immobilized proteins.
B. Binding of purified $Def1_{1\text{-}500\text{-}His}$, or $Def1_{1\text{-}500/CUEm\text{-}His}$ to HA antibody immobilized RNAPII or mono-ubiquitylated RNAPII. Western blot analysis was performed with Rpb1 (4H8), Def1 (anti-Def1) and Rpb3 (1Y26), after extensive washing and SDS-PAGE.

In order to find the correct substrate for the CUE domain - taking a less biased approach - $Def1_{1\text{-}500\text{-}His}$ and $Def1_{1\text{-}500/CUEm\text{-}His}$ were immobilised on cross-linkable, Affigel beads (BioRad) and incubated with irradiated crude cell extract. After washing, the bound proteins were resolved by SDS-PAGE and identified by mass spectrometry. Overall, there was a significant enrichment for RNAPII subunits, but no difference between the CUEm and wild-type protein resins. Ubp3, another confirmed Def1 interactor (Kvint et al., 2008), was also significantly enriched in both mutant and wild type pull-downs. Immunoprecipitations (IPs) of Def1, with and without the CUE mutation, displayed no difference in Rpb1 association (Figure 7.7A). Whilst Def1's CUE domain is essential for its function, its exact target remained elusive.

7.2.2 Def1 interacts with Ela1-Elc1 via its CUE domain

As the first, most obvious, theory for Def1's role in promoting RNAPII poly-ubiquitylation had been ruled out, an alternate possibility was investigated. Def1 - and, critically, its CUE domain - may be involved in the binding and recruitment of the E3 ligase required for the poly-ubiquitylation of RNAPII. The Elongin-Cullin complex is required for the sequential poly-ubiquitylation of pre-mono-ubiquitylated Rpb1 (Ribar et al., 2006, Ribar et al., 2007, Harreman et al., 2009). This Elongin-Cullin complex co-purifies as four identified subunits: Elc1 and Ela1 form a Skp1-F-box-like complex, usually implicated in selecting substrate; whereas Cul3 and Rbx1 form the structural and catalytic centre of the ubiquitin ligase, promoting the ubiquitin transfer to substrate. Indeed, null strains lacking components of the proposed ligase cannot poly-ubiquitylate Rpb1 (Ribar et al., 2006, Ribar et al., 2007).

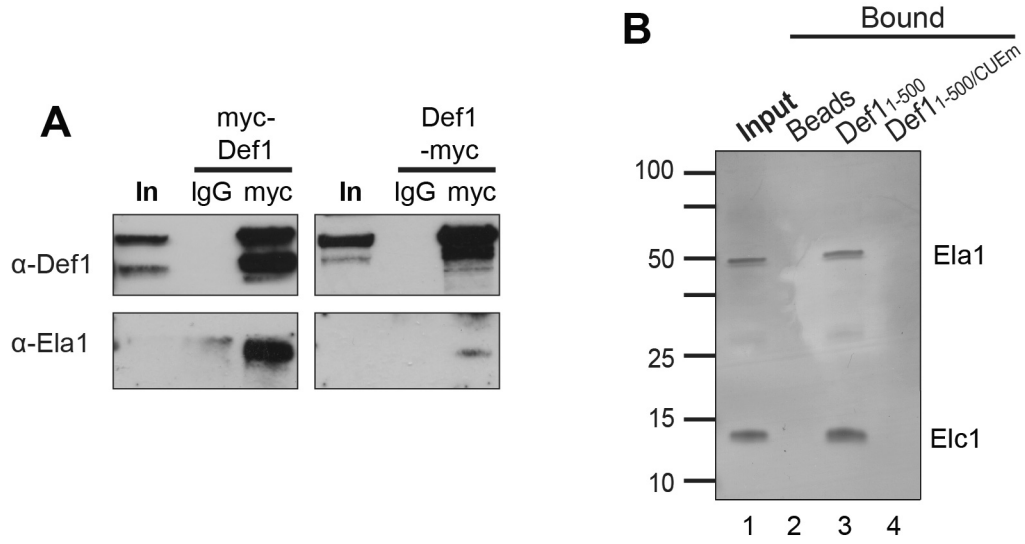

Figure 7.3: pr-Def1 binds Ela1-Elc1 via the CUE domain

A. Immunoprecipitation of N and C-terminally Myc tagged forms of Def1. Tagged strains (JSY1198 & JSY1207) were UV irradiated and allowed to recover for 1 hour before harvest for lysis. Immunoblot for Def1 and Ela1.
B. Silver stain gel of *in vitro* interaction between immobilised Def1 bait protein (covalently immobilised on Affigel beads) and recombinant Elc1-Ela1 heterodimer. 1% input for Elc1-Ela1 is shown.

N-terminally tagged Def1 interacts with the Ela1 subunit of the Elongin-Cullin ligase via co-immunoprecipitation (Figure 7.3 A, left panel). IP studies were performed using extracts derived from cells, irradiated with UV 1 hour prior to harvesting. When Def1 is tagged via its C-terminus, Ela1 association is dramatically reduced (Figure 7.3 A, right panel). This suggests that the active pr-Def1 form - not pulled out when the protein is C-terminally tagged - preferentially interacts with Ela1. Note that Ela1 could not be detected in the input extracts: both Ela1 and Elc1 are believed to be expressed at very low levels cells (Ghaemmaghami et al., 2003), and could not be visualised in extracts in this study. Co-immunoprecipitation of Def1 and Ela1 does not rule out the possibility that this interaction is indirect, via a common interacting partner. Indeed, as both proteins are thought to bind to stalled RNAPII after DNA damage, this co-precipitation might conceivably be mediated through polymerase association.

In order to ascertain whether the interaction between Ela1 and Def1 is direct, recombinant forms of the proteins were used. Ela1-Elc1 forms a hetero-dimer (Koth

et al., 2000). Elc1 contains a region with high homology to Skp1 and Ela1 is an F-box protein (Botuyan et al., 1999, Figure 7.5 A). The proteins have been proposed to interact via the C-terminus of Elc1 and N-terminus of Ela1 and, intriguingly, share opposite and extreme protein isoelectric points. We co-expressed His-tagged Elc1 and Ela1 in *E.coli*, and the complex co-purified at a 1:1 ratio. *E.coli* does not contain an identified ubiquitin system, so any proteins produced in this system would not be ubiquitylated. The recombinant proteins ran at the same molecular weight as the proteins purified from yeast (Figure 7.7 A and data not shown). After chemically cross-linking $Def1_{1\text{-}500\text{-}His}$ and $Def1_{1\text{-}500/CUEm\text{-}His}$ to beads, Ela1-Elc1 association could be tested. Both Elc1 and Ela1 associate with $Def1_{1\text{-}500\text{-}His}$ beads, but not with control beads or beads containing cross-linked $Def1_{1\text{-}500/CUEm\text{-}His}$ (Figure 7.3 B). The Def1 CUEm, which prevents Def1 toxicity and ubiquitin interaction, also prevents association with the Elongin-Cullin substrate adaptor. Notably, immobilising $Def1_{1\text{-}500\text{-}His}$ protein via its N-terminus reduced the association with the Ela1-Elc1 dimer (data not shown), suggesting the N-terminus of Def1 may somehow be involved in this interaction. As $Def1_{1\text{-}500\text{-}His}$ can associate with RNAPII and an Elc1-Ela1 dimer, we propose that pr-Def1 helps to target the Elongin-Cullin ligase to RNAPII (see further evidence in section 7.2.4).

7.2.3 Ela1 contains a C-terminal ubiquitin homology domain, with specificity for Def1

The CUE dependency of the Def1 interaction with Elc1-Ela1 raises an intriguing possibility; does Elc1 or Ela1 contain a ubiquitin homology (UbH) domain? As $Def1_{1\text{-}500\text{-}His}$ has been shown to interact with ubiquitin in a CUE-dependent manner (Figure 7.2 B), the binding to this domain is probably through a ubiquitin-like fold. Domains with homology to ubiquitin have been found via sequence annotation in 32 proteins in *S. cerevisiae* (SMART database), however due to low sequence conservation many other proteins have been predicted to contain UbH domains (Kiel and Serrano, 2006), based on the ubiquitin-domain superfold. The lack of biochemical and structural evidence to back-up the *in silico* identifications has left the list of proposed UbH domain proteins largely uncurated. Using the simplest

biochemical definition, one would assume that a UbH domain would bind to a UBD. Hence, the presence of a UbH domain can be tested through the binding of the proposed UbH-protein to a panel of UBDs. We found that the purified Ela1-Elc1 heterodimer complex not only specifically interacts with the CUE UBD of Def1, but also with all other UBD-containing polypeptides tested (Figure 7.4 A). Pure, recombinant Ela1-Elc1 binds to cross-linked resins containing full-length UBA domain-containing Dsk2, the UIM domains of Ataxin-3 and the tandem UIM domains of RAP80. This interaction is more or less equal, with the exception of some increased association with RAP80 and Ataxin-3 UIMs, possibly due to the presence of multiple UBDs, and hence a higher avidity for Ubiquitin or UbH domains.

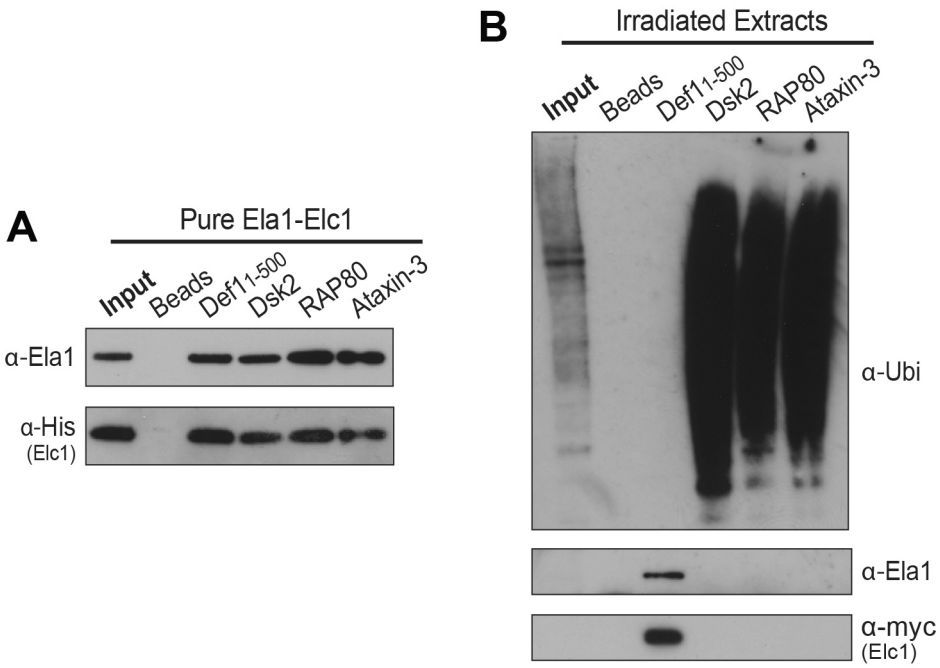

Figure 7.4: Ela1-Elc1 interacts with other UBD containing proteins *in vitro*.

A. Western blot displaying the interaction of Ela1 and His-Elc1 heterodimer with immobilized UBD containing proteins: $Def11_{-500}$, Dsk2 and the tandem UIMS from RAP80 and Ataxin-3. Immunoblotted using antibodies raised against Ela1 and His tag (Elc1).
B. Western blot of *ex vivo* Myc-Elc1 (JSY1116) extract incubated with the UBD resins listed above, immunoblotted for ubiquitin (P4D1), Ela1 and Elc1 (myc). As expected, Ela1 cannot be detected in the crude extract.

Whilst this *in vitro* experiment with pure proteins further indicates that the Ela1-Elc1 complex contains a UbH domain, it raises an important question: If any UBD containing protein can bind to Ela1-Elc1, how is specificity for Def1's CUE domain imparted? The *in vitro* experiments were performed with large excesses of pure protein and BSA, to prevent background binding and simulate protein crowding. The read-out does not provide much quantitative information on the affinities of these interactions, or how these interactions would fare in their proper cellular milieu.

In order to better simulate the *in vivo* environment, the same UBD-containing resins were incubated with UV-irradiated chromatin-enriched extracts taken from a Myc-tagged Elc1 strain (JSY1116). Whilst the Dsk2, RAP80 and Ataxin-3 polypeptides bound to a wide variety of ubiquitylated proteins - as indicated by the smear of proteins pulled-down that cross-react with a ubiquitin antibody (Figure 7.4 B, upper panel) - $Def1_{1\text{-}500\text{-}His}$ did not. Longer exposures revealed that immobilised $Def1_{1\text{-}500\text{-}His}$ could enrich ubiquitin-conjugated proteins, but far less efficiently than the other UBD resins tested. The immobilised $Def1_{1\text{-}500\text{-}His}$, however, did bind well to both Ela1 and Elc1 from the extract (Figure 7.4 B, lower panels). The other UBD containing proteins did not bind to Ela1 or Elc1 in the presence of extracted ubiquitylated proteins. Under these conditions, the proposed UbH domain contained within Ela1-Elc1 likely outcompeted the more abundant ubiquitin for Def1, to mediate specificity. Dsk2, RAP80 and Ataxin-3 exhibit chain specificities and can bind multiple ubiquitylated substrates (Funakoshi et al., 2002, Sobhian et al., 2007, Chai et al., 2004) leading to the promiscuity of binding observed. There was no detectable Ela1-Elc1 association with Dsk2, RAP80 or Ataxin-3, probably because protein enrichment was too low, and/or because the UbH domain is outcompeted by *bona fide* ubiquitin interactions with these proteins.

UbH domains typically have low sequence, but high structural homology to ubiquitin. As a result, direct alignment of sequences is often poor. Elc1 is a small protein, almost entirely assigned as a Skp1-like protein (Figure 7.5 A, upper), and the solution structure does not resemble ubiquitin (Botuyan et al., 2001). In contrast, Ela1 has an N-terminal F-box domain and no other identified downstream features. We aligned the C-terminus of Ela1 and found that it has remarkable homology to

ubiquitin (Figure 7.5 A, lower). Despite three large insertions in Ela1, many key ubiquitin residues were, if not conserved, then highly similar. The hydrophobic patch, Ile-44 in ubiquitin, appears to be conserved with residue Leu-289 of Ela1. Despite a high number of lysine residues in the C-terminus of Ela1, only Lys-27 and Lys-63 align near Ela1's lysines, and ubiquitin chains on Ela1 have not been reported. This same aligned section contains conserved residues at the appropriate positions postulated by Kiel and Serrano to predict a three-dimensional ubiquitin-like superfold (Kiel and Serrano, 2006).

Independent of the above sequence alignment, expression constructs were created with sections of Ela1 removed from the C-terminus, in an unbiased attempt to determine which part of Ela1 was required for the interaction with Def1. The N-terminal 143 residues of Ela1 contain the F-box motif and are sufficient to bind to Elc1 (Koth et al., 2000). Constructs expressing truncated proteins were generated, with 50 amino acids removed at intervals, between residues 150-379 of Ela1 (Figure 7.5 B, right). The proteins co-expressed and formed a complex with Elc1 (Figure 7.5 B, lanes1, 4 and 7), much like the full-length Ela1 protein (lane 10). When incubated with $Def1_{1\text{-}500\text{-}His}$ cross-linked beads, both Ela1 1-250 and 1-300 showed no appreciable binding (Figure 7.5 B, lane 3 and 6), as would be expected if the UbH fold was disrupted. Ela1 1-350 - lacking only the last 29 residues of Ela1 - did bind to immobilised $Def1_{1\text{-}500}$, but not as efficiently as the full-length protein (Figure 7.5 B, compare lanes 9 and 12). These data, partnered with the earlier findings (Figure 7.3 B), indicate that the UbH domain of Ela1 is directly recognised by Def1's CUE domain. It is probable that artificial removal of even a few residues at the C-terminus of Ela1 is enough to disrupt the UbH fold, but do not lead to Ela1 protein instability. The very C-terminal region of Ela1 may be important for this interaction; since strains with a tag added to the C-terminal of Ela1 show reduced ability to degrade Rpb1 after DNA damage (data not shown).

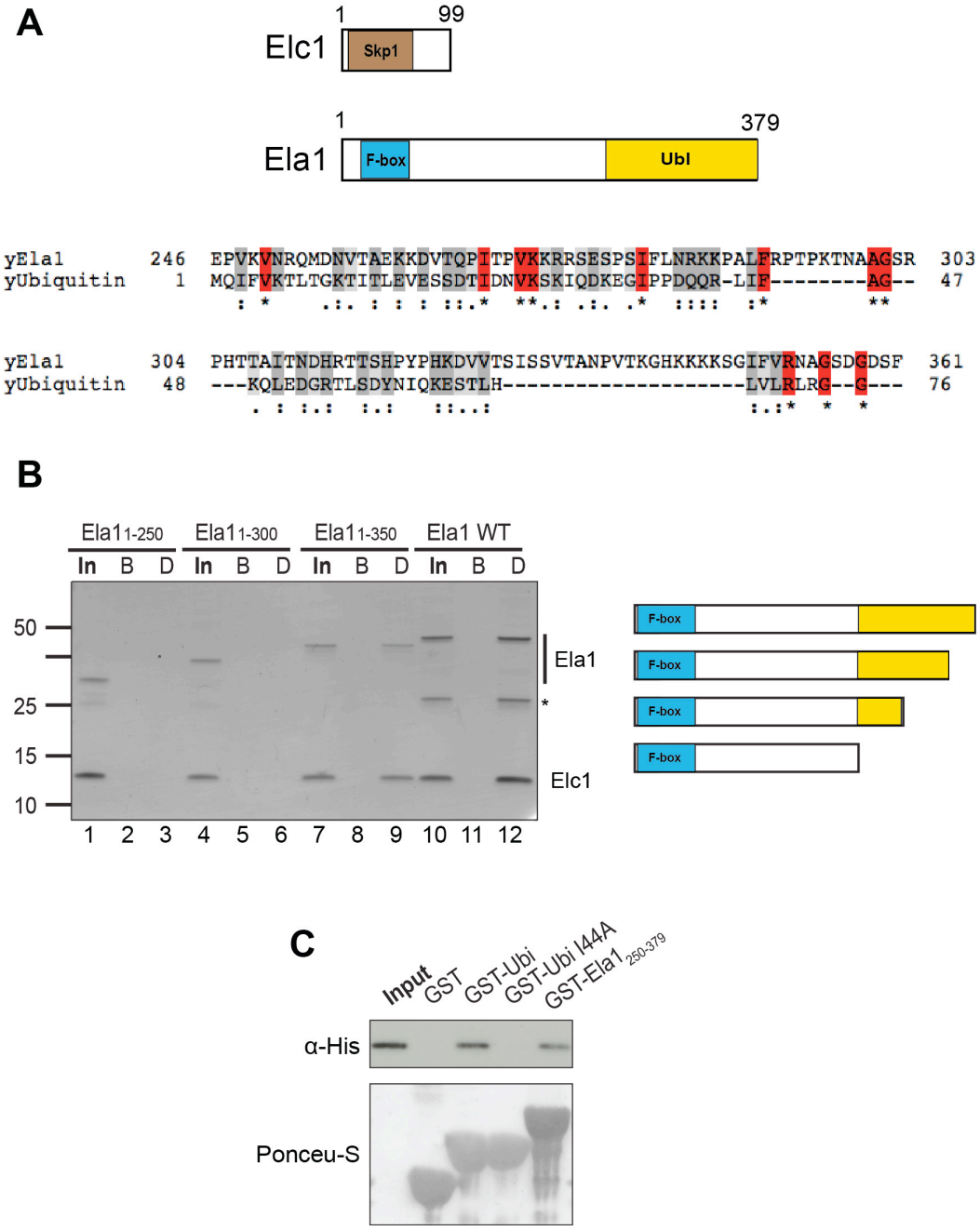

Figure 7.5: Ela1 contains a Ubiquitin-like domain

A. (Upper) schematic representation of Elc1 and Ela1 proteins, indicating the proposed domains, including the C-terminal UbH domain (yellow) in Ela1. (Lower) sequence alignment of the C-terminus of Ela1 with yeast ubiquitin. Similarly conserved residues are highlighted in grey and totally conserved residues highlighted in red. Alignment created using ClustalW (http://www.ebi.ac.uk/Tools/msa/clustalw2/).
B. (Left) Silver stain gel of *in vitro* interaction between immobilised $Def1_{1-500}$ and Ela1-Elc1 heterodimers with C-terminal deletions in Ela1. B=empty beads control, D=$Def1_{1-500}$-beads. Asterisk corresponds to a degradation product of Ela1 observed in this experiment. (Right) schematic of Ela1 proteins used in this assay.
C. Binding of purified, recombinant $Def1_{1-500}$ to immobilised GST, GST-ubiquitin, GST-ubiquitin I44A or GST-Ela1 250-379. 2.5% of input and bound proteins were loaded onto an SDS-PAGE

gel, followed by anti-Def1 immunoblotting. Ponceau-S is shown as a loading control for the immobilized proteins.

The C-terminal UbH domain of Ela1 is necessary for the interaction with $Def1_{1\text{-}500\text{-}His}$, but is the UbH domain sufficient to mediate this interaction? In order to test this possibility the last 129 residues of Ela1 were cloned into a GST expression vector and expressed. The resulting recombinant protein, GST-$Ela1_{250\text{-}379}$, was immobilised on glutathione beads in parallel with GST-Ubiquitin (positive control), GST-Ubiquitin I44A and GST alone (negative controls) (Figure 7.5 C, lower panel for loading). Pure, recombinant $Def1_{1\text{-}500\text{-}His}$ bound to GST-Ubiquitin, as described previously (Figure 7.2 B), and, importantly, also bound to GST-$Ela1_{250\text{-}379}$ (Figure 7.5 C). Whilst the interaction was weaker than for Def1 binding to ubiquitin, this suggests the C-terminus of Ela1 is sufficient to promote Def1 interaction *in vitro*. As immobilised $Def1_{1\text{-}500\text{-}His}$ exhibits specificity for Ela1-Elc1 over ubiquitylated proteins *ex vivo*, other regions of the Ela1-Elc1 complex must aid this interaction.

The C-terminus of Ela1 interacts with Def1, via a UbH–CUE interaction. This interaction is ablated when the CUE domain is mutated. Similarly, when Def1's CUE domain is mutated *in vivo*, Rpb1 ubiquitylation is reduced. If the key role of the CUE domain is to bind the C-terminus of Ela1 and recruit the Elongin-Cullin complex to persistently stalled RNAPII, removal of the UbH section should mirror mutation of the CUE domain. To test this hypothesis, a strain with genomically truncated Ela1 was created (*ela11-250,* JSY 1203). In this strain, Rpb1 was not degraded after 4-NQO treatment, in a manner akin to the cells completely lacking Ela1 protein (Figure 7.6 A). Poly-ubiquitylation of Rpb1 was similarly reduced when the C-terminus of Ela1 was absent (Figure 7.6 B). Def1 processing was unaffected in these strains. This suggests that removal of the C-terminus, including the UbH domain, of Ela1 functionally debilitates the Elongin-Cullin complex, in all probability because the protein can no longer interact with Def1. Critically, deletion of the C-terminus of Ela1 still allowed association with Elc1, in both a recombinant system (Figure 7.5 B) and in yeast IPs (Figure 7.6 C). The Elongin-Cullin complex can interact with RNAPII in Elc1 IPs (Harreman et al., 2009) (Figure 7.6 C, lane 3). This interaction is reduced in Elc1 IPs from the *ela1-250* strain (Figure 7.6 C, lane 6),

suggesting that RNAPII-Elongin-Cullin association is also mediated through the UbH domain, in all likelihood via Def1.

It is unclear from these experiments whether the truncated Ela1 can still form an active complex with the other subunits of the Cullin ligase. Recombinant expression of Cullin complexes is notoriously complicated. In addition, no commercial antibodies are available to the Cul3 or Rbx1 subunits of the Elongin-Cullin complex. No other substrates of the Elongin-Cullin complex have been identified in yeast, making the effect of the UbH domain removal hard to assess. However, as the interaction of $Ela1_{1\text{-}250}$ with Elc1 is maintained, and the Skp1 component is proposed to principally mediate the interaction with the cullin (Zheng et al., 2002), we hypothesise that the truncation of Ela1 does not affect the ubiquitin ligase directly. Instead, according to this hypothesis, the removal of the UbH domain inactivates the E3 ligase principally through preventing the interaction with Def1 and therefore RNAPII.

As the C-terminus of Ela1 is sufficient to allow association with Def1, and Def1 can also bind to ubiquitin, we investigated if ubiquitin could replace the UbH domain of Ela1. In order to achieve this, a strain expressing the first 250 amino acids of Ela1 followed by ubiquitin was created at the *ELA1* locus (*ela11-250-Ubi*; JSY1207). To ensure the ubiquitin was not inappropriately linked to other proteins, the last amino acid was mutated from glycine to valine (Zhao and Ulrich, 2010). The expression of Ela1 in the *ela11-250-Ubi* strain was equivalent to that of *ela11-250* and the wild-type Ela1 strain used (data not shown). However, addition of ubiquitin to the C-terminus of Ela1 did not seem to rescue the $ela1_{1\text{-}250}$ phenotype: Rpb1 degradation was not restored after DNA damage (Figure 7.6 D). This suggests that whilst the C-terminus of Ela1 can mimic ubiquitin, ubiquitin cannot replace the UbH domain to restore the Def1 interaction. The ubiquitylation status of Rpb1 and Elc1 interaction were not assayed in this strain. Immobilised ubiquitin can interact with Def1 *in vitro* (Figure 7.2 a), but Def1 did not bind ubiquitylated proteins strongly *ex vivo* in extracts (Figure 7.4 B). Possibly, replacing Ela1's UbH domain with ubiquitin did not provide the required specificity for the Def1-Ela1 interaction *in vivo*.

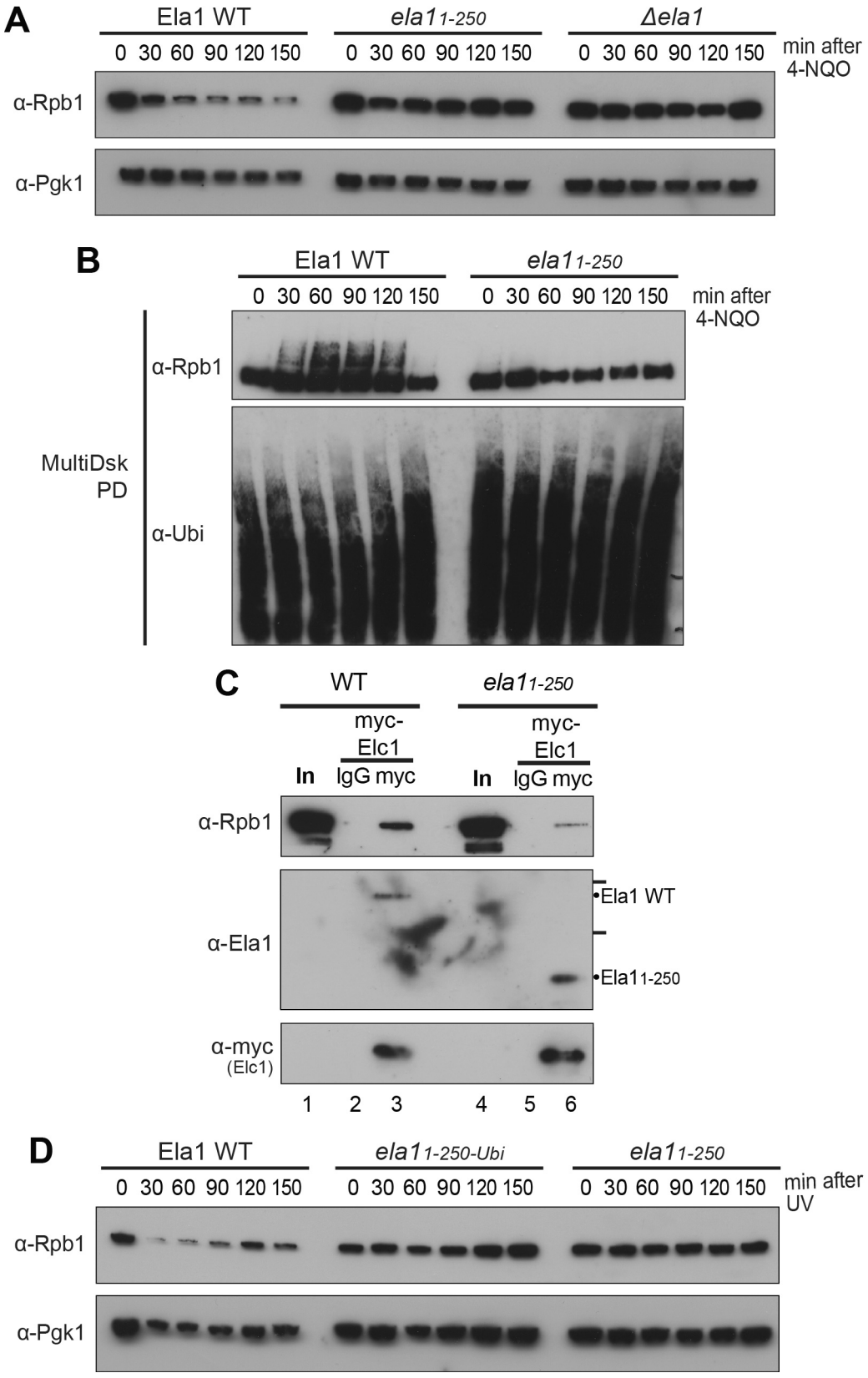

Figure 7.6: The UbH domain is necessary for Ela1 function *in vivo*

A. Western blot of extracts from Ela1 WT (JSY1204), *ela11-250* – where the last 129 amino acids had been genomically truncated - or *Δela1* (JSY1205) cells, were treated with 4-NQO at time point 0. The membrane was probed for Rpb1 (8WG16) and Pgk1.
B. MultiDsk pull-down from Ela1 WT and *ela11-250* strains. Western blot probed for ubiquitin (P4D1) and Rpb1 (4H8).
C. Immunoprecipitation of Myc-Elc1 in WT Ela1 and Ela11-250 strains. Western blot using anti-Rpb1 (4H8), anti-Def1, anti-myc (Elc1) and anti-Ela1. Note the black smear in the Ela1 blot is background signal.
D. Western blot of 4-NQO treated extracts from WT, *ela11-250* and *ela11-250-Ubiquitin* strains, probing for Rpb1 (8WG16) and Pgk1.

7.2.4 Def1 helps to bridge between RNAPII substrate and Elongin-Cullin ligase

pr-Def1, upon translocation to the nucleus, promotes the poly-ubiquitylation of RNAPII. It binds to a ubiquitin-like UbH in Ela1 and loss of this domain prevents the poly-ubiquitylation of Rpb1. As indicated above (Figure 7.6 C), the association of Def1 with Ela1 may have functional consequences. IPs of N-terminally tagged Def1 co-precipitate both RNAPII and Ela1 (Figure 7.3 A and Figure 7.7 A). Mutation of the CUE domain does not ablate RNAPII binding, but greatly reduces Ela1 binding (Figure 7.7 A, compare lane 3 and lane 6). Despite normal RNAPII association in this strain, Rpb1 poly-ubiquitylation is ablated (Figure 7.1 B). One possible model to explain this observation is that Def1 is acting as a bridging factor between enzyme (Elongin-Cullin) and substrate (stalled mono-ubiquitylated RNAPII). When the Def1-interacting UbH domain of Ela1 is removed, its interaction with RNAPII is reduced (Figure 7.6 C), supporting this model. Similarly, if Myc-Elc1 is immunoprecipitated in the *def1*$_{CUEm}$ strain, both the interaction with Def1 is reduced, as expected, but so to is the interaction with Rpb1 (Figure 7.7 B). The common factor in these interactions is Def1.

This interaction was reconstituted with purified components *in vitro*, to see if the proposed bridging ability of Def1 is direct and sufficient. RNAPII-HA was immobilised on HA-affinity beads. Def1$_{1\text{-}500\text{-}His}$ and Def1$_{1\text{-}500/CUEm\text{-}His}$, bound to immobilised RNAPII, but not to empty control beads (Figure 7.7 C, compare lanes 5-8). Def1 bound equally well to RNAPII, irrespective of the mutation in the CUE domain, as seen previously (Figure 7.2 B). The Ela1-Elc1 complex bound poorly to

RNAPII alone, with no detectable Elc1 binding (lane 10). Critically, this binding was substantially increased upon the addition of $Def1_{1\text{-}500\text{-}His}$ (lane12). Moreover, the ability of Def1 to bridge the interaction between RNAPII and Ela1-Elc1 was dependent on the CUE domain: even though $Def1_{1\text{-}500/CUEm\text{-}His}$ associated with RNAPII-containing beads as efficiently as its wild-type counterpart (compare lanes 6 and 8), it had little or no stimulatory effect on Ela1-Elc1 binding to RNAPII (compare lanes 12 and 14). Interestingly, the addition of Ela1-Elc1 also clearly increased Def1-RNAPII interaction (compare Def1 binding in lane 12 with that in 6, 8 and 14), contributing to a more stable RNAPII/Def1/Ela1-Elc1 ternary complex.

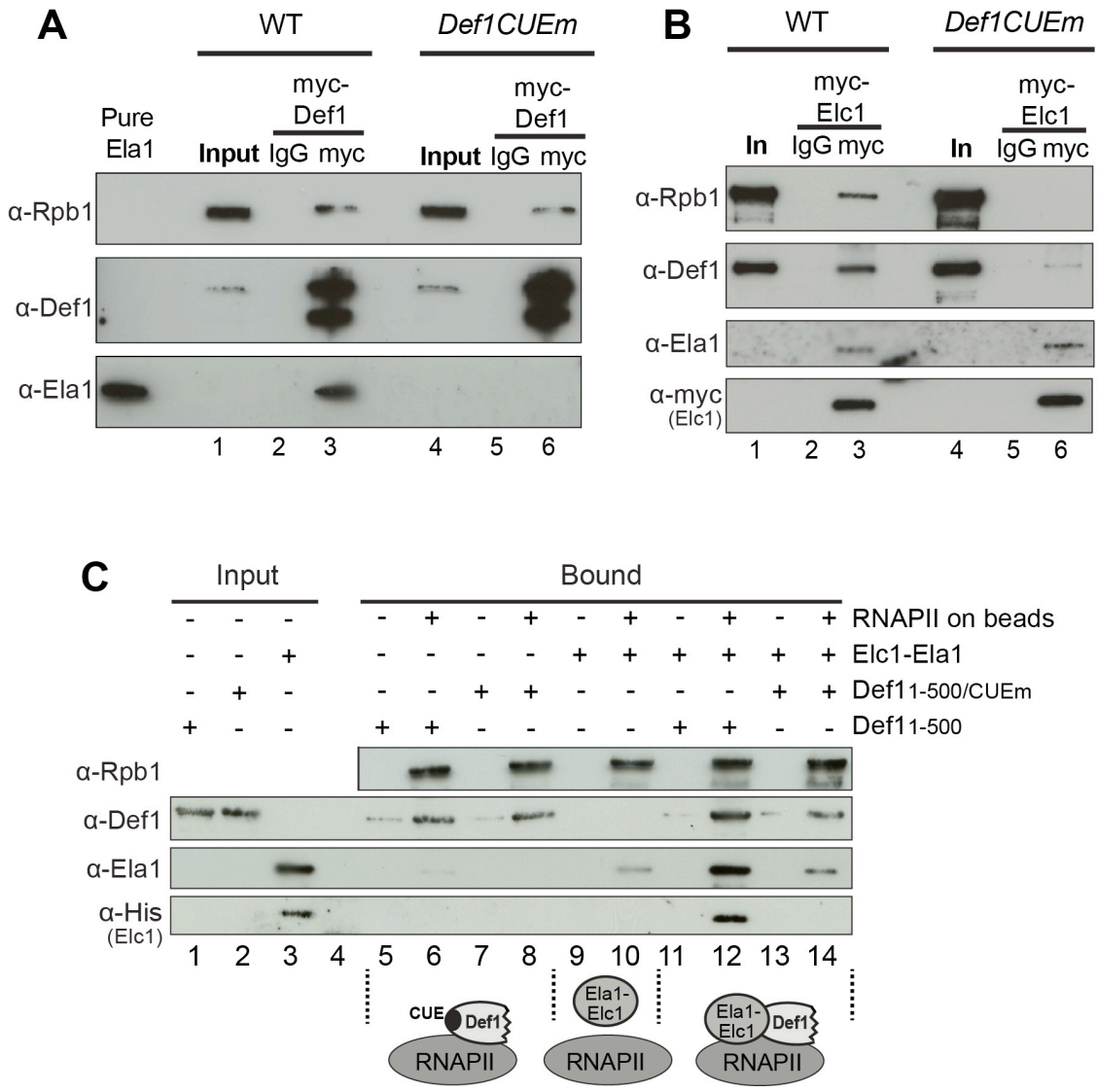

Figure 7.7: Def1 binds RNAPII and Ela1-Elc1

A. Immunoprecipitation of N-terminally Myc-tagged Def1, with and without mutation of the CUE domain (JSY1198 & JSY1199). Cells were UV irradiated and allowed to recover for one hour, before harvest and extraction of proteins. Immunoblot for Rpb1 (4H8), Def1 and Ela1. Pure Ela1 protein was loaded as an antibody control.
B. Immunoprecipitation of N-terminally Myc-tagged Elc1, with and without mutation of the CUE domain of Def1 (JSY1116 & JSY1202). Cells were UV irradiated and allowed to recover for one hour. Immunoblot for Rpb1 (4H8), Def1, Ela1 and Elc1 (anti-myc).
C. Binding of recombinant Ela1-Elc1 heterodimer to immobilized RNAPII (or empty control beads), in the absence or presence of recombinant $Def1_{1\text{-}500\text{-}His}$, or $Def1_{1\text{-}500/CUEm\text{-}His}$. Assay analysed by Western blotting. Schematics of results are shown below the relevant lanes.

There is some residual Ela1-Elc1/RNAPII interaction in both *in vitro* and IP assays. Whether this is a genuine interaction remains to be determined, but in all cases it is above the level of 'background' empty-control beads, suggesting there is an element of Elongin-Cullin-RNAPII interaction, not mediated through Def1. This interaction appears to be very weak, but may explain why the mutation of the CUE domain of Def1 reduces RNAPII-ubiquitylation, but does not completely prevent it. Removal of the C-terminal 129 residues of Ela1 prevents RNAPII-ubiquitylation to a greater extent, suggesting that this residual interaction may be via the C-terminal UbH of Ela1.

7.3 Conclusions

pr-Def1 toxicity is due to the dysregulated activity of the N-terminal ubiquitin-binding CUE domain. The principal target of the CUE domain is unmodified Ela1, which contains a ubiquitin-like, UbH domain. The UbH domain maps roughly to residues 250-379 of Ela1. Whilst the CUE domain can bind ubiquitin, we propose that the UbH-CUE domain interaction is specific to Ela1, ensuring that Def1 does not bind to ubiquitylated proteins and that other UBD-containing proteins do not bind Ela1.

If the interaction between Def1 and Ela1 is ablated, then the Elongin-Cullin interaction with its substrate is also decreased, preventing the targeting of the ligase to stalled RNAPII. Def1 binds to both the Elongin-Cullin complex and RNAPII, bridging the interaction between substrate and enzyme. In some ways, Def1 can be considered an additional subunit, or bridging factor, of the Elongin-Cullin complex,

and it is this bridging factor that imposes both the specificity to RNAPII and control of RNAPII-ubiquitylation after transcription stress.

Chapter 8. Discussion II

pr-Def1: A key Protein for the Poly-ubiquitylation of Rpb1

Work over the past decade, from multiple laboratories, has helped to elucidate the mechanism of Rpb1 poly-ubiquitylation and degradation (reviewed in Wilson et al., 2013, see introduction, 1.5.3). However, the mechanistic function of Def1 - one of the first factors identified to be involved in the Rpb1 poly-ubiquitylation process (Woudstra et al., 2002) – had not previously been expounded. Work presented in this thesis has suggested that Def1 acts at the confluence of a number of ubiquitin-related processes. Def1 becomes ubiquitylated, thus targeting it for partial proteolytic processing by the proteasome. The proteasome degrades the C-terminus of Def1 and releases a N-terminal fragment, which can then accumulate in the nucleus. Nuclear pr-Def1 binds to both stalled RNAPII and the Elongin-Cullin complex. Binding to the E3 ligase is mediated through Def1's CUE ubiquitin binding domain (UBD), whose principle target is the newly identified ubiquitin homology (UbH) domain of Ela1, rather than ubiquitin. This allows the recruitment of the Elongin-Cullin E3 complex to RNAPII, which in turn promotes Rpb1 poly-ubiquitylation and degradation by the proteasome (Figure 8.1).

8.1 The Mechanistic Role of Def1 in RNAPII Ubiquitylation

Rpb1 ubiquitylation and degradation occurs via a complex, multi-step mechanism (see Introduction 1.5.3) The initial, Rsp5-catalysed, Rpb1 mono-ubiquitylation is not dependent on Def1, but is accelerated by the protein *in vitro* (Woudstra et al., 2002, Somesh et al., 2005). The subsequent step is catalysed by another E3 ligase, the Elongin-Cullin complex, which takes over to perform poly-ubiquitylation (Ribar et al., 2006, Ribar et al., 2007, Harreman et al., 2009). The data presented in this thesis explains how Def1 fits into this complex scheme: through promoting efficient Rpb1 poly-ubiquitylation.

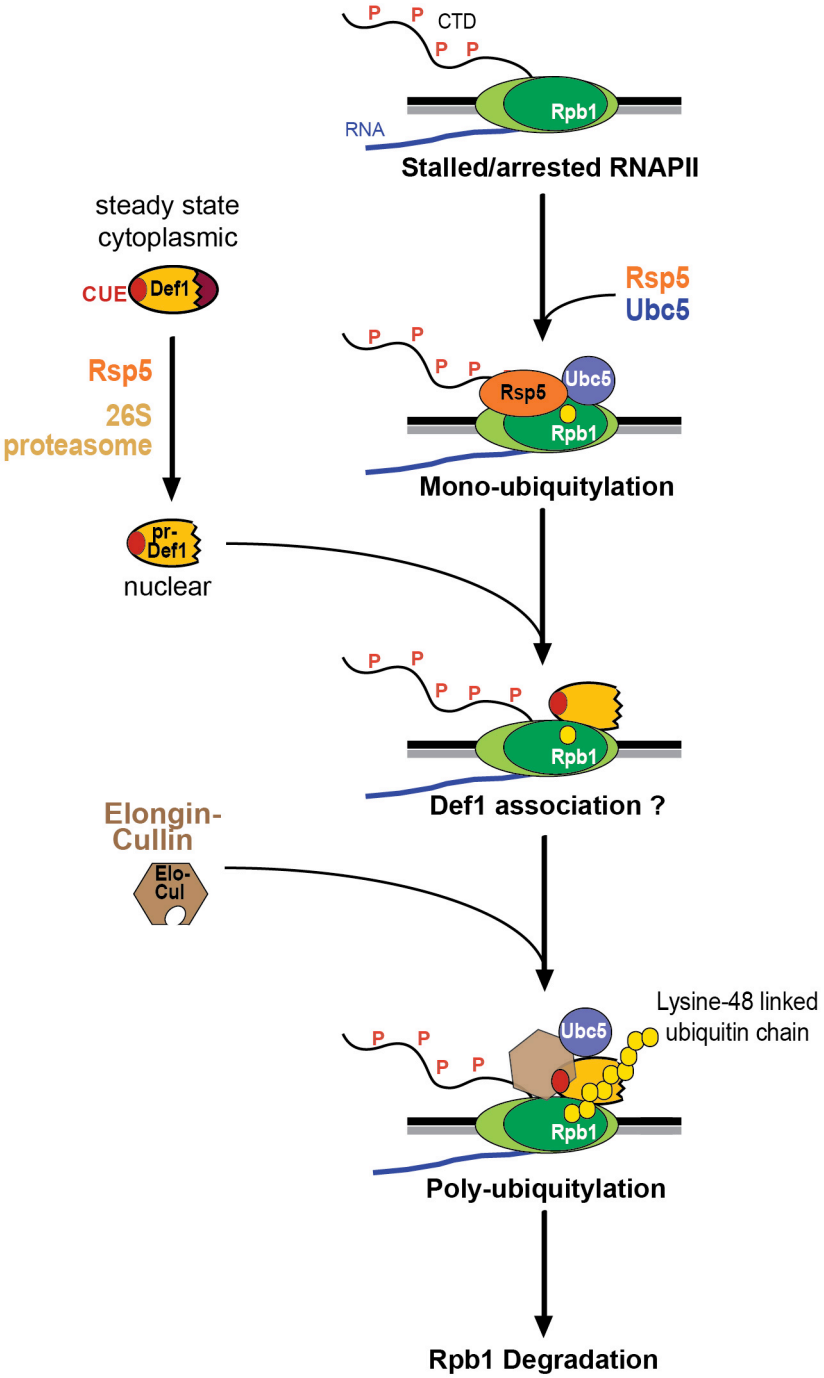

Figure 8.1: Proposed model of Def1-mediated Rpb1 poly-ubiquitylation

The processing of Def1 occurs concurrently with the emergence of poly-ubiquitylated Rpb1 and its subsequent degradation. These two processes are inherently interlinked, since expression of pr-Def1-like molecules is sufficient to induce Rpb1 poly-ubiquitylation in the absence of induced DNA damage. It is

interesting to note that the poly-ubiquitylation of Rpb1, observed when Def1 is cleaved by TEV protease (Figure 5.7 A), was less pronounced than normally observed after treating with a stalling agent, despite the production of similar levels of pr-Def1 and the mimicking, TEV-cut, pr*-Def1. It is possible that the TEV-cleaved Def1 was not as active as its properly processed, *in vivo*, counterpart. Similarly, multiple signals may be required to converge on stalled RNAPII to promote efficient poly-ubiquitylation, such as activation of the DNA damage response (DDR), which would be absent in this experiment. RNAPII stalling can activate the DDR (Derheimer et al., 2007, Chen et al., 2009) and may be important in Rpb1 poly-ubiquitylation (Michael Taschner, unpublished results). The processing of Def1 does not appear to be affected in preliminary experiments using DDR kinase null backgrounds (*Δmec1, Δtel1, Δrad9, Δdun1* and *Δrad53*; data not shown).

However, there was no induced RNAPII stall in the TEV experiment and as a result, little correct substrate for Rpb1 poly-ubiquitylation. In fact, it is surprising that any Rpb1 poly-ubiquitylation could be observed at all; the most likely explanation is that the cleaved Def1 is inappropriately recognising transiently stalled RNAPII and aberrantly causing its destruction. Under normal conditions this temporarily stalled RNAPII would be re-started by general elongation factors. Shifting the temperature sensitive $def1_{1\text{-}530}$ strain to 37°C was sufficient to promote wholesale Rpb1 degradation. This effect may be more pronounced than for the TEV cleaved Def1, as RNAPII stall may be induced at the elevated temperature (see below), producing more poly-ubiquitylation competent RNAPII. The toxicity of the truncated forms of Def1 may also be due to the aberrant activation of Rpb1 ubiquitylation, whereby the 'last-resort', back-up pathway artificially becomes the detrimental primary pathway of choice.

Indeed, the manner by which pr-Def1 is targeted to stalled, mono-ubiquitylated RNAPII is unclear. Def1 did not associate with mono-ubiquitylated RNAPII *in vitro*, but does with immobilised unmodified RNAPII (Figure 7.2 B). Targeting of the poly-ubiquitylation machinery to only persistently stalled RNAPII is paramount to prevent futile Rpb1 degradation. Poly-ubiquitylation cannot occur unless Rsp5 has first mono-ubiquitylated RNAPII, however there is a distinct, basal population of mono-ubiquitylated RNAPII in cells that does not appear to get degraded (see Discussion

I). Investigating how Rpb1 degradation is properly targeted to persistently stalled RNAPII is a key, unanswered, question remaining in the field.

Def1 is processed under a number of different cellular assaults (Figure 5.2); whether these conditions also induce persistent transcription stall is unclear. Elevated temperature results in Def1 processing. Heating bacterial RNAP does not increase the length of frequency of pausing *in vitro* (Mejia et al., 2008, Abbondanzieri et al., 2005). Indeed, the promoter proximal pause of a number of genes is relieved upon heat shock in metazoa (Nechaev et al., 2010). It remains to be investigated whether Rpb1 poly-ubiquitylation is promoted after heat stress, or ethanol treatment. Alternatively, Def1 processing may occur as a general response to cellular stress. Artificial activation of $Def1_{1\text{-}530}$, did not affect global or control protein levels (Figure 5.5 C), but other targets of pr-Def1 may exist. This study has focused on the role of Def1 in Rpb1 degradation, but Def1 has been implicated in a number of other diverse processes in the cell, from telomere maintenance to glutathione biosynthesis (Jordan et al., 2007, Manogaran et al., 2011, Chen et al., 2005, Cai et al., 2006, Suzuki et al., 2011). It would be interesting to investigate whether there is any potential role for the C-terminus of Def1 or pr-Def1 in these other cellular processes, and therefore, if there is any cross-talk with the Rpb1 poly-ubiquitylation pathway.

It is interesting to note that Def1 purifies with the RNAPII DUB, Ubp3 (Kvint et al., 2008). The band annotated as Def1 - from a low stringency Ubp3 purification – runs at just over 100kDa by SDS-PAGE; both too small to be the full-length (p120), and too large to be the processed (p90) Def1 protein. In the mass spectrometry experiment presented in this thesis, Ubp3 was highly enriched from UV-irradiated extracts by immobilised $Def1_{1\text{-}500\text{-}His}$. Whether there is a direct functional association between Def1 and Ubp3 requires further study. Conceivably, Def1 could promote Rpb1 poly-ubiquitylation through multiple mechanisms, including the inhibition of Ubp3.

Rpb1 poly-ubiquitylation is thought to be a last-resort mechanism, which is only used after unsuccessful TC-NER (Svejstrup, 2002). How the decision between TC-NER and Rpb1 poly-ubiquitylation is made is unclear (see 1.5.3.7). One possible

switching mechanism could be mediated through Def1. Full-length Def1 co-purifies from chromatin with the only TC-NER specific factor in yeast, Rad26 (Woudstra et al., 2002). Since this complex was not present in the non-chromatin fraction, and cells that lack Rad26 exhibit accelerated Rpb1 degradation: Rad26 appears to antagonise Def1 activity. The role of Rad26 in the processing and activation of Def1 is unclear. Speculatively, Rad26 could protect Def1 from processing in chromatin, therefore inhibiting Rpb1 degradation. The presence of Rad26 at stalled RNAPII complexes would suggest that the preferable TC-NER pathway is in progress. According to the current model, for the 'last-resort' back-up pathway to proceed, Rad26 would need to be inactivated or diffuse away from the Def1 complex. It would be interesting to investigate where Rad26 binds to Def1, and whether it still interacts with pr-Def1. No such interaction was investigated in this study.

Interestingly, Def1 is not required for Rpb1 degradation in the absence of Rad26 (Woudstra et al., 2002); suggesting Def1 is not absolutely mechanistically required for RNAPII poly-ubiquitylation. In support of this finding, pure Elongin-Cullin complex can catalyse the poly-ubiquitylation of RNAPII *in vitro*, in the absence of Def1 (Harreman et al., 2009). This Def1-independent degradation may be due to the weak Elongin-Cullin-RNAPII interaction observed (Figure 7.7 C), allowing some Rpb1 poly-ubiquitylation. Further investigation into the Rad26-Def1 switch is essential to help understand pathway choice after persistent transcription stall.

8.2 Regulated Ubiquitin Partial Proteasomal Processing as a Control Mechanism

Def1 is proteolytically cleaved to yield a processed fragment. The proteases responsible for the partial processing appear to be within the proteasome complex. Several similarities and differences between the partial proteolytic processing of Def1 and the other identified processed proteins have emerged throughout this

study. Partial proteasome processing was reconstituted *in vitro* with the relevant pure proteins. Previously, assays have been performed using cell extracts (Orian et al., 1995, Tian et al., 2005, Kravtsova-Ivantsiv et al., 2009) or with the 20S proteasome (Moorthy et al., 2006). The latter study concluded that processing was not reliant upon the 19S regulatory particle or ubiquitylation. Our studies have corroborated these findings with an important caveat: Neither the 19S nor ubiquitylation are absolutely required, but they do accelerate the processing reaction, perhaps achieving reaction rates that are more physiological. The 26S proteasome used in this assay is comprised of both the 20S core particle and 19S regulatory particles. The proteasome is known to differ in subunit composition; up to 20% of proteasomes in the cell include an accessory factor Blm1, which replaces the 19S regulatory particle (Schmidt et al., 2005). The *in vitro* system developed offers a unique opportunity to further study partial proteolytic processing.

Despite repeated attempts, the C-terminal fragment derived from Def1 processing could not be detected. The C-terminus was assumed to be degraded, as observed for other proteasomal processed proteins (Hoppe et al., 2000, Fan and Maniatis, 1991). The proteasome can act as an endo-protease, at internal initiation sites (Liu et al., 2003, Piwko and Jentsch, 2006, Kraut and Matouschek, 2011), as seems to be the case for Def1 (Figure 6.4 F). In order to degrade the C-terminus, the proteasome would have to work bi-directionally, as has been described previously (Liu et al., 2003, Piwko and Jentsch, 2006)(Figure 8.2 B).

Def1 is targeted to the proteasome by Rsp5 mediated mono-ubiquitylation. This is inducible upon DNA damage (Figures 3.4 C & 6.2 A), but the mechanism by which Rsp5 is targeted to Def1 is unclear. Pre-ubiquitylating Def1 alters the electrophoretic mobility of the full-length band, compared to non-ubiquitylated Def1 (Figure 6.1 C). Non-ubiquitylated, full-length Def1 can be processed *in vitro*, and this artificially created pr-Def1 runs at the equivalent size to the *in vivo* band (Figure 6.4 B). This would suggest that the *in vivo* pr-Def1 band is not modified by ubiquitin. However, full-length Def1 is ubiquitylated and this greatly accelerates processing *in vivo* (Figure 6.2 A). Furthermore, the identified ubiquitylation sites were found in the N-terminus of Def1. In fact, adding ubiquitylation reagents to the proteasome processing reaction can lead to the ubiquitin attachment of the processed band

(data not shown), suggesting ubiquitylation is still possible in this region. If pr-Def1 is not ubiquitylated then this moiety must be removed during the processing reaction. The 19S proteasome particle contains de-ubiquitylating activity (Verma et al., 2002, Guterman and Glickman, 2004). It is likely that the ubiquitin targeting signal on Def1 may be removed by one of these DUBs during proteasomal processing. However, it is important to note that the *in vivo* pr-Def1 band has not been directly confirmed to be un-ubiquitylated.

The processed bands of NF-κB and Ci are not ubiquitylated, whilst their full-length precursors are (Orian et al., 1999, Price and Kalderon, 2002). However, in these cases the ubiquitylation sites lie in the degraded region. The proteasomal initiation site is thought to be near the ubiquitylation site (Inobe et al., 2011). However the Def1 ubiquitylation sites are far from the proposed processing site, which has to be upstream from the proteasome initiation site. It is possible that ubiquitylated protein recognition is different in yeast. In support of this hypothesis, Spt23 and Mga2 both retain their ubiquitin moieties after processing (Rape et al., 2001). The reason why Def1 loses its ubiquitin is unclear and requires further study. One possibility is that Def1 is not recruited to the proteasome by one of the 19S UBD subunits, therefore alleviating the spatial distance constraints between the initiation site and the ubiquitylation site. Instead, Def1 might be recruited by one of the proteasome shuttle factors, allowing greater flexibility in Def1 proteasome binding (Figure 8.2 B). Further study is required to investigate this hypothesis, both genetically and biochemically.

Partial proteolysis occurs when the proteasome is blocked by a stop-transfer signal (see 1.1.7). Previous studies have shown that stop-transfer signals require both a low complexity region, which is followed by a tightly folded domain or strong protein-protein interactions (Lin and Ghosh, 1996, Rape et al., 2001, Tian et al., 2005). The low complexity region is poorly bound to the proteasome, whilst the stable domain(s) are refractive to 19S unwinding. The identity of the stop-transfer signal in Def1 is unclear, but Def1 can form multimers *in vivo* (Figure 5.8 B) and has extensive regions of low complexity (Figure 8.2 A).

CUE domains are able to dimerise (Kang et al., 2003), and some UBDs can prevent protein degradation by the proteasome (Heessen et al., 2005, Heinen et al., 2011). However, the N-terminal CUE domain of Def1 is probably too far from the proposed processing site to block the proteasome. Def1 is predicted to contain coiled-coil domains (Figure 5.8 D), which end just before the proposed processing site. Coiled-coil domains have been reported to be extremely stable, especially in glutamine rich regions (Fiumara et al., 2010). Indeed, others have previously reported that a glutamine rich region (residues 381-480) of Def1 runs uncharacteristically fast through a gel filtration column, suggesting that this section is capable forming coiled-coil based trimers or tetramers (Chen et al., 2005). Whether Def1 self-association is mediated through the coiled-coil domain is unclear, but such self-association may be critical in order to prevent the complete processivity of the proteasome, as has been observed for Spt23 and Mga2 (Rape et al., 2001).

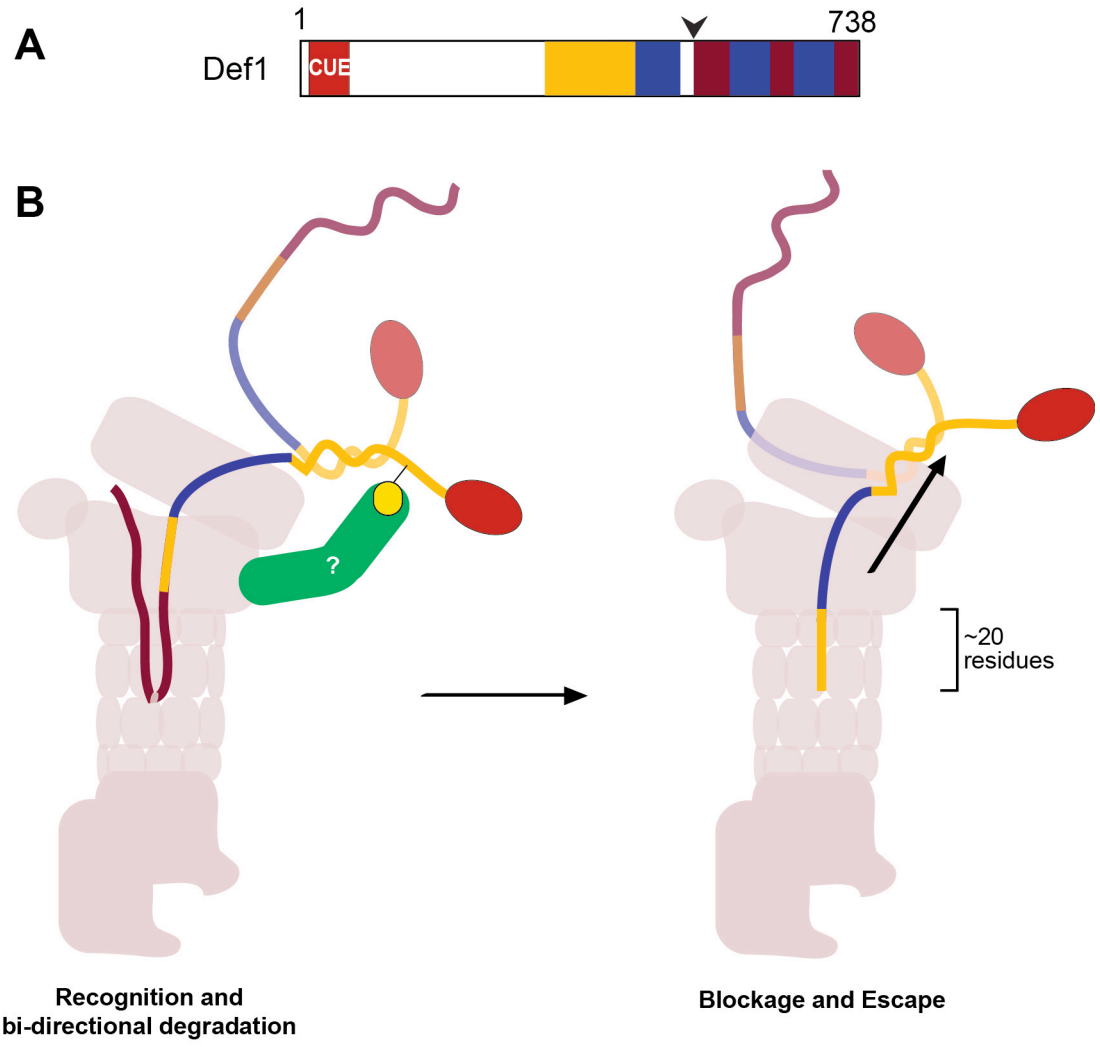

Figure 8.2: A model of Def1 partial proteasomal processing

A. Schematic of Def1 with the hypothesised stop transfer signals highlighted. Low complexity glutamine rich regions are highlighted in blue and the predicted coiled-coil oligomerisation domains in yellow. An arrow indicates the proposed site of processing. Note that the initiation site must lie downstream of this region
B. Def1 proteolytic processing may be split into two steps. In the first the mono-ubiquitylated form of Def1 is recognised, potentially by an unknown protein (green) and targeted to the proteasome. The initiation site, buried in the C-terminus, is degraded bi-directionally (brown section). This is potentially blocked by the glutamine rich region (dark blue) and the coiled-coil, oligomerisation domains, allowing Def1 escape. For clarity only one other interacting Def1 is shown, but the oligomerisation status is unclear. Model not to scale.

Glutamines account for 23% of all the residues in full-length Def1, with the area of highest density between Def1 residues 385-515. Poly-glutamine repeats reduce the unfolding ability of the proteasome in a length dependent manner (Kraut et al., 2012). The stop-transfer signal for the processed protein Sp1 has not been identified, but the protein does have regions of high glutamine content, prior to the identified processing site (Su et al., 1999; Figure 1.4). The hypothesised bi-partite stop-transfer signal of Def1, therefore, might be formed from the final predicted coiled-coil domain of Def1, followed by a glutamine rich, low complexity region. The distance from the outside of the 20S proteasome to the active sites is equivalent to 20 extended residues of a polypeptide chain (Piwko and Jentsch, 2006). Therefore it is conceivable that the proposed processing site, around residues 520-530, is chosen because it is 20 residues from this proposed stop-transfer signal (Figure 8.2 B). This is a highly speculative model, which could be investigated using the *in vitro* reaction described in this study.

If Def1 forms a homomultimer strong enough to block the proteasome, dissociation would require a large amount of unfolding energy. The Cdc48 ATPase is required for the dissociation of Spt23 and Mga2 from their unprocessed partners (Rape et al., 2001, Shcherbik et al., 2003). Whether Cdc48 also dissociates Def1 is unclear and difficult to assess, as it also has a role downstream in the 'last-resort' pathway: extracting poly-ubiquitylated Rpb1 from the RNAPII ternary complex on chromatin (Verma et al., 2011). It is interesting to note that both Ubx4/Ubx5 and the separate Ufd1-Npl4 substrate adaptors are required for proper Rpb1 degradation (Verma et al., 2011). Whilst Ubx4/Ubx5 is thought to directly feed poly-ubiquitylated Rpb1 into the proteasome, the authors of the aforementioned study did not speculate on the

role of Ufd1-Npl4 in the pathway. Ufd1-Npl4 depletion does not lead to increased Rpb1 poly-ubiquitylation, suggesting that these Cdc48 adaptors may be working upstream of the poly-ubiquitylation step of Rpb1 - possibly by promoting the dissociation of Def1 multimers.

Unlike site-specific proteases, which often only nick the polypeptide backbone, the proteasome actively digests proteins. As a result, the site of proteasome initiation does not necessarily correspond to the eventual site of processing. The exact site of processing was not successfully mapped in this study. Mass spectrometry proved unsuccessful and mutation around the processing site shifted the eventual processed C-terminus. pr-Def1 is not a single species, but appears as a doublet under some running conditions (for example in Figure 6.4 B). This either suggests multiple, different length processed proteins are produced, or that the processed proteins are post-translationally modified. However, the pr-Def1 doublet is also observed *in vitro* in the absence of post-translationally modifying proteins, suggesting that there is an inherent stoichasticity in the processing of Def1. It is interesting to note that processed Spt23 also appears as a collection of bands (Hoppe et al., 2000), suggesting partial processing can produce multiple products.

It appears that the regions that promote processing are redundant and poorly conserved. Internal deletion in processed proteins around the processing site does not prevent their processing (Sears et al., 1998, Piwko and Jentsch, 2006). Small deletions in Def1 affected both the full-length and processed band electrophoretic mobility and removal of residues surrounding the proposed processing site did not prevent processing. Furthermore, removal of the majority of the glutamine rich region or the terminal predicted coiled-coil domain did not prevent processing. However the extent of partial processing was unclear from this study, as there may have been some read-through by the proteasome leading to the total degradation of Def1.

Interestingly, removal of Def1 residues 500-600 did prevent processing of the protein, whilst the removal of residues 506-575 still allowed Def1 processing. There are many potential explanations for these observations. This form of Def1 may be lacking a degron sequence and, as a result, may not be ubiquitylated and targeted

to the proteasome. However, levels of $Def1_{\Delta 500\text{-}600}$ reduce after 4-NQO treatment, suggesting total degradation rather than partial processing is occurring. These findings suggest a role for this region, which is normally degraded, in preventing total degradation. Somewhat surprisingly, the strain expressing $Def1_{\Delta 500\text{-}600}$ was still able to degrade Rpb1 after DNA damage, suggesting processing may be unnecessary for the relocalisation of this truncated form of Def1. $Def1_{1\text{-}530}$, $Def1_{1\text{-}400}$ and $Def_{1\text{-}500}$ proteins may similarly not require processing for their action. Further work to bolster this interesting preliminary result is required. The ubiquitylation status, localisation and effect on Rpb1-poly-ubiquitylation all require investigation in the $Def1_{\Delta 500\text{-}600}$ strain. Furthermore, creating a strain with residues 575-600 deleted would prove very informative.

Considering the high toxicity of the pr-Def1-like molecules used in this study, it would be imperative that activated pr-Def1 is removed after it has performed its function. The pr-Def1 protein is extremely short-lived in cell extracts and $Def1_{1\text{-}500}$ rapidly disappears after the cessation of galactose induction (data not shown). Despite being unable to totally degrade Def1 previously, the proteasome may be able to degrade pr-Def1 after it has performed its function. Def1 is only tagged with mono-ubiquitin for partial proteasomal processing; poly-ubiquitylation - at another site on pr-Def1 or Def1 - could switch the signal to complete degradation, as has been observed for both NF-κB and Spt23 (Ciechanover et al., 2001, Siepe and Jentsch, 2009). Indeed, a number of other ubiquitylation sites in Def1 have been identified (Beltrao et al., 2012, Starita et al., 2012). The identity of the degradation-targeting ubiquitin ligase, assuming such a ligase exists, is unclear, but could be the Elongin-Cullin E3. Auto-ubiquitylation by cullin ring ligases (CRLs) of their bound substrate adaptor proteins has been reported (Zhou and Howley, 1998, Yen et al., 2012). Mechanistically, the directionality of proteasomal digestion determines whether a protein is partially or completely degraded (Tian et al., 2005, Kraut and Matouschek, 2011) thus complete degradation of pr-Def1 could be mediated by the proteasome, using a different initiation site. Alternatively, other cellular proteases could be implicated in the short half-life of pr-Def1.

8.3 Self Cleavage

Proteasomal processing is believed to be a two-step process: first the proteasome nicks the polypeptide backbone; then the processed-protein is progressively degraded up to a stop-transfer signal (Lin and Ghosh, 1996, Piwko and Jentsch, 2006). The proteasome may only be required for the second step in Def1 processing. Full-length Def1 used in this thesis was purified from yeast cells. Incubating this protein with inhibited proteasome or ubiquitylation components induces the formation of a pr-Def1-like band (Figures 6.4 C and 6.1 C). This may be due to contamination of active proteasome or other proteases in these assays. However, bacterially purified $Def1_{1\text{-}500}$ seemed to lose the C-terminal His tag upon binding to ubiquitin (Figure 7.2 A). Moreover, full-length Def1, purified from *E.coli* and incubated at room temperature, can also form a pr-Def1-like band, in the absence of any other agents (Kotryna Temcinaite, personal communication). This suggests that pure Def1 can exhibit an inherent instability, leading to the formation of a band similar to that exhibited in cells after DNA damage. One possible explanation could be that Def1 auto-catalytically cleaves itself.

Some proteins do have the capacity to cleave themselves. A group of proteins have been found to self-splice, post-translationally (reviewed in Paulus, 2000). These remove an internal section of a polypeptide (termed an intein) and reform the amide backbone. Alternatively, auto-proteolysis can be achieved through the use of a more recognisable internal peptidase domain. For example, caspases only activate upon self-dimerisation, where they are induced to cleave their neighbouring protein (Hengartner, 2000). The NPC subunit Nup145 self cleaves, with each half associated with opposite sides of the nuclear pore (Teixeira et al., 1997). The LexA repressor protein auto-cleaves as part of the bacterial SOS response, resulting in up-regulation of repair genes and promoting survival in the face of severe DNA damage (Schlacher and Goodman, 2007). How, or even if, Def1 auto-cleaves is not clear, but cleavage does seem to be promoted upon association with ubiquitin (Figure 7.2 A), RNAPII (Figure 7.2 B) or the proteasome

(Figure 6.4 D). No recognisable peptidase or intein-like domain can be found in Def1. Further experiments are required to assess these puzzling observations.

8.4 Dynamic Compartmentalisation as a Method to Prevent Protein Interactions

The shorter pr-Def1 is toxic when mis-expressed, compared to its full-length counterpart. § protein appears to function just as well as pr-Def1. Furthermore, the expression of the C-terminus of Def1 does not suppress the toxicity of the 1-500 section, suggesting that the C-terminus may not be acting as an auto-inhibitory domain. Instead, this toxicity is mediated at the cellular level; pr-Def1 can accumulate in the nucleus, whereas full-length Def1 cannot. The steady state cytoplasmic localisation of Def1 is dependent upon the equilibrium between nuclear import and rapid nuclear export. Upon transcription stall, export is prevented via removal of Def1's C-terminus, allowing the accumulation of pr-Def1 in the nucleus. Through dynamic compartmentalisation, the majority of Def1 is not allowed access to RNAPII, unless transcription has been stalled. The inducible movement of a toxic protein to the nucleus is not unprecedented. In mammalian cells, severe DNA-damage can elicit apoptosis, triggering the caspase-dependent cleavage of ICAD. This frees the nuclease CAD, promoting its entry to the nucleus, leading to DNA fragmentation (Nagata, 2000).

The C-terminus of Def1 can promote cytosolic location, through promoting the nuclear export of the protein (Figure 6.7). This was analysed by artificially appending the C-terminus of Def1 to an NLS-GFP sequence. The hybrid protein is present in both the nucleus and cytoplasm, suggesting that it is dynamically shuttling across the nuclear membrane, with the NLS targeting import and the C-terminus of Def1 targeting export. The artificial nature of the assay used in this thesis does not prove that the C-terminus of Def1 promotes export in the context of the full-length protein, but provides strong evidence for this function. The identity of the export signal in Def1's C-terminus is unclear. No short NES-like sequence could be found and the short Def1 500-540 section could not direct nuclear export

on its own (Figure 6.8 B). The glutamine rich nature of Def1's C-terminus may act as the export signal. Poly-glutamine tracts can promote nuclear export in *Drosophila* (Chan et al., 2011), but can also prevent nuclear import, by forming cytoplasmic aggregates (Park et al., 2013).

As the C-terminus of Def1 can promote nuclear export, this would suggest that full-length Def1 is dynamically shuttling between compartments, rather than excluded from the nucleus altogether. Previous biochemical work confirms this finding: full-length Def1 was purified from chromatin (Woudstra et al., 2002) and associates with the, primarily nuclear, RNAPII (Reid and Svejstrup, 2004). Furthermore, Def1 is cleaved by expression of the TEV protease, which contains a NLS, and is localised to the nucleus upon expression (Uhlmann et al., 2000). As a result, at least a small proportion of Def1 is present in the nucleus in unstressed conditions, presumably below the detection limit of the microscope used in this work. However, when transcription stall is induced pr-Def1 temporarily accumulates in the nucleus.

Def1 export does not appear to be dependent on the canonical CRM1-NES export pathway (Figure 6.8 A), and therefore must be reliant on one of the other, poorly characterised, karyopherin exportins or transportins. A possible indirect stress caused by transcription inhibition is the accumulation of proteins in the nucleus. A number of proteins - including but not limited to RNA processing factors - are dependent upon mRNA synthesis for their export (O'Hagan and Ljungman, 2004, Lee et al., 1999b). Whilst the exportin required for Def1 has not been identified, if Def1 were exported with mRNA then it would be expected to accumulate in the nucleus when RNAPII is inhibited: exactly what has been observed after UV-induced transcription inhibtion.

pr-Def1 is predicted to have a mass of approximately 60kDa (assuming processing at residue 520-530) and therefore is unlikely to be able to diffuse freely through the nuclear pore. Active import into the nucleus requires binding to an importin protein (Xu et al., 2010), the best characterised of which binds to a lysine-rich NLS on the cargo protein (Dingwall, 1991). A degenerate NLS can be identified within the CUE domain of Def1. Future mutation of this sequence would help to ascertain how Def1 is imported to the nucleus.

Alternatively, Def1 does not necessarily need to directly contact a karyopherin protein; it could piggyback on another transiting protein. Rsp5 dynamically shuttles between the nucleus and cytoplasm, and accumulates in the nucleus after UV irradiation (Cholbinski et al., 2011). Def1 can interact with Rsp5 *in vitro*, and could bind and translocate with Rsp5. Rsp5 targets specifically to stalled RNAPII (Somesh et al., 2005, Somesh et al., 2007), possibly helping to target Def1 to the correct location.

8.5 A New Component of the Elongin-Cullin Complex

The Elc1-Ela1 complex is akin to the Skp1/F-box substrate adaptor of CRLs (Koth et al., 2000). However, this complex does not seem to be able recognise its target protein RNAPII efficiently (Figure 7.7). This may be due, in part, to the artificial nature of the *in vitro* experiment employed; immobilised RNAPII was not phosphorylated, stalled on DNA, or mono-ubiquitylated. Indeed, Human Elongin A has been shown to associate with hyper-phosphorylated RNAPII (Yasukawa et al., 2008). However, in immunoprecipitations Ela1 association with RNAPII is dependent upon Def1 and its CUE domain. This suggests pr-Def1 is a bridging factor, which connects the Elongin-Cullin ligase to its target (Figure 8.3). CRLs typically employ different substrate adaptors, which can associate specifically during the cell cycle, or in response to external stimuli (Patton et al., 1998, Kaiser et al., 2006). Def1 may represent the first example of a discrete substrate-specific bridging factor being required for target recognition by a CRL, rather than an alternative, cullin binding, substrate adaptor.

The Def1 protein facilitates the interaction between the Elongin-Cullin ligase and its Rpb1 substrate. The exact progression of events has not been determined; it is unclear whether Def1 binds first to the stalled RNAPII or to the Elongin-Cullin complex. Furthermore, the manner in which the signal of persistently stalled RNAPII is transduced to promote Def1 processing is unclear. One attractive model

is that full-length Def1 is proteolytically processed at the site of stalled RNAPII on chromatin. As a small portion of Def1 is present in the nucleus constitutively, it could sample the stall-status of transcribing RNAPII complexes. Under normal conditions, RNAPII pauses and stalls tend to be transient, promoting the predominantly cytoplasmic steady state localisation of Def1. Any possible background Rpb1 poly-ubiquitylation required, due to inherent persistent transcription stalling (such as reported in Hobson et al., 2012), could be dealt with by this minor nuclear Def1 fraction.

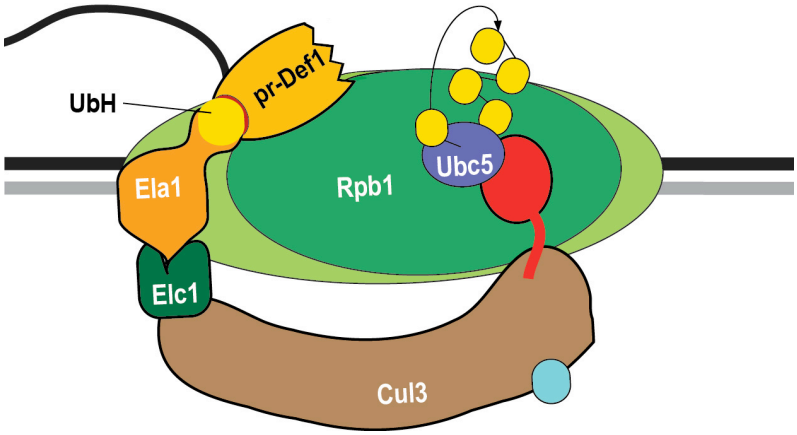

Figure 8.3: The proposed Elongin-Cullin complex and substrate

Proposed model of Elongin-cullin association with stalled RNAPII on chromatin, via pr-Def1. Activating Ubl Rub1 is coloured light blue. Ubiquitin moieties are coloured yellow. The dynamic catalytic RING finger protein, Rbx1, is coloured red. RNA is not included for clarity. pr-Def1 associates via its CUE domain with the UbH domain in Ela1. Not to scale.

However, in the presence of bulky helix-distorting DNA damage, RNAPII persistently arrests. Def1 associating with this RNAPII would be in close proximity to Rsp5, which is specifically targeted to stalled RNAPII only (Somesh et al., 2005, Somesh et al., 2007). Indeed, Rsp5 may even directly help to target Def1 to stalled RNAPII (see above). Furthermore, the proteasome directly associates with RNAPII, possibly at sites of stall (Auld et al., 2006, Gillette et al., 2004). As a result, Def1 ubiquitylation and subsequent proteasomal activation could be spatially localised - *in situ* - to its site of action. RNAPII-associated pr-Def1 could then recruit the

Elongin-Cullin complex. If this model is correct then pr-Def1 could not be considered to be a part of the Elongin-Cullin complex. Alternatively, pr-Def1 could associate with Elongin-Cullin and subsequently be recruited to sites of RNAPII persistent stall. It would be intriguing to investigate whether there are other substrates of the Elongin-Cullin ligase and if these are also mediated through Def1.

8.6 A Novel Ubiquitin Homology Domain

The CUE UBD of Def1 does not bind primarily to a ubiquitylated target. Instead, the CUE domain is required to recruit the Elongin-Cullin ligase, through a newly identified UbH domain in Ela1. The C-terminus of Ela1 has not previously been predicted to share homology with ubiquitin. However, ubiquitin shares 47% sequence similarity to the C-terminus of Ela1, and key functional residues defining the 3-dimensional fold seem to be conserved (Kiel and Serrano, 2006).

A UbH-UBD like interaction within a CRL has been reported previously (Ivantsiv et al., 2006). The UbH domain of the proteasome shuttling factor, Ddi, binds to the F-box protein Ufo1, via its UIM domain. This UbH-UBD like interaction within the SCF CRL is the opposite polarity of the interaction observed between Def1 and Ela1. Moreover, the interaction is required for the degradation of the F-box protein, not for the CRL catalytic poly-ubiquitylation function.

Def1 exhibits binding specificity to Ela1's UbH domain, compared to ubiquitin (Figure 7.4 B). Unsurprisingly, simple replacement of the UbH domain with ubiquitin did not rescue the Rpb1 poly-ubiquitylation function attributed to Ela1 in the Elongin-Cullin complex (Figure 7.6 D). In another example, replacement of the kinase IKKβ's UbH domain with ubiquitin abolishes kinase activity, whilst replacement with Rad23's UbH domain fully restored the function of the kinase (May et al., 2004). The CUE domain of Def1 appears to have a regular CUE fold, but the key conserved residues - mutated in this study - are not positioned similarly to other CUE domains, and as a result Def1 is unlikely to bind ubiquitin in the same

manner (James Omichinski, personal communication). The co-crystal structure of Def1's CUE domain with the UbH domain from Ela1 would be highly informative.

UBD-ubiquitin interactions are often weak and are consequently supplemented with accessory protein-specific interactions (Panier et al., 2012, Parker et al., 2007). Reported cases of UbH–UBD interactions vary from weaker than their cognate ubiquitin interactions (Raasi et al., 2004), to extremely stable (Chartron et al., 2012, Zhang et al., 2009). Usually, standard UBD-ubiquitin like contacts are conserved, but supplemented with specific electrostatic interactions. The CUE domain of Def1 might confer specificity directly, by displaying higher affinity to the UbH domain in Ela1 compared to ubiquitin. Alternatively, other binding surfaces of Def1, outside of the CUE domain, could contact the Ela1-Elc1 dimer. In order to investigate this further, shorter mutant Ela1-Elc1 and Def1 proteins could be purified. Preliminarily, the first 150 amino acids of Def1 (encompassing the majority of the CUE domain) could not interact with ubiquitin, whilst its binding to Ela1's C-terminus was not investigated.

In humans, the Elongin complex is comprised of three subunits, Elongin A, B, and C (Aso et al., 1995), which can form a CRL that catalyses the poly-ubiquitylation of Rpb1 (Yasukawa et al., 2008, Harreman et al., 2009). Budding yeast lack an Elongin B homologue (Koth et al., 2000) and Elongin A exhibits poor conservation with the C-terminus of yeast Ela1. Remarkably, the human Elongin B protein contains a UbH domain (Garrett et al., 1995). Therefore, the UbH of yeast Ela1 may have split onto a separate gene during evolution, which then became human Elongin B. Elongin B helps to stabilise Elongin C (Brower et al., 1999, Bullock et al., 2006), but critically its hydrophobic patch is free, possibly allowing interaction with other proteins, such as any possible human homologue of Def1.

8.7 Relevance to Higher Eukaryotes

Poly-glutamine expansion diseases are caused by trinucleotide CAG amplifications within the coding region. Nine different expanded proteins have been identified in the humans to date; all leading to related but separate neurodegenerative disorders (Schols et al., 2004). Proteolytic cleavage and release of the toxic fragment is thought to activate these disease proteins (Tarlac and Storey, 2003) and the poly-glutamine tract is able to interfere with the ubiquitin proteasome system (Venkatraman et al., 2004, Kraut et al., 2012). Current models suggest that the activated poly-glutamine proteins affect transcription (Tarlac and Storey, 2003), and that to perform this function they accumulate in the nucleus (Walsh et al., 2005). Exclusion of the poly-glutamine proteins from the nucleus prevents their toxicity (Yang et al., 2002). The many parallels to Def1 processing and activity are clear. The study of poly-glutamine expansion proteins is in its infancy and not yet at a molecular stage. The further study of Def1 and its function may help to elucidate the mechanism of toxicity in these neurodegenerative diseases.

A human homologue of Def1 has not yet been identified. However, considering the high conservation of the rest of the Rpb1 poly-ubiquitylation system (Table 1.5), it would be highly surprising for Def1's functions not to be conserved. The extensive low complexity regions within Def1 prevent the identification of direct sequence homologs. By amassing more data on the function of Def1 in yeast, the conserved requirements of a human Def1 could be ascertained. For example, assuming the conservation of the UbH within the Elongin-Cullin complex is not by chance, the human Def1 protein is likely to contain a UBD with specificity to this UbH. The future identification of the functional homologue of Def1 will be greatly aided by the knowledge gained from the yeast system.

Reference List

ABBONDANZIERI, E. A., SHAEVITZ, J. W. & BLOCK, S. M. 2005. Picocalorimetry of transcription by RNA polymerase. *Biophys J,* 89**,** L61-3.

ACCONCIA, F., SIGISMUND, S. & POLO, S. 2009. Ubiquitin in trafficking: the network at work. *Exp Cell Res,* 315**,** 1610-8.

AITCHISON, J. D. & ROUT, M. P. 2012. The yeast nuclear pore complex and transport through it. *Genetics,* 190**,** 855-83.

AKHRYMUK, I., KULEMZIN, S. V. & FROLOVA, E. I. 2012. Evasion of the innate immune response: the Old World alphavirus nsP2 protein induces rapid degradation of Rpb1, a catalytic subunit of RNA polymerase II. *J Virol,* 86**,** 7180-91.

AKHTAR, M. S., HEIDEMANN, M., TIETJEN, J. R., ZHANG, D. W., CHAPMAN, R. D., EICK, D. & ANSARI, A. Z. 2009. TFIIH kinase places bivalent marks on the carboxy-terminal domain of RNA polymerase II. *Mol Cell,* 34**,** 387-93.

AKHTAR, N., HAGAN, H., LOPILATO, J. E. & CORBETT, A. H. 2001. Functional analysis of the yeast Ran exchange factor Prp20p: in vivo evidence for the RanGTP gradient model. *Mol Genet Genomics,* 265**,** 851-64.

AL-MOGHRABI, N. M., AL-SHARIF, I. S. & ABOUSSEKHRA, A. 2003. UV-induced de novo protein synthesis enhances nucleotide excision repair efficiency in a transcription-dependent manner in S. cerevisiae. *DNA Repair (Amst),* 2**,** 1185-97.

ALBUQUERQUE, C. P., SMOLKA, M. B., PAYNE, S. H., BAFNA, V., ENG, J. & ZHOU, H. 2008. A multidimensional chromatography technology for in-depth phosphoproteome analysis. *Mol Cell Proteomics,* 7**,** 1389-96.

ANDRADE, M. A., PETOSA, C., O'DONOGHUE, S. I., MULLER, C. W. & BORK, P. 2001. Comparison of ARM and HEAT protein repeats. *J Mol Biol,* 309**,** 1-18.

ANINDYA, R., AYGUN, O. & SVEJSTRUP, J. Q. 2007. Damage-induced ubiquitylation of human RNA polymerase II by the ubiquitin ligase Nedd4, but not Cockayne syndrome proteins or BRCA1. *Mol Cell,* 28**,** 386-97.

ANINDYA, R., MARI, P. O., KRISTENSEN, U., KOOL, H., GIGLIA-MARI, G., MULLENDERS, L. H., FOUSTERI, M., VERMEULEN, W., EGLY, J. M. & SVEJSTRUP, J. Q. 2010. A ubiquitin-binding domain in Cockayne syndrome B required for transcription-coupled nucleotide excision repair. *Mol Cell,* 38**,** 637-48.

ARCHAMBAULT, J., LACROUTE, F., RUET, A. & FRIESEN, J. D. 1992. Genetic interaction between transcription elongation factor TFIIS and RNA polymerase II. *Mol Cell Biol,* 12**,** 4142-52.

ASO, T. & CONRAD, M. N. 1997. Molecular cloning of DNAs encoding the regulatory subunits of elongin from Saccharomyces cerevisiae and Drosophila melanogaster. *Biochem Biophys Res Commun,* 241**,** 334-40.

ASO, T., HAQUE, D., BARSTEAD, R. J., CONAWAY, R. C. & CONAWAY, J. W. 1996. The inducible elongin A elongation activation domain: structure, function and interaction with the elongin BC complex. *EMBO J,* 15**,** 5557-66.

ASO, T., LANE, W. S., CONAWAY, J. W. & CONAWAY, R. C. 1995. Elongin (SIII): a multisubunit regulator of elongation by RNA polymerase II. *Science,* 269**,** 1439-43.

AULD, K. L., BROWN, C. R., CASOLARI, J. M., KOMILI, S. & SILVER, P. A. 2006. Genomic association of the proteasome demonstrates overlapping gene regulatory activity with transcription factor substrates. *Mol Cell,* 21**,** 861-71.

AUNE, G. J., TAKAGI, K., SORDET, O., GUIROUILH-BARBAT, J., ANTONY, S., BOHR, V. A. & POMMIER, Y. 2008. Von Hippel-Lindau-coupled and transcription-coupled nucleotide excision repair-dependent degradation of RNA polymerase II in response to trabectedin. *Clin Cancer Res,* 14**,** 6449-55.

AZA-BLANC, P., RAMIREZ-WEBER, F. A., LAGET, M. P., SCHWARTZ, C. & KORNBERG, T. B. 1997. Proteolysis that is inhibited by hedgehog targets Cubitus interruptus protein to the nucleus and converts it to a repressor. *Cell,* 89**,** 1043-53.

BABON, J. J., SABO, J. K., SOETOPO, A., YAO, S., BAILEY, M. F., ZHANG, J. G., NICOLA, N. A. & NORTON, R. S. 2008. The SOCS box domain of SOCS3: structure and interaction with the elonginBC-cullin5 ubiquitin ligase. *J Mol Biol,* 381**,** 928-40.

BACHMAIR, A. & VARSHAVSKY, A. 1989. The degradation signal in a short-lived protein. *Cell,* 56**,** 1019-32.

BAGOLA, K., VON DELBRUCK, M., DITTMAR, G., SCHEFFNER, M., ZIV, I., GLICKMAN, M. H., CIECHANOVER, A. & SOMMER, T. 2013. Ubiquitin binding by a CUE domain regulates ubiquitin chain formation by ERAD E3 ligases. *Mol Cell,* 50**,** 528-39.

BAI, C., SEN, P., HOFMANN, K., MA, L., GOEBL, M., HARPER, J. W. & ELLEDGE, S. J. 1996. SKP1 connects cell cycle regulators to the ubiquitin proteolysis machinery through a novel motif, the F-box. *Cell,* 86**,** 263-74.

BAR-NAHUM, G., EPSHTEIN, V., RUCKENSTEIN, A. E., RAFIKOV, R., MUSTAEV, A. & NUDLER, E. 2005. A ratchet mechanism of transcription elongation and its control. *Cell,* 120**,** 183-93.

BASSI, C., HO, J., SRIKUMAR, T., DOWLING, R. J., GORRINI, C., MILLER, S. J., MAK, T. W., NEEL, B. G., RAUGHT, B. & STAMBOLIC, V. 2013. Nuclear PTEN controls DNA repair and sensitivity to genotoxic stress. *Science,* 341**,** 395-9.

BEAUDENON, S. L., HUACANI, M. R., WANG, G., MCDONNELL, D. P. & HUIBREGTSE, J. M. 1999. Rsp5 ubiquitin-protein ligase mediates DNA damage-induced degradation of the large subunit of RNA polymerase II in Saccharomyces cerevisiae. *Mol Cell Biol,* 19**,** 6972-9.

BECK, F., UNVERDORBEN, P., BOHN, S., SCHWEITZER, A., PFEIFER, G., SAKATA, E., NICKELL, S., PLITZKO, J. M., VILLA, E., BAUMEISTER, W. & FORSTER, F. 2012. Near-atomic resolution structural model of the yeast 26S proteasome. *Proc Natl Acad Sci U S A,* 109**,** 14870-5.

BECKER, J., MELCHIOR, F., GERKE, V., BISCHOFF, F. R., PONSTINGL, H. & WITTINGHOFER, A. 1995. RNA1 encodes a GTPase-activating protein specific for Gsp1p, the Ran/TC4 homologue of Saccharomyces cerevisiae. *J Biol Chem,* 270**,** 11860-5.

BELTRAO, P., ALBANESE, V., KENNER, L. R., SWANEY, D. L., BURLINGAME, A., VILLEN, J., LIM, W. A., FRASER, J. S., FRYDMAN, J. & KROGAN, N. J. 2012. Systematic functional prioritization of protein posttranslational modifications. *Cell,* 150**,** 413-25.

BENGAL, E., FLORES, O., KRAUSKOPF, A., REINBERG, D. & ALONI, Y. 1991. Role of the mammalian transcription factors IIF, IIS, and IIX during elongation by RNA polymerase II. *Mol Cell Biol,* 11**,** 1195-206.

BERG, J. M., TYMOCZKO, J. L., STRYER, L. & STRYER, L. 2002. *Biochemistry,* New York, W.H. Freeman.

BERNIER-VILLAMOR, V., SAMPSON, D. A., MATUNIS, M. J. & LIMA, C. D. 2002. Structural basis for E2-mediated SUMO conjugation revealed by a complex between ubiquitin-conjugating enzyme Ubc9 and RanGAP1. *Cell,* 108**,** 345-56.

BERTOLAET, B. L., CLARKE, D. J., WOLFF, M., WATSON, M. H., HENZE, M., DIVITA, G. & REED, S. I. 2001. UBA domains of DNA damage-inducible proteins interact with ubiquitin. *Nat Struct Biol,* 8**,** 417-22.

BHATIA, P. K., VERHAGE, R. A., BROUWER, J. & FRIEDBERG, E. C. 1996. Molecular cloning and characterization of Saccharomyces cerevisiae RAD28, the yeast homolog of the human Cockayne syndrome A (CSA) gene. *J Bacteriol,* 178**,** 5977-88.

BINTU, L., KOPACZYNSKA, M., HODGES, C., LUBKOWSKA, L., KASHLEV, M. & BUSTAMANTE, C. 2011. The elongation rate of RNA polymerase determines the fate of transcribed nucleosomes. *Nat Struct Mol Biol,* 18**,** 1394-9.

BIRGER, Y., WEST, K. L., POSTNIKOV, Y. V., LIM, J. H., FURUSAWA, T., WAGNER, J. P., LAUFER, C. S., KRAEMER, K. H. & BUSTIN, M. 2003. Chromosomal protein HMGN1 enhances the rate of DNA repair in chromatin. *EMBO J,* 22**,** 1665-75.

BOHR, V. A., SMITH, C. A., OKUMOTO, D. S. & HANAWALT, P. C. 1985. DNA repair in an active gene: removal of pyrimidine dimers from the DHFR gene of CHO cells is much more efficient than in the genome overall. *Cell,* 40**,** 359-69.

BOITEUX, S. & JINKS-ROBERTSON, S. 2013. DNA repair mechanisms and the bypass of DNA damage in Saccharomyces cerevisiae. *Genetics,* 193**,** 1025-64.

BOMAR, M. G., D'SOUZA, S., BIENKO, M., DIKIC, I., WALKER, G. C. & ZHOU, P. 2010. Unconventional ubiquitin recognition by the ubiquitin-binding motif within the Y family DNA polymerases iota and Rev1. *Mol Cell,* 37**,** 408-17.

BOMAR, M. G., PAI, M. T., TZENG, S. R., LI, S. S. & ZHOU, P. 2007. Structure of the ubiquitin-binding zinc finger domain of human DNA Y-polymerase eta. *EMBO Rep,* 8**,** 247-51.

BONNER, W. M. 1975. Protein migration into nuclei. II. Frog oocyte nuclei accumulate a class of microinjected oocyte nuclear proteins and exclude a class of microinjected oocyte cytoplasmic proteins. *J Cell Biol,* 64**,** 431-7.

BOTUYAN, M. V., KOTH, C. M., MER, G., CHAKRABARTTY, A., CONAWAY, J. W., CONAWAY, R. C., EDWARDS, A. M., ARROWSMITH, C. H. & CHAZIN, W. J. 1999. Binding of elongin A or a von Hippel-Lindau peptide stabilizes the structure of yeast elongin C. *Proc Natl Acad Sci U S A,* 96**,** 9033-8.

BOTUYAN, M. V., MER, G., YI, G. S., KOTH, C. M., CASE, D. A., EDWARDS, A. M., CHAZIN, W. J. & ARROWSMITH, C. H. 2001. Solution structure and dynamics of yeast elongin C in complex with a von Hippel-Lindau peptide. *J Mol Biol,* 312**,** 177-86.

BRADSHER, J. N., TAN, S., MCLAURY, H. J., CONAWAY, J. W. & CONAWAY, R. C. 1993. RNA polymerase II transcription factor SIII. II. Functional properties and role in RNA chain elongation. *J Biol Chem,* 268**,** 25594-603.

BREGMAN, D. B., HALABAN, R., VAN GOOL, A. J., HENNING, K. A., FRIEDBERG, E. C. & WARREN, S. L. 1996. UV-induced ubiquitination of RNA polymerase II: a novel modification deficient in Cockayne syndrome cells. *Proc Natl Acad Sci U S A,* 93**,** 11586-90.

BROWER, C. S., SHILATIFARD, A., MATHER, T., KAMURA, T., TAKAGI, Y., HAQUE, D., TREHARNE, A., FOUNDLING, S. I., CONAWAY, J. W. & CONAWAY, R. C.

1999. The elongin B ubiquitin homology domain. Identification of Elongin B sequences important for interaction with Elongin C. *J Biol Chem,* 274**,** 13629-36.

BRUECKNER, F., HENNECKE, U., CARELL, T. & CRAMER, P. 2007. CPD damage recognition by transcribing RNA polymerase II. *Science,* 315**,** 859-62.

BUCHELI, M. & SWEDER, K. 2004. In UV-irradiated Saccharomyces cerevisiae, overexpression of Swi2/Snf2 family member Rad26 increases transcription-coupled repair and repair of the non-transcribed strand. *Mol Microbiol,* 52**,** 1653-63.

BUCKING-THROM, E., DUNTZE, W., HARTWELL, L. H. & MANNEY, T. R. 1973. Reversible arrest of haploid yeast cells in the initiation of DNA synthesis by a diffusible sex factor. *Exp Cell Res,* 76**,** 99-110.

BULLOCK, A. N., DEBRECZENI, J. E., EDWARDS, A. M., SUNDSTROM, M. & KNAPP, S. 2006. Crystal structure of the SOCS2-elongin C-elongin B complex defines a prototypical SOCS box ubiquitin ligase. *Proc Natl Acad Sci U S A,* 103**,** 7637-42.

CAI, H., KAUFFMAN, S., NAIDER, F. & BECKER, J. M. 2006. Genomewide screen reveals a wide regulatory network for di/tripeptide utilization in Saccharomyces cerevisiae. *Genetics,* 172**,** 1459-76.

CHAI, Y., BERKE, S. S., COHEN, R. E. & PAULSON, H. L. 2004. Poly-ubiquitin binding by the polyglutamine disease protein ataxin-3 links its normal function to protein surveillance pathways. *J Biol Chem,* 279**,** 3605-11.

CHAN, W. M., TSOI, H., WU, C. C., WONG, C. H., CHENG, T. C., LI, H. Y., LAU, K. F., SHAW, P. C., PERRIMON, N. & CHAN, H. Y. 2011. Expanded polyglutamine domain possesses nuclear export activity which modulates subcellular localization and toxicity of polyQ disease protein via exportin-1. *Hum Mol Genet,* 20**,** 1738-50.

CHANG, A., CHEANG, S., ESPANEL, X. & SUDOL, M. 2000. Rsp5 WW domains interact directly with the carboxyl-terminal domain of RNA polymerase II. *J Biol Chem,* 275**,** 20562-71.

CHARLET-BERGUERAND, N., FEUERHAHN, S., KONG, S. E., ZISERMAN, H., CONAWAY, J. W., CONAWAY, R. & EGLY, J. M. 2006. RNA polymerase II bypass of oxidative DNA damage is regulated by transcription elongation factors. *EMBO J,* 25**,** 5481-91.

CHARTRON, J. W., VANDERVELDE, D. G. & CLEMONS, W. M., JR. 2012. Structures of the Sgt2/SGTA dimerization domain with the Get5/UBL4A UBL domain reveal an interaction that forms a conserved dynamic interface. *Cell Rep,* 2**,** 1620-32.

CHEN, P., JOHNSON, P., SOMMER, T., JENTSCH, S. & HOCHSTRASSER, M. 1993. Multiple ubiquitin-conjugating enzymes participate in the in vivo degradation of the yeast MAT alpha 2 repressor. *Cell,* 74**,** 357-69.

CHEN, X., DING, B., LEJEUNE, D., RUGGIERO, C. & LI, S. 2009. Rpb1 sumoylation in response to UV radiation or transcriptional impairment in yeast. *PLoS One,* 4**,** e5267.

CHEN, X., RUGGIERO, C. & LI, S. 2007. Yeast Rpb9 plays an important role in ubiquitylation and degradation of Rpb1 in response to UV-induced DNA damage. *Mol Cell Biol,* 27**,** 4617-25.

CHEN, Y. B., YANG, C. P., LI, R. X., ZENG, R. & ZHOU, J. Q. 2005. Def1p is involved in telomere maintenance in budding yeast. *J Biol Chem,* 280**,** 24784-91.

CHEUNG, A. C., SAINSBURY, S. & CRAMER, P. 2011. Structural basis of initial RNA polymerase II transcription. *EMBO J,* 30**,** 4755-63.

CHOLBINSKI, P., JASTRZEBSKA, Z., WYSOCKA-KAPCINSKA, M., PLOCHOCKA, D., GORNICKA, A., HOPPER, A. K. & ZOLADEK, T. 2011. Yeast ubiquitin ligase Rsp5 contains nuclear localization and export signals. *Eur J Cell Biol,* 90**,** 834-43.

CHURCHMAN, L. S. & WEISSMAN, J. S. 2011. Nascent transcript sequencing visualizes transcription at nucleotide resolution. *Nature,* 469**,** 368-73.

CICCIA, A. & ELLEDGE, S. J. 2010. The DNA damage response: making it safe to play with knives. *Mol Cell,* 40**,** 179-204.

CIECHANOVER, A., GONEN, H., BERCOVICH, B., COHEN, S., FAJERMAN, I., ISRAEL, A., MERCURIO, F., KAHANA, C., SCHWARTZ, A. L., IWAI, K. & ORIAN, A. 2001. Mechanisms of ubiquitin-mediated, limited processing of the NF-kappaB1 precursor protein p105. *Biochimie,* 83**,** 341-9.

COHEN, M., STUTZ, F., BELGAREH, N., HAGUENAUER-TSAPIS, R. & DARGEMONT, C. 2003. Ubp3 requires a cofactor, Bre5, to specifically de-ubiquitinate the COPII protein, Sec23. *Nat Cell Biol,* 5**,** 661-7.

COLLINS, G. A., GOMEZ, T. A., DESHAIES, R. J. & TANSEY, W. P. 2010. Combined chemical and genetic approach to inhibit proteolysis by the proteasome. *Yeast,* 27**,** 965-74.

COOK, A. G., FUKUHARA, N., JINEK, M. & CONTI, E. 2009. Structures of the tRNA export factor in the nuclear and cytosolic states. *Nature,* 461**,** 60-5.

COOK, W. J., JEFFREY, L. C., XU, Y. & CHAU, V. 1993. Tertiary structures of class I ubiquitin-conjugating enzymes are highly conserved: crystal structure of yeast Ubc4. *Biochemistry,* 32**,** 13809-17.

COPE, G. A., SUH, G. S., ARAVIND, L., SCHWARZ, S. E., ZIPURSKY, S. L., KOONIN, E. V. & DESHAIES, R. J. 2002. Role of predicted metalloprotease motif of Jab1/Csn5 in cleavage of Nedd8 from Cul1. *Science,* 298**,** 608-11.

COPPOTELLI, G., MUGHAL, N., MARESCOTTI, D. & MASUCCI, M. G. 2011. High avidity binding to DNA protects ubiquitylated substrates from proteasomal degradation. *J Biol Chem,* 286**,** 19565-75.

CRABTREE, H. G. 1928. The carbohydrate metabolism of certain pathological overgrowths. *Biochem J,* 22**,** 1289-98.

CRAMER, P., BUSHNELL, D. A. & KORNBERG, R. D. 2001. Structural basis of transcription: RNA polymerase II at 2.8 angstrom resolution. *Science,* 292**,** 1863-76.

CRICK, F. H. 1958. On protein synthesis. *Symp Soc Exp Biol,* 12**,** 138-63.

CZEKO, E., SEIZL, M., AUGSBERGER, C., MIELKE, T. & CRAMER, P. 2011. Iwr1 directs RNA polymerase II nuclear import. *Mol Cell,* 42**,** 261-6.

DAIGAKU, Y., DAVIES, A. A. & ULRICH, H. D. 2010. Ubiquitin-dependent DNA damage bypass is separable from genome replication. *Nature,* 465**,** 951-5.

DALAL, R. V., LARSON, M. H., NEUMAN, K. C., GELLES, J., LANDICK, R. & BLOCK, S. M. 2006. Pulling on the nascent RNA during transcription does not alter kinetics of elongation or ubiquitous pausing. *Mol Cell,* 23**,** 231-9.

DAMSMA, G. E., ALT, A., BRUECKNER, F., CARELL, T. & CRAMER, P. 2007. Mechanism of transcriptional stalling at cisplatin-damaged DNA. *Nat Struct Mol Biol,* 14**,** 1127-33.

DANIELSEN, J. M., SYLVESTERSEN, K. B., BEKKER-JENSEN, S., SZKLARCZYK, D., POULSEN, J. W., HORN, H., JENSEN, L. J., MAILAND, N. & NIELSEN, M. L. 2011. Mass spectrometric analysis of lysine ubiquitylation reveals promiscuity at site level. *Mol Cell Proteomics,* 10**,** M110 003590.

DANTUMA, N. P. & HOPPE, T. 2012. Growing sphere of influence: Cdc48/p97 orchestrates ubiquitin-dependent extraction from chromatin. *Trends Cell Biol,* 22**,** 483-91.

DASKALOGIANNI, C., APCHER, S., CANDEIAS, M. M., NASKI, N., CALVO, F. & FAHRAEUS, R. 2008. Gly-Ala repeats induce position- and substrate-specific regulation of 26 S proteasome-dependent partial processing. *J Biol Chem,* 283**,** 30090-100.

DATTA, A., BAGCHI, S., NAG, A., SHIYANOV, P., ADAMI, G. R., YOON, T. & RAYCHAUDHURI, P. 2001. The p48 subunit of the damaged-DNA binding protein DDB associates with the CBP/p300 family of histone acetyltransferase. *Mutat Res,* 486**,** 89-97.

DAULNY, A., GENG, F., MURATANI, M., GEISINGER, J. M., SALGHETTI, S. E. & TANSEY, W. P. 2008. Modulation of RNA polymerase II subunit composition by ubiquitylation. *Proc Natl Acad Sci U S A,* 105**,** 19649-54.

DAULNY, A. & TANSEY, W. P. 2009. Damage control: DNA repair, transcription, and the ubiquitin-proteasome system. *DNA Repair (Amst),* 8**,** 444-8.

DAVIES, A. A., NEISS, A. & ULRICH, H. D. 2010. Ubiquitylation of the 9-1-1 checkpoint clamp is independent of rad6-rad18 and DNA damage. *Cell,* 141**,** 1080-7.

DE BOER, J. & HOEIJMAKERS, J. H. 2000. Nucleotide excision repair and human syndromes. *Carcinogenesis,* 21**,** 453-60.

DEKKER, J., RIPPE, K., DEKKER, M. & KLECKNER, N. 2002. Capturing chromosome conformation. *Science,* 295**,** 1306-11.

DEN DULK, B., SUN, S. M., DE RUIJTER, M., BRANDSMA, J. A. & BROUWER, J. 2006. Rad33, a new factor involved in nucleotide excision repair in Saccharomyces cerevisiae. *DNA Repair (Amst),* 5**,** 683-92.

DERHEIMER, F. A., O'HAGAN, H. M., KRUEGER, H. M., HANASOGE, S., PAULSEN, M. T. & LJUNGMAN, M. 2007. RPA and ATR link transcriptional stress to p53. *Proc Natl Acad Sci U S A,* 104**,** 12778-83.

DIECKMANN, T., WITHERS-WARD, E. S., JAROSINSKI, M. A., LIU, C. F., CHEN, I. S. & FEIGON, J. 1998. Structure of a human DNA repair protein UBA domain that interacts with HIV-1 Vpr. *Nat Struct Biol,* 5**,** 1042-7.

DING, B., LEJEUNE, D. & LI, S. 2010. The C-terminal repeat domain of Spt5 plays an important role in suppression of Rad26-independent transcription coupled repair. *J Biol Chem,* 285**,** 5317-26.

DINGWALL, C. 1991. Transport across the nuclear envelope: enigmas and explanations. *Bioessays,* 13**,** 213-8.

DINH, T. N., NAGAHISA, K., HIRASAWA, T., FURUSAWA, C. & SHIMIZU, H. 2008. Adaptation of Saccharomyces cerevisiae cells to high ethanol concentration and changes in fatty acid composition of membrane and cell size. *PLoS One,* 3**,** e2623.

DONAHUE, B. A., FUCHS, R. P., REINES, D. & HANAWALT, P. C. 1996. Effects of aminofluorene and acetylaminofluorene DNA adducts on transcriptional elongation by RNA polymerase II. *J Biol Chem,* 271**,** 10588-94.

DONAHUE, B. A., YIN, S., TAYLOR, J. S., REINES, D. & HANAWALT, P. C. 1994. Transcript cleavage by RNA polymerase II arrested by a cyclobutane pyrimidine dimer in the DNA template. *Proc Natl Acad Sci U S A,* 91**,** 8502-6.

DONALDSON, K. M., YIN, H., GEKAKIS, N., SUPEK, F. & JOAZEIRO, C. A. 2003. Ubiquitin signals protein trafficking via interaction with a novel ubiquitin binding domain in the membrane fusion regulator, Vps9p. *Curr Biol,* 13**,** 258-62.

DONG, X., BISWAS, A., SUEL, K. E., JACKSON, L. K., MARTINEZ, R., GU, H. & CHOOK, Y. M. 2009. Structural basis for leucine-rich nuclear export signal recognition by CRM1. *Nature,* 458**,** 1136-41.

DOUGHERTY, W. G., PARKS, T. D., CARY, S. M., BAZAN, J. F. & FLETTERICK, R. J. 1989. Characterization of the catalytic residues of the tobacco etch virus 49-kDa proteinase. *Virology,* 172**,** 302-10.

DUAN, D. R., PAUSE, A., BURGESS, W. H., ASO, T., CHEN, D. Y., GARRETT, K. P., CONAWAY, R. C., CONAWAY, J. W., LINEHAN, W. M. & KLAUSNER, R. D. 1995. Inhibition of transcription elongation by the VHL tumor suppressor protein. *Science,* 269**,** 1402-6.

DUDA, D. M., BORG, L. A., SCOTT, D. C., HUNT, H. W., HAMMEL, M. & SCHULMAN, B. A. 2008. Structural insights into NEDD8 activation of cullin-RING ligases: conformational control of conjugation. *Cell,* 134**,** 995-1006.

EDDINS, M. J., CARLILE, C. M., GOMEZ, K. M., PICKART, C. M. & WOLBERGER, C. 2006. Mms2-Ubc13 covalently bound to ubiquitin reveals the structural basis of linkage-specific polyubiquitin chain formation. *Nat Struct Mol Biol,* 13**,** 915-20.

EDELMANN, M. J., IPHOFER, A., AKUTSU, M., ALTUN, M., DI GLERIA, K., KRAMER, H. B., FIEBIGER, E., DHE-PAGANON, S. & KESSLER, B. M. 2009. Structural basis and specificity of human otubain 1-mediated deubiquitination. *Biochem J,* 418**,** 379-90.

EGLOFF, S., SZCZEPANIAK, S. A., DIENSTBIER, M., TAYLOR, A., KNIGHT, S. & MURPHY, S. 2010. The integrator complex recognizes a new double mark on the RNA polymerase II carboxyl-terminal domain. *J Biol Chem,* 285**,** 20564-9.

ELETR, Z. M., HUANG, D. T., DUDA, D. M., SCHULMAN, B. A. & KUHLMAN, B. 2005. E2 conjugating enzymes must disengage from their E1 enzymes before E3-dependent ubiquitin and ubiquitin-like transfer. *Nat Struct Mol Biol,* 12**,** 933-4.

ELSASSER, S., CHANDLER-MILITELLO, D., MULLER, B., HANNA, J. & FINLEY, D. 2004. Rad23 and Rpn10 serve as alternative ubiquitin receptors for the proteasome. *J Biol Chem,* 279**,** 26817-22.

ELSASSER, S. & FINLEY, D. 2005. Delivery of ubiquitinated substrates to protein-unfolding machines. *Nat Cell Biol,* 7**,** 742-9.

ELSASSER, S., GALI, R. R., SCHWICKART, M., LARSEN, C. N., LEGGETT, D. S., MULLER, B., FENG, M. T., TUBING, F., DITTMAR, G. A. & FINLEY, D. 2002. Proteasome subunit Rpn1 binds ubiquitin-like protein domains. *Nat Cell Biol,* 4**,** 725-30.

EMRE, N. C., INGVARSDOTTIR, K., WYCE, A., WOOD, A., KROGAN, N. J., HENRY, K. W., LI, K., MARMORSTEIN, R., GREENBLATT, J. F., SHILATIFARD, A. & BERGER, S. L. 2005. Maintenance of low histone ubiquitylation by Ubp10 correlates with telomere-proximal Sir2 association and gene silencing. *Mol Cell,* 17**,** 585-94.

EPSHTEIN, V. & NUDLER, E. 2003. Cooperation between RNA polymerase molecules in transcription elongation. *Science,* 300**,** 801-5.

EXINGER, F. & LACROUTE, F. 1992. 6-Azauracil inhibition of GTP biosynthesis in Saccharomyces cerevisiae. *Curr Genet,* 22**,** 9-11.

FAESEN, A. C., DIRAC, A. M., SHANMUGHAM, A., OVAA, H., PERRAKIS, A. & SIXMA, T. K. 2011. Mechanism of USP7/HAUSP activation by its C-terminal ubiquitin-like domain and allosteric regulation by GMP-synthetase. *Mol Cell,* 44**,** 147-59.

FAESEN, A. C., LUNA-VARGAS, M. P. & SIXMA, T. K. 2012. The role of UBL domains in ubiquitin-specific proteases. *Biochem Soc Trans,* 40**,** 539-45.

FAN, C. M. & MANIATIS, T. 1991. Generation of p50 subunit of NF-kappa B by processing of p105 through an ATP-dependent pathway. *Nature,* 354**,** 395-8.

FENTEANY, G., STANDAERT, R. F., LANE, W. S., CHOI, S., COREY, E. J. & SCHREIBER, S. L. 1995. Inhibition of proteasome activities and subunit-specific amino-terminal threonine modification by lactacystin. *Science,* 268**,** 726-31.

FERDOUS, A., KODADEK, T. & JOHNSTON, S. A. 2002. A nonproteolytic function of the 19S regulatory subunit of the 26S proteasome is required for efficient activated transcription by human RNA polymerase II. *Biochemistry,* 41**,** 12798-805.

FIERZ, B., CHATTERJEE, C., MCGINTY, R. K., BAR-DAGAN, M., RALEIGH, D. P. & MUIR, T. W. 2011. Histone H2B ubiquitylation disrupts local and higher-order chromatin compaction. *Nat Chem Biol,* 7**,** 113-9.

FINLEY, D. 2009. Recognition and processing of ubiquitin-protein conjugates by the proteasome. *Annu Rev Biochem,* 78**,** 477-513.

FINLEY, D., ULRICH, H. D., SOMMER, T. & KAISER, P. 2012. The ubiquitin-proteasome system of Saccharomyces cerevisiae. *Genetics,* 192**,** 319-60.

FISCHER, E. S., SCRIMA, A., BOHM, K., MATSUMOTO, S., LINGARAJU, G. M., FATY, M., YASUDA, T., CAVADINI, S., WAKASUGI, M., HANAOKA, F., IWAI, S., GUT, H., SUGASAWA, K. & THOMA, N. H. 2011. The molecular basis of CRL4DDB2/CSA ubiquitin ligase architecture, targeting, and activation. *Cell,* 147**,** 1024-39.

FIUMARA, F., FIORITI, L., KANDEL, E. R. & HENDRICKSON, W. A. 2010. Essential role of coiled coils for aggregation and activity of Q/N-rich prions and PolyQ proteins. *Cell,* 143**,** 1121-35.

FOUSTERI, M., VERMEULEN, W., VAN ZEELAND, A. A. & MULLENDERS, L. H. 2006. Cockayne syndrome A and B proteins differentially regulate recruitment of chromatin remodeling and repair factors to stalled RNA polymerase II in vivo. *Mol Cell,* 23**,** 471-82.

FRADET-TURCOTTE, A., CANNY, M. D., ESCRIBANO-DIAZ, C., ORTHWEIN, A., LEUNG, C. C., HUANG, H., LANDRY, M. C., KITEVSKI-LEBLANC, J., NOORDERMEER, S. M., SICHERI, F. & DUROCHER, D. 2013. 53BP1 is a reader of the DNA-damage-induced H2A Lys 15 ubiquitin mark. *Nature,* 499**,** 50-4.

FRANGIONI, J. V. & NEEL, B. G. 1993. Solubilization and purification of enzymatically active glutathione S-transferase (pGEX) fusion proteins. *Anal Biochem,* 210**,** 179-87.

FUNAKOSHI, M., SASAKI, T., NISHIMOTO, T. & KOBAYASHI, H. 2002. Budding yeast Dsk2p is a polyubiquitin-binding protein that can interact with the proteasome. *Proc Natl Acad Sci U S A,* 99**,** 745-50.

FUSHMAN, D. & WALKER, O. 2010. Exploring the linkage dependence of polyubiquitin conformations using molecular modeling. *J Mol Biol,* 395**,** 803-14.

GAILLARD, H. & AGUILERA, A. 2013. Transcription coupled repair at the interface between transcription elongation and mRNP biogenesis. *Biochim Biophys Acta,* 1829**,** 141-50.

GARCIA-RUBIO, M. L. & AGUILERA, A. 2012. Topological constraints impair RNA polymerase II transcription and causes instability of plasmid-borne convergent genes. *Nucleic Acids Res,* 40**,** 1050-64.

GARRETT, K. P., ASO, T., BRADSHER, J. N., FOUNDLING, S. I., LANE, W. S., CONAWAY, R. C. & CONAWAY, J. W. 1995. Positive regulation of general

transcription factor SIII by a tailed ubiquitin homolog. *Proc Natl Acad Sci U S A,* 92**,** 7172-6.

GASCH, A. P., HUANG, M., METZNER, S., BOTSTEIN, D., ELLEDGE, S. J. & BROWN, P. O. 2001. Genomic expression responses to DNA-damaging agents and the regulatory role of the yeast ATR homolog Mec1p. *Mol Biol Cell,* 12**,** 2987-3003.

GENG, F., WENZEL, S. & TANSEY, W. P. 2012. Ubiquitin and proteasomes in transcription. *Annu Rev Biochem,* 81**,** 177-201.

GERBER, M., EISSENBERG, J. C., KONG, S., TENNEY, K., CONAWAY, J. W., CONAWAY, R. C. & SHILATIFARD, A. 2004. In vivo requirement of the RNA polymerase II elongation factor elongin A for proper gene expression and development. *Mol Cell Biol,* 24**,** 9911-9.

GHAEMMAGHAMI, S., HUH, W. K., BOWER, K., HOWSON, R. W., BELLE, A., DEPHOURE, N., O'SHEA, E. K. & WEISSMAN, J. S. 2003. Global analysis of protein expression in yeast. *Nature,* 425**,** 737-41.

GHOSH, A., SHUMAN, S. & LIMA, C. D. 2011. Structural insights to how mammalian capping enzyme reads the CTD code. *Mol Cell,* 43**,** 299-310.

GILLETTE, T. G., GONZALEZ, F., DELAHODDE, A., JOHNSTON, S. A. & KODADEK, T. 2004. Physical and functional association of RNA polymerase II and the proteasome. *Proc Natl Acad Sci U S A,* 101**,** 5904-9.

GILLETTE, T. G., YU, S., ZHOU, Z., WATERS, R., JOHNSTON, S. A. & REED, S. H. 2006. Distinct functions of the ubiquitin-proteasome pathway influence nucleotide excision repair. *EMBO J,* 25**,** 2529-38.

GLICKMAN, M. H., RUBIN, D. M., COUX, O., WEFES, I., PFEIFER, G., CJEKA, Z., BAUMEISTER, W., FRIED, V. A. & FINLEY, D. 1998. A subcomplex of the proteasome regulatory particle required for ubiquitin-conjugate degradation and related to the COP9-signalosome and eIF3. *Cell,* 94**,** 615-23.

GNATT, A. L., CRAMER, P., FU, J., BUSHNELL, D. A. & KORNBERG, R. D. 2001. Structural basis of transcription: an RNA polymerase II elongation complex at 3.3 A resolution. *Science,* 292**,** 1876-82.

GONZALEZ, F., DELAHODDE, A., KODADEK, T. & JOHNSTON, S. A. 2002. Recruitment of a 19S proteasome subcomplex to an activated promoter. *Science,* 296**,** 548-50.

GORSCH, L. C., DOCKENDORFF, T. C. & COLE, C. N. 1995. A conditional allele of the novel repeat-containing yeast nucleoporin RAT7/NUP159 causes both rapid cessation of mRNA export and reversible clustering of nuclear pore complexes. *J Cell Biol,* 129**,** 939-55.

GRABBE, C. & DIKIC, I. 2009. Functional roles of ubiquitin-like domain (ULD) and ubiquitin-binding domain (UBD) containing proteins. *Chem Rev,* 109**,** 1481-94.

GROISMAN, R., KURAOKA, I., CHEVALLIER, O., GAYE, N., MAGNALDO, T., TANAKA, K., KISSELEV, A. F., HAREL-BELLAN, A. & NAKATANI, Y. 2006. CSA-dependent degradation of CSB by the ubiquitin-proteasome pathway establishes a link between complementation factors of the Cockayne syndrome. *Genes Dev,* 20**,** 1429-34.

GROISMAN, R., POLANOWSKA, J., KURAOKA, I., SAWADA, J., SAIJO, M., DRAPKIN, R., KISSELEV, A. F., TANAKA, K. & NAKATANI, Y. 2003. The ubiquitin ligase activity in the DDB2 and CSA complexes is differentially regulated by the COP9 signalosome in response to DNA damage. *Cell,* 113**,** 357-67.

GU, W. & REINES, D. 1995. Identification of a decay in transcription potential that results in elongation factor dependence of RNA polymerase II. *J Biol Chem,* 270**,** 11238-44.

GUTERMAN, A. & GLICKMAN, M. H. 2004. Complementary roles for Rpn11 and Ubp6 in deubiquitination and proteolysis by the proteasome. *J Biol Chem,* 279**,** 1729-38.

GUZDER, S. N., HABRAKEN, Y., SUNG, P., PRAKASH, L. & PRAKASH, S. 1995. Reconstitution of yeast nucleotide excision repair with purified Rad proteins, replication protein A, and transcription factor TFIIH. *J Biol Chem,* 270**,** 12973-6.

GUZDER, S. N., HABRAKEN, Y., SUNG, P., PRAKASH, L. & PRAKASH, S. 1996a. RAD26, the yeast homolog of human Cockayne's syndrome group B gene, encodes a DNA-dependent ATPase. *J Biol Chem,* 271**,** 18314-7.

GUZDER, S. N., SOMMERS, C. H., PRAKASH, L. & PRAKASH, S. 2006. Complex formation with damage recognition protein Rad14 is essential for Saccharomyces cerevisiae Rad1-Rad10 nuclease to perform its function in nucleotide excision repair in vivo. *Mol Cell Biol,* 26**,** 1135-41.

GUZDER, S. N., SUNG, P., PRAKASH, L. & PRAKASH, S. 1996b. Nucleotide excision repair in yeast is mediated by sequential assembly of repair factors and not by a pre-assembled repairosome. *J Biol Chem,* 271**,** 8903-10.

GUZDER, S. N., SUNG, P., PRAKASH, L. & PRAKASH, S. 1999. Synergistic interaction between yeast nucleotide excision repair factors NEF2 and NEF4 in the binding of ultraviolet-damaged DNA. *J Biol Chem,* 274**,** 24257-62.

HA, S. W., JU, D. & XIE, Y. 2012. The N-terminal domain of Rpn4 serves as a portable ubiquitin-independent degron and is recognized by specific 19S RP subunits. *Biochem Biophys Res Commun,* 419**,** 226-31.

HANAWALT, P. C. & SPIVAK, G. 2008. Transcription-coupled DNA repair: two decades of progress and surprises. *Nat Rev Mol Cell Biol,* 9**,** 958-70.

HANNICH, J. T., LEWIS, A., KROETZ, M. B., LI, S. J., HEIDE, H., EMILI, A. & HOCHSTRASSER, M. 2005. Defining the SUMO-modified proteome by multiple approaches in Saccharomyces cerevisiae. *J Biol Chem,* 280**,** 4102-10.

HANOVER, J. A., LOVE, D. C., DEANGELIS, N., O'KANE, M. E., LIMA-MIRANDA, R., SCHULZ, T., YEN, Y. M., JOHNSON, R. C. & PRINZ, W. A. 2007. The High Mobility Group Box Transcription Factor Nhp6Ap enters the nucleus by a calmodulin-dependent, Ran-independent pathway. *J Biol Chem,* 282**,** 33743-51.

HANZELMANN, P., STINGELE, J., HOFMANN, K., SCHINDELIN, H. & RAASI, S. 2010. The yeast E4 ubiquitin ligase Ufd2 interacts with the ubiquitin-like domains of Rad23 and Dsk2 via a novel and distinct ubiquitin-like binding domain. *J Biol Chem,* 285**,** 20390-8.

HARIRINIA, A., VERMA, R., PUROHIT, N., TWAROG, M. Z., DESHAIES, R. J., BOLON, D. & FUSHMAN, D. 2008. Mutations in the hydrophobic core of ubiquitin differentially affect its recognition by receptor proteins. *J Mol Biol,* 375**,** 979-96.

HARLOW, E. & LANE, D. 1999. *Using antibodies : a laboratory manual,* Cold Spring Harbor, N.Y., Cold Spring Harbor Laboratory Press.

HARPER, S., BESONG, T. M., EMSLEY, J., SCOTT, D. J. & DREVENY, I. 2011. Structure of the USP15 N-terminal domains: a beta-hairpin mediates close association between the DUSP and UBL domains. *Biochemistry,* 50**,** 7995-8004.

HARREMAN, M., TASCHNER, M., SIGURDSSON, S., ANINDYA, R., REID, J., SOMESH, B., KONG, S. E., BANKS, C. A., CONAWAY, R. C., CONAWAY, J.

W. & SVEJSTRUP, J. Q. 2009. Distinct ubiquitin ligases act sequentially for RNA polymerase II polyubiquitylation. *Proc Natl Acad Sci U S A,* 106**,** 20705-10.

HARREMAN, M. T., KLINE, T. M., MILFORD, H. G., HARBEN, M. B., HODEL, A. E. & CORBETT, A. H. 2004. Regulation of nuclear import by phosphorylation adjacent to nuclear localization signals. *J Biol Chem,* 279**,** 20613-21.

HARTZOG, G. A., WADA, T., HANDA, H. & WINSTON, F. 1998. Evidence that Spt4, Spt5, and Spt6 control transcription elongation by RNA polymerase II in Saccharomyces cerevisiae. *Genes Dev,* 12**,** 357-69.

HAWLEY, D. K., WIEST, D. K., HOLTZ, M. S. & WANG, D. 1993. Transcriptional pausing, arrest, and readthrough at the adenovirus major late attenuation site. *Cell Mol Biol Res,* 39**,** 339-48.

HEESSEN, S., MASUCCI, M. G. & DANTUMA, N. P. 2005. The UBA2 domain functions as an intrinsic stabilization signal that protects Rad23 from proteasomal degradation. *Mol Cell,* 18**,** 225-35.

HEIDEMANN, M., HINTERMAIR, C., VOSS, K. & EICK, D. 2013. Dynamic phosphorylation patterns of RNA polymerase II CTD during transcription. *Biochim Biophys Acta,* 1829**,** 55-62.

HEINE, G. F., HORWITZ, A. A. & PARVIN, J. D. 2008. Multiple mechanisms contribute to inhibit transcription in response to DNA damage. *J Biol Chem,* 283**,** 9555-61.

HEINEMEYER, W., FISCHER, M., KRIMMER, T., STACHON, U. & WOLF, D. H. 1997. The active sites of the eukaryotic 20 S proteasome and their involvement in subunit precursor processing. *J Biol Chem,* 272**,** 25200-9.

HEINEN, C., ACS, K., HOOGSTRATEN, D. & DANTUMA, N. P. 2011. C-terminal UBA domains protect ubiquitin receptors by preventing initiation of protein degradation. *Nat Commun,* 2**,** 191.

HEMMING, S. A., JANSMA, D. B., MACGREGOR, P. F., GORYACHEV, A., FRIESEN, J. D. & EDWARDS, A. M. 2000. RNA polymerase II subunit Rpb9 regulates transcription elongation in vivo. *J Biol Chem,* 275**,** 35506-11.

HENGARTNER, M. O. 2000. The biochemistry of apoptosis. *Nature,* 407**,** 770-6.

HERRADOR, A., LEON, S., HAGUENAUER-TSAPIS, R. & VINCENT, O. 2013. A Mechanism for Protein Monoubiquitination Dependent on a trans-Acting Ubiquitin-binding Domain. *J Biol Chem,* 288**,** 16206-11.

HERSHKO, A., CIECHANOVER, A., HELLER, H., HAAS, A. L. & ROSE, I. A. 1980. Proposed role of ATP in protein breakdown: conjugation of protein with multiple chains of the polypeptide of ATP-dependent proteolysis. *Proc Natl Acad Sci U S A,* 77**,** 1783-6.

HINTERMAIR, C., HEIDEMANN, M., KOCH, F., DESCOSTES, N., GUT, M., GUT, I., FENOUIL, R., FERRIER, P., FLATLEY, A., KREMMER, E., CHAPMAN, R. D., ANDRAU, J. C. & EICK, D. 2012. Threonine-4 of mammalian RNA polymerase II CTD is targeted by Polo-like kinase 3 and required for transcriptional elongation. *EMBO J,* 31**,** 2784-97.

HITCHCOCK, A. L., KREBBER, H., FRIETZE, S., LIN, A., LATTERICH, M. & SILVER, P. A. 2001. The conserved npl4 protein complex mediates proteasome-dependent membrane-bound transcription factor activation. *Mol Biol Cell,* 12**,** 3226-41.

HJERPE, R., AILLET, F., LOPITZ-OTSOA, F., LANG, V., ENGLAND, P. & RODRIGUEZ, M. S. 2009. Efficient protection and isolation of ubiquitylated proteins using tandem ubiquitin-binding entities. *EMBO Rep,* 10**,** 1250-8.

HJERPE, R., THOMAS, Y., CHEN, J., ZEMLA, A., CURRAN, S., SHPIRO, N., DICK, L. R. & KURZ, T. 2012. Changes in the ratio of free NEDD8 to ubiquitin triggers NEDDylation by ubiquitin enzymes. *Biochem J,* 441**,** 927-36.

HOBSON, D. J., WEI, W., STEINMETZ, L. M. & SVEJSTRUP, J. Q. 2012. RNA polymerase II collision interrupts convergent transcription. *Mol Cell,* 48**,** 365-74.

HODEL, A. E., HARREMAN, M. T., PULLIAM, K. F., HARBEN, M. E., HOLMES, J. S., HODEL, M. R., BERLAND, K. M. & CORBETT, A. H. 2006. Nuclear localization signal receptor affinity correlates with in vivo localization in Saccharomyces cerevisiae. *J Biol Chem,* 281**,** 23545-56.

HODEL, M. R., CORBETT, A. H. & HODEL, A. E. 2001. Dissection of a nuclear localization signal. *J Biol Chem,* 276**,** 1317-25.

HODGES, J. L., LESLIE, J. H., MOSAMMAPARAST, N., GUO, Y., SHABANOWITZ, J., HUNT, D. F. & PEMBERTON, L. F. 2005. Nuclear import of TFIIB is mediated by Kap114p, a karyopherin with multiple cargo-binding domains. *Mol Biol Cell,* 16**,** 3200-10.

HOEGE, C., PFANDER, B., MOLDOVAN, G. L., PYROWOLAKIS, G. & JENTSCH, S. 2002. RAD6-dependent DNA repair is linked to modification of PCNA by ubiquitin and SUMO. *Nature,* 419**,** 135-41.

HOELLER, D., HECKER, C. M., WAGNER, S., ROGOV, V., DOTSCH, V. & DIKIC, I. 2007. E3-independent monoubiquitination of ubiquitin-binding proteins. *Mol Cell,* 26**,** 891-8.

HOFMANN, K. 2009. Ubiquitin-binding domains and their role in the DNA damage response. *DNA Repair (Amst),* 8**,** 544-56.

HOFMANN, K. & BUCHER, P. 1996. The UBA domain: a sequence motif present in multiple enzyme classes of the ubiquitination pathway. *Trends Biochem Sci,* 21**,** 172-3.

HOFMANN, R. M. & PICKART, C. M. 1999. Noncanonical MMS2-encoded ubiquitin-conjugating enzyme functions in assembly of novel polyubiquitin chains for DNA repair. *Cell,* 96**,** 645-53.

HOPPE, T., MATUSCHEWSKI, K., RAPE, M., SCHLENKER, S., ULRICH, H. D. & JENTSCH, S. 2000. Activation of a membrane-bound transcription factor by regulated ubiquitin/proteasome-dependent processing. *Cell,* 102**,** 577-86.

HUH, W. K., FALVO, J. V., GERKE, L. C., CARROLL, A. S., HOWSON, R. W., WEISSMAN, J. S. & O'SHEA, E. K. 2003. Global analysis of protein localization in budding yeast. *Nature,* 425**,** 686-91.

HUIBREGTSE, J. M., SCHEFFNER, M., BEAUDENON, S. & HOWLEY, P. M. 1995. A family of proteins structurally and functionally related to the E6-AP ubiquitin-protein ligase. *Proc Natl Acad Sci U S A,* 92**,** 2563-7.

HUIBREGTSE, J. M., YANG, J. C. & BEAUDENON, S. L. 1997. The large subunit of RNA polymerase II is a substrate of the Rsp5 ubiquitin-protein ligase. *Proc Natl Acad Sci U S A,* 94**,** 3656-61.

HURLEY, J. H., LEE, S. & PRAG, G. 2006. Ubiquitin-binding domains. *Biochem J,* 399**,** 361-72.

HUSNJAK, K. & DIKIC, I. 2012. Ubiquitin-binding proteins: decoders of ubiquitin-mediated cellular functions. *Annu Rev Biochem,* 81**,** 291-322.

HUSNJAK, K., ELSASSER, S., ZHANG, N., CHEN, X., RANDLES, L., SHI, Y., HOFMANN, K., WALTERS, K. J., FINLEY, D. & DIKIC, I. 2008. Proteasome subunit Rpn13 is a novel ubiquitin receptor. *Nature,* 453**,** 481-8.

HUTTEN, S. & KEHLENBACH, R. H. 2007. CRM1-mediated nuclear export: to the pore and beyond. *Trends Cell Biol,* 17**,** 193-201.

HWANG, C. S., SHEMORRY, A., AUERBACH, D. & VARSHAVSKY, A. 2010. The N-end rule pathway is mediated by a complex of the RING-type Ubr1 and HECT-type Ufd4 ubiquitin ligases. *Nat Cell Biol,* 12**,** 1177-85.

HWANG, W. W., VENKATASUBRAHMANYAM, S., IANCULESCU, A. G., TONG, A., BOONE, C. & MADHANI, H. D. 2003. A conserved RING finger protein required for histone H2B monoubiquitination and cell size control. *Mol Cell,* 11**,** 261-6.

INOBE, T., FISHBAIN, S., PRAKASH, S. & MATOUSCHEK, A. 2011. Defining the geometry of the two-component proteasome degron. *Nat Chem Biol,* 7**,** 161-7.

INUKAI, N., YAMAGUCHI, Y., KURAOKA, I., YAMADA, T., KAMIJO, S., KATO, J., TANAKA, K. & HANDA, H. 2004. A novel hydrogen peroxide-induced phosphorylation and ubiquitination pathway leading to RNA polymerase II proteolysis. *J Biol Chem,* 279**,** 8190-5.

IVANTSIV, Y., KAPLUN, L., TZIRKIN-GOLDIN, R., SHABEK, N. & RAVEH, D. 2006. Unique role for the UbL-UbA protein Ddi1 in turnover of SCFUfo1 complexes. *Mol Cell Biol,* 26**,** 1579-88.

IZBAN, M. G. & LUSE, D. S. 1992a. Factor-stimulated RNA polymerase II transcribes at physiological elongation rates on naked DNA but very poorly on chromatin templates. *J Biol Chem,* 267**,** 13647-55.

IZBAN, M. G. & LUSE, D. S. 1992b. The RNA polymerase II ternary complex cleaves the nascent transcript in a 3'----5' direction in the presence of elongation factor SII. *Genes Dev,* 6**,** 1342-56.

JANKE, C., MAGIERA, M. M., RATHFELDER, N., TAXIS, C., REBER, S., MAEKAWA, H., MORENO-BORCHART, A., DOENGES, G., SCHWOB, E., SCHIEBEL, E. & KNOP, M. 2004. A versatile toolbox for PCR-based tagging of yeast genes: new fluorescent proteins, more markers and promoter substitution cassettes. *Yeast,* 21**,** 947-62.

JARIEL-ENCONTRE, I., BOSSIS, G. & PIECHACZYK, M. 2008. Ubiquitin-independent degradation of proteins by the proteasome. *Biochim Biophys Acta,* 1786**,** 153-77.

JEON, H. B., CHOI, E. S., YOON, J. H., HWANG, J. H., CHANG, J. W., LEE, E. K., CHOI, H. W., PARK, Z. Y. & YOO, Y. J. 2007. A proteomics approach to identify the ubiquitinated proteins in mouse heart. *Biochem Biophys Res Commun,* 357**,** 731-6.

JIN, J., BAI, L., JOHNSON, D. S., FULBRIGHT, R. M., KIREEVA, M. L., KASHLEV, M. & WANG, M. D. 2010. Synergistic action of RNA polymerases in overcoming the nucleosomal barrier. *Nat Struct Mol Biol,* 17**,** 745-52.

JOHNSON, E. S. & GUPTA, A. A. 2001. An E3-like factor that promotes SUMO conjugation to the yeast septins. *Cell,* 106**,** 735-44.

JOHNSTON, J. A., JOHNSON, E. S., WALLER, P. R. & VARSHAVSKY, A. 1995. Methotrexate inhibits proteolysis of dihydrofolate reductase by the N-end rule pathway. *J Biol Chem,* 270**,** 8172-8.

JOHNSTON, J. A., WARD, C. L. & KOPITO, R. R. 1998. Aggresomes: a cellular response to misfolded proteins. *J Cell Biol,* 143**,** 1883-98.

JORDAN, P. W., KLEIN, F. & LEACH, D. R. 2007. Novel roles for selected genes in meiotic DNA processing. *PLoS Genet,* 3**,** e222.

JORGENSEN, P., NISHIKAWA, J. L., BREITKREUTZ, B. J. & TYERS, M. 2002. Systematic identification of pathways that couple cell growth and division in yeast. *Science,* 297**,** 395-400.

JOUVET, N., POSCHMANN, J., DOUVILLE, J., BULET, L. & RAMOTAR, D. 2010. Rrd1 isomerizes RNA polymerase II in response to rapamycin. *BMC Mol Biol,* 11**,** 92.

JOUVET, N., POSCHMANN, J., DOUVILLE, J., MARRAKCHI, R. & RAMOTAR, D. 2011. RNA polymerase II degradation in response to rapamycin is not mediated through ubiquitylation. *Biochem Biophys Res Commun,* 413**,** 248-53.

JUNG, Y. & LIPPARD, S. J. 2006. RNA polymerase II blockage by cisplatin-damaged DNA. Stability and polyubiquitylation of stalled polymerase. *J Biol Chem,* 281**,** 1361-70.

KAFFMAN, A., RANK, N. M., O'NEILL, E. M., HUANG, L. S. & O'SHEA, E. K. 1998. The receptor Msn5 exports the phosphorylated transcription factor Pho4 out of the nucleus. *Nature,* 396**,** 482-6.

KAISER, P., SU, N. Y., YEN, J. L., OUNI, I. & FLICK, K. 2006. The yeast ubiquitin ligase SCFMet30: connecting environmental and intracellular conditions to cell division. *Cell Div,* 1**,** 16.

KALDERON, D., RICHARDSON, W. D., MARKHAM, A. F. & SMITH, A. E. 1984. Sequence requirements for nuclear location of simian virus 40 large-T antigen. *Nature,* 311**,** 33-8.

KALISZEWSKI, P. & ZOLADEK, T. 2008. The role of Rsp5 ubiquitin ligase in regulation of diverse processes in yeast cells. *Acta Biochim Pol,* 55**,** 649-62.

KAMURA, T., BURIAN, D., YAN, Q., SCHMIDT, S. L., LANE, W. S., QUERIDO, E., BRANTON, P. E., SHILATIFARD, A., CONAWAY, R. C. & CONAWAY, J. W. 2001. Muf1, a novel Elongin BC-interacting leucine-rich repeat protein that can assemble with Cul5 and Rbx1 to reconstitute a ubiquitin ligase. *J Biol Chem,* 276**,** 29748-53.

KANG, R. S., DANIELS, C. M., FRANCIS, S. A., SHIH, S. C., SALERNO, W. J., HICKE, L. & RADHAKRISHNAN, I. 2003. Solution structure of a CUE-ubiquitin complex reveals a conserved mode of ubiquitin binding. *Cell,* 113**,** 621-30.

KANG, Y., ZHANG, N., KOEPP, D. M. & WALTERS, K. J. 2007. Ubiquitin receptor proteins hHR23a and hPLIC2 interact. *J Mol Biol,* 365**,** 1093-101.

KATHE, S. D., SHEN, G. P. & WALLACE, S. S. 2004. Single-stranded breaks in DNA but not oxidative DNA base damages block transcriptional elongation by RNA polymerase II in HeLa cell nuclear extracts. *J Biol Chem,* 279**,** 18511-20.

KAWAUCHI, J., INOUE, M., FUKUDA, M., UCHIDA, Y., YASUKAWA, T., CONAWAY, R. C., CONAWAY, J. W., ASO, T. & KITAJIMA, S. 2013. Transcriptional properties of mammalian Elongin A and its role in stress response. *J Biol Chem*.

KEE, Y., LYON, N. & HUIBREGTSE, J. M. 2005. The Rsp5 ubiquitin ligase is coupled to and antagonized by the Ubp2 deubiquitinating enzyme. *EMBO J,* 24**,** 2414-24.

KEE, Y., MUNOZ, W., LYON, N. & HUIBREGTSE, J. M. 2006. The deubiquitinating enzyme Ubp2 modulates Rsp5-dependent Lys63-linked polyubiquitin conjugates in Saccharomyces cerevisiae. *J Biol Chem,* 281**,** 36724-31.

KETTENBERGER, H., ARMACHE, K. J. & CRAMER, P. 2004. Complete RNA polymerase II elongation complex structure and its interactions with NTP and TFIIS. *Mol Cell,* 16**,** 955-65.

KIEL, C. & SERRANO, L. 2006. The ubiquitin domain superfold: structure-based sequence alignments and characterization of binding epitopes. *J Mol Biol,* 355**,** 821-44.

KIM, H. C. & HUIBREGTSE, J. M. 2009. Polyubiquitination by HECT E3s and the determinants of chain type specificity. *Mol Cell Biol,* 29**,** 3307-18.

KIM, H. T., KIM, K. P., LLEDIAS, F., KISSELEV, A. F., SCAGLIONE, K. M., SKOWYRA, D., GYGI, S. P. & GOLDBERG, A. L. 2007. Certain pairs of ubiquitin-conjugating enzymes (E2s) and ubiquitin-protein ligases (E3s) synthesize nondegradable forked ubiquitin chains containing all possible isopeptide linkages. *J Biol Chem,* 282**,** 17375-86.

KIM, J. K., PATEL, D. & CHOI, B. S. 1995. Contrasting structural impacts induced by cis-syn cyclobutane dimer and (6-4) adduct in DNA duplex decamers: implication in mutagenesis and repair activity. *Photochem Photobiol,* 62**,** 44-50.

KIM, W., BENNETT, E. J., HUTTLIN, E. L., GUO, A., LI, J., POSSEMATO, A., SOWA, M. E., RAD, R., RUSH, J., COMB, M. J., HARPER, J. W. & GYGI, S. P. 2011. Systematic and quantitative assessment of the ubiquitin-modified proteome. *Mol Cell,* 44**,** 325-40.

KIREEVA, M. L., HANCOCK, B., CREMONA, G. H., WALTER, W., STUDITSKY, V. M. & KASHLEV, M. 2005. Nature of the nucleosomal barrier to RNA polymerase II. *Mol Cell,* 18**,** 97-108.

KIREEVA, M. L., KOMISSAROVA, N., WAUGH, D. S. & KASHLEV, M. 2000. The 8-nucleotide-long RNA:DNA hybrid is a primary stability determinant of the RNA polymerase II elongation complex. *J Biol Chem,* 275**,** 6530-6.

KIRKPATRICK, D. S., WELDON, S. F., TSAPRAILIS, G., LIEBLER, D. C. & GANDOLFI, A. J. 2005. Proteomic identification of ubiquitinated proteins from human cells expressing His-tagged ubiquitin. *Proteomics,* 5**,** 2104-11.

KLEIGER, G., HAO, B., MOHL, D. A. & DESHAIES, R. J. 2009a. The acidic tail of the Cdc34 ubiquitin-conjugating enzyme functions in both binding to and catalysis with ubiquitin ligase SCFCdc4. *J Biol Chem,* 284**,** 36012-23.

KLEIGER, G., SAHA, A., LEWIS, S., KUHLMAN, B. & DESHAIES, R. J. 2009b. Rapid E2-E3 assembly and disassembly enable processive ubiquitylation of cullin-RING ubiquitin ligase substrates. *Cell,* 139**,** 957-68.

KLEIMAN, F. E., WU-BAER, F., FONSECA, D., KANEKO, S., BAER, R. & MANLEY, J. L. 2005. BRCA1/BARD1 inhibition of mRNA 3' processing involves targeted degradation of RNA polymerase II. *Genes Dev,* 19**,** 1227-37.

KOHDA, K., KAWAZOE, Y., MINOURA, Y. & TADA, M. 1991. Separation and identification of N4-(guanosin-7-yl)-4-aminoquinoline 1-oxide, a novel nucleic acid adduct of carcinogen 4-nitroquinoline 1-oxide. *Carcinogenesis,* 12**,** 1523-5.

KOMANDER, D., CLAGUE, M. J. & URBE, S. 2009. Breaking the chains: structure and function of the deubiquitinases. *Nat Rev Mol Cell Biol,* 10**,** 550-63.

KOMANDER, D., LORD, C. J., SCHEEL, H., SWIFT, S., HOFMANN, K., ASHWORTH, A. & BARFORD, D. 2008. The structure of the CYLD USP domain explains its specificity for Lys63-linked polyubiquitin and reveals a B box module. *Mol Cell,* 29**,** 451-64.

KOMANDER, D. & RAPE, M. 2012. The ubiquitin code. *Annu Rev Biochem,* 81**,** 203-29.

KOMEILI, A. & O'SHEA, E. K. 1999. Roles of phosphorylation sites in regulating activity of the transcription factor Pho4. *Science,* 284**,** 977-80.

KONG, S. E. & SVEJSTRUP, J. Q. 2002. Incision of a 1,3-intrastrand d(GpTpG)-cisplatin adduct by nucleotide excision repair proteins from yeast. *DNA Repair (Amst),* 1**,** 731-41.

KOSUGI, S., HASEBE, M., TOMITA, M. & YANAGAWA, H. 2008. Nuclear export signal consensus sequences defined using a localization-based yeast selection system. *Traffic,* 9**,** 2053-62.

KOTH, C. M., BOTUYAN, M. V., MORELAND, R. J., JANSMA, D. B., CONAWAY, J. W., CONAWAY, R. C., CHAZIN, W. J., FRIESEN, J. D., ARROWSMITH, C. H. & EDWARDS, A. M. 2000. Elongin from Saccharomyces cerevisiae. *J Biol Chem,* 275**,** 11174-80.

KRAUT, D. A., ISRAELI, E., SCHRADER, E. K., PATIL, A., NAKAI, K., NANAVATI, D., INOBE, T. & MATOUSCHEK, A. 2012. Sequence- and species-dependence of proteasomal processivity. *ACS Chem Biol,* 7**,** 1444-53.

KRAUT, D. A. & MATOUSCHEK, A. 2011. Proteasomal degradation from internal sites favors partial proteolysis via remote domain stabilization. *ACS Chem Biol,* 6**,** 1087-95.

KRAVTSOVA-IVANTSIV, Y., COHEN, S. & CIECHANOVER, A. 2009. Modification by single ubiquitin moieties rather than polyubiquitination is sufficient for proteasomal processing of the p105 NF-kappaB precursor. *Mol Cell,* 33**,** 496-504.

KROGAN, N. J., DOVER, J., WOOD, A., SCHNEIDER, J., HEIDT, J., BOATENG, M. A., DEAN, K., RYAN, O. W., GOLSHANI, A., JOHNSTON, M., GREENBLATT, J. F. & SHILATIFARD, A. 2003. The Paf1 complex is required for histone H3 methylation by COMPASS and Dot1p: linking transcriptional elongation to histone methylation. *Mol Cell,* 11**,** 721-9.

KRSMANOVIC, T. & KOLLING, R. 2004. The HECT E3 ubiquitin ligase Rsp5 is important for ubiquitin homeostasis in yeast. *FEBS Lett,* 577**,** 215-9.

KRUMMEL, B. & CHAMBERLIN, M. J. 1992. Structural analysis of ternary complexes of Escherichia coli RNA polymerase. Deoxyribonuclease I footprinting of defined complexes. *J Mol Biol,* 225**,** 239-50.

KUNZLER, M., TRUEHEART, J., SETTE, C., HURT, E. & THORNER, J. 2001. Mutations in the YRB1 gene encoding yeast ran-binding-protein-1 that impair nucleocytoplasmic transport and suppress yeast mating defects. *Genetics,* 157**,** 1089-105.

KURAOKA, I., ITO, S., WADA, T., HAYASHIDA, M., LEE, L., SAIJO, M., NAKATSU, Y., MATSUMOTO, M., MATSUNAGA, T., HANDA, H., QIN, J., NAKATANI, Y. & TANAKA, K. 2008. Isolation of XAB2 complex involved in pre-mRNA splicing, transcription, and transcription-coupled repair. *J Biol Chem,* 283**,** 940-50.

KUSHNIROV, V. V. 2000. Rapid and reliable protein extraction from yeast. *Yeast,* 16**,** 857-60.

KUZNETSOVA, A. V., MELLER, J., SCHNELL, P. O., NASH, J. A., IGNACAK, M. L., SANCHEZ, Y., CONAWAY, J. W., CONAWAY, R. C. & CZYZYK-KRZESKA, M. F. 2003. von Hippel-Lindau protein binds hyperphosphorylated large subunit of RNA polymerase II through a proline hydroxylation motif and targets it for ubiquitination. *Proc Natl Acad Sci U S A,* 100**,** 2706-11.

KVINT, K., UHLER, J. P., TASCHNER, M. J., SIGURDSSON, S., ERDJUMENT-BROMAGE, H., TEMPST, P. & SVEJSTRUP, J. Q. 2008. Reversal of RNA polymerase II ubiquitylation by the ubiquitin protease Ubp3. *Mol Cell,* 30**,** 498-506.

LAFRANCE-VANASSE, J., ARSENEAULT, G., CAPPADOCIA, L., CHEN, H. T., LEGAULT, P. & OMICHINSKI, J. G. 2012. Structural and functional characterization of interactions involving the Tfb1 subunit of TFIIH and the NER factor Rad2. *Nucleic Acids Res,* 40**,** 5739-50.

LAINE, J. P. & EGLY, J. M. 2006. When transcription and repair meet: a complex system. *Trends Genet,* 22**,** 430-6.

LANDER, G. C., ESTRIN, E., MATYSKIELA, M. E., BASHORE, C., NOGALES, E. & MARTIN, A. 2012. Complete subunit architecture of the proteasome regulatory particle. *Nature,* 482**,** 186-91.

LANGE, A., MILLS, R. E., LANGE, C. J., STEWART, M., DEVINE, S. E. & CORBETT, A. H. 2007. Classical nuclear localization signals: definition, function, and interaction with importin alpha. *J Biol Chem,* 282**,** 5101-5.

LAYFIELD, R., TOOTH, D., LANDON, M., DAWSON, S., MAYER, J. & ALBAN, A. 2001. Purification of poly-ubiquitinated proteins by S5a-affinity chromatography. *Proteomics,* 1**,** 773-7.

LEE, B. J., CANSIZOGLU, A. E., SUEL, K. E., LOUIS, T. H., ZHANG, Z. & CHOOK, Y. M. 2006. Rules for nuclear localization sequence recognition by karyopherin beta 2. *Cell,* 126**,** 543-58.

LEE, C., SCHWARTZ, M. P., PRAKASH, S., IWAKURA, M. & MATOUSCHEK, A. 2001a. ATP-dependent proteases degrade their substrates by processively unraveling them from the degradation signal. *Mol Cell,* 7**,** 627-37.

LEE, D., EZHKOVA, E., LI, B., PATTENDEN, S. G., TANSEY, W. P. & WORKMAN, J. L. 2005. The proteasome regulatory particle alters the SAGA coactivator to enhance its interactions with transcriptional activators. *Cell,* 123**,** 423-36.

LEE, D. H. & GOLDBERG, A. L. 1998a. Proteasome inhibitors cause induction of heat shock proteins and trehalose, which together confer thermotolerance in Saccharomyces cerevisiae. *Mol Cell Biol,* 18**,** 30-8.

LEE, D. H. & GOLDBERG, A. L. 1998b. Proteasome inhibitors: valuable new tools for cell biologists. *Trends Cell Biol,* 8**,** 397-403.

LEE, J. H., HWANG, G. S. & CHOI, B. S. 1999a. Solution structure of a DNA decamer duplex containing the stable 3' T.G base pair of the pyrimidine(6-4)pyrimidone photoproduct [(6-4) adduct]: implications for the highly specific 3' T --> C transition of the (6-4) adduct. *Proc Natl Acad Sci U S A,* 96**,** 6632-6.

LEE, K. B. & SHARP, P. A. 2004. Transcription-dependent polyubiquitination of RNA polymerase II requires lysine 63 of ubiquitin. *Biochemistry,* 43**,** 15223-9.

LEE, K. B., WANG, D., LIPPARD, S. J. & SHARP, P. A. 2002. Transcription-coupled and DNA damage-dependent ubiquitination of RNA polymerase II in vitro. *Proc Natl Acad Sci U S A,* 99**,** 4239-44.

LEE, M. S., HENRY, M. & SILVER, P. A. 1996. A protein that shuttles between the nucleus and the cytoplasm is an important mediator of RNA export. *Genes Dev,* 10**,** 1233-46.

LEE, S., NEUMANN, M., STEARMAN, R., STAUBER, R., PAUSE, A., PAVLAKIS, G. N. & KLAUSNER, R. D. 1999b. Transcription-dependent nuclear-cytoplasmic trafficking is required for the function of the von Hippel-Lindau tumor suppressor protein. *Mol Cell Biol,* 19**,** 1486-97.

LEE, S. J., SEKIMOTO, T., YAMASHITA, E., NAGOSHI, E., NAKAGAWA, A., IMAMOTO, N., YOSHIMURA, M., SAKAI, H., CHONG, K. T., TSUKIHARA, T. & YONEDA, Y. 2003. The structure of importin-beta bound to SREBP-2: nuclear import of a transcription factor. *Science,* 302**,** 1571-5.

LEE, S. K., YU, S. L., PRAKASH, L. & PRAKASH, S. 2001b. Requirement for yeast RAD26, a homolog of the human CSB gene, in elongation by RNA polymerase II. *Mol Cell Biol,* 21**,** 8651-6.

LEE, Y. D., WANG, J., STUBBE, J. & ELLEDGE, S. J. 2008. Dif1 is a DNA-damage-regulated facilitator of nuclear import for ribonucleotide reductase. *Mol Cell,* 32**,** 70-80.

LEIDECKER, O., MATIC, I., MAHATA, B., PION, E. & XIRODIMAS, D. P. 2012. The ubiquitin E1 enzyme Ube1 mediates NEDD8 activation under diverse stress conditions. *Cell Cycle,* 11**,** 1142-50.

LEJEUNE, D., CHEN, X., RUGGIERO, C., BERRYHILL, S., DING, B. & LI, S. 2009. Yeast Elc1 plays an important role in global genomic repair but not in transcription coupled repair. *DNA Repair (Amst),* 8**,** 40-50.

LI, S., DING, B., LEJEUNE, D., RUGGIERO, C., CHEN, X. & SMERDON, M. J. 2007. The roles of Rad16 and Rad26 in repairing repressed and actively transcribed genes in yeast. *DNA Repair (Amst),* 6**,** 1596-606.

LI, S. & SMERDON, M. J. 2002. Rpb4 and Rpb9 mediate subpathways of transcription-coupled DNA repair in Saccharomyces cerevisiae. *EMBO J,* 21**,** 5921-9.

LI, Y. F., KIM, S. T. & SANCAR, A. 1993. Evidence for lack of DNA photoreactivating enzyme in humans. *Proc Natl Acad Sci U S A,* 90**,** 4389-93.

LIN, L. & GHOSH, S. 1996. A glycine-rich region in NF-kappaB p105 functions as a processing signal for the generation of the p50 subunit. *Mol Cell Biol,* 16**,** 2248-54.

LINDAHL, T. & WOOD, R. D. 1999. Quality control by DNA repair. *Science,* 286**,** 1897-905.

LINDSEY-BOLTZ, L. A. & SANCAR, A. 2007. RNA polymerase: the most specific damage recognition protein in cellular responses to DNA damage? *Proc Natl Acad Sci U S A,* 104**,** 13213-4.

LIU, C. W., CORBOY, M. J., DEMARTINO, G. N. & THOMAS, P. J. 2003. Endoproteolytic activity of the proteasome. *Science,* 299**,** 408-11.

LIU, P., KENNEY, J. M., STILLER, J. W. & GREENLEAF, A. L. 2010. Genetic organization, length conservation, and evolution of RNA polymerase II carboxyl-terminal domain. *Mol Biol Evol,* 27**,** 2628-41.

LIU, S., CHEN, Y., LI, J., HUANG, T., TARASOV, S., KING, A., WEISSMAN, A. M., BYRD, R. A. & DAS, R. 2012. Promiscuous interactions of gp78 E3 ligase CUE domain with polyubiquitin chains. *Structure,* 20**,** 2138-50.

LIU, X., BUSHNELL, D. A. & KORNBERG, R. D. 2013. RNA polymerase II transcription: structure and mechanism. *Biochim Biophys Acta,* 1829**,** 2-8.

LOMMEL, L., BUCHELI, M. E. & SWEDER, K. S. 2000. Transcription-coupled repair in yeast is independent from ubiquitylation of RNA pol II: implications for Cockayne's syndrome. *Proc Natl Acad Sci U S A,* 97**,** 9088-92.

LOWE, E. D., HASAN, N., TREMPE, J. F., FONSO, L., NOBLE, M. E., ENDICOTT, J. A., JOHNSON, L. N. & BROWN, N. R. 2006. Structures of the Dsk2 UBL and UBA domains and their complex. *Acta Crystallogr D Biol Crystallogr,* 62**,** 177-88.

LUNA-VARGAS, M. P., FAESEN, A. C., VAN DIJK, W. J., RAPE, M., FISH, A. & SIXMA, T. K. 2011. Ubiquitin-specific protease 4 is inhibited by its ubiquitin-like domain. *EMBO Rep,* 12**,** 365-72.

LUO, Z., ZHENG, J., LU, Y. & BREGMAN, D. B. 2001. Ultraviolet radiation alters the phosphorylation of RNA polymerase II large subunit and accelerates its proteasome-dependent degradation. *Mutat Res,* 486**,** 259-74.

MACEDO-RIBEIRO, S., CORTES, L., MACIEL, P. & CARVALHO, A. L. 2009. Nucleocytoplasmic shuttling activity of ataxin-3. *PLoS One,* 4**,** e5834.

MAHROUR, N., REDWINE, W. B., FLORENS, L., SWANSON, S. K., MARTIN-BROWN, S., BRADFORD, W. D., STAEHLING-HAMPTON, K., WASHBURN, M. P., CONAWAY, R. C. & CONAWAY, J. W. 2008. Characterization of Cullin-box sequences that direct recruitment of Cul2-Rbx1 and Cul5-Rbx2 modules to Elongin BC-based ubiquitin ligases. *J Biol Chem,* 283**,** 8005-13.

MAIURI, P., KNEZEVICH, A., DE MARCO, A., MAZZA, D., KULA, A., MCNALLY, J. G. & MARCELLO, A. 2011. Fast transcription rates of RNA polymerase II in human cells. *EMBO Rep,* 12**,** 1280-5.

MAKHNEVYCH, T., LUSK, C. P., ANDERSON, A. M., AITCHISON, J. D. & WOZNIAK, R. W. 2003. Cell cycle regulated transport controlled by alterations in the nuclear pore complex. *Cell,* 115**,** 813-23.

MALASHKEVICH, V. N., KAMMERER, R. A., EFIMOV, V. P., SCHULTHESS, T. & ENGEL, J. 1996. The crystal structure of a five-stranded coiled coil in COMP: a prototype ion channel? *Science,* 274**,** 761-5.

MALIK, S., BAGLA, S., CHAURASIA, P., DUAN, Z. & BHAUMIK, S. R. 2008. Elongating RNA polymerase II is disassembled through specific degradation of its largest but not other subunits in response to DNA damage in vivo. *J Biol Chem,* 283**,** 6897-905.

MALIK, S. & BHAUMIK, S. R. 2012. Rad26p, a transcription-coupled repair factor, promotes the eviction and prevents the reassociation of histone H2A-H2B dimer during transcriptional elongation in vivo. *Biochemistry,* 51**,** 5873-5.

MALIK, S., CHAURASIA, P., LAHUDKAR, S., DURAIRAJ, G., SHUKLA, A. & BHAUMIK, S. R. 2010. Rad26p, a transcription-coupled repair factor, is recruited to the site of DNA lesion in an elongating RNA polymerase II-dependent manner in vivo. *Nucleic Acids Res,* 38**,** 1461-77.

MALIK, S., CHAURASIA, P., LAHUDKAR, S., UPRETY, B. & BHAUMIK, S. R. 2012. Rad26p regulates the occupancy of histone H2A-H2B dimer at the active genes in vivo. *Nucleic Acids Res,* 40**,** 3348-63.

MANOGARAN, A. L., HONG, J. Y., HUFANA, J., TYEDMERS, J., LINDQUIST, S. & LIEBMAN, S. W. 2011. Prion formation and polyglutamine aggregation are controlled by two classes of genes. *PLoS Genet,* 7**,** e1001386.

MANZO, S. G., ZHOU, Z. L., WANG, Y. Q., MARINELLO, J., HE, J. X., LI, Y. C., DING, J., CAPRANICO, G. & MIAO, Z. H. 2012. Natural product triptolide mediates cancer cell death by triggering CDK7-dependent degradation of RNA polymerase II. *Cancer Res,* 72**,** 5363-73.

MASPERO, E., VALENTINI, E., MARI, S., CECATIELLO, V., SOFFIENTINI, P., PASQUALATO, S. & POLO, S. 2013. Structure of a ubiquitin-loaded HECT ligase reveals the molecular basis for catalytic priming. *Nat Struct Mol Biol,* 20**,** 696-701.

MATSUURA, Y. & STEWART, M. 2004. Structural basis for the assembly of a nuclear export complex. *Nature,* 432**,** 872-7.

MATYSKIELA, M. E., LANDER, G. C. & MARTIN, A. 2013. Conformational switching of the 26S proteasome enables substrate degradation. *Nat Struct Mol Biol,* 20**,** 781-8.

MAURER, P., REDD, M., SOLSBACHER, J., BISCHOFF, F. R., GREINER, M., PODTELEJNIKOV, A. V., MANN, M., STADE, K., WEIS, K. & SCHLENSTEDT, G. 2001. The nuclear export receptor Xpo1p forms distinct complexes with NES transport substrates and the yeast Ran binding protein 1 (Yrb1p). *Mol Biol Cell,* 12**,** 539-49.

MAY, M. J., LARSEN, S. E., SHIM, J. H., MADGE, L. A. & GHOSH, S. 2004. A novel ubiquitin-like domain in IkappaB kinase beta is required for functional activity of the kinase. *J Biol Chem,* 279**,** 45528-39.

MAYER, A., HEIDEMANN, M., LIDSCHREIBER, M., SCHREIECK, A., SUN, M., HINTERMAIR, C., KREMMER, E., EICK, D. & CRAMER, P. 2012. CTD tyrosine

phosphorylation impairs termination factor recruitment to RNA polymerase II. *Science,* 336**,** 1723-5.

MAYER, A., LIDSCHREIBER, M., SIEBERT, M., LEIKE, K., SODING, J. & CRAMER, P. 2010. Uniform transitions of the general RNA polymerase II transcription complex. *Nat Struct Mol Biol,* 17**,** 1272-8.

MAYNE, L. V. & LEHMANN, A. R. 1982. Failure of RNA synthesis to recover after UV irradiation: an early defect in cells from individuals with Cockayne's syndrome and xeroderma pigmentosum. *Cancer Res,* 42**,** 1473-8.

MEIMOUN, A., HOLTZMAN, T., WEISSMAN, Z., MCBRIDE, H. J., STILLMAN, D. J., FINK, G. R. & KORNITZER, D. 2000. Degradation of the transcription factor Gcn4 requires the kinase Pho85 and the SCF(CDC4) ubiquitin-ligase complex. *Mol Biol Cell,* 11**,** 915-27.

MEINHART, A. & CRAMER, P. 2004. Recognition of RNA polymerase II carboxy-terminal domain by 3'-RNA-processing factors. *Nature,* 430**,** 223-6.

MEJIA, Y. X., MAO, H., FORDE, N. R. & BUSTAMANTE, C. 2008. Thermal probing of E. coli RNA polymerase off-pathway mechanisms. *J Mol Biol,* 382**,** 628-37.

MEVISSEN, T. E., HOSPENTHAL, M. K., GEURINK, P. P., ELLIOTT, P. R., AKUTSU, M., ARNAUDO, N., EKKEBUS, R., KULATHU, Y., WAUER, T., EL OUALID, F., FREUND, S. M., OVAA, H. & KOMANDER, D. 2013. OTU Deubiquitinases Reveal Mechanisms of Linkage Specificity and Enable Ubiquitin Chain Restriction Analysis. *Cell,* 154**,** 169-84.

MIKHAYLOVA, O., IGNACAK, M. L., BARANKIEWICZ, T. J., HARBAUGH, S. V., YI, Y., MAXWELL, P. H., SCHNEIDER, M., VAN GEYTE, K., CARMELIET, P., REVELO, M. P., WYDER, M., GREIS, K. D., MELLER, J. & CZYZYK-KRZESKA, M. F. 2008. The von Hippel-Lindau tumor suppressor protein and Egl-9-Type proline hydroxylases regulate the large subunit of RNA polymerase II in response to oxidative stress. *Mol Cell Biol,* 28**,** 2701-17.

MIN, J. H. & PAVLETICH, N. P. 2007. Recognition of DNA damage by the Rad4 nucleotide excision repair protein. *Nature,* 449**,** 570-5.

MITSUI, A. & SHARP, P. A. 1999. Ubiquitination of RNA polymerase II large subunit signaled by phosphorylation of carboxyl-terminal domain. *Proc Natl Acad Sci U S A,* 96**,** 6054-9.

MOCQUET, V., LAINE, J. P., RIEDL, T., YAJIN, Z., LEE, M. Y. & EGLY, J. M. 2008. Sequential recruitment of the repair factors during NER: the role of XPG in initiating the resynthesis step. *EMBO J,* 27**,** 155-67.

MOORTHY, A. K., SAVINOVA, O. V., HO, J. Q., WANG, V. Y., VU, D. & GHOSH, G. 2006. The 20S proteasome processes NF-kappaB1 p105 into p50 in a translation-independent manner. *EMBO J,* 25**,** 1945-56.

MORELAND, R. J., HANAS, J. S., CONAWAY, J. W. & CONAWAY, R. C. 1998. Mechanism of action of RNA polymerase II elongation factor Elongin. Maximal stimulation of elongation requires conversion of the early elongation complex to an Elongin-activable form. *J Biol Chem,* 273**,** 26610-7.

NA, X., DUAN, H. O., MESSING, E. M., SCHOEN, S. R., RYAN, C. K., DI SANT'AGNESE, P. A., GOLEMIS, E. A. & WU, G. 2003. Identification of the RNA polymerase II subunit hsRPB7 as a novel target of the von Hippel-Lindau protein. *EMBO J,* 22**,** 4249-59.

NACHURY, M. V. & WEIS, K. 1999. The direction of transport through the nuclear pore can be inverted. *Proc Natl Acad Sci U S A,* 96**,** 9622-7.

NAGATA, S. 2000. Apoptotic DNA fragmentation. *Exp Cell Res,* 256**,** 12-8.

NAKATOGAWA, H., SUZUKI, K., KAMADA, Y. & OHSUMI, Y. 2009. Dynamics and diversity in autophagy mechanisms: lessons from yeast. *Nat Rev Mol Cell Biol,* 10**,** 458-67.

NAKAZAWA, Y., SASAKI, K., MITSUTAKE, N., MATSUSE, M., SHIMADA, M., NARDO, T., TAKAHASHI, Y., OHYAMA, K., ITO, K., MISHIMA, H., NOMURA, M., KINOSHITA, A., ONO, S., TAKENAKA, K., MASUYAMA, R., KUDO, T., SLOR, H., UTANI, A., TATEISHI, S., YAMASHITA, S., STEFANINI, M., LEHMANN, A. R., YOSHIURA, K. & OGI, T. 2012. Mutations in UVSSA cause UV-sensitive syndrome and impair RNA polymerase IIo processing in transcription-coupled nucleotide-excision repair. *Nat Genet,* 44**,** 586-92.

NAVON, A. & GOLDBERG, A. L. 2001. Proteins are unfolded on the surface of the ATPase ring before transport into the proteasome. *Mol Cell,* 8**,** 1339-49.

NECHAEV, S., FARGO, D. C., DOS SANTOS, G., LIU, L., GAO, Y. & ADELMAN, K. 2010. Global analysis of short RNAs reveals widespread promoter-proximal stalling and arrest of Pol II in Drosophila. *Science,* 327**,** 335-8.

NEVILLE, M. & ROSBASH, M. 1999. The NES-Crm1p export pathway is not a major mRNA export route in Saccharomyces cerevisiae. *EMBO J,* 18**,** 3746-56.

NEWTON, K., MATSUMOTO, M. L., WERTZ, I. E., KIRKPATRICK, D. S., LILL, J. R., TAN, J., DUGGER, D., GORDON, N., SIDHU, S. S., FELLOUSE, F. A., KOMUVES, L., FRENCH, D. M., FERRANDO, R. E., LAM, C., COMPAAN, D., YU, C., BOSANAC, I., HYMOWITZ, S. G., KELLEY, R. F. & DIXIT, V. M. 2008. Ubiquitin chain editing revealed by polyubiquitin linkage-specific antibodies. *Cell,* 134**,** 668-78.

NG, J. M., VERMEULEN, W., VAN DER HORST, G. T., BERGINK, S., SUGASAWA, K., VRIELING, H. & HOEIJMAKERS, J. H. 2003. A novel regulation mechanism of DNA repair by damage-induced and RAD23-dependent stabilization of xeroderma pigmentosum group C protein. *Genes Dev,* 17**,** 1630-45.

NIELSEN, M. L., VERMEULEN, M., BONALDI, T., COX, J., MORODER, L. & MANN, M. 2008. Iodoacetamide-induced artifact mimics ubiquitination in mass spectrometry. *Nat Methods,* 5**,** 459-60.

NUDLER, E. 2012. RNA polymerase backtracking in gene regulation and genome instability. *Cell,* 149**,** 1438-45.

NUDLER, E., MUSTAEV, A., LUKHTANOV, E. & GOLDFARB, A. 1997. The RNA-DNA hybrid maintains the register of transcription by preventing backtracking of RNA polymerase. *Cell,* 89**,** 33-41.

O'HAGAN, H. M. & LJUNGMAN, M. 2004. Efficient NES-dependent protein nuclear export requires ongoing synthesis and export of mRNAs. *Exp Cell Res,* 297**,** 548-59.

OHNO, A., JEE, J., FUJIWARA, K., TENNO, T., GODA, N., TOCHIO, H., KOBAYASHI, H., HIROAKI, H. & SHIRAKAWA, M. 2005. Structure of the UBA domain of Dsk2p in complex with ubiquitin molecular determinants for ubiquitin recognition. *Structure,* 13**,** 521-32.

OLSEN, S. K. & LIMA, C. D. 2013. Structure of a ubiquitin E1-E2 complex: insights to E1-E2 thioester transfer. *Mol Cell,* 49**,** 884-96.

ORIAN, A., SCHWARTZ, A. L., ISRAEL, A., WHITESIDE, S., KAHANA, C. & CIECHANOVER, A. 1999. Structural motifs involved in ubiquitin-mediated processing of the NF-kappaB precursor p105: roles of the glycine-rich region and a downstream ubiquitination domain. *Mol Cell Biol,* 19**,** 3664-73.

ORIAN, A., WHITESIDE, S., ISRAEL, A., STANCOVSKI, I., SCHWARTZ, A. L. & CIECHANOVER, A. 1995. Ubiquitin-mediated processing of NF-kappa B

transcriptional activator precursor p105. Reconstitution of a cell-free system and identification of the ubiquitin-carrier protein, E2, and a novel ubiquitin-protein ligase, E3, involved in conjugation. *J Biol Chem,* 270**,** 21707-14.

ORPHANIDES, G., LEROY, G., CHANG, C. H., LUSE, D. S. & REINBERG, D. 1998. FACT, a factor that facilitates transcript elongation through nucleosomes. *Cell,* 92**,** 105-16.

OSTAPENKO, D. & SOLOMON, M. J. 2003. Budding yeast CTDK-I is required for DNA damage-induced transcription. *Eukaryot Cell,* 2**,** 274-83.

OTERO, G., FELLOWS, J., LI, Y., DE BIZEMONT, T., DIRAC, A. M., GUSTAFSSON, C. M., ERDJUMENT-BROMAGE, H., TEMPST, P. & SVEJSTRUP, J. Q. 1999. Elongator, a multisubunit component of a novel RNA polymerase II holoenzyme for transcriptional elongation. *Mol Cell,* 3**,** 109-18.

OZKAN, E., YU, H. & DEISENHOFER, J. 2005. Mechanistic insight into the allosteric activation of a ubiquitin-conjugating enzyme by RING-type ubiquitin ligases. *Proc Natl Acad Sci U S A,* 102**,** 18890-5.

PACOLD, M. E., SUIRE, S., PERISIC, O., LARA-GONZALEZ, S., DAVIS, C. T., WALKER, E. H., HAWKINS, P. T., STEPHENS, L., ECCLESTON, J. F. & WILLIAMS, R. L. 2000. Crystal structure and functional analysis of Ras binding to its effector phosphoinositide 3-kinase gamma. *Cell,* 103**,** 931-43.

PALOMBELLA, V. J., RANDO, O. J., GOLDBERG, A. L. & MANIATIS, T. 1994. The ubiquitin-proteasome pathway is required for processing the NF-kappa B1 precursor protein and the activation of NF-kappa B. *Cell,* 78**,** 773-85.

PAN, X., YE, P., YUAN, D. S., WANG, X., BADER, J. S. & BOEKE, J. D. 2006a. A DNA integrity network in the yeast Saccharomyces cerevisiae. *Cell,* 124**,** 1069-81.

PAN, Y., BAI, C. B., JOYNER, A. L. & WANG, B. 2006b. Sonic hedgehog signaling regulates Gli2 transcriptional activity by suppressing its processing and degradation. *Mol Cell Biol,* 26**,** 3365-77.

PANIER, S., ICHIJIMA, Y., FRADET-TURCOTTE, A., LEUNG, C. C., KAUSTOV, L., ARROWSMITH, C. H. & DUROCHER, D. 2012. Tandem protein interaction modules organize the ubiquitin-dependent response to DNA double-strand breaks. *Mol Cell,* 47**,** 383-95.

PARK, S. H., KUKUSHKIN, Y., GUPTA, R., CHEN, T., KONAGAI, A., HIPP, M. S., HAYER-HARTL, M. & HARTL, F. U. 2013. PolyQ Proteins Interfere with Nuclear Degradation of Cytosolic Proteins by Sequestering the Sis1p Chaperone. *Cell,* 154**,** 134-45.

PARKER, J. L., BIELEN, A. B., DIKIC, I. & ULRICH, H. D. 2007. Contributions of ubiquitin- and PCNA-binding domains to the activity of Polymerase eta in Saccharomyces cerevisiae. *Nucleic Acids Res,* 35**,** 881-9.

PARKER, J. L. & ULRICH, H. D. 2009. Mechanistic analysis of PCNA poly-ubiquitylation by the ubiquitin protein ligases Rad18 and Rad5. *EMBO J,* 28**,** 3657-66.

PARKS, T. D., HOWARD, E. D., WOLPERT, T. J., ARP, D. J. & DOUGHERTY, W. G. 1995. Expression and purification of a recombinant tobacco etch virus NIa proteinase: biochemical analyses of the full-length and a naturally occurring truncated proteinase form. *Virology,* 210**,** 194-201.

PASHKOVA, N., GAKHAR, L., WINISTORFER, S. C., YU, L., RAMASWAMY, S. & PIPER, R. C. 2010. WD40 repeat propellers define a ubiquitin-binding domain that regulates turnover of F box proteins. *Mol Cell,* 40**,** 433-43.

PATTON, E. E., WILLEMS, A. R., SA, D., KURAS, L., THOMAS, D., CRAIG, K. L. & TYERS, M. 1998. Cdc53 is a scaffold protein for multiple Cdc34/Skp1/F-box proteincomplexes that regulate cell division and methionine biosynthesis in yeast. *Genes Dev,* 12**,** 692-705.

PAULUS, H. 2000. Protein splicing and related forms of protein autoprocessing. *Annu Rev Biochem,* 69**,** 447-96.

PENG, J., SCHWARTZ, D., ELIAS, J. E., THOREEN, C. C., CHENG, D., MARSISCHKY, G., ROELOFS, J., FINLEY, D. & GYGI, S. P. 2003. A proteomics approach to understanding protein ubiquitination. *Nat Biotechnol,* 21**,** 921-6.

PETH, A., BESCHE, H. C. & GOLDBERG, A. L. 2009. Ubiquitinated proteins activate the proteasome by binding to Usp14/Ubp6, which causes 20S gate opening. *Mol Cell,* 36**,** 794-804.

PETROSKI, M. D. & DESHAIES, R. J. 2005. Mechanism of lysine 48-linked ubiquitin-chain synthesis by the cullin-RING ubiquitin-ligase complex SCF-Cdc34. *Cell,* 123**,** 1107-20.

PFANDER, B., MOLDOVAN, G. L., SACHER, M., HOEGE, C. & JENTSCH, S. 2005. SUMO-modified PCNA recruits Srs2 to prevent recombination during S phase. *Nature,* 436**,** 428-33.

PICKART, C. M. & ROSE, I. A. 1985. Functional heterogeneity of ubiquitin carrier proteins. *J Biol Chem,* 260**,** 1573-81.

PIERCE, N. W., KLEIGER, G., SHAN, S. O. & DESHAIES, R. J. 2009. Detection of sequential polyubiquitylation on a millisecond timescale. *Nature,* 462**,** 615-9.

PIERCE, N. W., LEE, J. E., LIU, X., SWEREDOSKI, M. J., GRAHAM, R. L., LARIMORE, E. A., ROME, M., ZHENG, N., CLURMAN, B. E., HESS, S., SHAN, S. O. & DESHAIES, R. J. 2013. Cand1 promotes assembly of new SCF complexes through dynamic exchange of F box proteins. *Cell,* 153**,** 206-15.

PIWKO, W. & JENTSCH, S. 2006. Proteasome-mediated protein processing by bidirectional degradation initiated from an internal site. *Nat Struct Mol Biol,* 13**,** 691-7.

POLO, S., SIGISMUND, S., FARETTA, M., GUIDI, M., CAPUA, M. R., BOSSI, G., CHEN, H., DE CAMILLI, P. & DI FIORE, P. P. 2002. A single motif responsible for ubiquitin recognition and monoubiquitination in endocytic proteins. *Nature,* 416**,** 451-5.

PONTING, C. P. 2002. Novel domains and orthologues of eukaryotic transcription elongation factors. *Nucleic Acids Res,* 30**,** 3643-52.

PRAG, G., MISRA, S., JONES, E. A., GHIRLANDO, R., DAVIES, B. A., HORAZDOVSKY, B. F. & HURLEY, J. H. 2003. Mechanism of ubiquitin recognition by the CUE domain of Vps9p. *Cell,* 113**,** 609-20.

PRAKASH, S. & PRAKASH, L. 2000. Nucleotide excision repair in yeast. *Mutat Res,* 451**,** 13-24.

PRAKASH, S., TIAN, L., RATLIFF, K. S., LEHOTZKY, R. E. & MATOUSCHEK, A. 2004. An unstructured initiation site is required for efficient proteasome-mediated degradation. *Nat Struct Mol Biol,* 11**,** 830-7.

PRICE, M. A. & KALDERON, D. 2002. Proteolysis of the Hedgehog signaling effector Cubitus interruptus requires phosphorylation by Glycogen Synthase Kinase 3 and Casein Kinase 1. *Cell,* 108**,** 823-35.

RAASI, S., ORLOV, I., FLEMING, K. G. & PICKART, C. M. 2004. Binding of polyubiquitin chains to ubiquitin-associated (UBA) domains of HHR23A. *J Mol Biol,* 341**,** 1367-79.

RAASI, S. & PICKART, C. M. 2003. Rad23 ubiquitin-associated domains (UBA) inhibit 26 S proteasome-catalyzed proteolysis by sequestering lysine 48-linked polyubiquitin chains. *J Biol Chem,* 278**,** 8951-9.

RAASI, S., VARADAN, R., FUSHMAN, D. & PICKART, C. M. 2005. Diverse polyubiquitin interaction properties of ubiquitin-associated domains. *Nat Struct Mol Biol,* 12**,** 708-14.

RAHIGHI, S., IKEDA, F., KAWASAKI, M., AKUTSU, M., SUZUKI, N., KATO, R., KENSCHE, T., UEJIMA, T., BLOOR, S., KOMANDER, D., RANDOW, F., WAKATSUKI, S. & DIKIC, I. 2009. Specific recognition of linear ubiquitin chains by NEMO is important for NF-kappaB activation. *Cell,* 136**,** 1098-109.

RAMSEY, K. L., SMITH, J. J., DASGUPTA, A., MAQANI, N., GRANT, P. & AUBLE, D. T. 2004. The NEF4 complex regulates Rad4 levels and utilizes Snf2/Swi2-related ATPase activity for nucleotide excision repair. *Mol Cell Biol,* 24**,** 6362-78.

RAPE, M., HOPPE, T., GORR, I., KALOCAY, M., RICHLY, H. & JENTSCH, S. 2001. Mobilization of processed, membrane-tethered SPT23 transcription factor by CDC48(UFD1/NPL4), a ubiquitin-selective chaperone. *Cell,* 107**,** 667-77.

RATNER, J. N., BALASUBRAMANIAN, B., CORDEN, J., WARREN, S. L. & BREGMAN, D. B. 1998. Ultraviolet radiation-induced ubiquitination and proteasomal degradation of the large subunit of RNA polymerase II. Implications for transcription-coupled DNA repair. *J Biol Chem,* 273**,** 5184-9.

REED, S. H. & GILLETTE, T. G. 2007. Nucleotide excision repair and the ubiquitin proteasome pathway--do all roads lead to Rome? *DNA Repair (Amst),* 6**,** 149-56.

REID, J. & SVEJSTRUP, J. Q. 2004. DNA damage-induced Def1-RNA polymerase II interaction and Def1 requirement for polymerase ubiquitylation in vitro. *J Biol Chem,* 279**,** 29875-8.

REID, J. & SVEJSTRUP, J. Q. 2006. An assay for studying ubiquitylation of RNA polymerase II and other proteins in crude yeast extracts. *Methods Enzymol,* 408**,** 264-73.

REINES, D., GHANOUNI, P., LI, Q. Q. & MOTE, J., JR. 1992. The RNA polymerase II elongation complex. Factor-dependent transcription elongation involves nascent RNA cleavage. *J Biol Chem,* 267**,** 15516-22.

RIBAR, B., PRAKASH, L. & PRAKASH, S. 2006. Requirement of ELC1 for RNA polymerase II polyubiquitylation and degradation in response to DNA damage in Saccharomyces cerevisiae. *Mol Cell Biol,* 26**,** 3999-4005.

RIBAR, B., PRAKASH, L. & PRAKASH, S. 2007. ELA1 and CUL3 are required along with ELC1 for RNA polymerase II polyubiquitylation and degradation in DNA-damaged yeast cells. *Mol Cell Biol,* 27**,** 3211-6.

ROBBINS, J., DILWORTH, S. M., LASKEY, R. A. & DINGWALL, C. 1991. Two interdependent basic domains in nucleoplasmin nuclear targeting sequence: identification of a class of bipartite nuclear targeting sequence. *Cell,* 64**,** 615-23.

ROCKX, D. A., MASON, R., VAN HOFFEN, A., BARTON, M. C., CITTERIO, E., BREGMAN, D. B., VAN ZEELAND, A. A., VRIELING, H. & MULLENDERS, L. H. 2000. UV-induced inhibition of transcription involves repression of transcription initiation and phosphorylation of RNA polymerase II. *Proc Natl Acad Sci U S A,* 97**,** 10503-8.

RODRIGO-BRENNI, M. C. & MORGAN, D. O. 2007. Sequential E2s drive polyubiquitin chain assembly on APC targets. *Cell,* 130**,** 127-39.

ROOS, M. D., SU, K., BAKER, J. R. & KUDLOW, J. E. 1997. O glycosylation of an Sp1-derived peptide blocks known Sp1 protein interactions. *Mol Cell Biol,* 17**,** 6472-80.

ROSENZWEIG, R., BRONNER, V., ZHANG, D., FUSHMAN, D. & GLICKMAN, M. H. 2012. Rpn1 and Rpn2 coordinate ubiquitin processing factors at proteasome. *J Biol Chem,* 287**,** 14659-71.

ROUT, M. P., BLOBEL, G. & AITCHISON, J. D. 1997. A distinct nuclear import pathway used by ribosomal proteins. *Cell,* 89**,** 715-25.

RYABOV, Y. & FUSHMAN, D. 2006. Interdomain mobility in di-ubiquitin revealed by NMR. *Proteins,* 63**,** 787-96.

SAEKI, H. & SVEJSTRUP, J. Q. 2009. Stability, flexibility, and dynamic interactions of colliding RNA polymerase II elongation complexes. *Mol Cell,* 35**,** 191-205.

SAEKI, Y., SAITOH, A., TOH-E, A. & YOKOSAWA, H. 2002a. Ubiquitin-like proteins and Rpn10 play cooperative roles in ubiquitin-dependent proteolysis. *Biochem Biophys Res Commun,* 293**,** 986-92.

SAHA, A. & DESHAIES, R. J. 2008. Multimodal activation of the ubiquitin ligase SCF by Nedd8 conjugation. *Mol Cell,* 32**,** 21-31.

SALGHETTI, S. E., CAUDY, A. A., CHENOWETH, J. G. & TANSEY, W. P. 2001. Regulation of transcriptional activation domain function by ubiquitin. *Science,* 293**,** 1651-3.

SALGHETTI, S. E., MURATANI, M., WIJNEN, H., FUTCHER, B. & TANSEY, W. P. 2000. Functional overlap of sequences that activate transcription and signal ubiquitin-mediated proteolysis. *Proc Natl Acad Sci U S A,* 97**,** 3118-23.

SANCAR, A. & RUPERT, C. S. 1978. Cloning of the phr gene and amplification of photolyase in Escherichia coli. *Gene,* 4**,** 295-308.

SANCAR, G. B. 2000. Enzymatic photoreactivation: 50 years and counting. *Mutat Res,* 451**,** 25-37.

SASAKI, T., FUNAKOSHI, M., ENDICOTT, J. A. & KOBAYASHI, H. 2005. Budding yeast Dsk2 protein forms a homodimer via its C-terminal UBA domain. *Biochem Biophys Res Commun,* 336**,** 530-5.

SCHAEFER, J. B. & MORGAN, D. O. 2011. Protein-linked ubiquitin chain structure restricts activity of deubiquitinating enzymes. *J Biol Chem,* 286**,** 45186-96.

SCHARF, A., GROZDANOV, P. N., VEITH, R., KUBITSCHECK, U., MEIER, U. T. & VON MIKECZ, A. 2011. Distant positioning of proteasomal proteolysis relative to actively transcribed genes. *Nucleic Acids Res,* 39**,** 4612-27.

SCHAUBER, C., CHEN, L., TONGAONKAR, P., VEGA, I., LAMBERTSON, D., POTTS, W. & MADURA, K. 1998. Rad23 links DNA repair to the ubiquitin/proteasome pathway. *Nature,* 391**,** 715-8.

SCHLACHER, K. & GOODMAN, M. F. 2007. Lessons from 50 years of SOS DNA-damage-induced mutagenesis. *Nat Rev Mol Cell Biol,* 8**,** 587-94.

SCHMIDT, M., HAAS, W., CROSAS, B., SANTAMARIA, P. G., GYGI, S. P., WALZ, T. & FINLEY, D. 2005. The HEAT repeat protein Blm10 regulates the yeast proteasome by capping the core particle. *Nat Struct Mol Biol,* 12**,** 294-303.

SCHNEIDER, B. L., SEUFERT, W., STEINER, B., YANG, Q. H. & FUTCHER, A. B. 1995. Use of polymerase chain reaction epitope tagging for protein tagging in Saccharomyces cerevisiae. *Yeast,* 11**,** 1265-74.

SCHOLS, L., BAUER, P., SCHMIDT, T., SCHULTE, T. & RIESS, O. 2004. Autosomal dominant cerebellar ataxias: clinical features, genetics, and pathogenesis. *Lancet Neurol,* 3**,** 291-304.

SCHRADER, E. K., HARSTAD, K. G. & MATOUSCHEK, A. 2009. Targeting proteins for degradation. *Nat Chem Biol,* 5**,** 815-22.

SCHWERTMAN, P., LAGAROU, A., DEKKERS, D. H., RAAMS, A., VAN DER HOEK, A. C., LAFFEBER, C., HOEIJMAKERS, J. H., DEMMERS, J. A., FOUSTERI, M., VERMEULEN, W. & MARTEIJN, J. A. 2012. UV-sensitive syndrome protein UVSSA recruits USP7 to regulate transcription-coupled repair. *Nat Genet,* 44**,** 598-602.

SCICCHITANO, D. A. 2005. Transcription past DNA adducts derived from polycyclic aromatic hydrocarbons. *Mutat Res,* 577**,** 146-54.

SEARS, C., OLESEN, J., RUBIN, D., FINLEY, D. & MANIATIS, T. 1998. NF-kappa B p105 processing via the ubiquitin-proteasome pathway. *J Biol Chem,* 273**,** 1409-19.

SEGURADO, M. & DIFFLEY, J. F. 2008. Separate roles for the DNA damage checkpoint protein kinases in stabilizing DNA replication forks. *Genes Dev,* 22**,** 1816-27.

SELBY, C. P., DRAPKIN, R., REINBERG, D. & SANCAR, A. 1997. RNA polymerase II stalled at a thymine dimer: footprint and effect on excision repair. *Nucleic Acids Res,* 25**,** 787-93.

SELBY, C. P. & SANCAR, A. 1993. Molecular mechanism of transcription-repair coupling. *Science,* 260**,** 53-8.

SELTH, L. A., SIGURDSSON, S. & SVEJSTRUP, J. Q. 2010. Transcript Elongation by RNA Polymerase II. *Annu Rev Biochem,* 79**,** 271-93.

SHABEK, N., HERMAN-BACHINSKY, Y., BUCHSBAUM, S., LEWINSON, O., HAJ-YAHYA, M., HEJJAOUI, M., LASHUEL, H. A., SOMMER, T., BRIK, A. & CIECHANOVER, A. 2012. The size of the proteasomal substrate determines whether its degradation will be mediated by mono- or polyubiquitylation. *Mol Cell,* 48**,** 87-97.

SHCHERBIK, N., ZOLADEK, T., NICKELS, J. T. & HAINES, D. S. 2003. Rsp5p is required for ER bound Mga2p120 polyubiquitination and release of the processed/tethered transactivator Mga2p90. *Curr Biol,* 13**,** 1227-33.

SHERMAN, F. 1991. Getting started with yeast. *Methods Enzymol,* 194**,** 3-21.

SHIH, S. C., PRAG, G., FRANCIS, S. A., SUTANTO, M. A., HURLEY, J. H. & HICKE, L. 2003. A ubiquitin-binding motif required for intramolecular monoubiquitylation, the CUE domain. *EMBO J,* 22**,** 1273-81.

SIEPE, D. & JENTSCH, S. 2009. Prolyl isomerase Pin1 acts as a switch to control the degree of substrate ubiquitylation. *Nat Cell Biol,* 11**,** 967-72.

SIERGIEJUK, E., SCOTT, D. C., SCHULMAN, B. A., HOFMANN, K., KURZ, T. & PETER, M. 2009. Cullin neddylation and substrate-adaptors counteract SCF inhibition by the CAND1-like protein Lag2 in Saccharomyces cerevisiae. *EMBO J,* 28**,** 3845-56.

SIGURDSSON, S., DIRAC-SVEJSTRUP, A. B. & SVEJSTRUP, J. Q. 2010. Evidence that transcript cleavage is essential for RNA polymerase II transcription and cell viability. *Mol Cell,* 38**,** 202-10.

SIKORSKI, R. S. & HIETER, P. 1989. A system of shuttle vectors and yeast host strains designed for efficient manipulation of DNA in Saccharomyces cerevisiae. *Genetics,* 122**,** 19-27.

SIMS, J. J. & COHEN, R. E. 2009. Linkage-specific avidity defines the lysine 63-linked polyubiquitin-binding preference of rap80. *Mol Cell,* 33**,** 775-83.

SINGH, J. & PADGETT, R. A. 2009. Rates of in situ transcription and splicing in large human genes. *Nat Struct Mol Biol,* 16**,** 1128-33.

SINGH, R. K., ZERATH, S., KLEIFELD, O., SCHEFFNER, M., GLICKMAN, M. H. & FUSHMAN, D. 2012. Recognition and cleavage of related to ubiquitin 1 (Rub1) and Rub1-ubiquitin chains by components of the ubiquitin-proteasome system. *Mol Cell Proteomics,* 11**,** 1595-611.

SIRKIS, R., GERST, J. E. & FASS, D. 2006. Ddi1, a eukaryotic protein with the retroviral protease fold. *J Mol Biol,* 364**,** 376-87.

SKOWYRA, D., CRAIG, K. L., TYERS, M., ELLEDGE, S. J. & HARPER, J. W. 1997. F-box proteins are receptors that recruit phosphorylated substrates to the SCF ubiquitin-ligase complex. *Cell,* 91**,** 209-19.

SMOLKA, M. B., ALBUQUERQUE, C. P., CHEN, S. H. & ZHOU, H. 2007. Proteome-wide identification of in vivo targets of DNA damage checkpoint kinases. *Proc Natl Acad Sci U S A,* 104**,** 10364-9.

SOBHIAN, B., SHAO, G., LILLI, D. R., CULHANE, A. C., MOREAU, L. A., XIA, B., LIVINGSTON, D. M. & GREENBERG, R. A. 2007. RAP80 targets BRCA1 to specific ubiquitin structures at DNA damage sites. *Science,* 316**,** 1198-202.

SOGAARD, T. M. & SVEJSTRUP, J. Q. 2007. Hyperphosphorylation of the C-terminal repeat domain of RNA polymerase II facilitates dissociation of its complex with mediator. *J Biol Chem,* 282**,** 14113-20.

SOLE, C., NADAL-RIBELLES, M., KRAFT, C., PETER, M., POSAS, F. & DE NADAL, E. 2011. Control of Ubp3 ubiquitin protease activity by the Hog1 SAPK modulates transcription upon osmostress. *EMBO J,* 30**,** 3274-84.

SOMESH, B. P., REID, J., LIU, W. F., SOGAARD, T. M., ERDJUMENT-BROMAGE, H., TEMPST, P. & SVEJSTRUP, J. Q. 2005. Multiple mechanisms confining RNA polymerase II ubiquitylation to polymerases undergoing transcriptional arrest. *Cell,* 121**,** 913-23.

SOMESH, B. P., SIGURDSSON, S., SAEKI, H., ERDJUMENT-BROMAGE, H., TEMPST, P. & SVEJSTRUP, J. Q. 2007. Communication between distant sites in RNA polymerase II through ubiquitylation factors and the polymerase CTD. *Cell,* 129**,** 57-68.

SPENCE, J., GALI, R. R., DITTMAR, G., SHERMAN, F., KARIN, M. & FINLEY, D. 2000. Cell cycle-regulated modification of the ribosome by a variant multiubiquitin chain. *Cell,* 102**,** 67-76.

SPIVAK, G. 2005. UV-sensitive syndrome. *Mutat Res,* 577**,** 162-9.

STALLONS, L. J. & MCGREGOR, W. G. 2010. Translesion synthesis polymerases in the prevention and promotion of carcinogenesis. *J Nucleic Acids,* 2010.

STAMENOVA, S. D., FRENCH, M. E., HE, Y., FRANCIS, S. A., KRAMER, Z. B. & HICKE, L. 2007. Ubiquitin binds to and regulates a subset of SH3 domains. *Mol Cell,* 25**,** 273-84.

STARITA, L. M., HORWITZ, A. A., KEOGH, M. C., ISHIOKA, C., PARVIN, J. D. & CHIBA, N. 2005. BRCA1/BARD1 ubiquitinate phosphorylated RNA polymerase II. *J Biol Chem,* 280**,** 24498-505.

STARITA, L. M., LO, R. S., ENG, J. K., VON HALLER, P. D. & FIELDS, S. 2012. Sites of ubiquitin attachment in Saccharomyces cerevisiae. *Proteomics,* 12**,** 236-40.

STROM, A. C. & WEIS, K. 2001. Importin-beta-like nuclear transport receptors. *Genome Biol,* 2**,** REVIEWS3008.

SU, K., ROOS, M. D., YANG, X., HAN, I., PATERSON, A. J. & KUDLOW, J. E. 1999. An N-terminal region of Sp1 targets its proteasome-dependent degradation in vitro. *J Biol Chem,* 274**,** 15194-202.

SUDOL, M. 1996. Structure and function of the WW domain. *Prog Biophys Mol Biol,* 65**,** 113-32.

SUGASAWA, K., OKAMOTO, T., SHIMIZU, Y., MASUTANI, C., IWAI, S. & HANAOKA, F. 2001. A multistep damage recognition mechanism for global genomic nucleotide excision repair. *Genes Dev,* 15**,** 507-21.

SULAHIAN, R., SIKDER, D., JOHNSTON, S. A. & KODADEK, T. 2006. The proteasomal ATPase complex is required for stress-induced transcription in yeast. *Nucleic Acids Res,* 34**,** 1351-7.

SULLIVAN, J. A., LEWIS, M. J., NIKKO, E. & PELHAM, H. R. 2007. Multiple interactions drive adaptor-mediated recruitment of the ubiquitin ligase rsp5 to membrane proteins in vivo and in vitro. *Mol Biol Cell,* 18**,** 2429-40.

SUN, Z. W. & ALLIS, C. D. 2002. Ubiquitination of histone H2B regulates H3 methylation and gene silencing in yeast. *Nature,* 418**,** 104-8.

SURYADINATA, R., HOLIEN, J. K., YANG, G., PARKER, M. W., PAPALEO, E. & SARCEVIC, B. 2013. Molecular and structural insight into lysine selection on substrate and ubiquitin lysine 48 by the ubiquitin-conjugating enzyme Cdc34. *Cell Cycle,* 12**,** 1732-44.

SUZUKI, T., YOKOYAMA, A., TSUJI, T., IKESHIMA, E., NAKASHIMA, K., IKUSHIMA, S., KOBAYASHI, C. & YOSHIDA, S. 2011. Identification and characterization of genes involved in glutathione production in yeast. *J Biosci Bioeng,* 112**,** 107-13.

SVEJSTRUP, J. Q. 2002. Mechanisms of transcription-coupled DNA repair. *Nat Rev Mol Cell Biol,* 3**,** 21-9.

SVEJSTRUP, J. Q. 2007. Contending with transcriptional arrest during RNAPII transcript elongation. *Trends Biochem Sci,* 32**,** 165-71.

SVEJSTRUP, J. Q., WANG, Z., FEAVER, W. J., WU, X., BUSHNELL, D. A., DONAHUE, T. F., FRIEDBERG, E. C. & KORNBERG, R. D. 1995. Different forms of TFIIH for transcription and DNA repair: holo-TFIIH and a nucleotide excision repairosome. *Cell,* 80**,** 21-8.

SWEDER, K. S. & HANAWALT, P. C. 1992. Preferential repair of cyclobutane pyrimidine dimers in the transcribed strand of a gene in yeast chromosomes and plasmids is dependent on transcription. *Proc Natl Acad Sci U S A,* 89**,** 10696-700.

SWEENEY, F. D., YANG, F., CHI, A., SHABANOWITZ, J., HUNT, D. F. & DUROCHER, D. 2005. Saccharomyces cerevisiae Rad9 acts as a Mec1 adaptor to allow Rad53 activation. *Curr Biol,* 15**,** 1364-75.

TAKAGI, Y., CHADICK, J. Z., DAVIS, J. A. & ASTURIAS, F. J. 2005a. Preponderance of free mediator in the yeast Saccharomyces cerevisiae. *J Biol Chem,* 280**,** 31200-7.

TAKAGI, Y., MASUDA, C. A., CHANG, W. H., KOMORI, H., WANG, D., HUNTER, T., JOAZEIRO, C. A. & KORNBERG, R. D. 2005b. Ubiquitin ligase activity of TFIIH and the transcriptional response to DNA damage. *Mol Cell,* 18**,** 237-43.

TAKAI, Y., SASAKI, T. & MATOZAKI, T. 2001. Small GTP-binding proteins. *Physiol Rev,* 81**,** 153-208.

TAN, S. 2001. A modular polycistronic expression system for overexpressing protein complexes in Escherichia coli. *Protein Expr Purif,* 21**,** 224-34.

TANOOKA, H. & TADA, M. 1975. Reparable lethal DNA damage produced by enzyme-activated 4-hydroxyaminoquinoline 1-oxide. *Chem Biol Interact,* 10**,** 11-8.

TARLAC, V. & STOREY, E. 2003. Role of proteolysis in polyglutamine disorders. *J Neurosci Res,* 74**,** 406-16.

TASCHNER, M., HARREMAN, M., TENG, Y., GILL, H., ANINDYA, R., MASLEN, S. L., SKEHEL, J. M., WATERS, R. & SVEJSTRUP, J. Q. 2010. A role for checkpoint

kinase-dependent Rad26 phosphorylation in transcription-coupled DNA repair in Saccharomyces cerevisiae. *Mol Cell Biol,* 30**,** 436-46.

TATUM, D., LI, W., PLACER, M. & LI, S. 2011. Diverse roles of RNA polymerase II-associated factor 1 complex in different subpathways of nucleotide excision repair. *J Biol Chem,* 286**,** 30304-13.

TAURA, T., KREBBER, H. & SILVER, P. A. 1998. A member of the Ran-binding protein family, Yrb2p, is involved in nuclear protein export. *Proc Natl Acad Sci U S A,* 95**,** 7427-32.

TAVERNA, D. M. & GOLDSTEIN, R. A. 2002. Why are proteins marginally stable? *Proteins,* 46**,** 105-9.

TEIXEIRA, M. T., SINIOSSOGLOU, S., PODTELEJNIKOV, S., BENICHOU, J. C., MANN, M., DUJON, B., HURT, E. & FABRE, E. 1997. Two functionally distinct domains generated by in vivo cleavage of Nup145p: a novel biogenesis pathway for nucleoporins. *EMBO J,* 16**,** 5086-97.

TENG, Y. & WATERS, R. 2000. Excision repair at the level of the nucleotide in the upstream control region, the coding sequence and in the region where transcription terminates of the Saccharomyces cerevisiae MFA2 gene and the role of RAD26. *Nucleic Acids Res,* 28**,** 1114-9.

TENNYSON, C. N., KLAMUT, H. J. & WORTON, R. G. 1995. The human dystrophin gene requires 16 hours to be transcribed and is cotranscriptionally spliced. *Nat Genet,* 9**,** 184-90.

TERLETH, C., VAN SLUIS, C. A. & VAN DE PUTTE, P. 1989. Differential repair of UV damage in Saccharomyces cerevisiae. *Nucleic Acids Res,* 17**,** 4433-9.

THROWER, J. S., HOFFMAN, L., RECHSTEINER, M. & PICKART, C. M. 2000. Recognition of the polyubiquitin proteolytic signal. *EMBO J,* 19**,** 94-102.

TIAN, L., HOLMGREN, R. A. & MATOUSCHEK, A. 2005. A conserved processing mechanism regulates the activity of transcription factors Cubitus interruptus and NF-kappaB. *Nat Struct Mol Biol,* 12**,** 1045-53.

TIJSTERMAN, M., VERHAGE, R. A., VAN DE PUTTE, P., TASSERON-DE JONG, J. G. & BROUWER, J. 1997. Transitions in the coupling of transcription and nucleotide excision repair within RNA polymerase II-transcribed genes of Saccharomyces cerevisiae. *Proc Natl Acad Sci U S A,* 94**,** 8027-32.

TIMNEY, B. L., TETENBAUM-NOVATT, J., AGATE, D. S., WILLIAMS, R., ZHANG, W., CHAIT, B. T. & ROUT, M. P. 2006. Simple kinetic relationships and nonspecific competition govern nuclear import rates in vivo. *J Cell Biol,* 175**,** 579-93.

TKACH, J. M., YIMIT, A., LEE, A. Y., RIFFLE, M., COSTANZO, M., JASCHOB, D., HENDRY, J. A., OU, J., MOFFAT, J., BOONE, C., DAVIS, T. N., NISLOW, C. & BROWN, G. W. 2012. Dissecting DNA damage response pathways by analysing protein localization and abundance changes during DNA replication stress. *Nat Cell Biol,* 14**,** 966-76.

TODO, T., TAKEMORI, H., RYO, H., IHARA, M., MATSUNAGA, T., NIKAIDO, O., SATO, K. & NOMURA, T. 1993. A new photoreactivating enzyme that specifically repairs ultraviolet light-induced (6-4)photoproducts. *Nature,* 361**,** 371-4.

TORNALETTI, S., PARK-SNYDER, S. & HANAWALT, P. C. 2008. G4-forming sequences in the non-transcribed DNA strand pose blocks to T7 RNA polymerase and mammalian RNA polymerase II. *J Biol Chem,* 283**,** 12756-62.

TOULOKHONOV, I., ZHANG, J., PALANGAT, M. & LANDICK, R. 2007. A central role of the RNA polymerase trigger loop in active-site rearrangement during transcriptional pausing. *Mol Cell,* 27**,** 406-19.

TREMPE, J. F., BROWN, N. R., LOWE, E. D., GORDON, C., CAMPBELL, I. D., NOBLE, M. E. & ENDICOTT, J. A. 2005. Mechanism of Lys48-linked polyubiquitin chain recognition by the Mud1 UBA domain. *EMBO J,* 24**,** 3178-89.

TSUI, C., RAGURAJ, A. & PICKART, C. M. 2005. Ubiquitin binding site of the ubiquitin E2 variant (UEV) protein Mms2 is required for DNA damage tolerance in the yeast RAD6 pathway. *J Biol Chem,* 280**,** 19829-35.

UHLMANN, F., WERNIC, D., POUPART, M. A., KOONIN, E. V. & NASMYTH, K. 2000. Cleavage of cohesin by the CD clan protease separin triggers anaphase in yeast. *Cell,* 103**,** 375-86.

UZUNOVA, K., GOTTSCHE, K., MITEVA, M., WEISSHAAR, S. R., GLANEMANN, C., SCHNELLHARDT, M., NIESSEN, M., SCHEEL, H., HOFMANN, K., JOHNSON, E. S., PRAEFCKE, G. J. & DOHMEN, R. J. 2007. Ubiquitin-dependent proteolytic control of SUMO conjugates. *J Biol Chem,* 282**,** 34167-75.

VAN DER VEEN, A. G. & PLOEGH, H. L. 2012. Ubiquitin-like proteins. *Annu Rev Biochem,* 81**,** 323-57.

VAN GOOL, A. J., VERHAGE, R., SWAGEMAKERS, S. M., VAN DE PUTTE, P., BROUWER, J., TROELSTRA, C., BOOTSMA, D. & HOEIJMAKERS, J. H. 1994. RAD26, the functional S. cerevisiae homolog of the Cockayne syndrome B gene ERCC6. *EMBO J,* 13**,** 5361-9.

VAN HOFFEN, A., KALLE, W. H., DE JONG-VERSTEEG, A., LEHMANN, A. R., VAN ZEELAND, A. A. & MULLENDERS, L. H. 1999. Cells from XP-D and XP-D-CS patients exhibit equally inefficient repair of UV-induced damage in transcribed genes but different capacity to recover UV-inhibited transcription. *Nucleic Acids Res,* 27**,** 2898-904.

VARADAN, R., ASSFALG, M., HARIRINIA, A., RAASI, S., PICKART, C. & FUSHMAN, D. 2004. Solution conformation of Lys63-linked di-ubiquitin chain provides clues to functional diversity of polyubiquitin signaling. *J Biol Chem,* 279**,** 7055-63.

VARADAN, R., ASSFALG, M., RAASI, S., PICKART, C. & FUSHMAN, D. 2005. Structural determinants for selective recognition of a Lys48-linked polyubiquitin chain by a UBA domain. *Mol Cell,* 18**,** 687-98.

VARADAN, R., WALKER, O., PICKART, C. & FUSHMAN, D. 2002. Structural properties of polyubiquitin chains in solution. *J Mol Biol,* 324**,** 637-47.

VENKATRAMAN, P., WETZEL, R., TANAKA, M., NUKINA, N. & GOLDBERG, A. L. 2004. Eukaryotic proteasomes cannot digest polyglutamine sequences and release them during degradation of polyglutamine-containing proteins. *Mol Cell,* 14**,** 95-104.

VERHAGE, R. A., VAN GOOL, A. J., DE GROOT, N., HOEIJMAKERS, J. H., VAN DE PUTTE, P. & BROUWER, J. 1996. Double mutants of Saccharomyces cerevisiae with alterations in global genome and transcription-coupled repair. *Mol Cell Biol,* 16**,** 496-502.

VERMA, R., ARAVIND, L., OANIA, R., MCDONALD, W. H., YATES, J. R., 3RD, KOONIN, E. V. & DESHAIES, R. J. 2002. Role of Rpn11 metalloprotease in deubiquitination and degradation by the 26S proteasome. *Science,* 298**,** 611-5.

VERMA, R., CHEN, S., FELDMAN, R., SCHIELTZ, D., YATES, J., DOHMEN, J. & DESHAIES, R. J. 2000. Proteasomal proteomics: identification of nucleotide-sensitive proteasome-interacting proteins by mass spectrometric analysis of affinity-purified proteasomes. *Mol Biol Cell,* 11**,** 3425-39.

VERMA, R., OANIA, R., FANG, R., SMITH, G. T. & DESHAIES, R. J. 2011. Cdc48/p97 mediates UV-dependent turnover of RNA Pol II. *Mol Cell,* 41**,** 82-92.

VERMA, R., OANIA, R., GRAUMANN, J. & DESHAIES, R. J. 2004. Multiubiquitin chain receptors define a layer of substrate selectivity in the ubiquitin-proteasome system. *Cell,* 118**,** 99-110.

VIJAY-KUMAR, S., BUGG, C. E. & COOK, W. J. 1987. Structure of ubiquitin refined at 1.8 A resolution. *J Mol Biol,* 194**,** 531-44.

VISPE, S., DEVRIES, L., CREANCIER, L., BESSE, J., BREAND, S., HOBSON, D. J., SVEJSTRUP, J. Q., ANNEREAU, J. P., CUSSAC, D., DUMONTET, C., GUILBAUD, N., BARRET, J. M. & BAILLY, C. 2009. Triptolide is an inhibitor of RNA polymerase I and II-dependent transcription leading predominantly to down-regulation of short-lived mRNA. *Mol Cancer Ther,* 8**,** 2780-90.

WAGNER, S. A., BELI, P., WEINERT, B. T., NIELSEN, M. L., COX, J., MANN, M. & CHOUDHARY, C. 2011. A proteome-wide, quantitative survey of in vivo ubiquitylation sites reveals widespread regulatory roles. *Mol Cell Proteomics,* 10**,** M111 013284.

WALMACQ, C., CHEUNG, A. C., KIREEVA, M. L., LUBKOWSKA, L., YE, C., GOTTE, D., STRATHERN, J. N., CARELL, T., CRAMER, P. & KASHLEV, M. 2012. Mechanism of translesion transcription by RNA polymerase II and its role in cellular resistance to DNA damage. *Mol Cell,* 46**,** 18-29.

WALSH, R., STOREY, E., STEFANI, D., KELLY, L. & TURNBULL, V. 2005. The roles of proteolysis and nuclear localisation in the toxicity of the polyglutamine diseases. A review. *Neurotox Res,* 7**,** 43-57.

WALTERS, K. J., LECH, P. J., GOH, A. M., WANG, Q. & HOWLEY, P. M. 2003. DNA-repair protein hHR23a alters its protein structure upon binding proteasomal subunit S5a. *Proc Natl Acad Sci U S A,* 100**,** 12694-9.

WANG, B., FALLON, J. F. & BEACHY, P. A. 2000. Hedgehog-regulated processing of Gli3 produces an anterior/posterior repressor gradient in the developing vertebrate limb. *Cell,* 100**,** 423-34.

WANG, G., YANG, J. & HUIBREGTSE, J. M. 1999. Functional domains of the Rsp5 ubiquitin-protein ligase. *Mol Cell Biol,* 19**,** 342-52.

WELCHMAN, R. L., GORDON, C. & MAYER, R. J. 2005. Ubiquitin and ubiquitin-like proteins as multifunctional signals. *Nat Rev Mol Cell Biol,* 6**,** 599-609.

WEN, W., MEINKOTH, J. L., TSIEN, R. Y. & TAYLOR, S. S. 1995. Identification of a signal for rapid export of proteins from the nucleus. *Cell,* 82**,** 463-73.

WILKINSON, C. R., SEEGER, M., HARTMANN-PETERSEN, R., STONE, M., WALLACE, M., SEMPLE, C. & GORDON, C. 2001. Proteins containing the UBA domain are able to bind to multi-ubiquitin chains. *Nat Cell Biol,* 3**,** 939-43.

WILSON, M. D., HARREMAN, M. & SVEJSTRUP, J. Q. 2013. Ubiquitylation and degradation of elongating RNA polymerase II: the last resort. *Biochim Biophys Acta,* 1829**,** 151-7.

WILSON, M. D., SAPONARO, M., LEIDL, M. A. & SVEJSTRUP, J. Q. 2012. MultiDsk: a ubiquitin-specific affinity resin. *PLoS One,* 7**,** e46398.

WINGET, J. M. & MAYOR, T. 2010. The diversity of ubiquitin recognition: hot spots and varied specificity. *Mol Cell,* 38**,** 627-35.

WINSOR, T. S., BARTKOWIAK, B., BENNETT, C. B. & GREENLEAF, A. L. 2013. A DNA damage response system associated with the phosphoCTD of elongating RNA polymerase II. *PLoS One,* 8**,** e60909.

WITHERS-WARD, E. S., MUELLER, T. D., CHEN, I. S. & FEIGON, J. 2000. Biochemical and structural analysis of the interaction between the UBA(2) domain of the DNA repair protein HHR23A and HIV-1 Vpr. *Biochemistry,* 39**,** 14103-12.

WOUDSTRA, E. C., GILBERT, C., FELLOWS, J., JANSEN, L., BROUWER, J., ERDJUMENT-BROMAGE, H., TEMPST, P. & SVEJSTRUP, J. Q. 2002. A Rad26-Def1 complex coordinates repair and RNA pol II proteolysis in response to DNA damage. *Nature,* 415**,** 929-33.

WYCE, A., XIAO, T., WHELAN, K. A., KOSMAN, C., WALTER, W., EICK, D., HUGHES, T. R., KROGAN, N. J., STRAHL, B. D. & BERGER, S. L. 2007. H2B ubiquitylation acts as a barrier to Ctk1 nucleosomal recruitment prior to removal by Ubp8 within a SAGA-related complex. *Mol Cell,* 27**,** 275-88.

XIAO, G., HARHAJ, E. W. & SUN, S. C. 2001. NF-kappaB-inducing kinase regulates the processing of NF-kappaB2 p100. *Mol Cell,* 7**,** 401-9.

XU, D., FARMER, A. & CHOOK, Y. M. 2010. Recognition of nuclear targeting signals by Karyopherin-beta proteins. *Curr Opin Struct Biol,* 20**,** 782-90.

XU, P., DUONG, D. M., SEYFRIED, N. T., CHENG, D., XIE, Y., ROBERT, J., RUSH, J., HOCHSTRASSER, M., FINLEY, D. & PENG, J. 2009a. Quantitative proteomics reveals the function of unconventional ubiquitin chains in proteasomal degradation. *Cell,* 137**,** 133-45.

XU, Z., WEI, W., GAGNEUR, J., PEROCCHI, F., CLAUDER-MUNSTER, S., CAMBLONG, J., GUFFANTI, E., STUTZ, F., HUBER, W. & STEINMETZ, L. M. 2009b. Bidirectional promoters generate pervasive transcription in yeast. *Nature,* 457**,** 1033-7.

YANG, W., DUNLAP, J. R., ANDREWS, R. B. & WETZEL, R. 2002. Aggregated polyglutamine peptides delivered to nuclei are toxic to mammalian cells. *Hum Mol Genet,* 11**,** 2905-17.

YAO, R., ZHANG, Z., AN, X., BUCCI, B., PERLSTEIN, D. L., STUBBE, J. & HUANG, M. 2003. Subcellular localization of yeast ribonucleotide reductase regulated by the DNA replication and damage checkpoint pathways. *Proc Natl Acad Sci U S A,* 100**,** 6628-33.

YASUKAWA, T., BHATT, S., TAKEUCHI, T., KAWAUCHI, J., TAKAHASHI, H., TSUTSUI, A., MURAOKA, T., INOUE, M., TSUDA, M., KITAJIMA, S., CONAWAY, R. C., CONAWAY, J. W., TRAINOR, P. A. & ASO, T. 2012. Transcriptional elongation factor elongin A regulates retinoic acid-induced gene expression during neuronal differentiation. *Cell Rep,* 2**,** 1129-36.

YASUKAWA, T., KAMURA, T., KITAJIMA, S., CONAWAY, R. C., CONAWAY, J. W. & ASO, T. 2008. Mammalian Elongin A complex mediates DNA-damage-induced ubiquitylation and degradation of Rpb1. *EMBO J,* 27**,** 3256-66.

YE, Y., BLASER, G., HORROCKS, M. H., RUEDAS-RAMA, M. J., IBRAHIM, S., ZHUKOV, A. A., ORTE, A., KLENERMAN, D., JACKSON, S. E. & KOMANDER, D. 2012. Ubiquitin chain conformation regulates recognition and activity of interacting proteins. *Nature,* 492**,** 266-70.

YEN, J. L., FLICK, K., PAPAGIANNIS, C. V., MATHUR, R., TYRRELL, A., OUNI, I., KAAKE, R. M., HUANG, L. & KAISER, P. 2012. Signal-induced disassembly of the SCF ubiquitin ligase complex by Cdc48/p97. *Mol Cell,* 48**,** 288-97.

YEN, Y. M., ROBERTS, P. M. & JOHNSON, R. C. 2001. Nuclear localization of the Saccharomyces cerevisiae HMG protein NHP6A occurs by a Ran-independent nonclassical pathway. *Traffic,* 2**,** 449-64.

YOH, S. M., CHO, H., PICKLE, L., EVANS, R. M. & JONES, K. A. 2007. The Spt6 SH2 domain binds Ser2-P RNAPII to direct Iws1-dependent mRNA splicing and export. *Genes Dev,* 21**,** 160-74.

YU, Y. B. 2002. Coiled-coils: stability, specificity, and drug delivery potential. *Adv Drug Deliv Rev,* 54**,** 1113-29.

ZEGERMAN, P. & DIFFLEY, J. F. 2010. Checkpoint-dependent inhibition of DNA replication initiation by Sld3 and Dbf4 phosphorylation. *Nature,* 467**,** 474-8.

ZHANG, D., CHEN, T., ZIV, I., ROSENZWEIG, R., MATIUHIN, Y., BRONNER, V., GLICKMAN, M. H. & FUSHMAN, D. 2009. Together, Rpn10 and Dsk2 can serve as a polyubiquitin chain-length sensor. *Mol Cell,* 36**,** 1018-33.

ZHANG, D., RAASI, S. & FUSHMAN, D. 2008. Affinity makes the difference: nonselective interaction of the UBA domain of Ubiquilin-1 with monomeric ubiquitin and polyubiquitin chains. *J Mol Biol,* 377**,** 162-80.

ZHANG, X., HORIBATA, K., SAIJO, M., ISHIGAMI, C., UKAI, A., KANNO, S., TAHARA, H., NEILAN, E. G., HONMA, M., NOHMI, T., YASUI, A. & TANAKA, K. 2012. Mutations in UVSSA cause UV-sensitive syndrome and destabilize ERCC6 in transcription-coupled DNA repair. *Nat Genet,* 44**,** 593-7.

ZHAO, S. & ULRICH, H. D. 2010. Distinct consequences of posttranslational modification by linear versus K63-linked polyubiquitin chains. *Proc Natl Acad Sci U S A,* 107**,** 7704-9.

ZHENG, N., SCHULMAN, B. A., SONG, L., MILLER, J. J., JEFFREY, P. D., WANG, P., CHU, C., KOEPP, D. M., ELLEDGE, S. J., PAGANO, M., CONAWAY, R. C., CONAWAY, J. W., HARPER, J. W. & PAVLETICH, N. P. 2002. Structure of the Cul1-Rbx1-Skp1-F boxSkp2 SCF ubiquitin ligase complex. *Nature,* 416**,** 703-9.

ZHOU, J., SCHWEIKHARD, V. & BLOCK, S. M. 2013. Single-molecule studies of RNAPII elongation. *Biochim Biophys Acta,* 1829**,** 29-38.

ZHOU, M., HALANSKI, M. A., RADONOVICH, M. F., KASHANCHI, F., PENG, J., PRICE, D. H. & BRADY, J. N. 2000. Tat modifies the activity of CDK9 to phosphorylate serine 5 of the RNA polymerase II carboxyl-terminal domain during human immunodeficiency virus type 1 transcription. *Mol Cell Biol,* 20**,** 5077-86.

ZHOU, P. & HOWLEY, P. M. 1998. Ubiquitination and degradation of the substrate recognition subunits of SCF ubiquitin-protein ligases. *Mol Cell,* 2**,** 571-80.

ZHOU, W. & DOETSCH, P. W. 1993. Effects of abasic sites and DNA single-strand breaks on prokaryotic RNA polymerases. *Proc Natl Acad Sci U S A,* 90**,** 6601-5.

ZHOU, W., REINES, D. & DOETSCH, P. W. 1995. T7 RNA polymerase bypass of large gaps on the template strand reveals a critical role of the nontemplate strand in elongation. *Cell,* 82**,** 577-85.

ZHU, X., MENARD, R. & SULEA, T. 2007. High incidence of ubiquitin-like domains in human ubiquitin-specific proteases. *Proteins,* 69**,** 1-7.

ZIV, I., MATIUHIN, Y., KIRKPATRICK, D. S., ERPAPAZOGLOU, Z., LEON, S., PANTAZOPOULOU, M., KIM, W., GYGI, S. P., HAGUENAUER-TSAPIS, R., REIS, N., GLICKMAN, M. H. & KLEIFELD, O. 2011. A perturbed ubiquitin landscape distinguishes between ubiquitin in trafficking and in proteolysis. *Mol Cell Proteomics,* 10**,** M111 009753.